INVESTIGATING THE ROLE OF THE MERCAPTURATE PATHWAY IN KIDNEY FUNCTION FOR THE IDENTIFICATION OF AN EARLY INDICATOR OF TUBULAR DYSFUNCTION

CLARA LÚCIA GONÇALVES DIAS

Tese para obtenção do grau de Doutor em Mecanismos de Doença e Medicina Regenerativa

Doutoramento em associação entre:

Universidade NOVA de Lisboa (Faculdade de Ciências Médicas | NOVA Medical School - FCM|NMS/UNL)

Universidade do Algarve (UAlg)

Janeiro, 2019

INVESTIGATING THE ROLE OF THE MERCAPTURATE PATHWAY IN KIDNEY FUNCTION FOR THE IDENTIFICATION OF AN EARLY INDICATOR OF TUBULAR DYSFUNCTION

Clara Lúcia Gonçalves Dias

Orientadores: Sofia de Azeredo Pereira, Professora Auxiliar, NOVA Medical School FCM|NMS/UNL

Miriam Karina Soto Rios, Médica, Hospital Fernando da Fonseca, EPE

Tese para obtenção do grau de Doutor em Mecanismos de Doença e Medicina Regenerativa

Doutoramento em associação entre:

Universidade NOVA de Lisboa (Faculdade de Ciências Médicas | NOVA Medical School - FCM|NMS/UNL)

Universidade do Algarve (UAlg)

PROGRAMAS DE DOUTORAMENTO FCT

Janeiro, 2019

The chapters presented in this thesis regarding experimental data corresponds to manuscripts in preparation for publishing. I hereby state that I have fully participated in the conception and execution of the experimental work, in the interpretation of the collected data and in the writing of the manuscripts. The work was approved by the Ethical Committee of Hospital Professor Doutor Fernando Fonseca, EPE and NMS|FCM-UNL (15/2017/CEFCM).

The experimental work was performed at CEDOC, Chronic Diseases Research Centre, Nova Medical School|Faculdade de Ciências Médicas da Universidade Nova de Lisboa, Hospital Professor Doutor Fernando Fonseca, EPE and at Instituto Português de Oncologia de Lisboa, Francisco Gentil.

FUNDING

Fundação para a Ciência e a Tecnologia (FCT, Portugal)

PD/BD/105892/2014 (to Clara Lúcia Gonçalves Dias) and EXPL/DTP-FTO/1792/2013 – HivKIomics: new insights on tubular injury and nephrotoxicity diagnosis and prediction in HIV-infected patients.

iNOVA4Health

201601-02-021 – (per)Sulfidomics: benchmarking mechanisms underlying drug toxicity and drug resistance in precision medicine. UID/Multi/04462/2013, a program financially supported by Fundação para a Ciência e Tecnologia / Ministério da Educação e Ciência, through national funds and co-funded by FEDER under the PT2020 Partnership Agreement is acknowledged.

Gilead Sciences, Inc.

PGG/032/2015 – Renal tubular lesion in HIV-infected patients: progression and interaction. Program Gilead-GÉNESE 2015

The scientific content of the present thesis originated:

Peer-reviewed papers

Gonçalves-Dias C, Morello J, Correia MJ, Coelho NR, Antunes AMM, Macedo MP, Monteiro EC, Soto K, Pereira SA. Mercapturate pathway in the tubulocentric perspective of diabetic kidney disease. Nephron, 2019, DOI: 10.1159/000494390.

Grácio PC, **Gonçalves-Dias C**, Lopes-Coelho F, Monteiro EC, Serpa J, da Silva CL, Pereira SA. Changes in N-acetyltransferase 8 in kidney tubular cell. Injury, recovery and mesenchymal stromal cell-based therapy (submitted).

Conference proceedings

Dias CG, Coelho NR, Grácio PC, Meneses MJ, Lima IS, Silva F, Serpa J, Soto K, Monteiro EM, Macedo MP, Pereira SA. Mercapturatos de dissulfetos de cisteína como marcadores de progressão de doença renal: comparação entre dois modelos animais de pré-diabetes. Rev Port Diab, 2018, 13(1)Suppl:37-40.

Dias CG, Coelho NR, Correia MJ, Grácio PC, Diogo LN, Monteiro EC, Pereira SA. Mercapturates of cysteine-*S*-disulfides for risk assessment of exposure-related hypertension and kidney dysfunction. Proceedings of the 2nd International DiMoPEx conference. J. Health Pollut., 2017, 8(17):S58-S59.

Dias CG, Campos P, Diogo LN, Trigo D, Correia MJ, Lemos AR, Monteiro EC, Soto K, Pereira SA. Kidney disease progression in HIV-infected patients related with the detoxification of endogenous electrophilic species. Abstracts of the 54th ERA-EDTA Congress. Nephrol. Dial. Transplant., 2017, 32(suppl 3):iii540-iii541

Dias CG, Diogo LN, Campos P, Lemos AR, Monteiro EC, Soto K, Pereira SA. Urinary N-acetyl cysteine and kidney disease progression in HIV-infected patients: a prospective study (Abstract). J. Am. Soc. Nephrol., 2016, 27:2016;952-3A.

Dias CG, Diogo LN, Trigo D, Campos P, Lemos AR, Morello J, Pacheco P, Monteiro EC, Soto K, Pereira SA. Urinary products of N-acetyltransferase 8 as indicators of kidney disease progression in HIV-infection. J. Int. AIDS Soc., 2016, 19(Suppl 7):166.

Oral presentations in scientific meetings

Gonçalves-Dias C, Soto K, Sancho-Martinez SM, Correia MJ, Coelho NR, Prieto-Vicente M, Monteiro EC, López-Hernández FJ, Pereira SA, Urinary mercapturates of cysteine-disulfides decrease in models of drug-induced acute kidney injury, XLIX Reunião da Sociedade Portuguesa de Farmacologia, XXXVII Reunião de Farmacologia Clínica e XVIII Reunião de Toxicologia, 2019, Porto, Portugal (accepted).

Dias CG, Coelho NR, Correia MJ, Lopes-Coelho F, Meneses MJ, Sousa-Lima I, Serpa J, Macedo MP, Soto K, Monteiro EC, Pereira SA. Cysteine disulfide stress is a common mechanism in kidney injury associated to metabolic inflammation models. XXXI Congresso Português de Nefrologia - Encontro Renal 2018, 2018, Vilamoura, Portugal.

Dias CG, Coelho NR, Grácio PC, Meneses MJ, Sousa-Lima I, Silva F, Serpa J, Soto K, Monteiro EC, Macedo MP, Pereira SA. Mercapturatos de dissulfetos de cisteína como marcadores de progressão de doença renal: comparação entre dois modelos animais de pré-diabetes. 14º Congresso Português de Diabetes, 2018, Vilamoura, Portugal.

Dias CG, Coelho NR, Correia MJ, Grácio PC, Lopes-Coelho F, Diogo LN, Serpa J, Monteiro EC, Pereira SA. Effect of chronic intermittent hypoxia in the temporal variation of mercapturates of cysteine-*S*-disulfides. XLVIII Reunião Anual da Sociedade Portuguesa de Farmacologia/ XXXVI Reunião de Farmacologia Clínica/ XVII Reunião de Toxicologia, 2018, Lisboa, Portugal.

Dias CG, Coelho NR, Correia MJ, Meneses MJ, Sousa-Lima I, Macedo MP, Monteiro EC, Pereira SA. Comparison of a marker of kidney disease progression between two animal models of pre-diabetes. Renal disease in obesity and diabetes. Advances in pathogenesis and therapeutics – Diabesity Working Group, 2017, Lisboa, Portugal

Dias CG, Diogo LN, Coelho NR, Pedro AR, Monteiro EC, Soto K, Pereira SA. Mercapturates of cysteine-*S*-disulfides in kidney disease progression: a one-year prospective study in a HIV-infected population. EMBO Workshop: Thiol oxidation in toxicity and signaling, 2017, Sant Feliu de Guíxols, Spain (1 minute elevator talk).

Dias CG, Coelho NR, Diogo LN, Pedro AR, Monteiro EC, Pereira SA. Temporal variation of mercapturates of cysteine-*S*-disulfides in hypertension. EMBO Workshop: Thiol oxidation in toxicity and signaling, 2017, Sant Feliu de Guíxols, Spain (1 minute elevator talk).

Dias CG, Correia MJ, Diogo LN, Campos P, Lemos AR, Morello J, Monteiro EC, Soto K, Pereira SA. uNAC as a novel marker of kidney disease progression in HIV-patients. XLVII Reunião Anual da Sociedade Portuguesa de Farmacologia/ XXXV Reunião de Farmacologia Clínica/ XVI Reunião de Toxicologia, 2017, Coimbra, Portugal.

Dias CG, Coelho NR, Diogo LN, Lemos AR, Morello J, Monteiro EC, Soto K, Pereira SA. Urinary *N*-acetylated cysteine-disulfides as indicators of kidney disease progression in HIV-infected patients. 7th European Congress of Pharmacology (EPHAR 2016), 2016, Istanbul, Turkey.

Poster presentations in scientific meetings

Gonçalves-Dias C, Soto K, Sancho-Martinez SM, Correia MJ, Coelho NR, Prieto-Vicente M, Monteiro EC, López-Hernández FJ, Pereira SA, Changes in mercapturates of cysteine-disulfides associate to acute kidney injury induced by cisplatin and gentamicin, ISN World Congress of Nephrology 2019, 2019, Melbourne, Australia (accepted).

Dias CG, Coelho NR, Correia MJ, Lopes-Coelho F, Meneses MJ, Sousa-Lima I, Serpa J, Macedo P, Soto K, Monteiro EC, Pereira SA. Renal cysteine-disulfide stress is a common feature of cardiometabolic diseases. I NoTeS Congress – Novel Therapeutic Strategies for Noncommunicable Diseases, 2018, Porto, Portugal

Dias CG, Campos P, Sequeira CO, Correia MJ, Coelho NR, Soto K, Monteiro EC, Pereira SA. Mercapturates of cysteine-*S*-disulfides in kidney dysfunction in HIV-infection. 1st Workshop on Human Biomonitoring in Portugal (1st HBM-PT), 2018, Lisboa, Portugal.

Dias CG, Coelho NR, Correia MJ, Grácio PC, Diogo LN, Monteiro EC, Pereira SA. Mercapturates of cysteine-*S*-disulfides for risk assessment of exposure-related hypertension and kidney dysfunction. DiMoPEx Working Groups Meeting, 2nd International conference on Pollution in living and working environments and health, 2017, Bentivoglio, Italy.

Dias CG, Diogo LN, Coelho NR, Pedro AR, Monteiro EC, Soto K, Pereira SA. Mercapturates of cysteine-*S*-disulfides in kidney disease progression: a one-year prospective study in a HIV-infected population. EMBO Workshop: Thiol oxidation in toxicity and signaling, 2017, Sant Feliu de Guíxols, Spain

Dias CG, Coelho NR, Diogo LN, Pedro AR, Monteiro EC, Pereira SA. Temporal variation of mercapturates of cysteine-*S*-disulfides in hypertension. EMBO Workshop: Thiol oxidation in toxicity and signaling, 2017, Sant Feliu de Guíxols, Spain.

Dias CG, Campos P, Diogo LN, Trigo D, Correia MJ, Lemos AR, Monteiro EC, Soto K, Pereira SA. Kidney disease progression in HIV-infected patients related with the detoxification of endogenous electrophilic species. 54th ERA-EDTA Congress, 2017, Madrid, Spain.

Dias CG, Diogo LN, Campos P, Lemos AR, Correia MJ, Morello J, Batista J, Monteiro EC, Soto K, Pereira SA. Mercapturate pathway and kidney disease progression in HIV-patients: a 1-year prospective study. ISN World Congress of Nephrology 2017, 2017, Mexico City, Mexico.

Dias CG, Diogo LN, Trigo D, Campos P, Lemos AR, Morello J, Pacheco P, Monteiro EC, Soto K, Pereira SA. Urinary products of *N*-acetyltransferase 8 as indicators of kidney disease progression in HIV-infected patients. HIV Drug Therapy Glasgow 2016, 2016, Glasgow, UK.

Awards

2018 – Best Poster (Cardiovascular area) at the I NoTeS Congress – Novel Therapeutic Strategies for Noncommunicable Diseases.

2018 – Best Oral Presentation (Basic Nephrology are) at the XXXI Congresso Português de Nefrologia - Encontro Renal 2018.

2017 – Registration award to attend the Renal disease in obesity and diabetes. Advances in pathogenesis and therapeutics – Diabesity Working Group. Lisboa, Portugal.

2017 – Travel award to attend the EMBO Workshop: Thiol oxidation in toxicity and signaling, Sant Feliu de Guíxols, Spain.

Para os meus pais, Florbela e Joaquim,

para os meus avós, Maria e António,

e para a minha irmã, Eva

Table of contents

List of tables

List of figures

List of acronyms and abbreviations

3TC	Lamivudine
ABC	Abacavir
ACR	Albumin-to-creatinine ratio
AKI	Acute kidney injury
ARV	Antiretroviral
ATP	Adenosine triphosphate
ATV	Atazanavir
AUC	Area under the curve
BCG	Bromocresol green albumin
BMI	Body mass index
BMP-7	Bone morphogenetic protein 7
BW	Body weight
cART	Combined antiretroviral therapy
CBS	Cystathionine beta-synthase
Ccl2	Chemokine (C-C motif) ligand 2
CDO	Cysteine dioxygenase
Chrebp	Carbohydrate-responsive element-binding protein
CIH	Chronic intermittent hypoxia
CISP	Cisplatin
CKD	Chronic kidney disease
CKD-EPI	Chronic kidney disease-epidemiology collaboration
CoA	Coenzyme A
Col1a2	Collagen, type I, alfa 2
Cr	Creatinine
CS	Calibration solutions
CTL	Control
CV	Coefficient of variation
Cys	Cysteine
Cys C	Cystatin c
Cys-CISP	Cysteine-cisplatin conjugate
CysGly	Cysteine-glycine
CysGly-CISP	Cysteine-glycine-cisplatin conjugate
CysGly-*S*-conjugate	Cysteine-glycine-*S*-conjugate
CysLT1	Cysteinyl leukotriene 1 receptor
CysLTs	Cysteinyl-leukotrienes
Cys-*S*-conjugate	Cysteine-*S*-conjugate
CysSCX	Cysteine-*S*-conjugates thioethers
CysSH	Free reduced cysteine
CysSSCoA	Cysteine-coenzyme A disulfide
CysSSCys	Cystine
CysSSG	Cysteine-glutathione disulfide
CysSSHCys	Cysteine-homocysteine disulfide
CysSSP	Protein cysteinylation
CysSSX	Cysteine-disulfides

DKD	Diabetic kidney disease
DNA	Deoxyribonucleic acid
DRV	Darunavir
EDTA	Ethylenediaminetetraacetic acid
EFV	Efavirenz
eGFR	Estimated glomerular filtration rate
EKD	Early kidney disease
Elovl2	Elongation of very long chain fatty acids like 2
EMT	Epithelial to mesenchymal transition
ER	Endoplasmic reticulum
ERK	Extracellular-signal-regulated kinase
ESRD	End-stage renal disease
ETV	Etravirine
Fbpase	Fructose 1,6 biphosphatase
FD	Fluorescence detection
FELASA	Federation for Laboratory Animal Science Associations
fl-gelsolin	Full-length gelsolin
Fn	Fibronectin
FTC	Emtricitabine
G	Gentamicin
GCS	Gamma-glutamylcysteine synthetase
GFR	Glomerular filtration rate
GGT	Gamma-glutamyltransferase
Glut2	Glucose transporter 2
GluCys	Glutamate-cysteine
GluCysSSP	Protein glutamylcysteinylation
GSH	Glutathione
GSH-CISP	Glutathione-cisplatin conjugate
GSH-*S*-conjugate	Glutathione-*S*-conjugate
GSSG	Oxidized glutathione
GSSX	Glutathione-disulfide
GST	Glutathione-*S*-transferase
HCys	Homocysteine
HCysSSHcys	Homocystine
HD	Hemodialysis
H&E	Hematoxylin and eosin
HFat	Hypercaloric diet
HFruct	High fructose diet
HIV	Human immunodeficiency virus
HLOQ	Higher limit of quantification
HOMA-IR	Homeostasis model assessment of insulin resistance
HPLC	High-performance liquid chromatography
Hprt	Hypoxanthine guanine phosphoribosyl transferase
Hspa5	Heat shock protein 5
IH	Intermittent hypoxia
IL-18	Interleukin 18

IQR	Interquartile range
IPGTT	Intra-peritoneal glucose tolerance test
KIM-1	Kidney injury molecule-l
LLOQ	Lower limit of quantification
LMW	Low molecular weight
LPV	Lopinavir
LTA4	Leukotriene A4
LTC4	Leukotriene C4
LTD4	Leukotriene D4
LTE4	Leukotriene E4
MDRD	Modification of diet in renal disease
MeOH	Methanol
MRP	Multidrug-resistance-associated protein
MSC	Mesenchymal stromal cell
MSC-CM	Mesenchymal stromal cell conditioned medium
NAC	*N*-acetylcysteine
NAC-Cys	Mercapturate of cysteine
N-acetyl-CysSSX	Mercapturates of cysteine-disulfides
N-acetyl-LTE4	Mercapaturate of leukotriene E4
NAC-NAC	*N*-acetylcysteine symmetric disulfide
NAC-Cys-*S*-conjugate	Mercapturate of cysteine-*S*-conjugate
NAG	*N*-acetyl-β-D-glucosaminidase
NAT8 or Nat8	*N*-acetyltransferase 8
NC	Normal control
NGAL	Neutrophil gelatinase associated lipocalin
NNRTI	Non-nucleoside reverse transcriptase inhibitor
NP	Non-progression
N(t)RTI	Nucleoside/nucleotide reverse transcriptase inhibitor
NVP	Nevirapine
Nx	Normoxic
OAT	Organic anion transporter
OSA	Obstructive sleep apnea
P	Progression
PBS	Phosphate buffered saline
pCr	Plasma creatinine
PI	Protease inhibitor
PI/r	Protease inhibitor boosted with ritonavir
QC	Quality control solution
qPCR	Quantitative real-time polymerase chain reaction
RC	Renal cortex
reg IIIb	Regenerating islet-derived protein III β
RM	Renal medulla
RT	Room temperature
SBD-F	7-fluorobenzofurazan-4-sulfonic acid ammonium salt
S-C	Sulfur-carbon bond
sCr	Serum creatinine

sCys C	Serum cystatin c
SD	Standard deviation
SEM	Standard error of the mean
Sglt2	Sodium/glucose co-transporter 2
SH	Sulfhydryl group
SIRT1	Sirtuin 1
SNP	Single nucleotide polymorphism
Srebp1a	Sterol regulatory element binding protein
S-S	Disulfide bond
TCA	Trichloroacetic acid
TCEP	Tris(2-carboxyethylphosphine)
TDF	Tenofovir
t-gelsolin	Gelsolin 43 kDa fragment
TGF-β1 or Tgfb1	Transforming growth factor-1
Tnfa	Tumor necrosis factor, alfa
uACR	Urinary albumin-to-creatinine ratio
uCr	Urinary creatinine
uCys	Urinary cysteine
uCysGly	Urinary cysteine-glycine
uLTE4	Urinary leukotriene E4
uNAC	Urinary surrogate of the mercapturates from cysteine-disulfides
uPCR	Urinary protein-to-creatinine ratio
UV	Ultraviolet
Vim	Vimentin
VL	Viral load
xCT	Glutamate/cystine antiporter

Acknowledgements

Em primeiro lugar, gostaria de agradecer à Professora Doutora Sofia de Azeredo Pereira pela orientação, motivação e voto de confiança que sempre depositou em mim. Agradeço também a paciência e a transmissão de ensinamentos e experiências. O seu notório entusiasmo pela ciência é contagiante e impulsiona os seus alunos a querer sempre saber mais e a dar todos os dias o seu melhor para o conseguir. A sua contribuição para este trabalho é inestimável e não tenho palavras para o descrever.

À Doutora Karina Soto, agradeço todo o apoio dado ao longo destes anos bem como a introdução ao mundo da nefrologia clínica.

Agradeço também à Professora Doutora Emília Monteiro, por toda a prontidão, simpatia e disponibilidade com que me recebeu no laboratório de Farmacologia Translacional. Obrigada por todo o conhecimento que me transmitiu e pela ajuda em questões que nem sempre foram fáceis de resolver.

À Professora Doutora Jacinta Serpa, agradeço a disponibilidade com que me recebeu no seu laboratório no IPO e todo o ensinamento que me transmitiu. Da mesma forma, agradeço também à Professora Doutora Paula Macedo toda a ajuda dada na área da diabetes, extendendo estes agradecimentos à Maria João Meneses e à Inês Lima.

À Doutora Alexandra Antunes, agradeço também a simpatia e disponibilidade com que sempre me recebeu. Da mesma forma, deixo aqui o meu agradecimento à Judit por toda a ajuda que me deu.

Não posso deixar de agradecer ao grupo do Laboratório de Farmacologia Translacional que ao longo destes anos conseguiu sempre suportar-me e animar-me. Sem vocês, esta tese nunca teria sido possível de realizar, o vosso espírito de entreajuda e motivação foram essenciais! Sinto-me uma sortuda por trabalhar nesta equipa e agradeço-vos do fundo do meu coração. João (Texuguinha), obrigada pela motivação nos momentos mais difíceis, por toda a ajuda e por todos os momentos de descontração que me proporcionaste. Nuno, obrigada por todos os teus "momentos à Nuno Coelho" que muito me fizeram rir e por toda a ajuda. Cat, não sei como agradecer toda a tua contribuição para este trabalho. Foste incansável, obrigada! Agradeço também aos membros antigos deste grupo, que ao longo destes anos foram passando pelo laboratório e de alguma forma contribuíram para a execução deste trabalho: à Aline, ao Nelson, à Rita Lemos e à Rita Pedro. Agradeço também à Patrícia e à Ana Hipólito, as minhas parceiras das células, que sempre me

ajudaram mesmo quando o meu humor não era o melhor. Agradeço ainda às pessoas dos grupos do lado, Joana Sacramento, Maria João Ribeiro, Bernardete, Cláudia, Inês, João, Filipe e Marisa, por todos os momentos de boa disposição no laboratório. Estendo este agradecimento também à Dr. Umbelina Caixas, à Professora Doutora Joana Batuca e à Professora Doutora Sílvia Conde.

Tenho também que agradecer a todas as pessoas que facilitaram a minha passagem pelo IPO. Filipa, obrigada por toda a tua paciência e ajuda e também pela tua calma nos momentos mais dramáticos! Obrigada ainda à Sofia Nunes, ao Cristiano, à Armanda, à Cindy e à Inês pelas horas de almoço e pelos momentos de descontração. Da mesma forma, agradeço também todo o apoio dado pelo Dr. Pedro Campos e pela Dra. Rita Theias.

Às minhas mais que amigas, Graça e Juliana, obrigada pelos nossos jantares, pelas fofoquices e sobretudo pelo apoio que me deram e que sei que sempre darão. As nossas reuniões quinzenais contribuíram, em muito, para a manutenção da minha sanidade mental!

Deixo ainda um especial agradecimento à minha "fofi" Nádia, que sempre me apoiou incondicionalmente e me ajudou em tudo. A tua amizade é muito valiosa para mim, obrigada por me animares quando eu mais preciso.

A ti Mauro, não sei como te agradecer. Sem ti, tudo isto teria sido bem mais difícil. Estiveste presente nos bons e nos maus momentos, apoiaste-me sem hesitares. Aturaste o meu mau feitio, os meus choros e desesperos. Obrigada por tudo!

Não posso deixar de agradecer a quem sempre me deu tudo: aos meus pais, Florbela e Joaquim. Tudo o que eu sou, devo-o a vocês. Vocês são tudo para mim, sempre acreditaram nas minhas capacidades e me motivaram para alcançar os meus objetivos. O vosso apoio incansável, os telefonemas intermináveis e a vossa dedicação foram pilares essenciais para conseguir finalizar esta etapa. Agradeço também à minha irmã, Eva, pelos conselhos, pelas idas ao shopping para relaxamento e pela paciência, muitas vezes necessária para me aturar. Ao meu avô António, a quem devo o bichinho de tudo querer saber. Obrigada pelos telefonemas de apoio e por nunca te esqueceres de quem está longe. E à minha avó Maria porque, apesar de já não seres quem eras, receberes-me sempre com um sorriso na cara e me fazeres acreditar que ainda sabes quem eu sou.

Aos restantes familiares e amigos, obrigada pelo apoio sempre demonstrado ao longo destes últimos 4 anos.

Abstract

The general objective of this project was to respond to a pressing need in clinical practice, which is the diagnosis of tubular dysfunction. This knowledge would not only allow the prediction of the early onset and progression of tubular dysfunction, but also the management of strategies to stop the progression of renal disease, which at present are non-existent. On the other hand, it would be of significant importance in the development of strategies to minimize tubular toxicity induced by drugs and substances used in diagnostic methods that pose a major challenge in clinical practice. It would also have added value in the preclinical tests in drug development.

There is a good correlation between the degree of damage to the tubulo-interstitial compartment and the deterioration of renal function. Moreover, the primary role of kidney as a detoxification organ renders it vulnerable to develop various forms of injury. Motivated by the relevant detoxification activity and its main expression in kidney proximal tubular cells, the mercapturate pathway was chosen as a starting point of this mechanistic-based investigation for a reliable biomarker reflective of tubular dysfunction. We were particularly interested in *N*-acetyltransferase 8 (NAT8), the last enzyme of the mercapturate pathway, that acetylates cysteine-*S*-conjugates (Cys-*S*-conjugates), rendering their urinary elimination. Cys-*S*-conjugates can be more toxic than the parent compounds. The formation of Cys-*S*-conjugates have been reported in inflammatory diseases and a hypothesis-based review of their contribution and the contribution of NAT8 as a balancer of their availability was built up exemplified by a tubular view of diabetic nephropathy.

As the kidney is highly susceptible to oxidative conditions and is exposed to relatively high concentrations of cysteine (Cys), which becomes easily oxidized, promoting the accumulation of its disulfides (in both the free and protein forms), we though that the measurement of Cys-S-conjugates which are disulfides could be a starting point for the identification of new markers of tubular dysfunction.

With the general goal of non-invasively evaluate kidney tubular dysfunction, it was first needed to develop a method that allowed to phenotype patients as higher or lower Cys-*S*-conjugates detoxifiers inspired on the activity of NAT8, which has been recognized as a nephroprotective factor mainly expressed in proximal tubular cells. This method

quantifies the mercapturates of Cys-*S*-conjugates that are disulfides (CysSSX). We measured the *N*-acetylcysteine moiety of these mercapturates, that we named uNAC, as a surrogate of detoxification of CysSSX. In **Chapter I**, the rationale for the mercapturates of CysSSX as indicators of tubular dysfunction and for method development and validation is presented. The developed method was validated and applied to urine from individuals with healthy kidney and kidney disease as well as to urine from mice and rats. We have shown that CysSSX are acetylated and eliminated in urine as mercapturates. Rats and mice showed higher levels of uNAC than man. No intra-individual variability was found for uNAC levels in urine samples from rats and mice. In addition, lower levels of uNAC were found in urine of four patients that progressed to chronic kidney disease (CKD) after an episode of acute kidney injury (AKI) in comparison with volunteers.

In order to evaluate the potential of uNAC as an early indicator of AKI, we measured uNAC concentrations in two animal models of drug-induced AKI (**Chapter II**). Cisplatin (CISP) was chosen because is a tubular toxicant that undergoes the mercapturate pathway and gentamicin (G) also promotes tubular dysfunction, but it does not undergo this metabolic circuitry. For this, male Wistar rats were allocated in individual metabolic cages and randomly divided into three groups: (1) control group (CTL), receiving daily vehicle intraperitoneal for 6 days; (2) cisplatin group (CISP), receiving a single intraperitoneal dose of cisplatin (5 mg/kg); and (3) gentamicin group (G), receiving gentamicin intraperitoneal (150 mg/kg) for 6 days. The levels of uNAC decreased prior to the increase in pCr, particularly in CISP model ($p < 0.001$). This tendency was also observed for rats treated with G, despite only reaching significance belatedly than CISP ($p = 0.044$).

Next, we were interested to know the inter-individual variability of uNAC in man and factors that could influence it. For that, uNAC was measured in a population of human-immunodeficiency virus (HIV)-infected patients as a proof-of-principle (**Chapter III**). The levels of uNAC varied highly (59%) among 242 HIV-infected patients. A multivariable analysis showed that the levels of uNAC were positively associated with estimated glomerular filtration rate (eGFR) ($p = 0.020$) and negatively associated with lamivudine use (3TC) ($p = 0.019$) and Black race ($p < 0.001$). Notably, a prospective analysis of uNAC in 118 HIV-infected patients allowed to discriminate patients on kidney disease progression from those that maintained a stable renal function, that might imply changes in cysteine disulfides availability and dynamics in kidney disease progression.

Thus, the next step was to evaluate the temporal changes of cysteine disulfides dynamics and uNAC in models of chronic diseases that affect the kidney, aiming to evaluate if they are prior to kidney dysfunction and also its relation to disease development (e.g. hypertension, insulin resistance). For that, we selected animal models associated with metabolic inflammation, namely two pre-diabetic mice models induced by high fructose (HFruct) or hypercaloric (HFat) diet for 15 weeks (**Chapter IV**); and a rat model of hypertension and insulin resistance induced by chronic intermittent hypoxia (CIH) to a maximum of 60 days (**Chapter V**). In the three models the disease progression and severity diseases are mild, being appropriated to study temporal changes of kidney tubular dysfunction and its relation to the development of hypertension and insulin resistance. HFat animals presented lower uNAC right after 1 week of exposure to the diet while the HFruct group presented a mild increase. Nevertheless, the increment on the chronicity of exposure to the diets decreased uNAC until the end of the study, that was particularly evident for HFat model (45% lower than Chow group, $p = 0.005$). Moreover, Cys availability and protein cysteinylation (CysSSP) increased in HFruct ($p = 0.046$, $p = 0.045$ and $p = 0.017$, respectively for total, free total and CysSSP); while HFat diet induced an overall decrease ($p = 0.028$, $p = 0.065$ and $p = 0.049$, respectively for total, free total and CysSSP fractions). Although no clear renal pathology was observed in both pre-diabetic groups at the end of the study, changes in urinary albumin-to-creatinine ratio (uACR) were earlier and more evident in the HFat, comparing with the HFruct group. HFat mice also presented higher renal expression of NAT8 ($p = 0.001$), fibrotic markers and enzymes of glucose and lipid metabolism. Both diets induced increases in the renal expression of inflammatory, epithelial to mesenchymal transition and endoplasmic reticulum stress markers.

In the first day of exposure to CIH, there was an acute increase of almost 100% in uNAC in comparison with normoxic (Nx) animals. Afterwards, its levels decreased overtime, reaching a difference of -80% in CIH versus Nx group ($p < 0.001$). Kidney NAT8 gene expression initially decreased at days 1 ($p = 0.006$ for renal cortex – RC; $p = 0.041$ for renal medulla – RM) and 7 ($p = 0.021$ for RC and $p = 0.024$ for RM) of CIH exposure, further increasing at 21 days when hypertension is established but prior to the establishment of insulin resistance, and decreased at 60 days ($p = 0.037$ for RC and $p = 0.024$ for RM), coincident with the previously reported increase in renal fibronectin expression. At 7 days of CIH exposure, an increase in renal total Cys ($p = 0.003$ for RC and $p = 0.001$ for RM) and CysSSP ($p = 0.041$ for RC and $p = 0.028$ for RM) was

observed, further decreasing with the chronicity of exposure to CIH ($p < 0.001$). An increase was also observed in the ratio of free Cys by CysSSX at day 7 ($p = 0.008$ for RC and $p = 0.017$ for RM), indicative of a more reduced state of Cys, decreasing from day 14 to 21 ($p < 0.001$) and returning to values closer to control conditions by the end of the experiment. Nevertheless, at the end of the study, no histological alterations were observed neither changes in uACR, despite there was a tendency to increase in CIH animals.

Herein, we provided evidence in order to respond to a lack of tubular dysfunction markers, a necessity that is mostly driven due to the need to better understand the pathophysiological mechanisms underlying it. Secondly, a method was developed to evaluate tubular dysfunction in a non-invasive manner. Lastly and although still very preliminary, new knowledge was herein provided based on a hypothesis that, as far as the author knowledge, is an innovative and never addressed issue that could pave the way for the identification of new mechanisms of inflammatory diseases through a tubulocentric perspective.

The preliminary data herein reported supports uNAC as an indicator of tubular dysfunction progression. Our approach shows that Cys-*S*-conjugate's dynamics changes throughout disease progression. The results support that this dynamic might be associated not only to adaptive mechanism, with increases in CysSSP and uNAC, but also to mechanisms of disease progression with the chronicity of injury, characterized by opposite changes on this dynamic. The translation of these results together with the deepening of this study might lead to the identification of new therapeutic targets to slow down or stop disease progression and to establish preventive strategies achieved through early diagnosis. Furthermore, the identification of a new marker could also help to evaluate the success of preventive/management strategies.

Keywords: acute kidney injury; biomarkers; chronic kidney injury; cysteine-disulfides; inflammation; mercapturates of cysteine-disulfides; *N*-acetyltransferase 8; nephrotoxicity; oxidation; tubular dysfunction.

Resumo

O objetivo geral deste projeto visou dar resposta a uma necessidade premente na prática clínica, que é o diagnóstico da disfunção tubular. Este conhecimento não só permitirá o diagnóstico precoce desta disfunção, como também o desenvolvimento de estratégicas terapêuticas que permitiam travar a progressão da doença renal, que neste momento são inexistentes. Por outro lado, teria uma importância significativa no desenvolvimento de estratégias para minimizar a toxicidade tubular induzida por fármacos e por substâncias utilizadas nos métodos de diagnóstico, que representam um desafio major na prática clínica. Por último, este conhecimento teria também valor acrescentado nos testes pré-clínicos do desenvolvimento de novos fármacos.

Existe uma forte correlação entre o grau de dano no compartimento túbulo-intersticial e o decréscimo da função renal. Além disso, o papel principal do rim como órgão de destoxificação torna-o vulnerável ao desenvolvimento de várias formas de lesão. Motivados pela actividade destoxificante relevante e pela sua principal expressão nas células tubulares proximais, a via dos mercapturatos foi escolhida como ponto de partida para esta investigação baseada no mecanismo para a identificação de um biomarcador fidedigno que reflita a disfunção tubular. O nosso interesse recaiu particularmente sobre a *N*-acetiltransferase 8 (NAT8), a última enzima da via do mercapturatos, que acetila os S-conjugados da cisteína (Cis-*S*-conjugados), possibilitando a sua eliminação urinária. Os Cis-*S*-conjugados podem ser mais tóxicos do que os seus compostos de origem. A formação dos Cis-*S*-conjugados já foi reportada em doenças inflamatórias e o nosso grupo escreveu uma revisão baseada numa hipótese da sua contribuição e da contribuição da NAT8 como um balanceador da sua disponibilidade, exemplificada por uma visão tubulocêntrica da nefropatia diabética.

Tendo em conta que o rim é altamente suscetível à oxidação e é exposto a concentrações relativamente altas de cisteína (Cis), que se torna facilmente oxidada promovendo a acumulação dos seus dissulfetos (nas suas formas livre e ligada a proteínas), considerámos que a quantificação dos dissulfetos poderia ser um ponto de partida para a identificação de novos marcadores de disfunção tubular.

Numa primeira etapa, foi desenvolvido um método não invasivo que permitiu fenotipar os doentes como menores ou maiores destoxificadores de Cis-*S*-conjugados, tendo por base a atividade da NAT8, que foi reconhecida como um fator nefroprotetor, expressa principalmente nas células tubulares proximais. Este método quantifica os mercapturatos dos Cis-*S*-conjugados que são dissulfetos (CisSSX). A fração de *N*-acetilcisteína destes mercapturatos foi quantificada, que denominamos de uNAC, como um equivalente da destoxificação dos CisSSX. No **Capítulo I**, é apresentado a justificação para os mercapturatos de CisSSX serem considerados indicadores de disfunção tubular e para o desenvolvimento e validação do método. O método desenvolvido foi validado e aplicado em urinas de indivíduos com rim saudável e com doença renal, bem como em urinas de murganhos e ratos. Neste capítulo foi demonstrado que os CisSSX são acetilados e eliminados na urina como mercapturatos. Tanto os ratos como os murganhos apresentaram níveis mais elevados de uNAC do que o homem. Não foi observada qualquer variabilidade intra-individual para os níveis de uNAC nas amostras de urina de ratos e murganhos. Além disso, foram observados níveis mais baixos de uNAC na urina de quatro doentes que progrediram para doença renal crónica (DRC) após um episódio de lesão renal aguda (LRA), em comparação com voluntários.

Com o intuito de avaliar o potencial do uNAC como indicador precoce de LRA, as concentrações de uNAC foram avaliadas em dois modelos animais de LRA induzida por fármacos (**Capítulo II**). A cisplatina (CISP) foi escolhida porque é uma toxina tubular que é metabolizada pela via dos mercapturatos. No caso da gentamicina (G), este fármaco também promove disfunção tubular, mas não é substrato da via dos mercapturatos. Para isso, ratos Wistar machos foram colocados em gaiolas metabólicas individuais e divididos aleatoriamente em três grupos: (1) grupo controlo (CTL), expostos ao veículo diariamente via intraperitoneal durante 6 dias; (2) grupo CISP, expostos a uma única dose (via intraperitoneal) de CISP (5 mg/kg); e (3) grupo G, expostos diariamente a uma dose de G (150 mg/kg) por via intraperitoneal durante 6 dias. Os níveis de uNAC diminuíram antes do aumento da pCr, particularmente no modelo da CISP ($p < 0.001$). Esta tendência também foi observada em ratos tratados com G, apesar de só atingir significância mais tardiamente que a CISP ($p = 0.044$).

De seguida, considerámos interessante avaliar a variabilidade inter-individual do uNAC e os fatores que poderiam influenciar os seus níveis. Para isso, os níveis de uNAC foram medidos numa população de doentes infetados pelo vírus da imunodeficiência humana (VIH) como prova de conceito (**Capítulo III**). Os níveis de uNAC variaram muito (59%) entre 242 doentes infetados pelo VIH. Através de uma análise multivariada foi demonstrado que os níveis de uNAC estavam associados positivamente com a taxa de filtração glomerular estimada (TFGe) ($p = 0.020$) e negativamente associada ao uso de lamivudina (3TC) ($p = 0.019$) e à raça negra ($p < 0.001$). Além disto, a análise prospetiva do uNAC em 118 doentes infetados pelo HIV permitiu discriminar doentes com progressão da doença renal daqueles que mantiveram uma função renal estável, o que pode implicar alterações na disponibilidade e dinâmica dos dissulfetos de cisteína na progressão da doença renal.

De seguida, fomos avaliar as alterações temporais da dinâmica dos dissulfetos de cisteína e do uNAC em modelos de doenças crónicas que afectam o rim, com o objectivo de avaliar se estas alterações precedem a disfunção renal e a sua relação com o desenvolvimento da doença (ex: hipertensão e resistência à insulina). Assim, foram selecionamos modelos animais associados à inflamação metabólica, dois modelos de murganho com pré-diabetes induzida por dieta rica em frutose (HFruct) e por dieta hipercalórica (HFat) durante 15 semanas (**Capítulo IV**); e um modelo de hipertensão e resistência à insulina induzido por hipoxia crónica intermitente (HCI) até um máximo de 60 dias (**Capítulo V**). Nos três modelos, a progressão e severidade da doença são moderadas, o que é apropriado para estudar alterações temporais da disfunção tubular renal e a sua relação com o desenvolvimento de hipertensão e resistência à insulina. Os animais HFat apresentaram menor eliminação de uNAC imediatamente após 1 semana de exposição à dieta, enquanto que o grupo HFruct apresentou um ligeiro aumento. No entanto, a cronicidade da exposição às dietas diminuiu os níveis de uNAC até ao final do estudo, que foi particularmente evidente para o modelo HFat (45% menor que o grupo controlo – Chow; $p = 0.005$). Além disso, as frações de Cis aumentaram no grupo HFruct ($p = 0.046$, $p = 0.045$ e $p = 0.017$, respetivamente para as formas total, livre total e ligada a proteínas da Cis), enquanto que a dieta HFat provocou uma diminuição geral ($p = 0.028$, $p = 0.065$ e $p = 0.049$, respetivamente, para as formas total, livre total e ligada a proteínas da Cis). Embora não tenha sido observada uma patologia renal clara nos grupos pré-diabéticos, alterações na relação albumina/creatinina na urina (uACR) foram observadas

mais cedo e mais evidentes no grupo HFat em comparação com o grupo HFruct. O grupo HFat também apresentou maior expressão renal de NAT8 (p = 0.001), de marcadores fibróticos e de enzimas do metabolismo da glucose e de lípidos. Ambas as dietas induziram aumentos na expressão renal de marcadores de inflamação, de transição epitelial para mesenquimal e de stress do retículo endoplasmático.

No primeiro dia de exposição à HCI, houve um aumento agudo de quase 100% de uNAC em comparação com animais normóxicos (Nx). Posteriormente, os níveis de uNAC diminuíram ao longo do tempo, atingindo uma diferença de -80% no grupo HCI versus Nx (p < 0.001). A expressão renal da NAT8 diminuiu inicialmente nos dias 1 (p = 0.006 para o córtex renal – CR; p = 0.041 para a medula renal – MR) e 7 (p = 0.021 para o CR e p = 0.024 para a MR) de exposição à HCI, aumentando aos 21 dias, quando a hipertensão foi estabelecida, mas antes do estabelecimento da resistência à insulina. Os níveis de uNAC voltaram a diminuir aos 60 dias (p = 0.037 para o CR e p = 0.024 para a MR), coincidente com o aumento mencionado anteriormente da expressão de fibronectina renal. Aos 7 dias de exposição à HCI, observou-se no rim um aumento da Cis total (p = 0.003 para o CR e p = 0.001 para a MR) e CisSSP (p = 0.041 para o CR e p = 0.028 para a MR), diminuindo ainda mais com a cronicidade da exposição à HCI (p < 0.001). Foi também observado um aumento do rácio de Cis livre/CisSSX no dia 7 (p = 0.008 para o CR e p = 0.017 para a MR), indicativo de um estado mais reduzido da Cis, diminuindo do dia 14 para 21 (p < 0.001) e regressando a valores mais próximos das condições de controlo no final do ensaio. No entanto, no fim do estudo não foram observadas alterações histológicas nem alterações nos níveis de uACR, apesar de haver uma tendência de aumento nos animais exposto à HIC.

Este trabalho forneceu provas para responder à falta de marcadores de disfunção tubular, uma necessidade que deriva maioritariamente ao facto de ser importante compreender melhor os mecanismos patofisológicos inerentes a esta condição. Em segundo lugar, foi desenvolvido um método para avaliar a disfunção tubular de forma não invasiva. Por fim, e apesar de serem ainda dados preliminares, este trabalho gerou conhecimentos novos baseados numa hipótese que, tanto quanto sabemos, é um assunto inovador e que nunca antes foi abordado, e que pode guiar na identificação de novos mecanismos de doenças inflamatórias através de uma perspetiva tubulocêntrica.

Os dados preliminares aqui reportados suportam o uNAC como um indicador de progressão de disfunção tubular. A nossa abordagem mostra que a dinâmica dos Cis-*S*-conjugados está alterada ao longo da progressão da doença. Os resultados sugerem que esta dinâmica pode estar associada não só a mecanismos de adaptação, com aumentos na CisSSP e uNAC, mas também a mecanismos de progressão de doença que a cronicidade da lesão, caracterizado por alterações opostas nesta dinâmica. A translação destes resultados juntamente com o aprofundamento deste estudo pode levar à identificação de novos alvos terapêuticos para desacelerar ou parar a progressão da doença e para estabelecer estratégicas preventivas alcançadas pelo diagnóstico precoce. Além disso, a identificação de um novo marcador pode também ajudar a avaliar o sucesso das estratégias de prevenção e gestão.

Palavras-chave: biomarcadores; lesão renal aguda; lesão renal crónica; disfunção tubular; dissulfetos de cisteína; inflamação; mercapturatos de dissulfetos de cisteína; *N*-acetiltransferase 8; nefrotoxicidade; oxidação.

INTRODUCTION

INTRODUCTION

1. Kidney disease as one of the most important diseases of our time

It is estimated that 5-10 million people die annually from kidney disease which should be considered, right next to cancer, diabetes, cardiovascular disease and chronic respiratory disease, as one of the most important disease of our time (Luyckx, Tonelli and Stanifer, 2018). Acute insults to the kidney are common in hospital settings, usually developed from hemorrhage, sepsis, drug toxicity and use of a contrast agent (Feehally, 2016; Ozkok and Ozkok, 2017). On the other hand, chronic injury associated with diabetes, aging or hypertension, all growing concerns in the modern society, promotes progression to fibrosis (James, Hemmelgarn and Tonelli, 2010; Ortiz *et al.*, 2014). Other factors influencing this kind of injury include infectious diseases (e.g. human immunodeficiency virus (HIV)-infection), environmental pollution, exposure to pesticides, analgesic abuse, herbal medications, use of unregulated food additives and also genetic factors (Jha *et al.*, 2013).

The handicap for the prevention and management of kidney disease is the limited ability of the current markers of kidney function for an early diagnosis of injury progression. The identification of a non-invasive marker reflecting the underlying pathophysiologic mechanism of kidney disease will not only improve the current knowledge of kidney disease, but also assist on the identification of new therapeutic targets to treat and prevent the progression of kidney disease. A major concern in this context is the lack of markers of proximal tubular cell function and of drugs that are able to stop renal dysfunction.
Kidney injury can trigger both adaptive and maladaptive responses, with the early adaptive response often becoming maladaptive over time, leading to a progressive decline in the anatomic and functional integrity of the kidney (Bonventre, 2015).

The kidney is a highly differentiated organ, with nearly 30 different cell types that modulate complex physiologic processes, including endocrine function, blood pressure regulation, intra-glomerular hemodynamics, solute and water transport, acid-base balance and metabolic waste excretion (George and Neilson, 2015). The functional unit of the kidney is the nephron that is composed by: a) a glomerulus (that is encased by the Bowman's capsule) that is able to filter the blood; b) a tubule (divided into proximal tubule, loop of Henle and distal tubule) that, through sequential events of reabsorption and secretion, progressively forms urine and c) a collecting duct that carries the urine into a collecting system that will ultimately lead to the elimination of urine (Reilly, Bulger

and Kriz, 2007; Li and Wingert, 2013; George and Neilson, 2015). The kidney has an outer zone, commonly known as the cortex region, and an inner zone that is divided between the medullary and papillary regions (**Figure 1**). The majority of nephrons are found throughout the cortex, with glomeruli and proximal tubule located in the mid-to-outer cortex, while their tubule loops and the collecting duct system inhabit predominantly the inner zones of the medulla and the papilla (Li and Wingert, 2013; George and Neilson, 2015) (**Figure 1**).

In humans, nephrogenesis (i.e., the formation of nephrons) is ceased at 36 weeks of gestation, with an average value of 1 million nephrons formed in each healthy kidney (Bertram *et al.*, 2011). This fact has tremendous consequences, as renal disease is associated with a reduction on the functional nephrons (Bonventre, 2015).

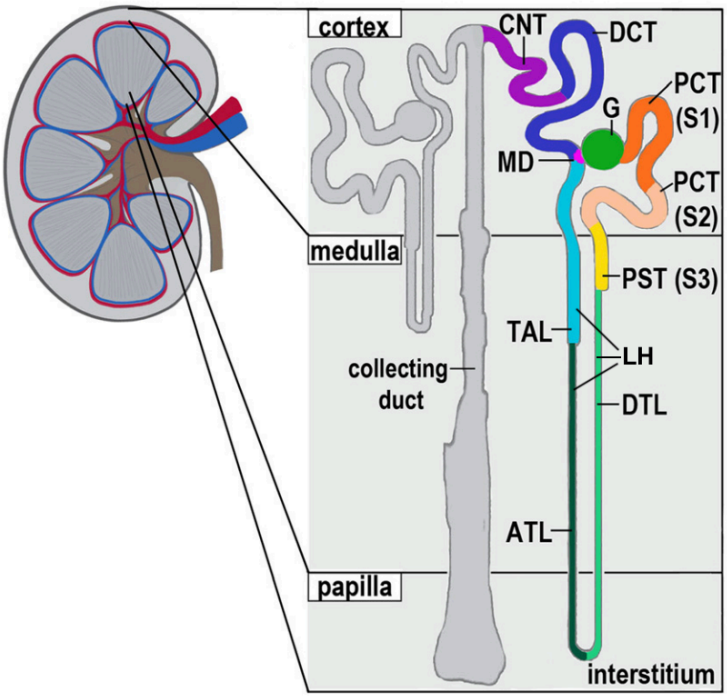

Figure 1 – Schematic representation of the kidney sections with details on the components of the nephron and their locations. The kidney is divided into cortex (outer zone), medulla and papilla (both comprising the renal inner zone) sections. As the functional unit of the kidney, the nephron is divided into glomerulus and a tubular and duct region. While both glomeruli and proximal tubule are majorly found in the cortical section, the tubule loops and the collecting duct are predominantly found in medullary and papillary zones. Adapted from Li and Wingert, 2013.
ATL: ascending thin limb; CNT: connecting tubule; DCT: distal convoluted tubule; DTL: descending thin limb; G: glomerulus; LH: loop of Henle; MD: macula densa; PCT: proximal convoluted tubule; PST: proximal straight tubule; S1: segment 1; S2: segment 2; S3: segment 3; TAL: thick ascending limb.

Kidney disease can either be classified into acute kidney injury (AKI) or chronic kidney disease (CKD). While AKI involves a rapid loss of kidney function from sudden injury (e.g. ischemia, toxin, sepsis) (Venkatachalam *et al.*, 2010; Bonventre and Yang, 2011),

CKD is understood as a temporal progressive loss of kidney function triggered by fibrosis and erosion of normal tissue (El Nahas and Bello, 2005). In fact, CKD is currently viewed as an increasing public health concern, contributing to the rising worldwide non-communicable disease burden (Jha *et al.*, 2013). Furthermore, CKD could culminate with organ failure, known as end-stage renal disease (ESRD or stage 5 CKD) (El Nahas and Bello, 2005; Schedl, 2007; Venkatachalam *et al.*, 2010; Bonventre and Yang, 2011; Bonventre, 2015). The progression to ESRD is a considerable socioeconomic burden, not only to the patients and their families but also to the healthcare system (Weiner, 2009). These consequences arise from the need for renal replacement therapy with dialysis and transplantation, with the concomitant intensive long-term care (Li and Wingert, 2013). The incidence of AKI has increased in the last two decades in parallel with an increase in ESRD (Leung, Tonelli and James, 2013), which in turn, has exceeded that expected upon prediction from CKD prevalence (Hsu *et al.*, 2004). As a consequence, the current knowledge is now formulating the hypothesis that not only cumulative episodes of AKI lead to CKD but also that preexisting CKD increases the risk of AKI (Hsu *et al.*, 2008; Leung, Tonelli and James, 2013).

1.1. Acute kidney injury (AKI)

AKI is a common complication among hospitalized patients. While the incidence of AKI in general ward has been reported to be 4.3% from community-acquired (due to volume depletion, adverse effects of medications and obstruction of the urinary tract) and 2.1% from hospital-acquired AKI (induced by sepsis, major surgical procedures, critical illness involving heart or liver failure and administration of intravenous iodinated contrast and nephrotoxic medication), this number rises to 58% in the setting of intensive care units (Wonnacott *et al.*, 2014; Hoste *et al.*, 2015; Waikar and Bonventre, 2015; Kashani *et al.*, 2017). Episodes of severe AKI often requires dialysis with a concomitant increase in the risk of development of ESRD. Clinical diagnosis of AKI encompasses an increase in serum creatinine (sCr) (increase of 0.3 mg/dL within 48 h or 1.5 times higher than baseline within 1 week), commonly associated with decreased urine volume (less than 0.5 mL/kg/h for 6 h) (KDIGO AKI Work Group, 2012; Waikar and Bonventre, 2015). Hence, AKI staging is defined by sCr and urine output (KDIGO AKI Work Group, 2012). AKI episodes can be derived from prerenal azotemia (associated with hypovolemia, decreased cardiac output and medications that interfere with renal autoregulatory

responses such as nonsteroidal anti-inflammatory drugs and inhibitors of angiotensin II), intrinsic renal parenchymal disease (induced by sepsis, ischemia and nephrotoxins of both endogenous and exogenous sources) and postrenal obstruction (triggered by bladder outlet obstruction, bilateral pelvoureteral obstruction or unilateral obstruction in case of a solitary functioning kidney) (KDIGO AKI Work Group, 2012; Waikar and Bonventre, 2015).

Importantly, drug-induced AKI is a serious matter frequently faced by clinicians (Perazella, 2009) and is reported in about 8 to 60% if hospital-acquired AKI (Schetz *et al.*, 2005). Nephrotoxic agents have the potential to promote injury in all kidney compartments, an effect that occurs due to the combination of patient's risk factors and the innate toxicity of this compounds. Therefore, drug-induced AKI will be the consequence of patient-specific, kidney-related and drug-associated factors, which combination can determine AKI, several tubulopathies, glomerular disease and CKD (Perazella and Luciano, 2015). Hence, recognizing these factors should be the first step to reduce nephrotoxicity. The nephrotoxic potential of several different therapeutic agents have been documented, including antimicrobial agents, chemotherapeutics, analgesics, among others (Perazella, 2005).

For instance, antibiotics such as gentamicin (G) (Kacew and Bergeron, 1990; Quiros *et al.*, 2010; Ferreira *et al.*, 2011; López-Novoa *et al.*, 2011) and the anticancer drug cisplatin (CISP) (Sánchez-González *et al.*, 2011; Sancho-Martínez *et al.*, 2012, 2018) are common causes of tubular toxicity. Researchers have developed different animal models of AKI not only to understand the pathophysiology of the onset of AKI but also to explore the drug-induced toxicity.

Still, there is an inability for approaching drug-induced kidney injury during pharmacological development; different urinary proteins have been proposed as kidney safety biomarkers but only in nonclinical studies (McDuffie, 2018). Moreover, as early assessment of drug-induced kidney injury by biomarker level changes is not yet available, histopathology changes currently remains the gold-standard for diagnosing kidney damage (Makris and Spanou, 2016). Emerging biomarkers should be combined with traditional markers and histopathology to enable early detection of damage in animal models.

1.2. Chronic kidney disease (CKD)

CKD affects about 10-15% of the worldwide population (Levin *et al.*, 2017) and is currently defined as abnormalities of kidney structure or function, present for more than 3 months, with implications for health (KDIGO CKD Work Group, 2013). Its classification is based on cause, estimated glomerular filtration rate (eGFR) (eGFR < 60 mL/min/1.73m^2) and albuminuria (albumin excretion ratio > 30 mg for 24 h urine collection or albumin-to-creatinine ratio – ACR > 30 mg/g of creatinine for spot first morning urine) categories (KDIGO CKD Work Group, 2013).

Factors that increase the risk of CKD include small gestation birth weight, childhood obesity, hypertension, diabetes mellitus, autoimmune disease, advanced age, African ancestry, family history of kidney disease, previous episode of AKI as well as the presence of proteinuria, abnormal urinary sediment or structural abnormalities of the urinary tract (Bargman and Skorecki, 2015). Nevertheless, the five most frequent causes of CKD are diabetic nephropathy, glomerulonephritis, hypertension-associated CKD (includes vascular and ischemic kidney disease and primary glomerular disease with associated hypertension), autosomal dominant polycystic kidney disease and other cystic and tubulointerstitial nephropathies (Bargman and Skorecki, 2015).

Stages of CKD are stratified as a way of predicting the risk of progression of CKD (**Figure 2**). While stages 1 and 2 are not usually associated with any symptoms (KDIGO CKD Work Group, 2013), the decline on glomerular filtration rate (GFR) progresses to stages 3 and 4 is linked with a more prominent clinical and laboratory complications of CKD. Among them, the most evident are anemia and its associated easy fatigability, decreased appetite leading to malnutrition, abnormalities in calcium, phosphorus, mineral-regulating hormones (calcitriol, parathyroid hormone and fibroblast growth factor 23) and sodium, potassium, water and acid-base homeostasis (KDIGO CKD Work Group, 2013; Bargman and Skorecki, 2015). Nevertheless, kidney failure is traditionally considered as the most serious outcome of CKD (KDIGO CKD Work Group, 2013).

The pathophysiology of CKD has been linked with two distinct mechanisms of damage, the initial ones, which are specific to the underlying etiology (e.g. genetically determined abnormalities in kidney development or integrity, immune complex deposition and inflammation in certain types of glomerulonephritis, or toxin exposure in certain diseases of the renal tubules and interstitium) and the ones associated to progression, involving hyperfiltration and hypertrophy of viable nephrons, that are a common consequence of

the long-term reduction of renal mass, irrespective of its etiology (Bargman and Skorecki, 2015).

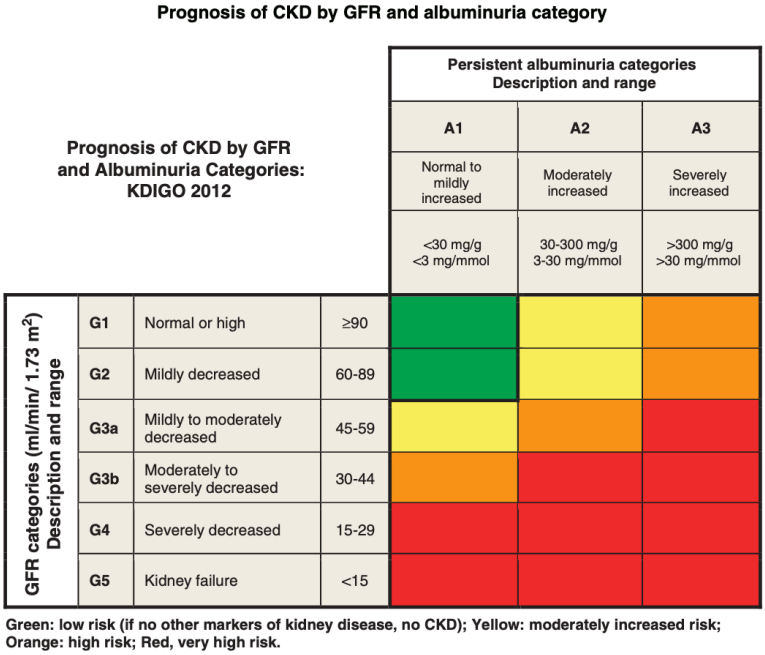

Figure 2 – Stages of CKD by Kidney Disease Improving Global Outcome (KDIGO). Staging of CKD is currently based on assessing both eGFR and 24h-albuminuria (24h urine collection) or ACR (spot first morning urine) (KDIGO CKD Work Group, 2013).
ACR: albumin-to-creatinine ratio; eGFR: estimated glomerular filtration rate

2. Current limitations on the detection and management of kidney disease

One of the major limitations on the detection and management of kidney disease is the unavailability of valid markers of tubular dysfunction, which limits the development of new drugs able to stop or revert disease progression. Given the complexity of disease processes and the multiple factors that affect progression over time, there is a great need to understand the pathophysiological mechanisms underlying the usual development of renal disease. As so, for the detection and management of kidney disease progression there is a need for non-invasive indicators that reflect the pathophysiologic mechanisms. The identification of biomarkers with this profile will not only improve the current knowledge of the complex condition that kidney disease is, but also increase the ability to predict and modulate response to therapy.

Traditionally, the assessment of kidney function is performed through eGFR based on demographic factors and sCr (Levey *et al.*, 2009) and, in a more unconventional way, using serum cystatin c (sCys C) alone or in combination with sCr (Inker *et al.*, 2012). The renal handling of creatinine (Cr) involves glomerular filtration and tubular secretion (Gutiérrez *et al.*, 2014). This last process becomes a serious issue since, as kidney function declines, tubular secretion of Cr increases in a proportional way to the decrease in its glomerular filtration, resulting in a significant overestimation of true GFR (Ferguson and Waikar, 2012). Moreover, as the end product of creatine, the majority of Cr is generated from muscle, meaning that Cr concentration is highly dependent on muscle mass (Perrone, Madias and Levey, 1992). Also, Cr production in patients with liver disease is decreased (Cocchetto, Tschanz and Bjornsson, 1983). As so, the use of sCr to asses kidney function in conditions associated with decreased lean body mass and an increased prevalence of liver disease should be performed with caution. Also, there is hard evidence showing that the progression of kidney disease can begin before the significant rise of sCr levels (Ferguson and Waikar, 2012). For instance, it has been shown that a rise in the levels of sCr does not occur until nearly 50% of nephrons are nonfunctional (Waikar, Betensky and Bonventre, 2009).

In contrast to Cr, all nucleated cells produce cystatin c (Cys C), which is freely filtered in the glomerulus and catabolized by tubular cells (Tenstad *et al.*, 1996). Cys C is not only affected by lean mass (Macdonald *et al.*, 2006) but also by the inflammatory marker C-reactive protein (Knight *et al.*, 2004).

The above-mentioned disadvantages of sCr and sCys C limits their use and have been boosting the investigation of newly accurate and precise markers of kidney dysfunction.

For instance, kidney injury molecule-l (KIM-1), an immunoglobulin superfamily cell-surface protein, is only upregulated on the surface of injured kidney epithelial cells (Ichimura *et al.*, 1998). In this scenario, the protein functions as a phosphatidylserine receptor, promoting the phagocytosis of apoptotic bodies and necrotic debris, hence transforming these cells into semiprofessional phagocytes (Ichimura *et al.*, 2008). As so, a role for KIM-1 in renal recovery and tubular regeneration has been proposed. Events of ischemia-reperfusion upregulates KIM-1, specifically present in proliferating dedifferentiated epithelial cells of the proximal tubule 48 hours after injury (Ichimura *et al.*, 1998). Additionally, an increase in urinary KIM-1 was also observed after renal injury induce by ischemia (Han *et al.*, 2002) and also by nephrotoxins including S-(1,1,2,2-

tetrafluoroethyl)-L-cysteine, folic acid, and CISP (Ichimura *et al.*, 2004). This increase seems to be related with the shedding of the extracellular component of KIM-1 (immunoglobulin and muccin domains) (Bailly *et al.*, 2002).

Another novel biomarker is neutrophil gelatinase associated lipocalin (NGAL), that can be considered as both an indicator of AKI and also a therapeutic agent that protects the kidney from ischemia. NGAL is a bacteriostatic agent with the ability to sequestrate iron-siderophores, preventing their uptake by bacterial pathogens (Flo *et al.*, 2004). The formation of this complex between NGAL and iron-siderophores has also been proposed to convert renal progenitors into epithelial tubules, hence inducing tubulogenesis in the metanephric mass (Yang *et al.*, 2002). Although with constitutive expression in neutrophils, inflammation triggers epithelial cells to express NGAL (Nielsen *et al.*, 1996; Cowland *et al.*, 2003). In fact, NGAL is highly upregulated at the transcript and proteins levels after ischemic or nephrotoxic kidney injury (Mishra *et al.*, 2003; Mishra, Mori, Ma, Kelly, Barasch, *et al.*, 2004). In urine, elevated NGAL is detectable as early as 3 hours after injury in animal models of renal ischemia-reperfusion (Mishra *et al.*, 2003). Nevertheless, in the setting of cardiopulmonary bypass-associated AKI, it only took 2 hours to observe the increase in both plasma and urine NGAL (Mishra *et al.*, 2005). The potential use of NGAL as a therapeutic agent is link with its canonical function previously mentioned. Administration of iron-siderophore-loaded NGAL was shown to protect the kidney before, during or even after ischemia-reperfusion injury (Mishra, Mori, Ma, Kelly, Yang, *et al.*, 2004; Mori *et al.*, 2005).

The proinflammatory interleukin 18 (IL-18) is also on the role for a biomarker of AKI, as its renal levels increase in response to different injury stimulus including ischemia-reperfusion (Melnikov *et al.*, 2001) as well as administration of glycerol (Homsi, Janino and De Faria, 2006) and CISP (Faubel *et al.*, 2007).

In the clinical setting, several biomarkers were studied for the early detection of AKI, before the falling of GFR (Vaidya *et al.*, 2008; Soto and Devarajan, 2016). Recently, urinary KIM-1, Cys C and NGAL were shown to predict the nephrotoxicity of platin-based drugs earlier than sCr (Abdelsalam *et al.*, 2018; George, Joy and Aleksunes, 2018). Furthermore, KIM-1 and NGAL are good markers of acute and chronic tubular injury associated with aminoglycosides exposure (McWilliam *et al.*, 2018).

There are many more putative biomarkers of kidney dysfunction that have been described, and several literature reviews have been recently published in general (Kotani, Kimura

and Gugliucci, 2011; Alge and Arthur, 2015; Klein *et al.*, 2016; Tan, Yap and Qian, 2016; Rysz *et al.*, 2017), hence confirming the pertinence of this issue. Nevertheless, there are still gaps in the current knowledge of kidney disease. The translation of the results obtained in animal models to clinical studies is not always linear and from the wide list of new discovered biomarkers that are reported on a regular basis, very few of them reach the clinical setting (Yerramilli *et al.*, 2016).

In fact, we have evaluated the performance of several biomarkers that were described in literature (Campos, Ortiz and Soto, 2016), including klotho and paraoxonase-1, for an HIV-infected population and no direct associations were obtained with kidney dysfunction in those patients (Dias, Casimiro, *et al.*, 2015; Dias, Maia, *et al.*, 2015; Campos *et al.*, 2016).

In this context, it is important to have into account the value of the proximal tubule as relevant player in kidney injury. In fact, evidence has been recently given that the proximal tubule is the primary sensor and effector in the progression of CKD as well as AKI (Chevalier, 2016). This specific region of the nephron is packed with mitochondria and highly dependent on oxidative phosphorylation (Simmons, Bogusky and Humes, 1980; Basile, Anderson and Sutton, 2012; Chevalier, 2016), which in turn makes the proximal tubule particularly vulnerable to oxidative injury. Specifically, recurrent tubular injury leads to a pattern of CKD in humans that is associated with tubular atrophy, interstitial chronic inflammation and fibrosis, vascular rarefaction and glomerulosclerosis (Bonventre, 2015). These facts suggest that looking into specific metabolic pathways of the proximal tubular cells could be a strategy for the prevention and management of kidney disease.

Having this into account and together with the unsuccessful outcomes on the study of literature markers, we moved on to investigate a new marker. We developed a concept supported by the team experience in mechanisms of drug toxicity related to drug metabolism and we got into a predominant detoxification pathway of proximal tubular cells that was supported by association studies (Juhanson *et al.*, 2008; Chambers *et al.*, 2010; Köttgen *et al.*, 2010; Tin *et al.*, 2013), the mercapturate pathway.

3. The mercapturate pathway is a hallmark of proximal tubular cell function

The mercapturate pathway has been associated to kidney function and is mainly expressed in renal proximal tubular cells (Chambers *et al.*, 2010; Datta *et al.*, 2010; De Carvalho *et al.*, 2011), predominantly in cortical regions (Chambers *et al.*, 2010). The mercapturate pathway has been described as a metabolic detoxification circuitry for electrophilic species generated under inflammatory and oxidative conditions (Habig, Pabst and Jakoby, 1974) (**Figure 3**).

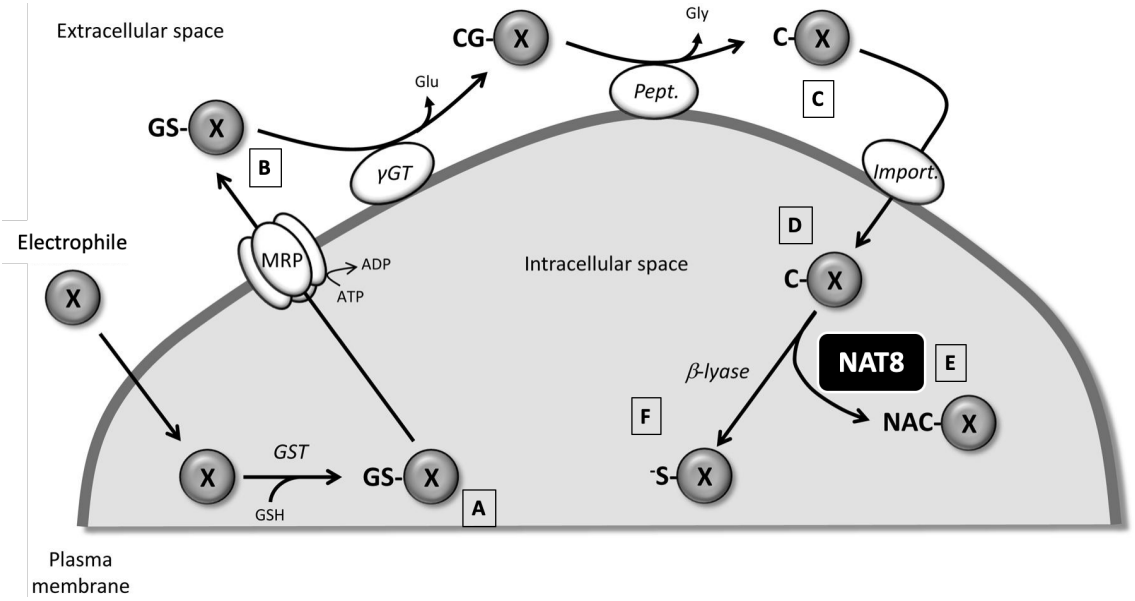

Figure 3 – The mercapturate pathway in proximal tubular cells. Upon conjugation of the electrophile with GSH (**A**), the conjugate is excreted from cells for further degradation (**B**). Extracellularly, glutathione-*S*-conjugates are catabolized in cysteine-glycine-*S*-conjugates by GGT and cysteine-*S*-conjugates by cysteinyl-glycine dipeptidase or aminopeptidase-M (**C**). These final conjugates are able to enter the proximal tubular cell (**D**) and suffer acetylation by NAT8 **(E),** being eliminated in urine. Alternatively, cysteine-*S*-conjugates might also undergo β-elimination through β-lyase activity, forming reactive intermediates with nephrotoxic features (**F**). Adapted from (Ramsay and Dilda, 2014). γGT: gamma-glutamyltransferase; CG-X: cysteine-glycine-*S*-conjugate; C-X: cysteine-*S*-conjugate; Glu: glutamate; Gly: glycine; GSH: glutathione; GST: glutathione-*S*-transferase; GS-X: glutathione-*S*-conjugate; MRP: multi-drug resistance association protein; NAC-X: mercapturate; NAT8: *N*-acetyltransferase 8; Pept: cysteinyl-glycine dipeptidase or aminopeptidase-M; $^{-}$S-X: highly reactive intermediate; X – electrophile.

The enzymes of the mercapturate pathway have endogenous functions in the kidney and may have evolved to detoxify endogenous reactive toxic intermediates rather than only xenobiotics (Bernstrom and Hammarstrom, 1986; Huber *et al.*, 1990; Deol, 2015). Endogenous compounds undergoing the mercapturate pathway include cysteinyl-leukotrienes (CysLTs) (Veiga-da-Cunha *et al.*, 2010), glucose (Szwergold, 2006),

catecholamines (Magnay *et al.*, 2001) and lipid peroxidation products (Ntimbane *et al.*, 2008; Feroe, Attanasio and Scinicariello, 2016), whereas paracetamol (Jian *et al.*, 2009) and CISP (Townsend *et al.*, 2003) are examples of xenobiotics.

Any cell under inflammatory or oxidative conditions can produce glutathione (GSH) conjugates upon the intracellular conjugation of GSH with an electrophile, generating covalent glutathione-*S*-conjugates (GSH-*S*-conjugates), usually mediated by glutathione-*S*-transferase (GST) (Ballatori *et al.*, 2009) (**Figure 3-A**), which can be of both endogenous (e.g. disulfides: glutathione-disulfide GSSX) (Wang and Ballatori, 1998) and exogenous (e.g. CISP: glutathione-cisplatin conjugate GSH-CISP) (Townsend *et al.*, 2003) sources. However, as cells are not able to catabolize these conjugates, they are excreted and degraded by peripheral tissues that express gamma-glutamyltransferase (GGT) in the extracellular border of cell membrane (**Figure 3-B**). This is the first enzyme of the mercapturate pathway. Extracellularly, GSH-*S*-conjugates are catabolized in cysteine-glycine-*S*-conjugates (CysGly-*S*-conjugates) by GGT and cysteine-*S*-conjugates (Cys-*S*-conjugates) by cysteinyl-glycine dipeptidase or aminopeptidase-M, all enzymes that are expressed at the brush border of tubular cells (Hughey *et al.*, 1978; Griffith, 1981; Hanigan, 1998) (**Figure 3-C**). Afterwards, Cys-*S*-conjugates, which can be either cysteine-disulfides (CysSSX, eg. cysteine-homocysteine disulfide, CysSSHCys) or not (e.g. cysteine-cisplatin conjugate, Cys-CISP), enter the tubular cell via various transporters including organic anion transport polypeptides and cystine/cysteine importers (Commandeur, Stijntjes and Vermeulen, 1995; Hinchman, Rebbeor and Ballatori, 1998; Garnier *et al.*, 2014) (**Figure 3-D**). At this stage and under normal conditions, only CysSSX would be reduced, yielding free cysteine (Cys), which becomes available to perform its several physiological actions (Bannai and Tateishi, 1986). On the other hand, other Cys-*S*-conjugates including Cys-CISP are detoxified through the acetylation by the activity of the enzyme *N*-acetyltransferase 8 (NAT8) (**Figure 3-E**), forming a mercapturate generally more polar and more water soluble than the parental compound, that can be eliminated in urine (majorly) or bile (minor) (Ballatori *et al.*, 2009; Veiga-da-Cunha *et al.*, 2010). The later might undergo enterohepatic circulation by the effect of intestinal microflora (Guhlmann, Hagmann and Keppler, 1987).

The acetylation of Cys-*S*-conjugates by NAT8 is the final step of the mercapturate pathway. Although the remaining enzymes are also expressed in liver small intestine, lung, brain, spleen and pancreas, enabling the formation of Cys-*S*-conjugates outside the kidney (Commandeur, Stijntjes and Vermeulen, 1995), the expression of NAT8 is almost

and exclusively limited to the proximal tubular cells (Chambers *et al.*, 2010; Veiga-da-Cunha *et al.*, 2010). Also, the pathway might currently have an underestimated importance, as shown by the recent reported nephroprotective effects of NAT8 (Juhanson *et al.*, 2008; Chambers *et al.*, 2010; Köttgen *et al.*, 2010; Tin *et al.*, 2013).

The precursors of Cys-*S*-conjugates have a rapid extracellular metabolism through this pathway, resulting in shorter half-lives than their Cys-*S*-conjugates, which are more stable and readily detected in biologic fluids (Kanaoka and Boyce, 2014). Also, mercapturates of Cys-*S*-conjugates are very well known in pharmacology/toxicology field since their biomonitoring in urine have for long been used as biomarkers of exposure to xeno-electrophiles (Mathias and Bhymer, 2016).

The mercapturate pathway has also been studied as a way for target delivering prodrugs to drug-resistant tumors of kidney (Ramsay and Dilda, 2014). Specifically, both GST and GGT are highly expressed in cancer cells and represents an important factor in the appearance of a more aggressive and resistant phenotype. Targeting tumors with GST or GGT-activated drugs has been proven to be a successful strategy in driving the activation of cytotoxic compounds within the tumors (Sequist *et al.*, 2009; Vergote *et al.*, 2010; Horsley *et al.*, 2013).

Cys-*S*-conjugates in the proximal tubular cell might also undergo *β*-elimination through *β*-lyase activity, forming reactive intermediates that have been strongly related to kidney injury (Möller-Hartmann and Siegers, 1991; Townsend *et al.*, 2003; Cooper and Pinto, 2006; Lash, 2007; Cooper, Pinto, *et al.*, 2008; Cooper, Younis, *et al.*, 2008; Cooper *et al.*, 2011) (**Figure 3-F**). *β*-lyases catalyze the cleavage of Cys-*S*-conjugates into a potentially toxic thiol (sulfur)-containing fragment and dehydroalanine, which very rapidly hydrolyzes to ammonia and pyruvate (Commandeur, Stijntjes and Vermeulen, 1995). In rat, *β*-lyase is present mainly in cytosol and, to a lesser extent, in mitochondria. Differently, in man, a considerable *β*-lyase activity was found in microsomes. Studies performed in rat have shown that this activity is absent in the glomeruli and distal tubule. Regarding distribution in the proximal tubule, there are conflicting data on the segments involved (Jones *et al.*, 1988; MacFarlane *et al.*, 1989). The involvement of *β*-lyase-mediated bioactivation of Cys-*S*-conjugates in nephrotoxicity has been demonstrated for several toxicants (Commandeur, Stijntjes and Vermeulen, 1995; Cristofori, Sauer and Trevisan, 2015).

In accordance, a nephroprotective role has been attributed to the tubular enzyme NAT8 that promotes the urinary elimination of these compounds (Veiga-da-Cunha *et al.*, 2010), counteracting *β*-lyase activity, avoiding their reabsorption into the bloodstream and promotion of systemic metabolic-inflammation. Evidence supporting that NAT8 is nephroprotective came majorly from association studies (Juhanson *et al.*, 2008; Chambers *et al.*, 2010; Köttgen *et al.*, 2010; Tin *et al.*, 2013). The study of Juhanson and colleagues (2008) (Juhanson *et al.*, 2008) included 137 controls and 157 hypertensive patients with and without nephropathy and identified single nucleotide polymorphisms (SNPs) in the promoter region of NAT8 associated with systolic blood pressure and renal function (eGFR). In particular, minor alleles of NAT8 (of the same SNP) were found to be related with lower blood pressure and higher eGFR. The authors hypothesized that this effect was explained by the reduced susceptibility of the minor alleles to transcriptional suppression, hence guarantying availability of NAT8. In 2010, Chambers and co-authors (Chambers *et al.*, 2010) reported an association between common genetic variations in NAT8 gene and Cr, Cys C, eGFR and CKD in a population of 16,626 Europeans. On the same year, the CKDGen consortium performed a meta-analysis of genome-wide association data in 67,093 Caucasian individuals and found that NAT8 was a susceptibility locus for reduced renal function, estimated by eGFR obtained separately with both Cr and Cys C and also CKD (Köttgen *et al.*, 2010). Moreover, NAT8 was the only kidney locus identified that was associated with eGFR in all three different genome-wide scans performed in 9049 European Americans (Tin *et al.*, 2013).

More recently, the role of NAT8 has been investigated in regenerative processes of the kidney tubular cell (Omata *et al.*, 2016). Omata and co-authors (2016) found a reduction of NAT8 transcript levels upon exposure to transforming growth factor-1 (TGF-β1), using an in vitro model of dedifferentiation/re-epithelization of human proximal tubular cells. This cytokine promoted cell dedifferentiation, an event initiator of repair process in early stages of renal injury. TGF-β1 withdrawing after dedifferentiation did not prevented re-epithelization in NAT8 knock-down cells. The authors suggested that the recovery process may be independent of the activity of NAT8. In addition, the difficulty in developing NAT8 knockout rats (Fu *et al.*, 2014) and absence of tools to pharmacologically address NAT8 hinders to get hard evidence on the nephroprotective role of this enzyme. Nevertheless, the effect of probenecid, an inhibitor of the peritubular transport of organic anions, was described to impact NAT8 activity. The enzymatic activity of partially purified NAT8 from pig kidney cortex-derived microsomes decreased 40% and 61% in the presence of 2 or 5 mM probenecid, respectively (Aigner *et al.*, 1996). As so, this

drug, in addition to the inhibitor effect on mercapturic acid transport, might also inhibit the acetylation of Cys-*S*-conjugates. Nevertheless, this study is limited by the purification technique used which led to a 45% loss of enzymatic activity. Recently, we have investigated the effects of mesenchymal stromal cell conditioned medium (MSC-CM) on tubular epithelial cells exposed to TGF-β1 (dedifferentiation) and after TGF-β1 withdrawal (re-epithelization) (Grácio, 2017; Grácio *et al.*, 2018). We have observed that prolonged injury was associated with a decrease in NAT8 expression. The re-epithelization was biphasic with a decrease of NAT8 followed by a late rescue. When MSC-CM was used in the absence of a harmful stimulus, it promoted re-epithelization, which was not related with increase in NAT8 expression. Contrastingly, MSC-CM addition was associated with marked recovery of NAT8 transcription under continued TGF-β1 exposure. To the best of our knowledge, this is the first report of the paracrine effects of human mesenchymal stromal cells (MSCs) on NAT8 in the kidney and the relevance of NAT8 to maintain regenerative potential when tubular epithelial cells undergo dedifferentiation (Grácio, 2017; Grácio *et al.*, 2018).

The above-mentioned facts support that the mercapturate pathways is a hallmark of proximal tubular cell function and that NAT8 activity is nephroprotective plausibly by avoiding systemic accumulation of Cys-*S*-conjugates.

4. Cysteine-*S*-conjugates are features of inflammatory conditions

Cys-*S*-conjugates have primarily vascular and hemodynamic properties (Lewis and Austen, 1984), being potent vasoconstrictors (Rosenthal and Pace-Asciak, 1983; Badr, Brenner and Ichikawa, 1987; Shastri *et al.*, 2001) with ability to enhance the permeability of the postcapillary venules (Leng *et al.*, 1988). Therefore, the elimination of these conjugates could have nephroprotective consequences. It has been shown that Cys-*S*-conjugates are involved in glucose-stimulated insulin secretion (Guo *et al.*, 2018), and have pro-inflammatory (Magnay *et al.*, 2001), cytotoxic (Townsend *et al.*, 2003; Stern, Bruno, Hennig, *et al.*, 2005; Stern, Bruno, Horton, *et al.*, 2005; Dvash *et al.*, 2015) and immunogenic (Salauze *et al.*, 2005) properties, all processes potentially involved in the development of kidney dysfunction.

These Cys-*S*-conjugates seem to have significantly higher half-life than the precursors and are the plausible ones responsible for the biological effects (Szwergold, 2006; Kanaoka and Boyce, 2014). The effects of Cys-*S*-conjugates have been underestimated,

probably because the mercapturate pathway has been classically considered a detoxification route for xenobiotics. Although, it is known that, for instance, Cys-CISP is more toxic to tubular cells than CISP (Townsend *et al.*, 2003). Another example, the Cys-*S*-conjugate of paracetamol is related to its nephrotoxicity, but not to its hepatotoxicity (Stern, Bruno, Hennig, *et al.*, 2005). On the other hand, treatment of cystinuria patients with tiopronin leads to the formation of a soluble mixed disulfide between the drug and Cys and was shown to reduce both the urinary excretion of cystine (the oxidized form of Cys, cystine, CysSSCys) and the formation of renal cystine stones due to the low solubility of Cys, common features of this condition (Lindell, Denneberg and Jeppsson, 1995).

Cys-*S*-conjugates can be categorized according with the formation of a sulfur-carbon (S-C) or a disulfide (S-S) bond between the sulfhydryl group (SH) of Cys and the compound that is being conjugated, into thioethers (CysSCX) (**Figure 4A**) or CysSSX (**Figure 4B**), respectively. For simplification purposes, the thioethers will from now on be called Cys-*S*-conjugates.

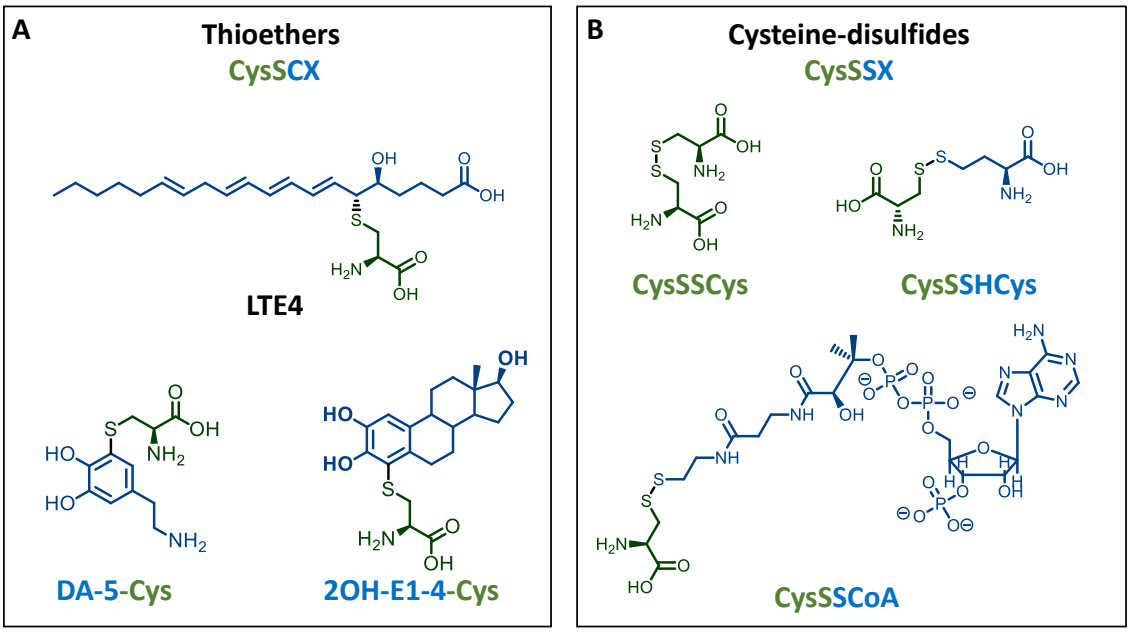

Figure 4 – Cysteine-*S*-conjugates categorized in thioethers and cysteine disulfides. According with the type of bond formed between the sulfhydryl of Cys and the compound that is being conjugated, cysteine-*S*-conjugates can either be thioethers (with a sulfur-carbon bond) (**A**) or cysteine disulfides (with a disulfide bond) (**B**).
2OH-E1-4-Cys: cysteine conjugate of 2-hydroxyestrone; CysSCX: thioether cysteine-*S*-conjugates; CysSSCoA: cysteine-coenzyme A disulfide; CysSSCys: cystine; CysSSHCys: cysteine-homocysteine disulfide; CysSSX: cysteine-disulfides; DA-5-Cys: cysteine-dopamine conjugate; LTE: leukotriene E4.

4.1. Thioether cysteine-*S*-conjugates: relevance for kidney disease and other inflammatory conditions

The formation of CysLTs is the best described example among endogenous thioether compounds generated through the mercapturate pathway (Wang and Ballatori, 1998; Veiga-da-Cunha *et al.*, 2010). CysLTs are products of arachidonic acid metabolism and key mediators of inflammatory conditions (Funk, 2001; Haeggström and Funk, 2011; Di Gennaro and Haeggström, 2012), responsible for enhancing the conversion of arachidonic acid into the short-lived leukotriene A4 (LTA4) (Samuelsson *et al.*, 1987). LTA4 is further conjugated with GSH to yield a GSH-*S*-conjugate (leukotriene C4, LTC4) that is expelled from cells. Extracellular LTC4 undergo a two-step catabolic process originating respectively the CysGly-*S*-conjugate (leukotriene D4, LTD4) and Cys-*S*-conjugate (leukotriene E4, LTE4) through the mercapturate pathway (Haeggström and Funk, 2011; Di Gennaro and Haeggström, 2012). These compounds are generally termed CysLTs, although these denominations fully suits only for LTE4, which has the longer half-life (Kanaoka and Boyce, 2014).

The synthesis and release of CysLTs by the kidney have been described (Petric, Nicholson and Ford-Hutchinson, 1995; Dvash *et al.*, 2015). The role of leukotrienes in kidney diseases was recently reviewed (Rubinstein and Dvash, 2018) and was demonstrated that they are able to reduce renal blood flow and GFR by triggering vasoconstriction. On the other hand, they can promote immune and non-immune-mediated kidney damage and oxidative intracellular stress (Dvash *et al.*, 2015). The selective inhibition of CysLTs is being investigated in several models of kidney disease (Rubinstein and Dvash, 2018), but their nephroprotection ability in man is still unknown.

Under inflammatory conditions, the temporal changes in urinary CysLTs elimination were paralleled with their biosynthesis enzyme activity in renal cortical microsomes (Petric and Ford-Hutchinson, 1994). Urinary CysLTs levels increased in initial stages and decreased along kidney disease progression, supporting an early role for CysLTs in the development of subsequent functional changes (Petric and Ford-Hutchinson, 1994). CysLTs were also reported to promote angiotensin II release, increase mean arterial pressure, decrease cardiac output, renal blood flow and eGFR (Badr *et al.*, 1984; Assem and Abdullah, 1987). Additionally, several studies showed the association of CysLTs biosynthesis with drug-induced nephrotoxicity (Rubinstein and Dvash, 2018). In an *in vitro* approach, aristolochic acid I-induced tubular injury was associated with CysLTs

release, via extracellular-signal-regulated kinase (ERK) pathway activation (Yang *et al.*, 2011). Additionally, diabetic kidney disease (DKD) was associated with lower urinary LTE4 concentrations (Rafnsson and Bäck, 2013). A multivariate analysis revealed that only eGFR was an independent predictor of urinary LTE4 concentrations. Currently there is no evidence to support if this implicates a role for circulating LTE4 in its own urinary excretion, a decrease in its renal formation or an increase in its elimination as a mercapturate (*N*-acetyl-LTE4) rather than in the LTE4 form.

Even though, several aspects on CysLTs are missing such as their synthesis and mechanism of action in immune and non-immune-mediated kidney damage. Also, the receptor responsible for LTE4 effects is still to be clarified (Thompson-Souza, Gropillo and Neves, 2017), although evidence from one study has suggested GPR99 as a new receptor sensitive to LTE4 (Kanaoka, Maekawa and Austen, 2013). Moreover, the methodology employed for the quantification of the mercapturate pathway-derived *S*-conjugates should allow the discrimination between GSH-*S*-conjugates, Cys-*S*-conjugates and mercapturates in serum and urine and their association with kidney disease progression.

Changes in the levels of several thioether endogenous Cys-*S*-conjugates have been reported in other inflammatory conditions rather than kidney disease. **Table 1** summarizes the clinical studies that evaluated the levels of specific Cys-*S*-conjugates, their associations with disease and factors that influenced them. In this literature review, we also included the results obtained for the GSH-*S*- and *N*-acetylcysteine- (NAC)-Cys-*S*-conjugates, due to their upstream and downstream connection with Cys-*S*-conjugates in the mercapturate pathway.

For instance, increases in LDT4 and LTE4 were observed in exhaled breath condensate of patients with pneumoconiosis derived from asbestos and silica exposure (Pelclova *et al.*, 2012). Higher levels of CysLTs in exhaled breath condensate were detected in patients with more severe radiological sign of asbestosis in comparison with mild asbestosis. Interestingly, urine LTD4 and LTE4 correlated positively with kidney failure in silicosis patients (Pelclova *et al.*, 2012). The value of quantification of CysLTs in saliva as an alternative diagnostic strategy in aspirin-intolerant asthma has been previously described (Ono *et al.*, 2011). Although CysLTs increased in this fluid in comparison with aspirin-tolerant asthma and healthy subjects, only the increase in urinary LTE4 in these patients was associated with severe aspirin-intolerant asthma (Ono *et al.*, 2011). The role of

CysLTs has also been investigated in autistic children, together with 8-isoprostane (Qasem, Al-Ayadhi and El-Ansary, 2016), a sensitive indicator of bioactive products of lipid peroxidation and oxidative stress (Janicka *et al.*, 2010). The authors proposed of both CysLTs and 8-isoprostane as markers of early recognition of autistic patients through sensory deficits phenotypes, suggesting that the quantification of this markers might facilitate early intervention (Qasem, Al-Ayadhi and El-Ansary, 2016). On another issue, the release of CysLTs in urine was assessed in patients suffering from spontaneous intracerebral hemorrhage, and correlated positively with hematoma volume (Winking *et al.*, 1998). The effect of hematoma removal in the release of CysLTs was also assessed by diving the patients in two different groups of treatment, one with surgery and the other with conservative treatment. Differences in urinary CysLTs were only found for the surgically treated patients, who presented lower levels 5 days after surgery in comparison with the concentration detected prior to the surgery (Winking *et al.*, 1998). An increase in both urine and plasma CysLTs during cardiac surgery with cardiopulmonary bypass was observed, and was greater in patients with moderate-to-severe chronic obstructive pulmonary disease than patients without the condition (de Prost *et al.*, 2011). This increase may be related with the higher lung and airway production of CysLTs and neutrophil activation in chronic obstructive pulmonary disease patients. CysLTs were also found to be increased in gingival crevicular fluid in periodontitis conditions and also in subjects with atherosclerotic plaques, regardless of periodontal status (Bäck *et al.*, 2007). Moreover, Celik and collaborators assessed the effect of smoking in the exhaled breath condensate levels of LTE4 and LTD4 in asthmatic patients (Celik *et al.*, 2013). LTE4 levels were increased in both asthmatic groups in relation to control (CTL) non-smoking group, whereas LTD4 was only increased in asthmatic smokers, suggesting that CysLTs synthesis increase in smoking asthmatics. The authors also speculated on the importance of adding leukotriene receptor antagonists in smoking asthmatics as a blocker of the effects of LTD4 (Celik *et al.*, 2013).

On the other hand, urinary LTE4 levels were also increased in patients admitted with acute chest pain derived from acute myocardial infarction and unstable angina (Carry *et al.*, 1992), in coronary artery disease before and after coronary artery bypass surgery (Allen *et al.*, 1993). Furthermore, a recent work by Gautier-Veyret and co-authors reported that intermittent hypoxia (IH) is an inducer of CysLTs pathway activation and contributes to the obstructive sleep apnea (OSA)-induced atherogenesis (Gautier-Veyret *et al.*, 2018). In this study, history of cardiovascular event, age and severity of hypoxia

influenced independently the levels of urine LTE4, which were increased in OSA-cardiovascular event free patients. Urinary LTE4 was also associated with intima-media thickness, suggesting the activation of CysLTs pathway as a driver of vascular remodeling in OSA. Additionally, they showed that pharmacological blockade of cysteinyl leukotriene 1 receptor (CysLT1) in mice prevented IH-induced atherogenesis, hence representing a new therapeutic target for reducing cardiovascular risk (Gautier-Veyret *et al.*, 2018). Similarly, increased elimination of LTE4 in urine was identified in OSA in relation to obesity, and to a lesser extent, hypoxia severity (Stanke-Labesque *et al.*, 2009). Episodes of acute asthma exacerbations were also associated with increases urinary elimination of LTE4 (Green *et al.*, 2004). On the other hand, the increased urinary excretion of LTE4 has been associated with diabetes (Hardy *et al.*, 2005; Boizel *et al.*, 2010), suggesting that hyperglycemia activates arachidonic acid metabolism and consequent CysLTs formation. Intensive glycemic control is able to reduce its elimination in patients with type 1 diabetes, although no changes were observed in type 2 diabetes (Hardy *et al.*, 2005; Boizel *et al.*, 2010).

Besides CysLTs, there are also reports with altered levels of Cys-S-conjugates of catechols. One example is the case of 5-*S*-Cys-dopa, formed by the rapid binding of dopaquinone, a highly reactive molecule, to Cys. Oxidation of 5-*S*-Cys-dopa leads to production of pheomelanin, a yellow to reddish melanin, although a significant portion of 5-*S*-Cys-dopa leaks into the bloodstream and has been associated with the progression of melanoma (Wakamatsu *et al.*, 2002). For instance, increases in serum 5-*S*-Cys-dopa have been reported in patients with melanoma and associated with poor prognosis and shorter survival times (Wimmer *et al.*, 1997; Banfalvi *et al.*, 2000; Wakamatsu *et al.*, 2002; Sato *et al.*, 2003; Umemura *et al.*, 2017). Additionally, immunochemotherapy has been shown to decrease 5-*S*-Cys-dopa levels in serum with concomitant longer survival times (Wimmer *et al.*, 1997).

Cys-*S*-conjugates of catechols have also been reported in neurological conditions. For instance, conjugates of both Cys and GSH with the catechols L-3,4-dihydroxyphenylalanine, dopamine and 3,4-dihydroxyphenylacetic acid were found in postmortem brain samples of Parkinson's disease patients (Spencer *et al.*, 1998). Specifically, the authors found increased concentrations of the 5-*S*-Cys-conjugates of the three catechols in substantia nigra and substantia innominata which suggest acceleration of L-3,4-dihydroxyphenylalanine/dopamine oxidation occurs in Parkinson's disease. Nevertheless, as all patients were under L-3,4-dihydroxyphenylalanine treatment, this

suggestion warrants further elucidation in patients without L-3,4-dihydroxyphenylalanine treatment before effectively stating that this is a primary feature of the disease (Spencer *et al.*, 1998). The 5-*S*-Cys conjugates of these catechols had been previously studied in three brain sections, namely substantia nigra, putamen and caudate nucleus from individuals with or without neurological disorders (Fornstedt *et al.*, 1989). In this report, the samples were divided according with macro- and microscopically judged degree of depigmentation and neuronal loss within the substantia nigra. The main findings of this work were that the levels of the catechols decreased with the degree of depigmentation and degeneration. Additionally, while no differences were found the levels of their Cys-*S*-conjugates, the authors observed an increase in the ratio of Cys-catechol by catecholamine concentration in the more depigmented and degenerated substantia nigra group, except for the dopamine ratio in putamen (Fornstedt *et al.*, 1989). The authors proposed that depigmentation and degeneration of dopaminergic substantia nigra neurons seem to correlate with enhanced rates of autooxidation, possibly due to an impaired antioxidant capacity.

On the other, the levels of 5-*S*-Cys-dopamine were similar in cerebrospinal fluid samples of control individuals and synucleinopathy patients with both parkinsonian (Parkinson's disease and parkinsonian multiple system atrophy) and no parkinsonian components (pure autonomic failure). Nevertheless, the levels of 3,4-dihydroxyphenylacetic acid were decreased only in Parkinson's disease and parkinsonian multiple system atrophy, with a consequent increase by 2-fold in 5-*S*-Cys-dopamine/3,4-dihydroxyphenylacetic acid ratio in these patients (Goldstein *et al.*, 2016). The authors were not able to identify factors that could cause this difference. However, evidence from previous works suggested that this might happen due to decreased antioxidant capacity (since it would shift the balance from catechols to catecholquinones and finally to Cys-catechol products) (Carlsson and Fornstedt, 1991) as well as decreased activity of aldehyde dehydrogenase (the enzyme responsible for the formation of 3,4-dihydroxyphenylacetic acid), which has been reported in both Parkinson's disease (Goldstein *et al.*, 2013) and parkinsonian multiple system atrophy (Goldstein *et al.*, 2015) conditions. In similarity, a decrease in cerebrospinal fluid homovanillic acid, the ultimate metabolite of dopamine, was found in Parkinson's disease patients 5 days after chronic L-3,4-dihydroxyphenylalanine therapy withdrawal, that was associated with an increase in the ratio of 5-*S*-Cys-Dopamine/ homovanillic acid (Cheng *et al.*, 1996). The authors hypothesized that the translocation

of GSH or Cys into neuromelanin-pigmented dopaminergic cell bodies in the substantia nigra might represent an early event in the pathogenesis of Parkinson's disease.

Catechol estrogens, namely 2- and 4-hydroxyestrone (or estradiol) can also conjugate with GSH, Cys and *N*-acetylcysteine (NAC) and their urinary levels were found to be increased in healthy subjects relatively to patients with breast cancer (Gaikwad *et al.*, 2008; Gaikwad, Yang, Pruthi, *et al.*, 2009), non-Hodgkin lymphoma (Gaikwad, Yang, Weisenburger, *et al.*, 2009) and Parkinson's disease (Gaikwad *et al.*, 2011). Additionally, the ratio of depurinating estrogen deoxyribonucleic acid (DNA) adducts by estrogen metabolites and conjugates (where the conjugates with GSH, Cys and NAC were included) is higher in cases of thyroid and ovarian cancer in comparison with healthy individuals (Zahid *et al.*, 2013, 2014).

Interestingly, glucose can also generate cysteine-*S*-conjugates that are far more stable than glucose-GSH. In specific, higher urinary levels of glucose-Cys were detected in patients with diabetes (Szwergold, 2006).

Hence, endogenous thioether Cys-*S*-conjugates are associated with innumerous and different inflammatory chronic conditions. Nevertheless, these compounds have in common the detoxification by the proximal tubular cells. That might motivate a tubulocentric perspective for multiple inflammatory conditions, which has been performed in the current year (Gonçalves-Dias *et al.*, 2019).

4.2. Cysteine-disulfide conjugates and disulfide stress: the kidney as a primordial organ for Cys accumulation and oxidation

The Cys-residue of the strong antioxidant GSH is the most abundant small-molecule thiol in cells whereas extracellularly, Cys is predominantly found in its free oxidized form (cystine) (Rossi et al., 2009). In liver, the majority of Cys is rapidly incorporated into GSH which is then exported (Lu, 2009). GSH is hence distributed by the blood to cells that have high GGT activity, such as kidney proximal tubular cells (De Carvalho et al., 2011), that catabolize GSH to Cys (Dröge et al., 1991; Pitts, 1995) for its release in the peripheral circulation (Stipanuk *et al.*, 2002). For this reason, some peripheral tissues may be exposed to relatively high concentrations of Cys such as the kidney.

The key regulatory enzymes of Cys metabolism are cysteine dioxygenase (CDO), that converts Cys into cysteine-sulfinate and 3) gamma-glutamylcysteine synthetase (GCS) that competes with CDO for the use of Cys as substrate for the formation of GSH (Bella, Hahn and Stipanuk, 1999; Stipanuk *et al.*, 2002, 2006). Additionally, Cys availability is also dependent on other pathways including coenzyme A (coA) synthesis and hydrogen sulfide production (Stipanuk et al., 2006).

Nevertheless, hepatic CDO plays a dominant role in the regulation of Cys levels, with a rapidly drop on its turnover upon the increase of intracellular Cys levels (Bagley and Stipanuk, 1995; Bella *et al.*, 1999; Bella, Hahn and Stipanuk, 1999; Stipanuk *et al.*, 2002, 2006). In fact, the maintenance of low levels of Cys in the body is critical due to the toxic effects elicited by excess Cys is plasma. Increased plasma levels of Cys were reported in inflammatory conditions such as rheumatoid arthritis (Bradley et al., 1994), systemic lupus erythematosus (Gordon et al., 1992), cardiovascular disease (Özkan, Özkan and Şimşek, 2002; De Chiara et al., 2012), metabolic syndrome (Mohorko et al., 2015), in both diabetic and non-diabetic patients with CKD (Suzuki et al., 2014; Pastore et al., 2015) as well as in the neurological disorders Parkinson's disease, Alzheimer's disease and motor neuron disease (Heafield et al., 1990). The value of these results is, however, limited due to the quantification of the total fraction of Cys rather than its different forms, since the predominant fraction of Cys in plasma is its oxidized form (Rossi et al., 2009) and changes on this proportion could trigger toxic effects. In rats, the expression and activity of CDO in the kidney is less than half of the hepatic one (Tsuboyama et al., 1996). This could be one of the reasons why the ratio of Cys to GSH increases 4 times in the kidney while it decreases 2 to 3 fold in the liver from the newborn to the adult period in rats (States, Foreman and Segal, 1987). However, contrarily to the data obtained in rats, CDO was not detected in human kidney (Tsuboyama-Kasaoka *et al.*, 1999).

Both Cys and GSH have important roles in maintaining the homeostasis of the metabolizing cells. Cys *per se* is essential for growth and development due to its involvement in protein synthesis, transsulfuration and transmethylation pathways (Hirakawa and Baker, 1985; Finkelstein, Martin and Harris, 1986) and is an important constituent of most proteins, establishing disulfide bridges that determine protein's tertiary structure. Further, it is the sulfhydryl group of Cys that allows GSH to perform its reducing function. In fact, Cys is less likely to remain reduced in an oxidative environment than GSH (Jones et al., 2000; Grunwell et al., 2015) and the reaction of Cys with reactive compounds forming Cys-*S*-conjugates has been reported to be far more

stable and faster than the reaction with GSH (Szwergold, 2006) and with higher half-lives than its precursors (Kanaoka and Boyce, 2014).

On the other hand, the kidney is exposed to relatively high concentrations of Cys (Dröge *et al.*, 1991; Pitts, 1995; Stipanuk *et al.*, 2002) and is a primordial organ for oxidation due to its high metabolic rate and strong dependence on oxidative phosphorylation to produce energy (Simmons, Bogusky and Humes, 1980; Basile, Anderson and Sutton, 2012; Chevalier, 2016). Nearly 80 meq Na/g kidney/day are reabsorbed by the intact mammalian kidney across the renal tubules, accounting approximately 70% of oxygen utilization by the kidney (Lewy *et al.*, 1973). Hence, meeting this demand requires the tubular cells to generate a significant amount of adenosine triphosphate (ATP), whose preferential energy substrate are non-esterified free fatty acids, mainly palmitate, and to a lesser degree, lactate, pyruvate and citrate (Lewy *et al.*, 1973). In fact, the proximal tubule does not utilize glucose, but is the only part of the kidney with the appropriate enzymes for gluconeogenesis (Mather and Pollock, 2011).

It is well established the degree of damage to the tubulointerstitial compartment correlated with the deterioration of renal function (Tramonti and Kanwar, 2013; Tonolo and Cherchi, 2014). On this regard and having into account the above-mentioned facts linking the kidney and Cys, the regulation of Cys availability might be an important factor to consider in kidney disease. Diet content (mainly), protein breakdown and GSH recycling, that occurs mainly in renal tubule through the mercapturate pathway contribute to Cys availability, as well as Cys metabolism that is high in liver and adipose tissue (Lu, 1999). As so, the metabolism of Cys is pivotal in keeping its levels below the threshold of toxicity (Stipanuk et al., 2006). Of note, the mean normal levels of total Cys in plasma is about 190 to 250 μM (Özkan, Özkan and Şimşek, 2002; Davis *et al.*, 2006; Rossi *et al.*, 2009) and Cys in plasma exists mainly in oxidized form (Ashfaq *et al.*, 2006).

In fact, the promotion of toxicity by Cys is related to the formation of its auto-oxidative products, namely CysSSX (Vina et al., 1983; Munday, 1989; Poole, 2015), playing important roles in redox cycling and/or regulation of enzymes and transcription factors involved in cell signaling processes (Forman, Maiorino and Ursini, 2010; Poole, 2015).

The formation of CysSSX occurs through a disulfide bond between Cys with other low molecular weight (LMW) thiol-containing molecule, including GSH, Cys, coenzyme A (CoA) or homocysteine (HCys) yielding cysteine-glutathione disulfide (CysSSG), CysSSCys, cysteine-coenzyme A disulfide (CysSSCoA) and CysSSHCys, respectively

(Wang and Ballatori, 1998; Moreno *et al.*, 2014; Coelho *et al.*, 2018). We have previously shown an increase in the formation of CysSSX at the kidney at early stages of disease in an animal model of systemic hypertension (Coelho et al., 2018), characterized by increased oxidative and inflammatory status (Abuyassin et al., 2018). Moreover increased formation of LMW disulfides namely CysSSCys and homocystine (HCysSSHcys) together with increased protein cysteinylation (CysSSP) and glutamylcysteinylation (GluCysSSP) (i.e. the oxidation of Cys residues in protein with, respectively, free Cys and glutamate-cysteine – GluCys) has been described as a redox signaling mechanism associated with acute organ inflammation (Moreno et al., 2014). This mechanism was named disulfide stress and represents a new paradigm in inflammatory/oxidative conditions, as it is independent of the classical view of GSH redox status. Furthermore, targets of this disulfide stress (i.e. oxidation of Cys residues) have important roles in DNA repair, cell proliferation, apoptosis, endoplasmic reticulum (ER) stress and inflammatory response (Moreno *et al.*, 2014). This could be seen as a double-edged sword since in one hand, oxidation of the Cys residues might result in functional inactivation of enzymes (e.g. ribonuclease inhibitor, APE1, PP2A) while in other hand it could induce an adaptive response to oxidative stress through the activation of both the unfolded protein response, by the oxidation of protein isomerase disulfide (Parakh and Atkin, 2015) and the antioxidant response element, through oxidation of Keap1 with consequent activation of Nrf2 (Taguchi, Motohashi and Yamamoto, 2011; Levonen *et al.*, 2014; Poole, 2015). Interestingly, no changes in GSH oxidation or protein glutathionylation were observed in a model of acute organ injury. This is in accordance with the fact that the redox state of GSH in plasma is not equilibrated with the pool of Cys (which is far larger in plasma than GSH), eliciting different responses to chemical toxicants and physiologic stimuli, suggesting that oxidative stress may be better defined as a disruption of redox signaling and control rather than the redox state of GSH (Jones, 2006). Moreover, it seems that disulfide stress might be a good mechanism for regulation of proteins (through activation of the unfolded protein response and the antioxidant response element), while the formation of LWM disulfides might induce an opposite reaction. For instance, CysSSCys can accumulate in lysosomes, which promotes mitochondrial depolarization and the induction of redox-sensitive genes (Sumayao *et al.*, 2016). Additionally, a recent review evaluating the relative solute retention of several compounds in uremia through the ratio of the mean of all reported uremic concentrations measured (M) in patients to the normal concentration (N) measured in healthy controls, revealed that plasma Cys (that is mainly

in its oxidized form, cystine) was among the 18 solutes with the ratio M/N, ranging between one and two (positioned in number 8 of 18) (Duranton *et al.*, 2012).

Under oxidative stress conditions, CysSSX might be directly formed in proximal tubular cells, independently of GSH levels (Jones et al., 2000; Grunwell et al., 2015). Also, CysSSX might reach tubular cells upon the catabolism of GSSX generated plausibly by any cell, through the mercapturate pathway, by the mechanism above-mentioned (sequential hydrolysis by GGT and cysteinyl-glycine dipeptidase or aminopeptidase-M) and finally transported into the tubular cell. As so, under chronic injury, the kidney might be exposed to high and potentially toxic concentrations of CysSSX, that together with the increased susceptibility of the kidney for oxidation (Simmons, Bogusky and Humes, 1980; Basile, Anderson and Sutton, 2012; Chevalier, 2016) might perpetuate the effects of CysSSX accumulation, promoting injury of proximal tubular cells.

In fact, increased levels of plasma CysSSCys have been reported in conditions associated with kidney dysfunction. For instance, higher levels of CysSSCys were detected in patients under hemodialysis (HD) (Wlodek et al., 2001; Suzuki et al., 2018). A recent study showed that increased concentrations of CysSSCys were associated with older age, longer HD duration, HD-associated hypotension and higher body mass index (BMI), demonstrating that higher CysSSCys levels predicted the cardiovascular-related and all-cause mortality in these patients (Suzuki et al., 2018). Additionally, patients with coronary artery disease also presented higher levels of CysSSCys, that, among other factors, were associated with impaired renal function as demonstrated by a lower eGFR (Patel et al., 2016). On the other hand, although no changes were observed in CysSSCys in a population of patients with different stages of CKD, the redox potential of Cys increased with disease progression towards a more oxidized state of Cys (Rodrigues et al., 2012).

Regarding the levels of CysSSX in studies with animal models, rats exposed to chronic intermittent hypoxia, mimicking co-morbidities of OSA, presented an increased in renal concentrations of CysSSX in an early phase of disease (Coelho et al., 2018). In another model, a drop in plasma and renal levels of total Cys was observed 24 hours right after injection of CISP in rats, although the individual levels of Cys and CysSSCys could not be evaluated (Ezaki et al., 2017).

Similarly to the thioether Cys-*S*-conjugates, changes in CysSSX have also been reported in other inflammatory conditions, although the reports are only regarding plasma samples

(**Table 1**). Specifically, the levels of CysSSCys were increased in plasma samples from coronary artery disease patients, representing greater oxidant burden on this setting (Patel et al., 2016). The increase in CysSSCys was accompanied by a reduction of GSH, indicating a low intracellular reducing capacity. Furthermore, a high ratio of CysSSCys/GSH was observed and was associated with a 2-fold increase in risk of mortality over a mean of 5 years, regardless of age and other risk factors such as inflammation. Factors contributing for the increase in CysSSCys were older age, female sex, higher BMI, lower eGFR as well as the presence of hypertension and diabetes (Patel et al., 2016). In fact, other reports have shown that increased plasma CysSSCys is associated with ageing (Ashfaq et al., 2006; Giustarini et al., 2006), diabetes (Ashfaq et al., 2008) as well as hypertension and higher BMI (Ashfaq et al., 2008; Dhawan et al., 2011). In an otherwise healthy population, CysSSCys was also positively associated with Framingham risk score (used to estimate the 10-year cardiovascular risk of an individual). Moreover, a higher level of oxidized metabolites, namely CysSSCys and CysSSG was associated with worse endothelial function (Ashfaq et al., 2008). In critically ill children, decreased vitamin D was associated with a more oxidative status of Cys (Alvarez et al., 2018). Additionally, impaired microvascular function and increase necrotic core was related with a higher ratio of CysSSCys/GSH, reflective of higher oxidative stress, in patients with coronary atherosclerotic heart disease (Dhawan et al., 2011). Higher intima-media thickness correlated with a higher profile of plasma levels of CysSSCys and also higher redox potential of GSH (more oxidized), although after adjusting for traditional risk factors and inflammation, only the latter remained a predictor of intima-media thickness in a manner that was both independent of and additive to the Framingham risk score (Ashfaq et al., 2006). Oxidation of Cys, shown by an increase in CysSSCys and the redox potential of Cys (more oxidized) was associated with decrease responsiveness to the systemic glucocorticoid triamcinolone in children with difficult-to-treat asthma (Stephenson et al., 2015).

The effect of antioxidant supplementation on plasma CysSSCys levels has also been studied. In a randomized, double-blind placebo-controlled clinical trial of patients with history of sporadic colorectal adenoma, supplementation with an antioxidant micronutrient combination lead to a reduction in plasmatic levels of CysSSCys, an effect that was further pronounced in nonsmoking patients (Hopkins et al., 2010). However, standard or modified (containing micronutrients and minimal lipids alone) parenteral nutrition had no effect on the levels of CysSSCys or the redox potential of both GSH and

Cys, that increased over time in patients undergoing bone marrow transplantation following chemotherapy (Jonas et al., 2000).

In summary, the study of CysSSX seems to be still poorly explored in relation of what is known for other Cys-*S*-conjugates. Nevertheless, evidence shows that increased levels of CysSSX are associated with both kidney dysfunction and other inflammatory conditions.

Table 1 – Endogenous cysteine-*S*-conjugates (thioethers and disulfides) in inflammatory conditions.

Conjugates	Study aim/rationale	Biological sample and patients' characteristics	Method, ranges or cut-offs	Results Metabolite levels, association with disease	Reference
CysLTs	Evaluate the impact of systemic diseases, pharmaceuticals and diet on CysLTs in EBC and correlation of respiratory disorders with plasma and urine CysLTs.	EBC, plasma and urine samples from 82 patients with pneumoconiosis – 45 from asbestos exposure (mean age 70 yo; 53% men) and 37 from silica exposure (mean age 69 yo; 97% men); and 27 CTLs; subjects with systemic disorders were present in all groups.	LC-ESI-MS/MS	• ↑ LTD4 and LTE4 in pneumoconiosis *versus* CTL group in EBC; • ↑ urine LTD4 and plasma LTE4 in asbestosis *versus* CTL group; • ↑ CysLTs in severe asbestosis *versus* mild asbestosis in EBC; • In CTL group, plasma LTE4 was correlated with nephrolithiasis (+) and fibrates; • In asbestosis group, plasma LTC4 was correlated with steroids; • In silicosis group, urine LTD4 was correlated with kidney failure (+), urine LTE4 with kidney failure (+) and salicylates, and plasma LTE4 with vitamin C and E.	(Pelclova *et al.*, 2012)
	Clarify the types of CysLTs in saliva and evaluate them in AIA patients; Compare the levels of CysLTs between saliva and urine.	Saliva and urine samples from 26 non-smoking asthmatic patients: 15 AIA (mean age 51 yo; 40% men) and 11 ATA (mean age 55 yo; 36% men); and 10 CTLs; AIA patients were also divided in mild (n=6) and mild (n=9) asthma.	Purification by HPLC followed by EIA (LLOD: 13 pg/mL).	• LTC4 (30%), LTD4 (32%) and LTE4 (38%) were detectable in saliva in similar amounts; • ↑ CysLTs in saliva of AIA *versus* other groups; • CysLTs correlated with LTB4 in saliva in all groups (+); • ↑ LTE4 in urine of AIA *versus* other groups; • No association between urine LTE4 and CysLTs in saliva; • ↑ LTE4 in urine of severe AIA patients.	(Ono *et al.*, 2011)
	Determine the correlation of 8-isoprostane, CysLTs, age and autism severity scales to clarify the role of oxidative stress and inflammation in the etiopathology of autism.	Plasma samples from 44 autistic children (mean age 7 yo) and 40 CTLs (mean age 7 yo). Autistic cases were all simple and tested negative for the fragile X gene mutations.	ELISA	• ↑ CysLTs and 8-isoprostane in autistic *versus* CTL group; • CysLTs correlated with 8-isoprostane (+); • SSP test correlated with CysLTs and 8-isoprostane (-).	(Qasem, Al-Ayadhi and El-Ansary, 2016)
	Quantify CysLTs in urine of spontaneous ICH patients; compare the release of CysLTs with the edema volume; assess the effect of hematoma removal in the release of CysLTs.	Urine samples from 17 spontaneous ICH patients (mean age 58 yo; 53% men): 12 treated surgically and 5 treated conservatively. Samples were collected before treatment and during 5 days of treatment.	HPLC	• CysLTs were correlated with hematoma volume (+); • ↓ CysLTs 5 days after surgery in comparison with before surgery; • No differences with conservative treatment	(Winking *et al.*, 1998)
	Study CysLTs changes during and after cardiac surgery with CPB and the differences between patients with and without COPD.	Plasma and urine samples from patients undergoing cardiac surgery with CPB: 9 with moderate-to-severe COPD (mean age 69 yo; 78% men) and 10 non-smoker CTLs (mean age 64 yo; 60% men).	ELISA	• ↑ CysLTs in urine with time, in both groups, but more evident in COPD patients; • ↑ CysLTs in plasma of COPD patients between baseline and admission to ICU.	(de Prost *et al.*, 2011)

		Samples were collected after intubation (baseline), at the end of CPB, after CPB and 2h after admission in ICU.			
	Detect the formation of CysLTs and atherosclerosis in subjects with and without periodontitis.	GCF samples of 19 subjects with periodontitis (mean age 55 yo; 63% men; 13 with atherosclerotic plaques) and 16 CTLs (mean age 53 yo; 44% men; 5 with atherosclerotic plaques).	EIA	• > subjects with atherosclerotic plaques in periodontitis *versus* CTL; • ↑ CysLTs than LTB4 in GCF; • ↑ CysLTs in periodontitis subjects with high PLI; • ↑ CysLTs in subjects with atherosclerotic plaques, even when dividing between periodontitis and CTL subjects.	(Bäck *et al.*, 2007)
	Evaluate the effect of smoking in LDT4 and LTE4 levels in asthma	EBC samples from 59 asthmatic patients – 30 smokers (mean age 34 yo; 50% men) and 29 non-smokers (mean age 34 yo; 48% men); and 29 CTLs (mean age 34 yo; 48% men; non-smokers).	ELISA	• ↑ LTD4 in asthmatic smokers *versus* other groups; • ↑ LTE4 in asthmatic *versus* CTL group; • LTE4 correlates with the ratio of forced expiratory volume in one second by forced vital capacity (measure of airway obstruction) in asthmatic smokers (-).	(Celik *et al.*, 2013)
LTE4	Assess *in vivo* release of LTE4 during and after an ischemic episode.	Urine samples from 16 AMI (mean age 51 yo; 88% men) and 14 UA patients (mean age 52 yo; 21% men); and 8 clinical (88% mean) and 10 normal (50% men) CTLs. Samples were collected upon admission with acute chest pain and 3 days after.	HPLC followed by RIA	• ↑ LTE4 in MIA and UA at admission *versus* CTL groups; • ↑ LTE4 on admission than 3 days after in AMI and UA groups;	(Carry *et al.*, 1992)
	Study the relation between the systemic CysLTs synthesis and stable CAD and changes after bypass surgery	Urine samples from 13 CAD patients (mean age 59 yo; 100% men) and 12 CTLs (mean age 44 yo; 100% men; no previous history of CAD). For CAD patients, samples were collected in the preoperative and for up to 7 days after.	Solid-phase extraction, HPLC purification and RIA	• ↑ LTE4 in preoperative CAD *versus* CTL group; • ↑ LTE4 2 days after surgery *versus* preoperative in CAD group;	(Allen *et al.*, 1993)
	Identify the determinants on the activation of CysLTs pathway and the role of CysLTs in OSA-related atherosclerosis	Urine samples from 170 OSA patients (mean age 57 yo; 81 % men) – 136 CVE free and 34 with previous CVE; and 20+9 CTLs (mean age 52 yo; 52% men).	LC-MS	• Whole cohort: LTE4 was independently influenced by age, min SaO_2 and history of CVE and was correlated with IMT (+); • ↑ LTE4 in OSA CVE free patients *versus* CTL group and was independently related to min SaO_2 and traditional risk factors of the 10-year cardiovascular risk score.	(Gautier-Veyret *et al.*, 2018)

	Monitor urine LTE4 in OSA; to determine the influence of obesity and other confounders on; to examine the mechanisms involved through transcriptional profiling of CysLTs pathway in; and to investigate the effect of continuous positive air pressure (CPAP) on LTE4.	Urine samples from 40 nonobese OSA patients (mean age 49 yo; 85% men) and 25 CTLs (mean age 45 yo; 72% men). A group of 72 OSA patients (mean age 51 yo; 81% men) was included to study confounder factors of LTE4. All were nonsmokers.	LC-MS; LLOD: 10 pg/mL	• ↑ LTE4 in nonobese OSA versus CTL group; • In nonobese OSA patients, LTE4 was correlated with % of time spent with SaO_2<90% (+); • In the 72 OSA patients, BMI and % of time spent with SaO_2<90% were identified as independent predictors of LTE4; • CPAP ↓ LTE4 by 22% only in OSA patients with normal BMI.	(Stanke-Labesque *et al.*, 2009)
	Analyze CysLTs activation in asthma during treatment in the ED and 2 weeks after; determine whether the degree of airflow limitation is correlated with activation of CysLTs pathway.	Urine samples from 184 patients with acute asthma at the ED (mean age 35 yo). Samples were collected at the ED and 2 weeks after.	HPLC followed by RIA.	• ↑ LTE4 during asthma exacerbations *versus* 2 weeks later; • LTE4 was correlated with FEV_1 (+) over the 2-week interval.	(Green *et al.*, 2004)
	Evaluate urinary excretion of LTE4 in patients with T1D and the influence of glycemic control in this excretion	Urine samples from 34 T1D patients – 20 with GMC (median age 39 yo; 55% men) and 14 with PMC (median age 41 yo; 50% men) and 28 CTLs (median age 39 yo; 43% men), all nonsmokers.	LC-MS	• ↑ LTE4 in T1D *versus* CTL group; • ↑ LTE4 in T1D patients with PMC *versus* CTL group;	(Hardy *et al.*, 2005)
	Investigate the effect on LTE4 and 11-dehydro-TXB2 of a 3-month improvement of glycemic control by intensive insulin treatment in diabetes.	Urine samples from 20 T1D (mean age 37 yo; 35% men) and 19 T2DM patients (mean age 58 yo; 68% men), all nonsmokers.	LC-MS; detection range: 10-100 pg/mL	• ↓ LTE4 after intensive insulin treatment (-32%) in T1D but not in T2DM groups.	(Boizel *et al.*, 2010)
5-*S*-CD	Retrospective evaluation of the usefulness of serum 5-*S*-CD as a biomarker for prognosis and early detection of relapse of MM.	Serum samples of 120 patients with MM (mean age 64 yo; 41% men).	HPLC; Normal range: 1.5-8 nmol/L but the cut-off has been established to be 10 nmol/L.	• ↑ 5-*S*-CD in advanced stages (III and IV) versus early stages (0–II) patients; • In patients with advanced stages, 5-*S*-CD>15.0 nmol/L correlated with a poor prognosis; • 5-*S*-CD>10 nmol/L in 11/14 patients with disease progression during follow up.	(Umemura *et al.*, 2017)
	Case report for diagnosis of rectal malignant melanoma with 5-*S*-CD.	Serum sample from woman with 84 yo diagnosed with rectal MM.	Method was not specified; Normal range: 1.5-8 nmol/L.	• Before tumor resection: 5-*S*-CD levels were 26 nmol/L; • 3 months after surgery: 5-*S*-CD levels were 12.6 nmol/L 3 (still>10 nmol/L) and CT scan confirmed multiple liver and lung metastasis.	(Sato *et al.*, 2003)
	Usefulness of serum 5-*S*-CD in following melanoma progression and prognosis.	Serum samples from 218 melanoma patients (mean age 55 yo; 51% men).	HPLC-EC; Upper limit of normal range: 10 nmol/L	• 5-*S*-CD>10 nmol/L in stage IV patients; • Elevation of 5-*S*-CD preceded or occurred at the same time of clinical detection of visceral metastasis in, respectively, 33% and 37% of cases; • ↑ 5-*S*-CD was associated with shorter survival time.	(Wakamatsu *et al.*, 2002)

	Serum 5-S-CD-levels as a useful marker for monitoring tumor progression and regression due to immunochemotherapy cycles in metastasizing MM and its value for prognosis and therapy response.	Serum samples from 11 patients with metastatic MM (mean age 47 yo; 64% men).	HPLC-EC; Upper limit of normal range: 3.2 ng/mL (10 nmol/L); Variations of 0.2 ng/mL were taken ↓ or ↑	• Before and after therapy, mean 5-*S*-CD were 4.3 ng/mL and 94.3 ng/mL, respectively; • ↓ and ↑ in 5-*S*-CD was observed in, respectively 68% and 32% of therapy cycles; • Declines in 5-*S*-CD in > 68% of therapy cycles had longer survival time.	(Wimmer *et al.*, 1997)
	Levels of 5-*S*-CD in different stages of malignant melanoma, and its value on the extent of metastasis.	Serum sample from 252 patients with MM (51% men).	HPLC; Upper limit of normal range: 10 nmol/L.	• ↑ 5-*S*-CD in symptomatic *versus* asymptomatic patients; • ↑ 5-*S*-CD in stage III *versus* stage I and II patients; • ↑ 5-*S*-CD in stage III *versus* primary tumor, lymph node and lung metastasis symptoms; • ↑ 5-*S*-CD correlated with tumor burden.	(Banfalvi *et al.*, 2000)
5-*S*-Cys and 5-*S*-GSH conjugates of DA, L-DOPA and DOPAC	Quantification of 5-*S*-Cys- and 5-*S*-GSH-catechol conjugates in brain tissue and changes on their levels in PD.	Postmortem brain samples from 6 PD patients with PD (mean age 77 yo, L-DOPA therapy) and 6 CTLs (mean age 81 yo); Brains were dissected into 11 regions.	HPLC-EC	• Detectable conjugates in most brain regions, with higher levels in SN and PUT; • ↓ 5-*S*-glutathionyl- *versus* 5-*S*-cysteinyl-conjugates; • ↓ conjugates in PD with the exception of 5-*S*-cysteinyl-conjugates that were ↑ in SN and SI.	(Spencer *et al.*, 1998)
5-*S*-Cys conjugates of DA, L-DOPA and DOPAC	Investigate the connection between SN's degenerative changes and the occurrence of 5-*S*-Cys-catechol conjugates and their ratio with the catecholamines.	Postmortem brain samples (SN, PUT and CN sections) from 17 individuals (72-90 yo; 41% men); Samples were divided according to degree of depigmentation and neuronal loss within SN.	HPLC-EC	• ↓ DA, DOPAC and DOPA in depigmented group in SN; • No differences for Cys-DA among groups; • ↑ 5-*S*-Cys-catechol conjugates/catecholamine ratio in the more depigmented and degenerated SN group, except for the DA ratio in PUT.	(Fornstedt *et al.*, 1989)
5-*S*-Cys-DA	Assess the value of increased Cys-DA/DOPAC ratio CSF as a specific biomarker of parkinsonism.	CSF samples from 24 PD patients (mean age 61 yo, 58% men); 32 MSA-P (mean age 60 yo; 66% men); 18 PAF (mean age 63 yo; 67% men) and 32 CTLs (mean age 53 yo; 53% men). Patients were not under levodopa or monoamine oxidase inhibitor treatment.	HPLC-EC	• ↓ DOPAC in PD and MSA-P versus PAF and CTL groups; • Cys-DA levels were similar among groups; • Cys-DA/DOPAC >2-fold in PD and MSA-P than PAF and CTL groups; • Cys-DA/DOPAC was correlated with putamen/occipital ratios (-) and washout fractions of ^{18}F-fluorodopa-derived radioactivity (+).	(Goldstein *et al.*, 2016)
	Evaluate the levels of Cys-DA, homovanillic acid (HVA) and their ratio in CSF samples of PD patients.	CSF samples from 20 PD patients (mean age 69 yo, 85% men) and 16 CTLs (mean age 60 yo years, 63 % men); Samples under and 5 days after L-DOPA withdrawal.	HPLC-EC	• ↓ HVA in PD patients after L-DOPA withdrawal *versus* CTLs; • No differences for Cys-DA among groups; • ↑ Cys-DA/HVA ratio in PD after L-DOPA withdrawal *versus* CTLs.	(Cheng *et al.*, 1996)

Cys, GSH and NAC conjugates of 2-OHE$_1$(E$_2$) and 4-OHE$_1$(E$_2$)	To test if estrogen metabolites, conjugates and depurinating DNA adducts differ between healthy women and women with breast cancer or at high risk for breast cancer.	Urine samples from 12 women with high-risk for breast cancer (mean age 52 yo), 17 with breast cancer (mean age 54 yo) and 46 CTLs (mean age 50 yo).	UPLC/MS-MS detection	• ↑ Cys, GSH and NAC conjugates of 2-OHE$_1$(E$_2$) in CTL *versus* other groups.	(Gaikwad *et al.*, 2008)
	Analyze the urinary levels of estrogen metabolites, conjugates and depurinating DNA adducts and their association with breast cancer.	Urine samples from 40 women with high risk for breast cancer (median age 57 yo) and 40 with newly diagnosed with breast cancer (median age 58 yo) and CTLs (median age 45 yo), all without estrogen-containing treatment.	UPLC/MS-MS detection	• ↑ Cys, GSH and NAC conjugates of 2-OHE$_1$(E$_2$) and 4-OHE$_1$(E$_2$) in CTL *versus* other groups.	(Gaikwad, Yang, Pruthi, *et al.*, 2009)
	Determine if the estrogen depurinating DNA adducts are involved in the etiology of NHL.	Urine samples from 15 NHL patients (median age 59 yo; 100% men) and 30 CTLs (median age 60; 100% men).	UPLC/MS-MS detection	• ↑ Cys, GSH and NAC conjugates of 4-OHE$_1$(E$_2$) in CTL *versus* NHL group.	(Gaikwad, Yang, Weisenburger, *et al.*, 2009)
	Assess if high levels of estrogen DNA adducts are associated with PD.	Urine samples from 20 PD patients (mean age 62 yo; 75% men; all under levodopa) and 40 CTLs (mean age 63 yo; 75% men)	UPLC/MS-MS detection	• ↑ Cys, GSH and NAC conjugates of 4-OHE$_1$(E$_2$) in CTL *versus* PD group.	(Gaikwad *et al.*, 2011)
	Investigate the role of estrogen metabolism in thyroid cancer	Urine samples from 40 women with thyroid cancer (mean age 47 yo) and 40 CTL women (mean age 47 yo).	UPLC/MS-MS; the ratio of depurinating estrogen DNA adducts by metabolites and conjugates was obtained.	• ↑ ratio in thyroid cancer than CTL group.	(Zahid *et al.*, 2013)
	Investigate the role of estrogen metabolism in ovarian cancer	Urine samples from 33 women with ovarian cancer (mean age 58 yo) and 34 CTL women (mean age 58 yo).	UPLC/MS-MS; the ratio of depurinating estrogen DNA adducts by metabolites and conjugates was obtained.	• ↑ ratio in ovarian cancer than CTL group.	(Zahid *et al.*, 2014)
Glucose-Cys	Assess if α-thiolamines such as Cys is a good candidate to fulfill the role of general trans-glycating agent	Urine samples from 5 patients with diabetes and 2 normoglycemic subjects	SIM	• ↑ Glucose-Cys in diabetes than normoglycemic subjects.	(Szwergold, 2006)

CysSSCys	Examine the association of emerging aminothiol markers of non-free radical mediated oxidative stress with clinical outcomes.	Plasma samples from 1411 subjects prior to undergoing coronary angiography for investigation or management of CAD (mean age 63 yo; 66% men).	HPLC-FD	• A multivariable model showed that older age, female sex, ↑ BMI, ↓ eGFR, presence of diabetes and HTN were independently associated with ↑ CysSSCys; • ↑ CysSSCys was associated with risk of death; • ↑ CysSSCys/GSH leads to a 2-fold increase in risk of mortality over a mean of 5 years, regardless of age and other risk factors such as inflammation.	(Patel *et al.*, 2016)
	Assess whether there is a shift of the thiol/disulfide balance during aging	Plasma samples from 41 healthy individuals (age between 21 and 92 yo; 41% men)	HPLC-FD	• Aging was correlated with ↑ CysSSCys.	(Giustarini *et al.*, 2006)
	Effects of an antioxidant micronutrient combination on oxidative and inflammatory biomarkers in sporadic colorectal adenoma.	Pilot, randomized, double-blind, placebo-controlled clinical trial. Plasma samples from 47 patients with in patients with a history of sporadic colorectal adenoma: 23 under placebo (median age 59 yo; 52% men) and 24 under antioxidant treatment (median age 61 yo; 50% men).	HPLC	• ↓ CysSSCys in the antioxidant (-39%) *versus* placebo group; • In the antioxidant group, ↓ CysSSCys was more pronounced in nonsmokers (-35%) *versus* smokers (-12%).	(Hopkins *et al.*, 2010)
CysSSCys and CysSSG	Assess oxidative stress in the bloodstream as a reliable predictor of endothelial function in healthy adults.	Plasma samples from 124 healthy nonsmokers subjects without any known cardiovascular risk factors (mean age 44 yo; 40% men). In A subset of individuals with HTN, diabetes or BMI≥30 was analyzed (n=41).	HPLC-FD	• CysSSCys was correlated with age (+), BMI (+), HTN (+) and Framingham risk score; • ↑ CysSSCys in patients with HTN, diabetes or BMI≥30 *versus* the remaining individuals; • CysSSG was correlated with TG (-), HDL (+), HTN (+); • Endothelium-dependent vasodilation correlated with CysSSCys (-) and CysSSG (-).	(Ashfaq *et al.*, 2008)
CysSSCys and GSSG	Investigate the relationship between vitD status and GSH and Cys redox and immunity in critically ill children.	Plasma samples of 50 critically ill children (mean age 12 yo; 56% men) that were stratified by vitD levels: <20 ng/dl (n=29); 20-30 ng/dL (n=8) and ≥30 ng/dL (n=13).	HPLC	• ↓ vitD associated with ↓ CysSH/CysSSCys and ↑ E_hCysSH/CysSSCys; • ↑ vitD associated with ↓ GSSG.	(Alvarez *et al.*, 2018)
	Determine if higher oxidative stress is associated with impaired coronary microvascular function and plaque necrotic core content	Plasma samples from 47 patients undergoing cardiac catheterization (mean age 58 yo; 64% men).	HPLC	• ↑ CysSSCys/GSH associated with impaired microvascular function and greater necrotic core; • ↑ CysSSCys in patients with ↑ BMI and HTN.	(Dhawan *et al.*, 2011)
	Characterize systemic Cys oxidation and its association with inflammatory and clinical features in children with asthma	Plasma and PBMCs samples from 99 children with asthma (median age 12 yo; 67% men) and 15 CTLs (median age 10	HPLC	• ↓ CysSH and ↑ CysSSCys and E_hCysSH/CysSSCys in plasma of asthmatic *versus* CTL group; • ↑ GSSG in PBMCs of asthmatic *versus* CTL group;	(Stephenson *et al.*, 2015)

		yo; 20% men). Response to triamcinolone treatment was assessed in 57 children.		• The lowest CysSH and highest E_hCysSH/CysSSCys were found in children with severe asthma; • ↑ E_hCysSH/CysSSCys and ↓ CysSH in triamcinolone non-responders at both the baseline and the 2-week after treatment visits.	
	Investigate the relationship between biomarkers of oxidative stress and early atherosclerosis.	Plasma samples from 114 healthy nonsmokers subjects without known clinical atherosclerosis (mean age 44 yo; 41% men).	HPLC-FD	• ↑ IMT correlated with both CysSSCys (+) and E_hGSH/GSSG (+); • Age correlated with GSH/GSSG (+) and CysSSCys (+); • Multivariable analysis showed that only E_hGSH/GSSG was an independent predictor of IMT.	(Ashfaq *et al.*, 2006)
	Determine the effect of high-dose chemotherapy in circulating antioxidants in patients undergoing BMT and if administration of standard PN (sPN) maintains systemic antioxidant concentrations compared with modified PN (mPN) containing micronutrients and minimal lipids alone.	Double-blind, controlled, randomized clinical trial. Plasma samples from 24 BMT patients (mean age 40 yo; 58% men). Patients were divided into treatment with sPN (mean age 41 yo; 36% men) and mPN (mean age 38 yo; 69% men). Samples were collected before chemotherapy and BMT (baseline) and 1, 3, 7, 10 and 14 days after BMT.	HPLC-FD	• ↑ E_hGSH/GSSG, E_hCys/CysSSCys and CysSSCys over time, regardless of PN treatment type.	(Jonas *et al.*, 2000)

↑: higher; ↓: lower; (-): negative correlation; (+): positive correlation; 2-$OHE_1(E_2)$, 2-hydroxyestrone (estradiol); 4-$OHE_1(E_2)$, 4-hydroxyestrone (estradiol); 5-*S*-CD: 5-*S*-Cysteinyl-dopa; 5-*S*-Cys-DA: 5-*S*-Cysteinyl-dopamine; AIA: aspirin-intolerant asthma; AMI: acute myocardial infarction; ATA: aspirin-tolerant asthma; BMI: body mass index; BMT: bone marrow transplantation; CAD: coronary artery disease; CoA-SSG: coenzyme A-glutathione disulfide; COPD: chronic obstructive pulmonary disease; CPAP: continuous positive air pressure; CPB: cardiopulmonary bypass; CRP: C-reactive protein; CTL: controls; CSF: cerebrospinal fluid; CVD: cardiovascular disease; CVE: cardiovascular event; Cys: cysteine; CysSH: free cysteine; CysLTs: cysteinyl-leukotrienes; CysSSCys: cystine; CysSSG: cysteine-glutathione disulfide; DA: dopamine; CN: caudate nucleus; DOPAC; 3,4-dihydroxyphenylacetic acid EBC: exhaled breath condensate; ED: emergency department; eGFR: estimated glomerular filtration rate; E_h: redox potential; EIA: enzyme immunoassay; ELISA: enzyme-linked immunosorbent assay; FEV_1: forced expiratory volume in 1 second; GCF: gingival crevicular fluid; GCM: good metabolic control; GSH: glutathione; GSSG: oxidized glutathione; HD: hemodialysis; HDL: high-density lipoprotein; HPLC: high-performance liquid chromatography; HPLC-EC: high-performance liquid chromatography with electrochemical detection; HPLC-FD: high-performance liquid chromatography with fluorescence detection; HTN: hypertension; HVA: homovanillic acid; ICH: intracerebral hemorrhage; ICU: intensive care unit; IMT: intima-media thickness; L-DOPA; L-3,4-dihydroxyphenylalanine; LC-ESI-MS/MS: liquid chromatography − electrospray ionization − tandem mass spectrometry; LC-MS: liquid chromatography-tandem mass spectrometry ; LLOD: lower limit of detection; LTB4: leukotriene B4; LTC4: leukotriene C4; LTD4: leukotriene D4; LTE4: leukotriene E4; min SaO_2: minimal oxygen saturation; MM: malignant melanoma; MSA-P: parkinsonian multiple system atrophy; NAC_ *N*-acetylcysteine; NHL: non-Hodgkin lymphoma; OSA: obstructive sleep apnea; PAF: pure autonomic failure; PBMCs: peripheral blood mononuclear cells; PCM: poor metabolic control; PD: Parkinson's disease; PLI: dental plaque index; PN: parenteral nutrition; PUT: putamen; RIA: radioimmunoassay; SI: substantia innominata; SIM: selective ion monitoring; SN: substantia nigra; SSP: short sensory profile; T1D: type 1 diabetes; T2DM: type 2 diabetes mellitus; TG: triglycerides; UA: unstable angina; UPLC/MS-MS: ultraperformance liquid chromatography – tandem mass spectrometry; vit: vitamin D; yo: years old.

5. Urinary mercapturates for biomonitoring in kidney disease

Based on the previously exposed association of NAT8 and kidney function (Juhanson *et al.*, 2008), urinary mercapturates may be used as a hallmark of proximal tubular cells capability to detoxify Cys-*S*-conjugates. As mentioned, this enzyme is highly and almost exclusively expressed in proximal tubular cells (Chambers *et al.*, 2010). In addition, mercapturates are measured in urine, rendering them feasible for biomonitoring purposes (Mathias and Bhymer, 2016; Dias *et al.*, 2017). In fact, urinary mercapturates of several xenobiotics have been used for biomonitoring of environmental and occupational exposure (Mathias and Bhymer, 2016). Thereby, the generation of mercapturates is considered a feature of proximal tubular cells (Hughey *et al.*, 1978; Lash, 2007).

As mentioned, there are dozens of endogenous compounds undergoing the mercapturate pathway (Wang and Ballatori, 1998). There has been an association between mercapturates of endogenous compounds and kidney disease. The urinary elimination of the mercapturate *N*-acetyl-LTE4 is increased in inflammatory conditions (Petric and Ford-Hutchinson, 1994) and with cyclosporine A treatment (Butterly *et al.*, 2000). Moreover, severe nephrotoxicity induced by a high dose of iron nitrilotriacetate increased the concentration of mercapturates derived from 4-hydroxynonenal in both plasma and kidneys of rats right after 5 hours of administration (Mally *et al.*, 2007). This effect was not observed in low doses of iron nitrilotriacetate neither with the administration of potassium bromate. Four-hydroxynonenal is a lipid peroxidation product and normal constituent of mammalian cell membranes, considered a highly potent reactive species that promotes propagation and amplification of the effects elicited by free radicals (Ntimbane *et al.*, 2008).

In fact, several potentially toxic metabolites originated from both endogenous (e.g. leukotrienes, prostaglandins, hepoxilin, nitric oxide, hydroxyalkenals, ascorbic acid, dihydroxyphenylalanine, dopamine, maleic acid) and exogenous (e.g. drugs, natural toxins, environmental pollutants) sources are eliminated from the body after their conversion to the corresponding mercapturate (Boyland and Chasseaud, 1969; Chasseaud, 1979; Dekant, Vamvakas and Anders, 1989; Stevens and Jones, 1989; Hinchman *et al.*, 1991; Hinchman and Ballatori, 1994; Dawn and Ballatori, 1998; Hinchman, Rebbeor and Ballatori, 1998; Wang and Ballatori, 1998).

Changes in the mercapturates of endogenous Cys-*S*-conjugates have also been reported in other inflammatory conditions. For instance, acrolein is a dietary, environmental

pollutant and lipid metabolism-derived electrophile associated to diabetic dysmetabolism and two of its urinary mercapturates were associated with diabetes and insulin resistance (Feroe, Attanasio and Scinicariello, 2016). Urinary acrolein mercapturates are increased in diabetic patients and are related to glycemic control parameters, but not with lipid metabolism nor albumin to creatinine ratio (Daimon *et al.*, 2003), whereas in Alzheimer's disease patients, its levels were found to be decreased (Tsou *et al.*, 2018).

Additionally, urinary mercapturates of 4-hydroxynonenal are decreased in patients with impaired glucose tolerance (Ntimbane *et al.*, 2008). On the other hand, mercapturates of 4-hydroxynonenal and 4-oxo-2-nonenal, another lipid peroxidation product, are elevated in urine of smokers and decrease significantly following smoking cessation, further showing the relevance of mercapturates as markers of *in vivo* oxidative stress. (Kuiper *et al.*, 2010)

In rats, treatment with bromotrichloromethane, an inducer of lipid peroxidation, increased the amount of urinary 1,4-hydroxynonene mercapturic acid, a mercapturate derived from 4-hydroxynonenal, compared to its normal basal levels (Peiro *et al.*, 2005; Guéraud *et al.*, 2006). Similarly, increased urinary elimination of several mercapturates derived from 4-hydroxynonenal and 4-oxo-2-nonenal was observed after treatment of rats with carbon tetrachloride, an established animal model of acute oxidative stress (Kuiper *et al.*, 2008).

The transport of mercapturates for elimination is still a debating issue, but evidence shows that the probenecid-sensitive organic anion transport (OAT) system might be involved (Inoue, Okajima and Morino, 1981; Burckhardt and Burckhardt, 2003; Burckhardt, 2012). For instance, intravenous administration of S-benzyl-N-acetyl-L[U-^{14}C] cysteine (10 µmol/Kg) in rats lead to a very rapidly decrease in plasma level radioactivity with concomitant increase in the renal one. However, after 2 minutes, these levels decreased rapidly and a consequent increase of radioactive in the urine was observed (Inoue, Okajima and Morino, 1981). More than 98% of the radioactivity in urine was accounted for by the intact form of the mercapturate. Both renal accumulation and excretion into urine were inhibited by intravenously administration of probenecid (350 µmol/Kg).

In 2001, Pombrio and colleagues tested the hypothesis that renal clearance of mercapturates is partially mediated by the kidney OAT-1 (Pombrio *et al.*, 2001). The OAT-1 is highly expressed in the kidney, particularly localized in the basolateral membrane of the S2 segment of the renal proximal tubule (Sweet, Miller and Pritchard, 1999; Tojo *et al.*, 1999), where mercapturates are secreted within the nephron (Stevens

and Jones, 1989). Using several *N*-acetyl-Cys-*S*-conjugates, the authors proved that these compounds are substrates of OAT-1. Once taken up into renal proximal tubular cells, mercapturic acids may then be secreted into tubular fluid for excretion in urine. However, the exact mechanism of transport across the apical membrane is still to be elucidated. In fact, this should have been a top priority in these studies, as evidence shows that the majority of the mercapturates of Cys-*S*-conjugates are formed *in vivo* within the proximal tubular cell due to the almost exclusively expression of NAT8 (Chambers *et al.*, 2010; Veiga-da-Cunha *et al.*, 2010). As so, the formed mercapturates require a transporter for its urinary elimination at the apical membrane.

Summarizing, there is evidence on the biomonitoring of mercapturates of endogenous compounds in man and its relation to kidney disease and other inflammatory conditions. Although there are dozens of endogenous compounds undergoing the mercapturate pathway (Wang and Ballatori, 1998), information is still missing such as the contribution of each particular mercapturate in kidney disease. The inability of proximal tubular cells to detoxify Cys-*S*-conjugates, through NAT8 activity, might perpetuate injury. This dysfunction in proximal tubular cell activity can be monitored through the quantification of mercapturates of Cys-*S*-conjugates in urine. A better understanding of the impairment on the mercapturate pathway triggering kidney dysfunction may help to find out new therapeutic approaches and strategies for early prediction and biomonitoring of disease.

RATIONALE & HYPOTHESIS

RATIONALE & HYPOTHESIS

The general aim was to discover a bioindicator of progression of kidney disease. This is relevant because kidney disease impacts global morbidity and mortality by increasing the risk associated with major killers including diabetes, hypertension and HIV-infection (Kassebaum *et al.*, 2016; Wang *et al.*, 2016). Moreover, the renal injury acquired in the hospital setting by contrast agents, drugs and sepsis (Feehally, 2016; Ozkok and Ozkok, 2017) is also a serious health problem and a heavy weight in the global burden of kidney disease. Importantly, as the proximal tubule is considered to be the primary sensor and effector in the progression of both AKI and CKD, the study of specific pathways of proximal tubular cells might shed a light on the critical issue that kidney disease represents today.

For that and based on the literature, we merged genes that were reported to be highly expressed in kidney proximal tubular cells, associated to kidney function through genome-wide association studies and related to detoxification pathways. It is known that genes contributing to normal fetal renal programming and kidney function in adult life have been signalized in the etiology of kidney disease (Zandi-Nejad, Luyckx and Brenner, 2006). This motivated a targeted-screening of genes involved in renal metabolic pathways (Samani, 2003; Chambers *et al.*, 2010) that allowed the identification NAT8 (Juhanson *et al.*, 2008).The knowledge on NAT8 actions has been hampered by its late association to both disease (Juhanson *et al.*, 2008) and the mercapturate pathway (Juhanson *et al.*, 2008; Chambers *et al.*, 2010; Veiga-da-Cunha *et al.*, 2010). Moreover, there are no available pharmacological tools to manipulate NAT8 levels that together with reported difficulties in generating a viable NAT8 knock-out model in rat (Fu *et al.*, 2014) further contribute for this gap on the knowledge. However, it is now recognized that NAT8 is almost exclusively expressed in kidney proximal tubular cells (Ozaki *et al.*, 1998; Chambers *et al.*, 2010) and has been implicated in:

- protection against elevated systolic blood pressure and kidney failure in hypertensive patients (Juhanson *et al.*, 2008);
- development and maintenance of kidney's structure, function (Ozaki *et al.*, 1998) and detoxification pathways (Lock *et al.*, 2006; Veiga-da-Cunha *et al.*, 2010; Deol and Josephy, 2017);
- adaptive response after electrophilic-stress-related injury of renal tubular cell (Fu *et al.*, 2014) and hepatocyte (Liu and Pravia, 2010; Omata *et al.*, 2016) characterized by an increase on the expression of the enzyme.

A hypothesis-oriented investigation is herein presented, underlying that NAT8 activity is related to kidney disease in inflammatory conditions because it controls the balance of Cys-*S*-conjugates. Upon oxidative/inflammatory injury exposure, Cys-*S*-conjugates are generated as part of an adaptive response and their concentration are controlled by NAT8 activity mainly in kidney proximal tubular cells. The exposure to environmental noxious factors (nephrotoxicants) that undergo the mercapturate pathway or endogenous Cys-*S*-conjugates generated upon injury might lead to a misbalance of the detoxification of these conjugates and promote kidney disease progression. As a consequence, Cys-*S*-conjugates will be retained in the course of renal dysfunction and impact multiple organ and systems. This occurs in a temporal and dose dependent manner. Urinary products of NAT8 activity in proximal tubular cells (the mercapturates of Cys-*S*-conjugates) might be indicators of kidney tubule function. This is a never addressed concept that has a rationale strongly supported by literature data:

- the clearance of Cys-*S*-conjugates is controlled by NAT8 activity which protects against elevated systolic blood pressure and kidney failure in hypertensive patients (Juhanson *et al.*, 2008);
- there are dozens of endogenous Cys-*S*-conjugates described with relation to common features of inflammatory conditions including oxidative stress, inflammation and activation of sympathetic nervous system. Examples include Cys-*S*-conjugates of catecholamines, prostaglandins, leukotrienes or steroids (Wang and Ballatori, 1998; Gonçalves-Dias *et al.*, 2019);
- Cys-*S*-conjugates are stable metabolites that can be measured in biological fluids and can slowly accumulate over time (Kanaoka and Boyce, 2014);
- Cys-*S*-conjugates have been associated to several actions including vasoconstriction (Rosenthal and Pace-Asciak, 1983; Badr, Brenner and Ichikawa, 1987; Shastri *et al.*, 2001), cytotoxicity (Townsend *et al.*, 2003; Stern, Bruno, Hennig, *et al.*, 2005; Stern, Bruno, Horton, *et al.*, 2005; Dvash *et al.*, 2015), inflammation and immunogenicity (Salauze *et al.*, 2005).

Endogenous Cys-*S*-conjugates that accumulate can circulate because the Cys-*S*-conjugate has higher half-life than the prior compounds and they are associated with different inflammatory chronic conditions (as reviewed in **Table 1**). Nevertheless, these compounds have in common the detoxification by the proximal tubular cells as mercapturates that might motivate tubulocentric perspectives for multiple inflammatory

conditions, such the one recently reported by us regarding diabetic kidney disease (Gonçalves-Dias *et al.*, 2019). A short preview of the article is herein presented, with the mechanistic hypothesis shown in **Figure 5**.

In Clinical Practice: Mini-review Nephron, DOI: 10.1159/000494390

MERCAPTURATE PATHWAY IN THE TUBULOCENTRIC PERSPECTIVE OF DIABETIC KIDNEY DISEASE

Clara Gonçalves-Dias[a], Judit Morello[b], M. João Correia[a], Nuno R. Coelho [a], Alexandra M.M. Antunes [b], Maria Paula Macedo [a,c,d], Emília C. Monteiro [a], Karina Soto [a,e], Sofia de A. Pereira [a,§]

[a] CEDOC, Chronic Diseases Research Centre, NOVA Medical School|Faculdade de Ciências Médicas, Universidade NOVA de Lisboa, Campo dos Mártires da Pátria, Lisboa, Portugal; [b] Centro de Química Estrutural (CQE), Instituto Superior Técnico, Universidade de Lisboa, Av. Rovisco Pais, Lisboa, Portugal; [c] Portuguese Diabetes Association Education and Research Center (APDP-ERC), Lisboa, Portugal; [d] Departamento de Ciências Médicas, Universidade de Aveiro, Aveiro, Portugal; [e] Department of Nephrology, Hospital Fernando Fonseca, Lisboa, Portugal; [§] Corresponding author

Abstract

Background: The recent growing evidence that the proximal tubule underlies the early pathogenesis of DKD is unveiling novel and promising perspectives. This pathophysiological concept links tubulointerstitial oxidative stress, inflammation, hypoxia, and fibrosis with the progression of DKD. In this new angle for DKD, the prevailing molecular mechanisms on proximal tubular cells emerge as an innovative opportunity for prevention and management of DKD as well as to improve diabetic dysmetabolism.

Summary: The mercapturate pathway is a classical metabolic detoxification route for xenobiotics that is emerging as an integrative circuitry detrimental to resolve tubular inflammation caused by endogenous electrophilic species. Herein we review why and how it might underlie DKD.

Key Messages: The mercapturate pathway is a hallmark of proximal tubular cell function, and cysteine-*S*-conjugates might represent targets for early intervention in DKD. Moreover, the biomonitoring of urinary mercapturates from metabolic inflammation products might be relevant for the implementation of preventive/management strategies in DKD.

Keywords: Cysteine-*S*-conjugates · Diabetic nephropathy · Mercapturic acids · *N*-Acetyltransferase-8 · Renal proximal tubular cells

Summary and Perspectives in Mercapturate Involvement in DKD

The inability of proximal tubular cells to detoxify Cys-*S*-conjugates, through NAT8 activity, might perpetuate metabolic inflammation and dysmetabolism and supports that the mercapturate pathway underlies the tubulocentric perspective of DKD. This dysfunction in proximal tubular cell activity can be monitored through the quantification of mercapturates of Cys-*S*-conjugates in urine.

A better understanding of the mercapturate pathway impairment triggering early DKD is necessary. Such knowledge may help to find out new therapeutic approaches and strategies for early prediction and biomonitoring of DKD.

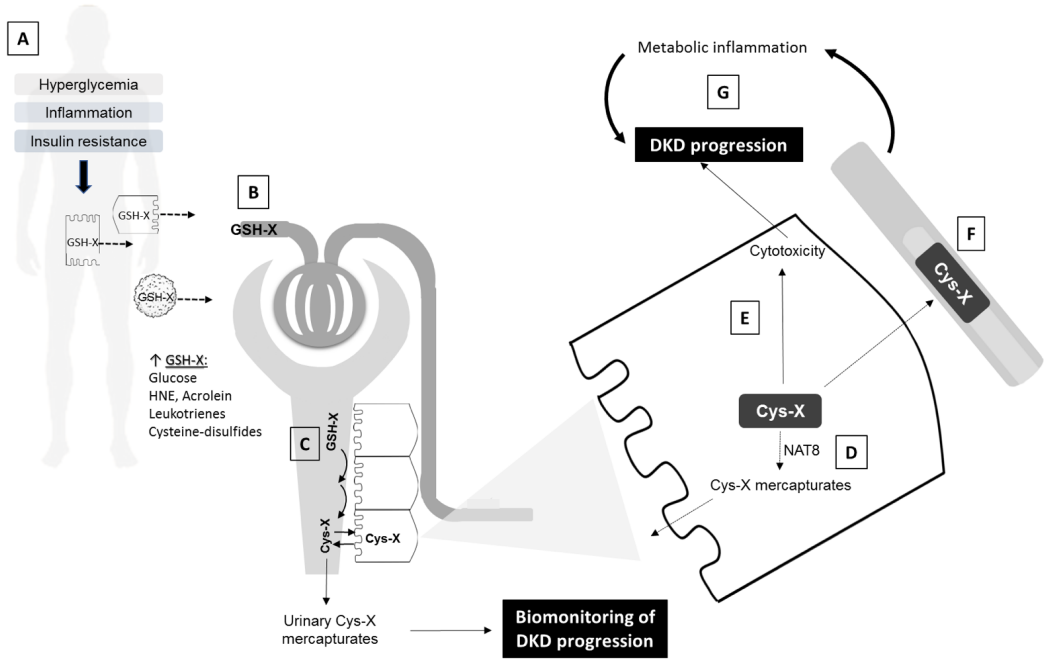

Figure 5 – Mechanistic hypothesis of MAP role in the tubulocentric view of diabetic kidney disease (DKD) billed up on literature review herein presented. (a) GSH-*S*-conjugates (GSH-X) of electrophiles increase in inflammatory conditions in both immune and nonimmune cells, (**b**) being excreted into the bloodstream and have a short half-life due to its rapid (c) metabolization at the external apical membrane of proximal tubular cells. The generated cysteine-*S*-conjugate (Cys-X) may have one of 3 fates. (**d**) They may be detoxified by *N*-acetyltransferase 8 (NAT8), generating mercapturates that are eliminated in urine, (**e**) they may be bioactivated to highly cytotoxic species or (**f**) they may be reabsorbed into the bloodstream, (**g**) perpetuating metabolic inflammatory processes and DKD progression (Gonçalves-Dias *et al.*, 2019).
Cys-X: cysteine-*S*-conjugate; DKD: diabetic kidney disease; GSH-X: glutathione-*S*-conjugate; HNE: 4-hydroxynonenal; NAT8: *N*-acetyltransferase 8.

GENERAL & SPECIFIC AIMS

GENERAL and SPECIFIC AIMS

The general aim was to discover a bioindicator of progression of tubular kidney disease and contribute to the knowledge of NAT8 function in the mechanisms underlying kidney tubular dysfunction with different etiologies.

The current work is focused on the evaluation of renal handling of the endogenous Cys-*S*-conjugates that are disulfides (CysSSX).

Specifically, this work intended to:

- develop and validate a phenotyping method for NAT8 activity (**Chapter I**);
- quantify the renal tubular detoxification of CysSSX in animal models of drug-induced AKI, comparing drugs that undergo the mercapturate pathway (CISP) and those that do not (G) (**Chapter II**);
- investigate the effect of antiretroviral drugs on the excretion of mercapturates of CysSSX in HIV-infection and other factors of variability for CysSSX detoxification as well as prospectively evaluate changes in the detoxification of CysSSX with the progression of kidney disease (**Chapter III**);
- investigate Cys availability and dynamics and the temporal variation of mercapturates of CysSSX in two animal models of pre-diabetes (**Chapter IV**) and a model of hypertension (**Chapter V**).

CHAPTER I

A mechanistic-based approach to non-invasively quantify the kidney ability to detoxify cysteine-disulfides

CHAPTER I

A mechanistic-based approach to non-invasively quantify the kidney ability to detoxify cysteine-disulfides

I.1. Rationale & Objectives

The first specific objective of our work was to develop a method that would allow us to phenotype the activity of NAT8. We focused on CysSSX as evidence shows that, similarly to the Cys-*S*-conjugates which are thioethers rather than disulfides (CysSCX), CysSSX might be detoxified by the action of NAT8 (Deol and Josephy, 2017). Thus, we hypothesized that the quantification of mercapturates of CysSSX will be indicative of the capability of kidney to detoxify CysSSX and NAT8 activity. The contribution of CysSSX for disulfide stress signaling and its effects in kidney are still to be unveiled, but it might contribute to an adaptive response to an acute insult (Moreno *et al.*, 2014; Coelho *et al.*, 2018). Our general aim was to find out a strategy to non-invasively measure tubular disulfide stress in kidney. Thereby, we developed a method to quantify mercapturates of CysSSX (*N*-acetyl-CysSSX) in urine samples (**Figure I.1**) and we applied it to evaluate the capability of kidney to detoxify CysSSX in rodents, volunteers and patients after an episode of AKI.

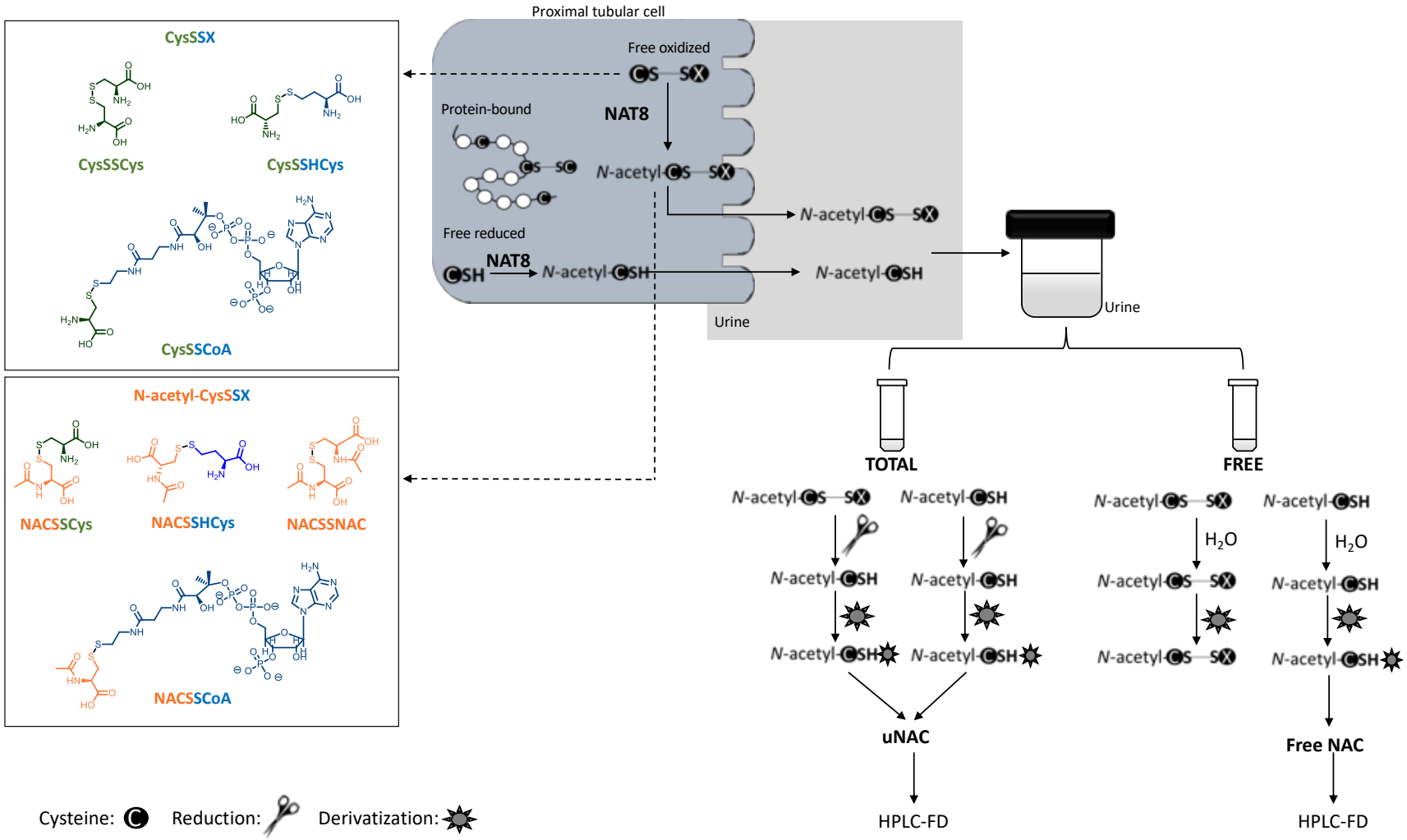

Figure I.1 – Rationale for method development. Cysteine-disulfides (CysSSX) are detoxified by N-acetyltransferase 8 (NAT8) forming mercapturates (N-acetyl-CysSSX) that are eliminated in urine. The developed method was able to quantify urinary mercapturates of cysteine-disulfides, using uNAC as a surrogate. The method takes advantage of a reducing agent that selectively reduces disulfide bonds followed by derivatization with a selective fluorescent reagent for thiol groups. uNAC can then be monitored through fluorescence detection in a high-performance liquid chromatography system (HPLC-FD). This strategy allowed the quantification of both reduced cysteine and oxidized cysteine-disulfides. For the measurement of the free NAC, the same protocol is followed, although with no addition of the reducing agent, allowing the derivatization of only the naturally free NAC.

CoA: coenzyme A; Cys: cysteine; CysSSX: cysteine-disulfides; HCys: homocysteine; HPLC-FD: high-performance liquid chromatography with fluorescence detection; NAC: N-acetylcysteine; N-acetyl-CysSSX: mercapturates of cysteine-disulfides; NAT8: N-acetyltransferase 8; uNAC: urinary surrogate of mercapturates from cysteine-disulfides.

I.2. Methods

I.2.1. Method development

The formation of CysSSX occurs through a disulfide bond between Cys with other LMW thiol-containing molecule, including GSH, Cys, CoA or HCys yielding CysSSG, CysSSCys, CysSSCoA and CysSSHCys, respectively (Wang and Ballatori, 1998; Moreno *et al.*, 2014; Coelho *et al.*, 2018).

Our strategy, aimed to evaluate the capability of kidney to detoxify CysSSX and to address renal disulfide stress, was based on three basic premises: a) insult-triggered disulfide stress in kidney increases CysSSX formation (Coelho *et al.*, 2018); b) Cys-*S*-conjugates are acetylated by NAT8 activity and are eliminated in urine as mercapturates (Veiga-da-Cunha *et al.*, 2010; Deol and Josephy, 2017); and c) NAT8 is almost exclusively expressed in kidney and is related to kidney function (Juhanson *et al.*, 2008; Chambers *et al.*, 2010; Veiga-da-Cunha *et al.*, 2010). This encouraged us to develop a method to quantify urinary mercapturates of CysSSX (*N*-acetyl-CysSSX) (**Figure I.1**).

For that, we used a reducing agent, tris(2-carboxyethylphosphine) (TCEP), that allows the selective reduction of disulfide bonds, converting the oxidized form to the corresponding reduced thiol, i.e. *N*-acetylcysteine (**Figure I.1**) (Burns *et al.*, 1991). We named as uNAC the *N*-acetylcysteine moiety formed upon reduction of urinary *N*-acetyl-CysSSX and we used it as a surrogate of *N*-acetyl-CysSSX (**Figure I.1**). By using a fluorescent reagent selective for thiol groups, 7-fluorobenzofurazan-4-sulfonic acid ammonium salt (SBD-F) (Imai, Toyo'oka and Watanabe, 1983), uNAC can be quantified through fluorescence detection (FD), affording high sensitivity to the method (Grilo *et al.*, 2017). The coupled chromatographic step allows the separation of uNAC from the other endogenous thiols such as cysteine-glycine (CysGly), GSH, Cys, CoA, cysteamine and HCys (sections I.2.2.3. and I.2.2.4.).

We have evaluated the ability of the method to distinguish uNAC from NAC in urine (section I.2.3.7.). Moreover, we ascertain that the uNAC that is being quantified is a surrogate of *N*-acetyl-CysSSX that is excreted from renal tubular cells and not from other cells further undergoing glomerular filtration. To this end, we quantified the levels of uNAC in serum samples from volunteers, following the protocols described in sections I.2.2.3. and I.2.2.4. (**Figure I.1**). The levels of free NAC were also quantified, employing the protocol described in section I.2.3.7. (**Figure I.1**). Actually, if uNAC formed at the

hepatocytes is excreted in bile and not in plasma with subsequent filtration by the glomerulus, the levels of uNAC would not be detectable in serum samples.

Serum samples were collected from volunteers with normal kidney function, as confirmed by a glomerular filtration rate higher than 90 mL/min/1.73m^2.

I.2.2 Method description

I.2.2.1. Chemicals

High-performance liquid chromatography (HPLC)-grade solvents were purchased from *VWR* (Belgium). All reagents were purchased from *Sigma-Aldrich* (USA), except for trichloroacetic acid (TCA), which was purchased from *Roth* (Germany).

I.2.2.2. Stock and calibration solutions

Calibration solutions (CS) were prepared from successive dilutions in phosphate buffered saline (PBS 1x) to obtain eight different concentrations of NAC, namely, 2.1875, 6.25, 12.5, 18.75, 25, 150, 400 and 600 µM.

I.2.2.3. Reduction and derivatization

An initial volume of 50 µL of each CS, quality control solution (QC) or sample were treated with TCEP (100 g/L, 5 µL) in reverse osmosis water for reduction of disulfide bonds. After an incubation period of 30 min at room temperature (RT), proteins were precipitated by mixing with 45 µL of TCA (100 g/L) in 1 mM ethylenediaminetetraacetic acid (EDTA). The mixture was then centrifuged (13,000 *g*, 10 min, 4 ˚C) and the supernatant collected into a new tube containing 5 µL of 1.55 M sodium hydroxide, 62.5 µL of 125 mM sodium tetraborate buffer (pH 9.5) with 4 mM EDTA, and 25 µL of SBD-F (1 g/L) prepared in the same buffer. The final mixture was vortexed and incubated in the dark, at 60 °C for 1 h, to complete derivatization of free sulfhydryl groups.

I.2.2.4. Chromatographic conditions

The solutions prepared as described in section 2.2.3. were analyzed by HPLC-FD on a Shimadzu LC-10AD VP (Shimadzu Scientific Instruments Inc) system, using a reversed-phase C18 LiChroCART 250x4 column (LiChrospher 100 RP-18, 5µm, VWR, USA), at 29 °C, as previously described (Nolin, McMenamin and Himmelfarb, 2007; Grilo *et al.*, 2017). The detector was set at excitation and emission wavelengths of 385 and 515 nm, respectively. The mobile phase consisted of 100 mM acetate buffer (pH 4.5) and methanol (MeOH) [99:1 (v/v)]. The analytes were separated in an isocratic elution mode, at a flow rate of 0.8 mL/min for 20 min.

I.2.3. Method validation

The validation criteria were defined according to standard procedures for bioanalytical methods (European Medicines Agency, 2012). For this purpose, the criteria assessed included linearity, lower limit of quantification (LLOQ), higher limit of quantification (HLOQ), and four QC samples were prepared to obtain concentrations independently from CS. Selectivity, carry-over effect, accuracy, intra- and inter-assay precision and stability after freezing cycles were also evaluated.

I.2.3.1. Selectivity and carry-over effect.

Blank samples of PBS, MeOH or mobile phase were prepared as described in section 2.2.3. The carry-over effect was studied by preparing and injecting into the HPLC system three blank samples of PBS after the analysis of the highest CS sample.

I.2.3.2 Linearity

Three calibration curves were prepared from different stock solutions. Each calibration curve contained eight CSs ranging from 2.1875 to 600 µM of NAC (namely, 2.1875, 6.25, 12.5, 18.75, 25, 150, 400 and 600 µM). Linearity was assessed by plotting the curves by linear regression of the chromatographic peak area (mAU*min) as a function of NAC concentration (µM). The average back-calculated concentrations were also assessed. The slopes and Y-intercept of the curves were compared in order to access reproducibility.

I.2.3.3. Lower and higher limits of quantification

The LLOQ was defined as the lowest concentration of NAC that could be quantified with acceptable accuracy and precision. For this, six samples with a concentration of 2.1875 µM were analyzed for the accuracy and the intra- and inter-assay precisions. Additionally, the same was performed for the validation of the HLOQ.

I.2.3.4. Accuracy

Accuracy was defined as the closeness to the theoretical concentration of the QC samples. To study the accuracy of the method, six samples from the LLOQ and the HLOQ, as well as four QC samples with concentrations within the established concentration range (QC1 = 3.125 µM; QC2 = 9.375 µM; QC3 = 50 µM and QC4 = 300 µM) were analyzed. The accuracy of the method was calculated as the ratio between the measured and theoretical concentrations, expressed in percentage.

I.2.3.5. Intra- and inter-assay precision

The precision of the method was defined as the closeness between multiple measures. Intra- and inter-assay precision were assessed by analysis of six samples of LLOQ, HLOQ and QC. While intra-assay precision was assessed by the coefficient of variation (CV) obtained from analytical runs on the same day, the inter-assay precision was evaluated using the CV obtained on different days. The calculation of the precision was performed assuming that its value would ideally be 100%, subtracting the obtained CV.

I.2.3.6. Stability and storage conditions

Stability tests were carried out to ensure that the concentration of uNAC is not affected during sample preparation, sample analysis or even during storage. To this end, urine samples from volunteers were collected to a) readily quantify uNAC; b) store at RT for 2 h and for 6 h; c) store at 4 °C for 2 h and for 6 h; and d) store at -80 °C and unfreeze. The stability was also investigated in samples stored at -80 °C for 1, 6 and 12 months after collection.

I.2.3.7. Quantification of uNAC vs. free NAC

The ability to differentiate uNAC from free NAC in urine was also evaluated (**Figure I.1**). Thiols might be present in urine in different fractions, the protein-bound and the unbound/free fractions, which includes disulfides and free reduced forms (Grilo *et al.*, 2017; Sutton *et al.*, 2018).

To measure each fraction, we adapted the protocol previously described (Grilo *et al.*, 2017) (**Figure I.1**). The sum of all fractions corresponds to the total urinary NAC content, herein called uNAC. To quantify free NAC that do not require the reducing step, as it is present in its reduced sulfhydryl form, freshly collected urine samples from volunteers, referred in section 2.1, were firs submitted to protein precipitation with TCA, followed by centrifugation (13,000 g, 10 min, at 4 °C). Then, samples were incubated with reverse osmosis water for 30 min at RT. The use of reverse osmosis water instead of the reducing agent TCEP allows the posterior derivatization exclusively of the naturally free NAC (**Figure I.1**), following the protocol described in section I.2.2.3. For quantification of uNAC, a surrogate of mercapturates derived from CysSSX, samples from the same volunteers were analyzed by performing the protocol described in I.2.2.3.

I.2.4. Method applicability

I.2.4.1. uNAC in urine of rats and mice

Experiments were performed using male Wistar Crl:WI (Han) and male C57BL/6 mice obtained from the NOVA Medical School rodent facility. Animals were housed in polycarbonate cages with wire lids and maintained under standard laboratory conditions as follows: artificial 12 h light/dark cycles at RT. Animals were maintained on a standard laboratory diet (SDS diets RM1 for rats and RM3 for mice, Special Diets Services) and reverse osmosis water, both *ab libitum*. While the RM1 diet has 2.2 g/Kg of methionine and 2.4 g/Kg of CysSSCys, the RM3 diet has 3.6 g/Kg of methionine and 3.5 g/Kg of CysSSCys. Urine samples were collected at different time-points. Animals were specific-pathogen-free according to Federation for Laboratory Animal Science Associations (FELASA) recommendations (Mähler *et al.*, 2014). All applicable institutional and governmental regulations concerning the ethical use of animals were followed, according to the NIH Principles of Laboratory Animal Care (NIH Publication 85 23, revised 1985), the European guidelines for the protection of animals used for scientific purposes

(European Union Directive 2016/63/EU) and the Portuguese Law nº 113/2013. The experimental procedures received prior approval by the Institutional Ethics Committee of the NOVA Medical School for animal care and use in research (protocol nº 15/2017/CEFCM) for rats and Portuguese Directorate-General for Food and Veterinary that regulates the animal care and use in research (protocol nº 0421/000/000/2017) for mice.

The levels of uNAC were obtained using the procedure described in section I.2.2.3 and I.2.2.4.

I.2.4.2. uNAC in patients with kidney disease

To obtain a proof-of-principle of the impact of kidney dysfunction in uNAC, its levels were quantified in urine samples from patients after an episode of AKI employing the same procedure described in sections I.2.2.3. and I.2.2.4. The levels of uNAC were then compared with the levels obtained in urine samples from volunteers (quantified in section I.2.3.7.).

I.2.5. Statistical analysis

Statistical analysis was performed using GraphPad Prism® version 5.0 (GraphPad Software Inc., San Diego, CA, USA). Data are presented in percentage, mean ± standard error of the mean (SEM) or mean ± standard deviation (SD) or median ± interquartile range (IQR), whenever applicable. Variability among data is expressed in CV. The *F*-test was used to explore differences between the slopes and elevations of the calibration curves and to ascertain the influence of the concentrations on the chromatographic signal area. Comparisons among groups were performed using paired t-test, unpaired t-test or one-way ANOVA, whenever applicable. Significance was set at $p < 0.05$.

I.3. Results & Discussion

I.3.1. Method development

To establish if uNAC can be used as a surrogate of CysSSX excreted by kidney tubular cells, by the action of NAT8, serum samples from five volunteers (median [IQR] age of 39 [28-54] years old, 60% men, all Caucasian) were submitted to the protocol, described in sections I.2.2.3. and I.2.3.7. for quantification of uNAC and free NAC, respectively. Neither uNAC nor free NAC were found in all serum samples tested (**Figure I.2**). This suggests that uNAC is a marker of *N*-acetylation of CysSSX in the kidney. It is known that cysteine-*S*-conjugates are acetylated by NAT8 which is predominantly expressed in human kidney tubular cells, being also present in substantially lower levels in hepatocytes (Chambers *et al.*, 2010). The absence of uNAC in serum might indicate that either the mercapturates from the liver are formed in small amounts and/or they are excreted into the bile and thus not found in circulation. As such, uNAC present in urine, i.e. the *N*-acetyl-CysSSX, are not derived from the glomerular filtrate but rather from tubular cells where the expression of NAT8 is the highest (Chambers *et al.*, 2010).

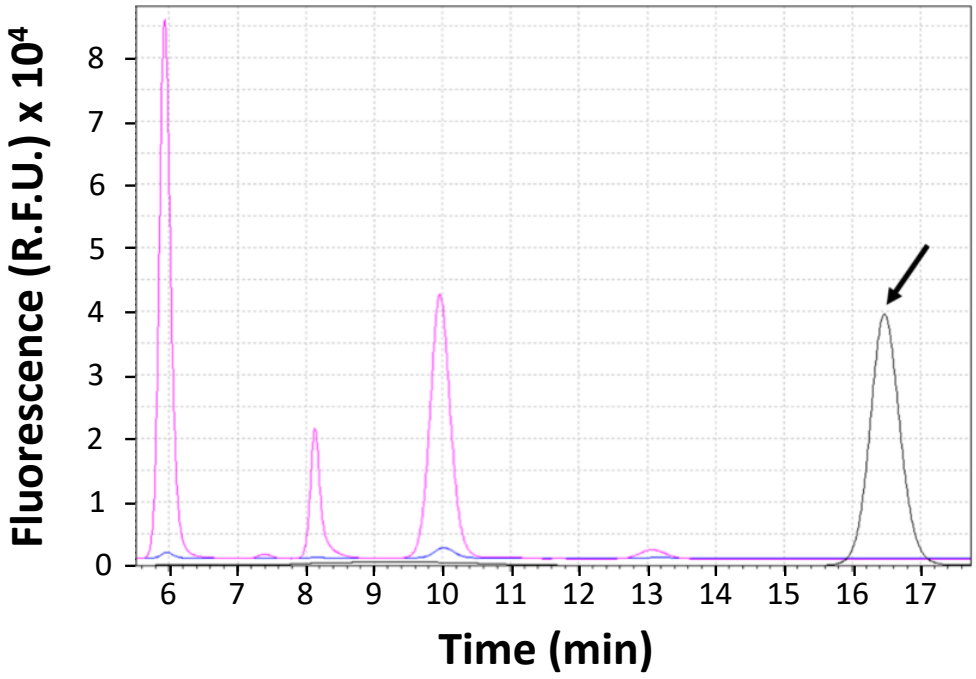

Figure I.2 – Representative chromatograms of NAC (black arrow). No uNAC or free NAC were detected in serum samples. In black, a chromatogram for calibration solution; In pink, uNAC (oxidized + reduced + protein-bound fractions) and in blue, free NAC fraction in a serum sample of a volunteer.

The methodology used is able to measure the total fraction of mercapturates from CysSSX (the free and protein-bounded). However, to the best of our knowledge, protein *N*-acetyl-

cysteinylation by NAT8 has never been described in literature. Nonetheless, as CysSSP, i.e. the formation of a disulfide bond between a free Cys and a Cys residue in proteins, was described in kidney (Coelho *et al.*, 2018), these conjugates will be plausible substrates of NAT8. Nevertheless, since urine from healthy kidneys is not enriched in proteins, we have not addressed this topic in this work. This can be easily performed by promoting protein precipitation prior to the reducing step and should be evaluated in models of kidney disease.

Free NAC was also not expected to be observed, taking into consideration previous reports showing that free NAC levels are only detectable in serum or plasma samples after oral administration of the drug *N*-acetylcysteine (Tsikas *et al.*, 1998).

In fact, the acetylation of Cys in the kidney seems to be the only process whereby endogenous NAC is produced. This explains the fact that NAC can only be found in urine but not in plasma (Hannested and Sörbo, 1979). Therefore, the obtained results support that the approach herein employed is able to distinguish *N*-acetyl-CysSSX formed in tubular cells from those formed in hepatocytes, by measuring uNAC in urine.

I.3.2. Method description

I.3.2.1. Optimization of reduction and derivatization steps

The general approach for the quantification of thiols initially requires the generation of free thiols from disulfides, a process accomplished by the use of a reducing agent such as TCEP (Burns *et al.*, 1991). This step is required for quantification of the total and of the oxidized fractions of thiols (free and protein-bound, as this is the only way for the sulfhydryl groups to be available for subsequent derivatization). Other authors have taken advantage of the properties conferred by TCEP (Kuśmierek and Bald, 2008), while the quantification was performed in a reversed-phase ion-pair liquid chromatography with ultraviolet (UV) absorption at 355 nm. Herein, we employed FD to minimize the interferences from other biological substances characteristic of absorption methods, especially in the UV range (Peng *et al.*, 2012).

On the other hand, thiols have physicochemical properties, including high polarity and water-solubility, that renders their extraction from biological matrices nearly impossible without a derivatization process (Kuśmierek *et al.*, 2009). As thiols are not spontaneously

fluorescent (Jakubowski and Głowacki, 2011), this step needs to be performed with a fluorescent probe that selectively reacts with the free sulfhydryl group of the thiol in order to generate a derivative that is strongly fluorescent, hence enabling a highly sensitive and precise measurement (Imai, Toyo'oka and Watanabe, 1983; Kuśmierek *et al.*, 2009).

Taking advantage of a previously reported method (Grilo *et al.*, 2017), we added NAC to the analytical run and were able to reduce the initial volumes of samples, CS and reagents to half of those previously employed without any changes in the chromatographic peak area.

I.3.2.2. Optimization of chromatographic conditions

The development of this methodology required the optimization of several chromatographic conditions namely a) mobile phase – isocratic elution using different concentrations of acetate buffer with MeOH in several proportions; b) stationary phase – two C18 columns of different lengths were tested (LiChroCART 125-4 and C18 LiChroCART 250x4) with different temperatures (from 23 to 35 °C) and c) flow rate – 0.6 and 0.8 mL/min were tested. As far as we know, this is the first method specifically developed with the goal of quantifying the mercapturates of CysSSX.

Using an isocratic elution with 1% MeOH in 100 mM acetate buffer (pH 4.5) on a C18 LiChroCART 250x4 column at 29 °C, the chromatographic peak of NAC eluted at 16.5 min, totally separated from the retention time of the remaining thiols (Cys: 5.9 min, HCys: 8.1 min; CysGly: 10.0 min; cysteamine: 10.5 min CoA: 11.8 min and GSH: 13.1 min).

A few methods have been developed for pharmacokinetics studies of the drug *N*-acetylcysteine that would also allow the quantification of uNAC, even though laborious, require high amounts of sample and employ other reducing and labelling agents (Hannested and Sörbo, 1979; Ventura *et al.*, 1999; Kuśmierek and Bald, 2008). However, it is important to highlight that these methods were not developed to investigate *N*-acetyl-CysSSX nor its potential as non-invasive indicators of renal injury. One of the plausible reasons to explain the absence of studies investigating the meaning of altered levels of *N*-acetyl-CysSSX in urine might be the lack of information regarding NAT8 and disulfide stress, that is recent as is their relation with renal function (Juhanson *et al.*, 2008; Chambers *et al.*, 2010; Veiga-da-Cunha *et al.*, 2010; Moreno *et al.*, 2014; Coelho *et al.*, 2018).

The novelty of our approach is based on the association between disulfide stress and increased CysSSX with NAT8 activity and their detoxification as mercapturates. This is, in fact, the first report aiming at the quantification of uNAC as a surrogate of the urinary mercapturates derived from CysSSX and that provides first-hand evidence that its formation occurs in the kidney.

I.3.3. Method validation

I.3.3.1. Selectivity and carry-over effect

The injection of blank samples of PBS, MeOH or mobile phase (100 mM acetate buffer (pH 4.5) and MeOH [99:1 (v/v)]) showed no interference with uNAC. Additionally, the injection of three blank samples after the higher CS (600 µM) showed no carry-over effect.

I.3.3.2. Linearity

Linearity was assessed using three calibration curves containing eight CSs ranging from 2.1875 to 600 µM of NAC. Linear regression proved to be the most suitable model for fitting the experimental data (*Runs Test,* $p > 0.05$). The concentration of the standard samples significantly influenced the chromatographic signal area (*F* test $p < 0.001$). Additionally, no differences were found between the slopes and elevations of the calibration curves. The correlation coefficients, r^2, of the calibration curves were >0.99, showing a good adjustment of all calibration curves. The 95% confidence interval for the intercept contained zero, indicating that the concentration of the CSs was the only factor with significant influence on the chromatographic peak area.

The observed back-calculated values were close to the expected ones at each tested concentration. The CVs were lower than 13% for higher and lower limits and 12% for the remaining standards.

I.3.3.3. Lower and higher limits of quantification

The LLOQ was set at 2.1875 µM, and the CV of multiple measurements was 5%. Although concentrations lower than 2.1875 µM were also tested, the chromatographic peaks were not distinguishable from background noise. This LLOQ allows the quantification of NAC at urinary levels reported (Mårtensson and Hermansson, 1984). The HLOQ was defined at 600 µM, with CV of several measures lower than 12%. The accuracy and intra- and inter-assay precisions of LLOQ and HLOQ are presented in **Table I.1**.

Table I.1 – Mean accuracy, intra- and inter-assay precision of the method.

Sample (µM)	Accuracy (%)	Intra-assay precision (%)	Inter-assay precision (%)
LLOQ (2.1875)	96	96	95
QC1 (3.125)	98	95	96
QC2 (9.375)	104	97	95
QC3 (50)	105	98	98
QC4 (300)	110	96	98
HLOQ (600)	102	97	88

HLOQ: higher limit of quantification; LLOQ: lower limit of quantification; QC: quality control solution

I.3.3.4. Accuracy

The accuracy ranged from 87 to 114% for LLOQ and HLOQ and from 102 to 112% for QC samples (**Table I.1**).

I.3.3.5. Intra- and inter-assay precision

The intra-assay precision was 96% and 97% for LLOQ and HLOQ, respectively, and 95-98% for the remaining QCs. As for the inter-assay precision, the obtained values were 88 and 95% for the LLOQ and HLOQ and 95-98% for the QCs (**Table I.1**). The obtained results further support the use of this method to quantify with accuracy and precision the levels of uNAC in biological samples.

I.3.3.6. Stability and storage conditions

The variations in uNAC levels in urine samples subjected to different storage conditions are presented in **Table I.2**. No significant differences were found in uNAC concentrations obtained for all samples from the same volunteer under the several tested conditions.

Table I. 2– Stability of uNAC in urine samples from volunteers subjected to different storage conditions.

	Condition							
Temperature	RT		4 °C		-80 °C			
Time	2 h	6 h	2 h	6 h	24 h	1 m	6 m	12 m
uNAC [a] (%)	104 ± 5	107 ± 5	98 ± 4	113 ± 3	109 ± 4	117 ± 5	106 ± 6	97 ± 6

[a] Mean ± SEM; uNAC expressed as % of values quantified readily after collection; h: hour; m: month; RT: room temperature; uNAC: urinary surrogate of mercapturates from cysteine-disulfides

The presented results are particularly important for clinical studies, where the logistics of sample procurement, its storage, lifecycle and delivery to the laboratory are often difficult to manage. Similarly to mercapturates of endogenous CysSSX, the levels of several mercapturates derived from both endogenous (e.g. acrolein, 4-hydroxy-2-nonenal) and exogenous substances (e.g. flupirtine, 1-vinyl-2-pyrrolidones, thioTEPA, acrylamide, acrylonitrile, benzene, 1,3-butadiene, crotonaldehyde, ethylene, ethylene oxide, *N*,*N*-dimethylformamide, vinyl chloride, propylene oxide, styrene, toluene, propylene oxide) were found to be fairly stable when subjected to different storage conditions or several freeze-thaw cycles (Alary *et al.*, 1998; Van Maanen and Beijnen, 1999; Schettgen, Musiol and Kraus, 2008; Cosnier *et al.*, 2012; Pluym *et al.*, 2015; Scheuch *et al.*, 2015; Bertram, Schettgen and Kraus, 2016).

I.3.3.7. Quantification of uNAC vs. free NAC

Urinary levels of uNAC (58 [44-69] µM) were higher than free NAC (9 [8-13] µM) (Paired t-test, $p = 0.001$). The levels of free NAC represent 13-24% of uNAC (**Table I.3**).

Table I.3 – Quantification of uNAC vs. free NAC in urine samples from volunteers.

Sample	Age	Sex	uNAC (µM)	free NAC (µM)	free NAC (% of uNAC)
1	27	F	67	12	18
2	29	M	70	14	20
3	68	M	33	8	24
4	39	F	58	9	16
5	39	M	54	7	13

F: female; M: male; uNAC: urinary surrogate of mercapturates from cysteine-disulfides; NAC: *N*-acetylcysteine

The presence of endogenous free NAC in urine samples was already reported in volunteers (Hannested and Sörbo, 1979). Free NAC levels in urine varied from 3 to 7 µM and represented 18-26% of uNAC, results that are in accordance with our findings. In fact, the acetylation of Cys in the kidney seems to be the only process whereby endogenous free NAC is present in urine (Hannested and Sörbo, 1979), although this represent a small contribution to uNAC. The presence of free NAC in urine has been also described as a result of oral administration of NAC (Shih and Schulman, 1969).

Our results support the hypothesis that CysSSX might undergo acetylation by NAT8, forming mercapturates that are eliminated in urine. uNAC can hence be used as a surrogate of these mercapturates and the difference between free NAC and uNAC results from this acetylation step.

I.3.4. Method applicability

I.3.4.1. uNAC in urine of rats and mice

The levels of uNAC were quantified in urine samples from rat (n=13 male rats, 12 weeks of age, mean ± SD body weight, BW, 303 ± 28 g) and mouse (n=13 male mice, 5 weeks of age, 19 ± 2 g BW). There were no temporal differences in uNAC levels for both species (**Figure I.3**). uNAC levels found in both rat and mouse samples are higher than the ones quantified in human samples. These results might indicate that there are species differences regarding the elimination of uNAC and hence the mercapturate pathway. In fact, rat livers dosed with l-chloro-2,4-dinitrobenzen excreted lower amounts of its mercapturate and higher quantity of the GSH-conjugate in bile whereas the opposite was found in guinea pig livers (Hinchman *et al.*, 1991). On the other hand, the metabolism of acrylamide in humans is apparently more prone for GSH conjugation rather than conversion to glycidamide when compared with rats and mice (Li *et al.*, 2016). Differences on the expression of the enzymes of the mercapturate pathway have also been reported. For instance, rats and mice have very low hepatic but very high renal activities of GGT in comparison with guinea pig, pig, macaque monkey and man (Hinchman and Ballatori, 1990). Species differences were also found for dipeptidases activity, although in a lower magnitude than the one observed for GGT (Hinchman and Ballatori, 1990).

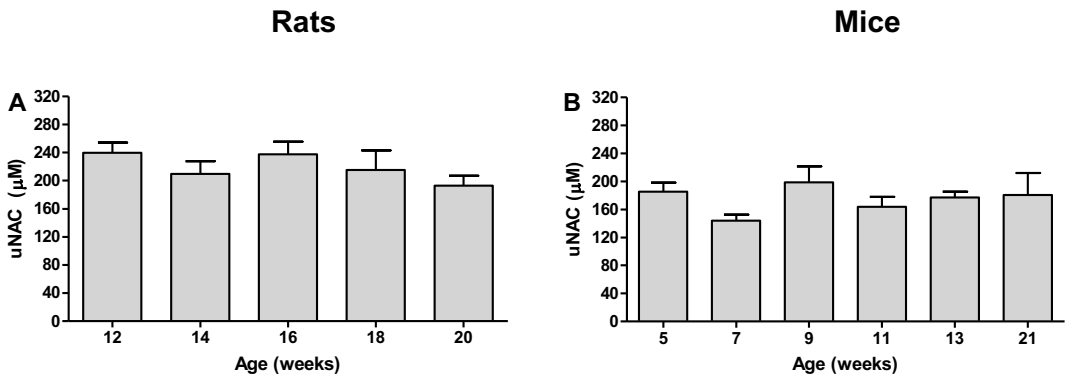

Figure I.3 – Temporal variation of uNAC in urine samples from rats (A) and mice (B). The intra-individual variability in uNAC levels was low in control conditions for both species (n= 5 to 13 per week).
uNAC: urinary surrogate of mercapturates from cysteine-disulfides.

I.3.4.2. uNAC in patients with kidney disease

uNAC levels were quantified in four patients after an episode of AKI. Anthropometric and clinical data are presented in **Table I.4**. Lower levels of uNAC were found in urine of patients after an episode of AKI (23 [16-41] µM) in comparison with volunteers (58 [44-69] µM) (Unpaired t-test, $p = 0.016$). All AKI patients progressed to chronic kidney disease. These findings support that uNAC might represent an added value for the diagnosis and monitoring of kidney tubular injury. Nevertheless, an increase in uNAC in this setting was expected as an adaptive mechanism. However, these results require further elucidation, as the samples were not collected neither right after the episode nor at the same time for the 4 patients.

I.4. Conclusions

The developed and validated HPLC-FD method is able to quantify the levels of mercapturates derived from endogenous CysSSX, herein called uNAC. This method might be applied in clinical studies aiming to investigate NAT8 and disulfide stress in kidney tubular dysfunction in man as well as in animal models of kidney tubular disease.

Table I.4 – Anthropometric and clinical data from patients with an episode of AKI.

Patients	A	B	C	D
Age (years)	74	85	56	23
Sex	M	F	F	M
Race	NB	B	NB	NB
Co-morbidities	DM, CVD	CVD	-	CVD
AKI etiology	CRSd	NSAIDs	RPGN (Wegener)	MHT, TMA
AKI SCr (mg/dL)	2.3	3	3.13	4.5
AKI eGFR[a] (mL/min/1.73m^2)	27	16	16	17
AKI grade	2	1	3	3
Urine sampling time (days after AKI)	17	2	17	6
SCr (mg/dL)	2.95	2.19	3.12	4.31
eGFR (mL/min/1.73m^2)	20	23	16	18
uNAC (µM)	45	17	15	28

[a] calculated with CKD-EPI equation using serum creatinine; AKI: acute kidney injury; B: black; CRSd: cardiorenal syndrome; CVD: cardiovascular disease; DM: diabetes mellitus; eGFR: estimated glomerular filtration rate; F: female; M: male; MHT: malignant hypertension; NB: non-Black; NSAIDs: non-steroidal anti-inflammatory drugs; RPGN: rapidly progressive glomerulonephritis; SCr: serum creatinine; TMA: thrombotic microangiopathy; uNAC: urinary surrogate of mercapturates from cysteine-disulfides.

CHAPTER II

Changes in mercapturates of cysteine-disulfides associate to acute kidney injury induced by cisplatin and gentamicin

CHAPTER II

Changes in mercapturates of cysteine-disulfides associate to acute kidney injury induced by cisplatin and gentamicin

II.1. Rationale & Objectives

The kidney is a major target for chemical and drug toxicities. One of the most important functions of the kidney is the clearance of endogenous waste products, but also the metabolism and excretion of exogenous agents (George and Neilson, 2015). This primary role for removing exogenous drugs and toxins makes the kidney vulnerable to develop various forms of injury. AKI is characterized by a rapid decline in kidney function over a period of hours or days. It was demonstrated that AKI determines worse kidney and patient outcomes (Soto *et al.*, 2016). The major cause of intrinsic AKI is acute tubular necrosis that results mainly from ischemic or nephrotoxic injury.

Herein, we used a targeted mechanistic-based approach, centered on the mercapturate pathway as a metabolic controller of CysSSX in kidney tubular cells. Encouraged by the increased formation of disulfides that was described in acute organ failure (Moreno *et al.*, 2014) and knowing that kidney tubular cells are likely to be exposed to high concentrations of CysSSX, we hypothesized that their detoxification would involve the formation of mercapturates that would be a protective factor in AKI. Supported by a literature review we defined the scheme presented in **Figure II.1** and we aimed at quantifying the temporal changes of three urinary metabolites: mercapturates of CysSSX (uNAC, marker of detoxification of Cys-*S*-conjugates that are disulfides plausibly through NAT8 activity), total cysteine (uCys) (measure of CysSSX filtration and reabsorption) and total cysteine-glycine (uCysGly) (measure of GSH turnover) in animal models of AKI-induced by tubular nephrotoxins.

It must be highlighted that both drugs are deleterious for the tubule, but CISP undergoes the mercapturate pathway and G does not, and this justifies the choice of our models. Cys in its reduced state is essential as the rate-limiting synthesis factor of the antioxidant GSH (Rathbun and Murray, 1991). Oxidized glutathione, i.e., GSH-*S*-conjugates, which can be of both endogenous (eg. disulfides, GSSX) (Wang and Ballatori, 1998) and exogenous (eg. CISP, GSH-CISP) (Nunes and Serpa, 2018) sources, might be released mainly by liver and degraded by peripheral tissues that express GGT in the extracellular border of

cell membrane (De Carvalho *et al.*, 2011). This is the first enzyme of the mercapturate pathway, a metabolic circuit that is mainly expressed in kidney tubular cells (Chambers *et al.*, 2010). Extracellularly, GSH-*S*-conjugates are catabolized in CysGly-*S*-conjugates by GGT and Cys-*S*-conjugates by cysteinyl-glycine dipeptidase or aminopeptidase-M, all enzymes that are expressed at the brush border of tubular cells (Hughey *et al.*, 1978; Griffith, 1981; Hanigan, 1998). This Cys-*S*-conjugate, which can be disulfides (CysSSX, eg. CysSSHCys) or not (Cys-CISP), enter the tubular cell. At this stage and under normal conditions, Cys would be reduced, being available to perform its several physiological actions (Bannai and Tateishi, 1986).

Drug-induced toxicity models were herein used as proof-of-concept, but the study of nephrotoxicity is pertinent as it is a problematic burden for health and economy worldwide, affecting 25% of the 100 most used drugs in intensive care units (Taber and Mueller, 2006). In addition, it is one of the major causes leading to candidate drop during the drug discovery process of otherwise pharmacologically relevant molecules (Loghman-Adham *et al.*, 2012).

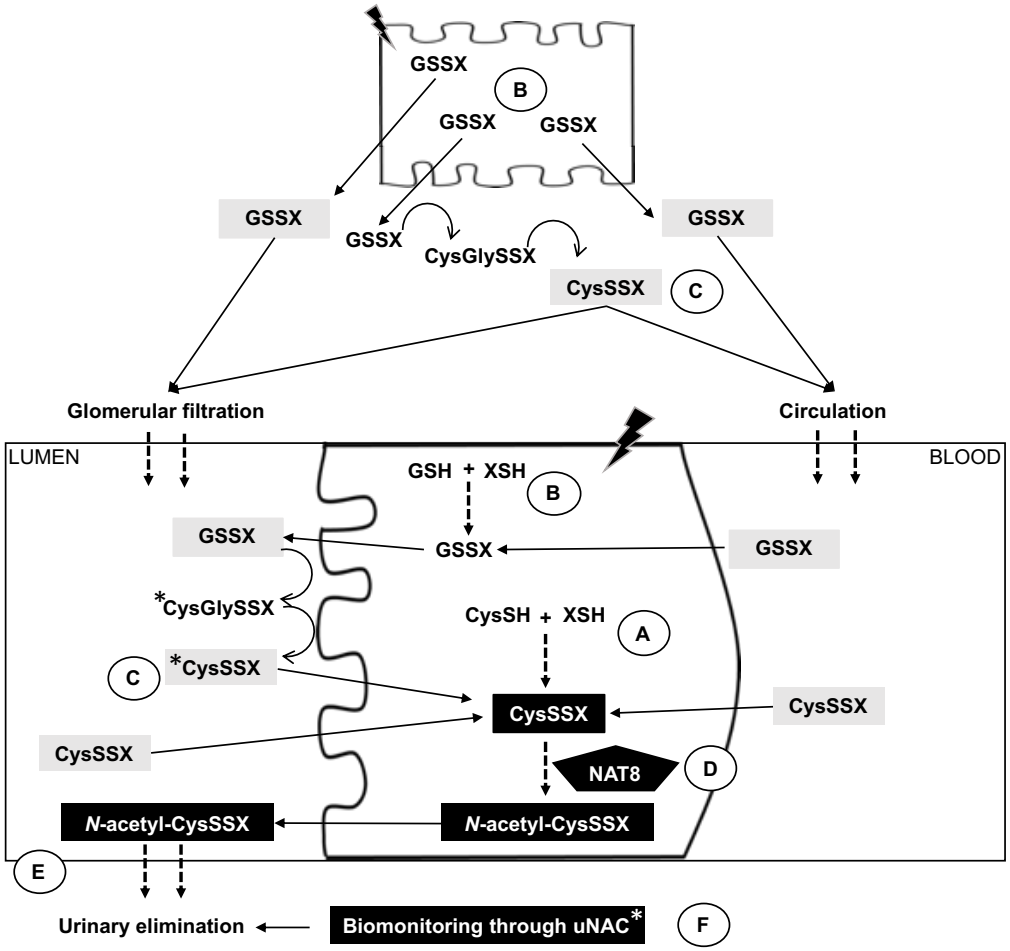

Figure II.1 – Formation of CysSSX and their elimination in proximal tubular cells through the mercapturate pathway. CysSSX increase in tubular cell. (**A**) Oxidative injury triggers the direct formation of CysSSX in proximal tubular cells in a process that is independent of GSH levels. (**B**) CysSSX might also be delivered to proximal tubular cells through the catabolism of GSSX generated intracellularly by any cell. These GSSX are then converted into CysSSX by enzymes expressed at the brush border membrane through the mercapturate pathway. This conversion of GSSX in CysSSX occurs mainly and almost exclusively in kidney tubular cells (**C**). **CysSSX decrease in tubular cell** – The intracellular detoxification of CysSSX seems to be dependent on their acetylation plausibly by NAT8 (**D**), forming mercapturates that are readily eliminated in urine (**E**). The formation of these mercapturates can be monitored through the quantification of uNAC, that is the N-acetyl moiety common to all mercapturates from CysSSX (**F**).
* urinary quantifications performed in this work; CysGlySSX: cystine-glycine-dissulfides; CysSH: cysteine; CysSSX: cysteine-disulfides; GSH: glutathione; GSSX: glutathione-disulfides; N-acetyl-CysSSX: mercapturates of cysteine-disulfides; NAT8: N-acetyltransferase 8; uNAC: urinary surrogate of the mercapturates from cysteine-disulfides; XSH: thiol.

II.2. Animals & Methods

II.2.1. Animals and experimental protocol

Urine samples from AKI animal models (Ferreira *et al.*, 2011) were kindly provided by Dr. Francisco J. López-Hernández from Institute of Biomedical Research of Salamanca (IBSAL) & University of Salamanca (USAL), Department of Physiology and Pharmacology, Salamanca, Spain (**Figure II.2**). Animals were treated in accordance with the *Declaration of Helsinki Principles* and the Guiding Principles in the Care and Use of Animals stated in the international regulations and in the following European and national institutions: *Conseil de l'Europe* (published in the Official Daily N. L358/1-358/6, 18

December 1986), Spanish Government (published in Boletín Oficial del Estado N. 67, pp 8509-8512, 18 March 1988, and Boletín Oficial del Estado N. 256, pp 31349-31362, 28 October 1990). Male Wistar rats (200–250 g, n = 6 *per* group) were allocated under controlled environmental conditions in individual metabolic cages, for 24 h urine samples collection. Rats were randomly divided into three groups: (1) CTL group (CTL), receiving daily vehicle (0.9% NaCl) intraperitoneal for 6 days; (2) gentamicin group (G), receiving gentamicin intraperitoneal (150 mg/kg body weight per day) for 6 days; and (3) cisplatin group (CISP), receiving a single intraperitoneal dose of cisplatin (5 mg/kg body weight *per* day). At the end of the experiment kidneys were perfused by the aorta with saline (0.9% NaCl) and immediately dissected. One kidney was fixed in buffered 3.7% p-formaldehyde for histological studies. Blood samples were also obtained in heparinized capillaries at different time points by a small incision in the tail tip. Plasma was obtained and kept at - 80 ºC until use as well as urine after being cleared by centrifugation.

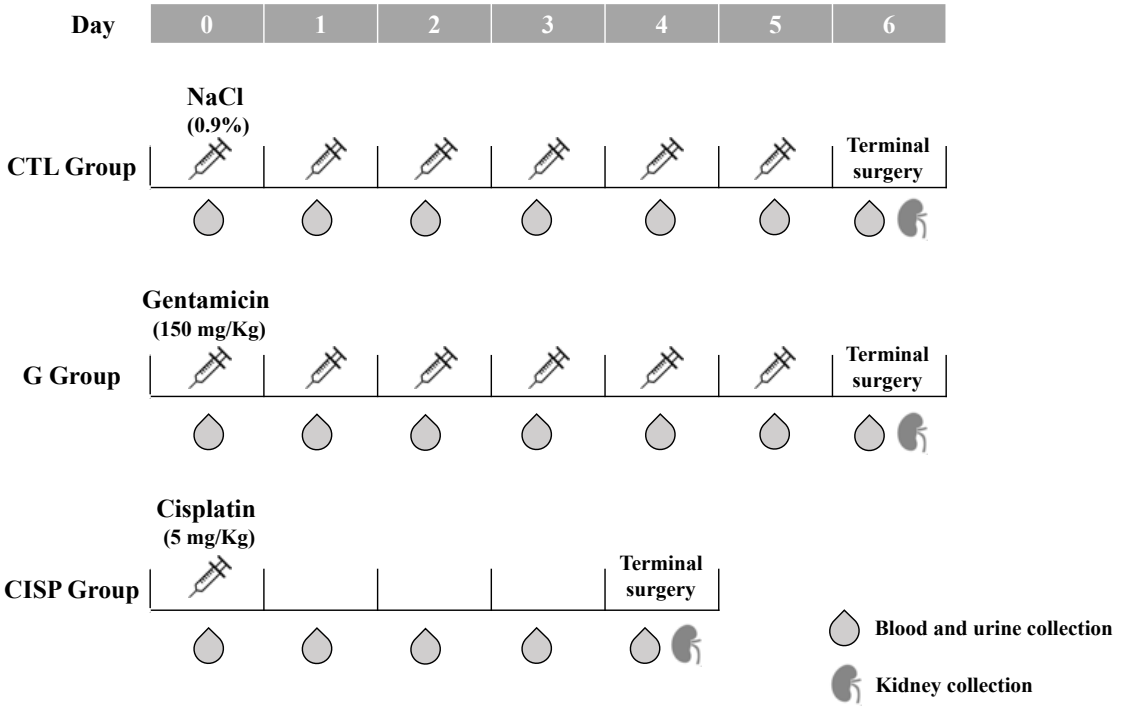

Figure II.2 – Experimental design. Wistar rats (n = 6 animals per group) were allocated under controlled environmental conditions in individual metabolic cages, for 24 h urine samples collection. Rats were randomly divided into three groups: (1) control group (CTL), receiving daily vehicle (NaCl 0.9%) intraperitoneal for 6 days; (2) gentamicin group (G), receiving gentamicin intraperitoneal (150 mg/kg body weight per day) for 6 days; and (3) cisplatin group (CISP), receiving a single intraperitoneal dose of cisplatin (5 mg/kg body weight per day).
CISP: cisplatin; CTL: control; G: gentamicin.

II.2.2. Histological studies

Paraffin blocks were obtained and 5 µm tissue sections were stained with hematoxylin and eosin (H&E). Photographs were taken using an Olympus BX51 microscope connected to an Olympus DP70 color digital camera (Olympus, Barcelona, Spain).

II.2.3. Biochemical measurements

Plasma Cr (pCr) levels were measured using an automated analyzer Reflotron (Roche Diagnostics, Barcelona, Spain).

The levels of uNAC, uCys (as a measure of CysSSX filtration and reabsorption) and uCysGly (as a measure of GSH turnover) were quantified in urine by HPLC-FD (**Chapter I**) (Grilo *et al.*, 2017; Coelho *et al.*, 2018).

II.2.4. Statistical analysis

Statistical analysis was performed using GraphPad Prism® version 7.0 (GraphPad Software Inc., San Diego, CA, USA). Data are presented as mean ± SEM. Whenever applicable, data was analyzed through One-way ANOVA with *Dunnett's* multiple comparisons test or Two-way ANOVA with *Bonferroni's* multiple comparisons test. Statistical significance for all tests was set at the level of $p < 0.05$.

II.3. Results

II.3.1 Characterization of AKI-induced by G and CISP

Severe AKI was associated with high mortality (50%) in the G group, and surviving animals coursed with a small but significant weight loss and polyuria, whereas no mortality was observed in the CISP model. Given that, in most cases and types of AKI, most of the damage is located in the outer cortical and medullary areas, these two regions have been analyzed and photographed (**Figure II.3**). The histological analysis by H&E stain revealed a clear tubular necrosis in both AKI models, with loss of the integrity, detachment and vacuolization of epithelial cells and widespread tubular obstruction with hyaline casts. No gross modification of the glomeruli was evident.

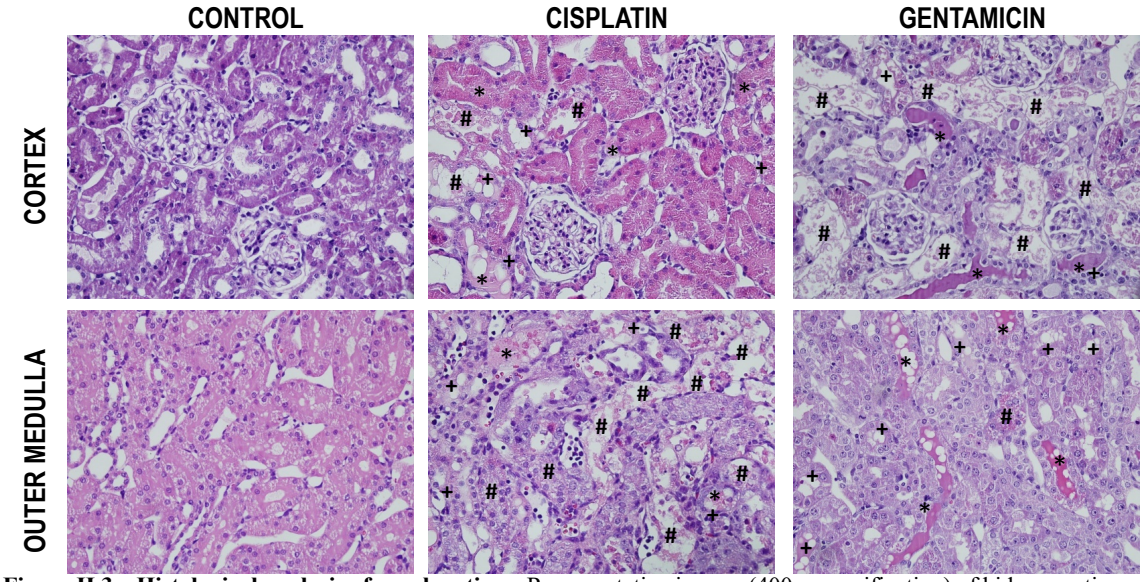

Figure II.3 – Histological analysis of renal sections. Representative images (400x magnification) of kidney sections, cortex and outer medulla, stained with H&E from CTL, CISP and G groups. CISP and G induced massive tubular necrosis. * Hyaline tubular casts; # detachment epithelial tubular cells; + vacuolization in tubular cells. All symbols represent phenomena of acute tubular necrosis.

II.3.2. Biochemical measurements

II.3.2.1. Quantification of pCr

pCr levels were quantified as a temporal marker of renal changes, remaining unchanged in the CTL group (0.55 ± 0.05 mg/dL) and increasing after 4 days of CISP treatment (2.55 ± 0.56 mg/dL, $p < 0.001$, **Figure II.4A**) and after 5 days of G treatment (3.3 ± 0.4 mg/dL, $p < 0.001$, **Figure II.4B**).

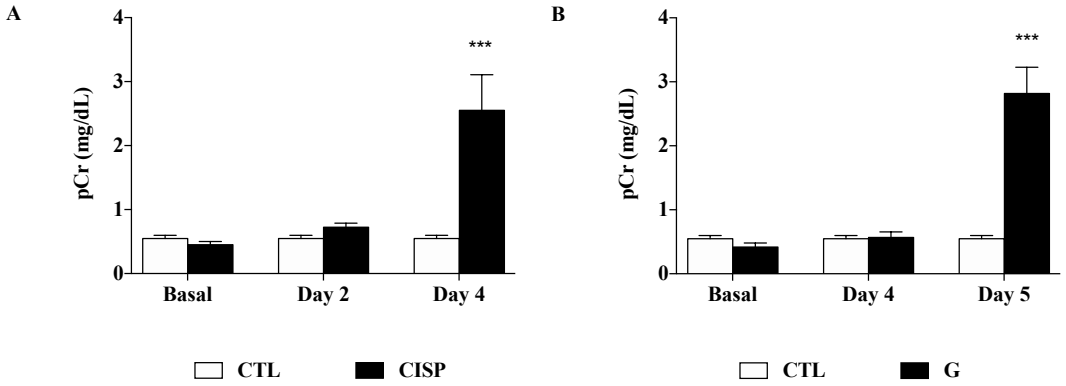

Figure II.4 – pCr levels. pCr levels increased after 4 days of CISP administration (**A**) and after 5 days of treatment with G (**B**) (n = 6 animals per group).
*** Two-way ANOVA with *Bonferroni's* multiple comparison test, versus CTL group; CISP: cisplatin group; CTL: control group; G: gentamicin; pCr: plasma creatinine; *** $p < 0.001$

II.3.2.2. uNAC assessment

To investigate tubular detoxification of CysSSX in both AKI-models, the levels of uNAC were quantified in urine as a surrogate of the mercapturates of CysSSX. Temporal changes of uNAC in the CISP model were prior to the increase in pCr. Comparing with basal state (163 ± 6 µM), the levels of uNAC decreased 2 days after administration of CISP (64 ± 10 µM), further decreasing at day 4 (47 ± 3 µM, $p < 0.001$, **Figure II.5A**). This tendency was also observed for rats treated with G, despite with lower levels of basal uNAC excretion (basal state 97 ± 14 µM) and only reaching significance at day 5 (37 ± 7 µM, $p = 0.044$, **Figure II.5B**).

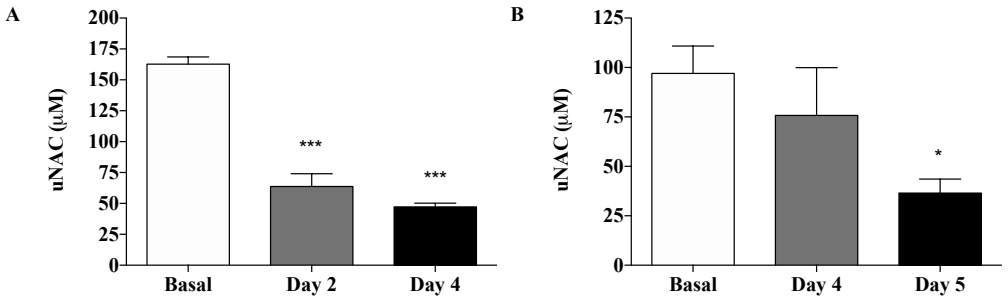

Figure II.5 – Temporal variation of uNAC levels. A decrease in the levels of uNAC was found 2 days after CISP treatment, worsening at day 4 (**A**). A similar trend was observed in rats treated with G although only after 5 days of treatment (**B**) (n = 6 animals per group).
* or *** One-way ANOVA with *Dunnett's* multiple comparison test, versus Basal state; uNAC: urinary surrogate of the mercapturates from cysteine-disulfides; * $p < 0.05$; *** $p < 0.001$.

II.3.2.3. Determination of uCys and uCysGly

To further understand the contribution of CysSSX filtration and reabsorption, we quantified the temporal variation of uCys. The onset of changes in uCys was coincident with the alterations observed for pCr, although in a higher magnitude for CISP (319 ± 24 µM *versus* 56 ± 3 µM obtained in basal state, $p < 0.001$, **Figure II.6A**) than for the G group (53 ± 11 µM versus 27 ± 3 µM obtained in basal state, $p = 0.039$, **Figure II.6B**).

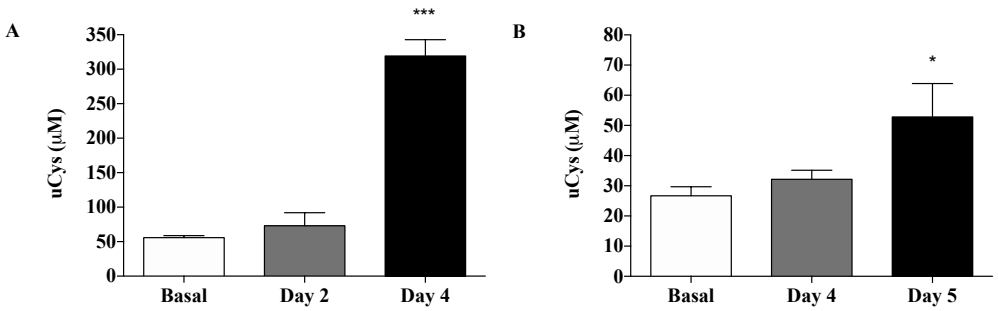

Figure II.6 – Variation of uCys throughout study time as a measure of CysSSX filtration and reabsorption. An increase in the levels of uCys was observed **A.** 4 days after CISP administration and **B.** on day 5 of G treatment (n = 6 animals per group).
* or *** One-way ANOVA with *Dunnett's* multiple comparison test, versus Basal state; uCys: urinary cysteine as a measure of CysSSX filtration and reabsorption; * $p < 0.05$; *** $p < 0.001$

On the other hand, the effect of GSH turnover might also account for changes in renal tubule. For this reason, uCysGly was also quantified. While a decrease in the levels of uCysGly was observed for the CISP group at day 2 (18 ± 2 μM) and day 4 (9 ± 2 μM) in relation to basal state (33 ± 3 μM) ($p < 0.001$, **Figure II.7A**), no changes were observed for the G group (**Figure II.7B**).

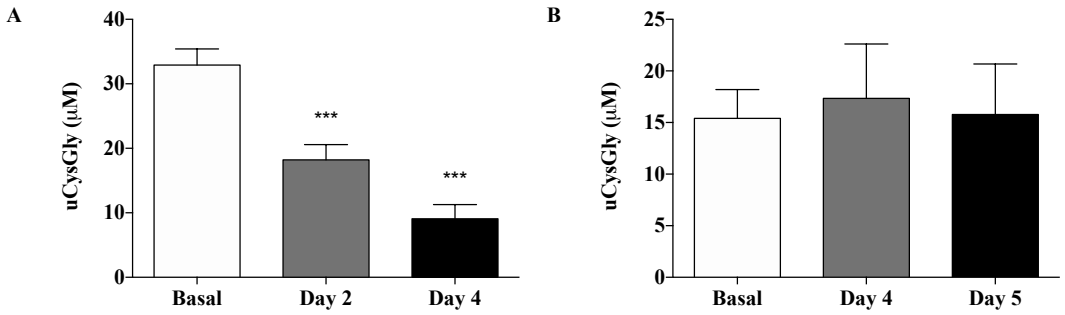

Figure II.7 – Temporal changes of uCysGly as a measure of GSH turnover. A decrease in the levels of uCysGly was found 2 days after CISP administration, further decreasing at day 4 (**A**). Treatment with G had no effect on uCysGly (**B**) (n = 6 animals per group).
* One-way ANOVA with *Dunnett's* multiple comparison test, versus Basal state; uCysGly: urinary cysteine as a measure GSH turnover; *** $p < 0.001$

The main results obtained for both models are depicted at **Table II.1**.

Table II.1 – Summary of the temporal renal changes observed.

	CISP (5 mg/Kg)	G (150 mg/Kg)
Day 2	↓ **uNAC** ↓ uCysGly	
Day 4	↑ plasma Cr ↑ uCys	
Day 5	-	↑ plasma Cr ↑ uCys and ↓ **uNAC**

CISP: cisplatin; Cr: creatinine; G: gentamicin; uCys: urinary cysteine as a measure of CysSSX filtration and reabsorption; uCysGly: urinary cysteine as a measure GSH turnover; uNAC: urinary surrogate of the mercapturates from cysteine-disulfides.

II.4. Discussion

Herein, we have shown that uNAC decreases according to decreased kidney function mediated by nephrotoxicity of CISP and G. In both models, uNAC decreased before the increase of pCr and might suggest that changes on the detoxification of CysSSX might underlie AKI-episodes induced by both CISP and G drugs. Consequently, uNAC might represent an early biomarker of drug induced-AKI, particularly for drugs undergoing the mercapturate pathway, such as CISP.

The rationale for this hypothesis-driven study was the fact that as kidney is enriched in Cys (Dröge *et al.*, 1991; Pitts, 1995) and a primordial organ for oxidation (Simmons, Bogusky and Humes, 1980; Basile, Anderson and Sutton, 2012; Chevalier, 2016), high concentrations of CysSSX are toxic (Vina *et al.*, 1983; Munday, 1989; Coelho *et al.*, 2018), the renal handling of CysSSX could add relevant data on the mechanism underlying kidney injury. In fact, an increased formation of CysSSX has been previously reported in a model of acute organ injury (Moreno *et al.*, 2014). Thus, our approach was to investigate the detoxification of CysSSX in animal models of drug-induced AKI. For this, we selected two drugs, CISP and G, whose wide used is limited by the frequent development of AKI episodes (Madias and Harrington, 1978; Goldstein and Mayor, 1983; López-Novoa *et al.*, 2011; Vicente-Vicente *et al.*, 2017). The nephrotoxicity elicited by both drugs affects mainly the proximal tubular cells (Markowitz and Perazella, 2005; Ferreira *et al.*, 2011) which seems to be mediated through oxidative reactions (Pedraza-Chaverrí *et al.*, 2000; Al-Majed *et al.*, 2002; Karahan *et al.*, 2005; Aydinoz *et al.*, 2007; Randjelovic *et al.*, 2012; Ozkok and Edelstein, 2014; Hosohata, 2016; Vicente-Vicente *et al.*, 2017; Soni *et al.*, 2018). CISP and G have also been associated with renal ER stress (Peyrou, Hanna and Cribb, 2007; López-Novoa *et al.*, 2011; Kong *et al.*, 2013; Xu, Wang and Li, 2014; Jaikumkao *et al.*, 2016; Randjelovic *et al.*, 2017; Yan *et al.*, 2018), which is an important aspect to have into account since NAT8 is predominantly expressed in the microsomes of proximal tubular cells (Chambers *et al.*, 2010; Veiga-da-Cunha *et al.*, 2010). Furthermore, the accumulation of the oxidized form of Cys in lysosomes promotes mitochondrial injury with consequent proximal tubular cell dysfunction (Sumayao *et al.*, 2016).

CISP and G are widely used and frequently associated with AKI complications (Goldstein and Mayor, 1983; López-Novoa *et al.*, 2011; Perazella and Luciano, 2015). Clinically, high doses of G have been shown to produce nephrotoxicity in 10 to 20% of cases (Kacew and Bergeron, 1990; Walker, Barri and Shah., 1999; Vicente-Vicente *et al.*, 2017) and in up to 58% in the ICU setting (Oliveira *et al.*, 2009). G's kidney toxicity is characterized mostly by tubular damage, although glomerular and vascular alterations are also detected in a dose-dependent manner (López-Novoa *et al.*, 2011).

The administration of G induced a marked acute renal failure with an associated mortality of nearly 50% after 6 days of treatment (Ferreira *et al.*, 2011). Rats from this group

presented lower weight and Cr clearance, higher levels of plasma urea, proteinuria, higher excretion of *N*-acetyl-β-D-glucosaminidase (NAG), KIM-1 and bone morphogenetic protein 7 (BMP-7), and higher urinary flow (Ferreira *et al.*, 2011). Regarding the CISP model, rats develop an overt renal failure demonstrated by increase in plasma urea, higher excretion of NAG and decrease in creatinine clearance.

The authors identified increases in regenerating islet-derived protein III β (reg IIIb) and gelsolin (both the full-length, fl-gelsolin, and the fragment of 43 kDa, t-gelsolin) in the gentamicin-induced AKI model, differentiating the nephrotoxicity evoked by this drug in relation to CISP. While reg IIIb was overexpressed in the kidneys and eliminated in the urine, urinary gelsolin was delivered to the kidneys by glomerular filtration (Ferreira *et al.*, 2011). The temporal profile of renal damage was further elucidated. **Table II.2** summarizes the temporal variations of renal markers of the animal models (Ferreira *et al.*, 2011). For simplification purposes, the table shows only the time at each marker starts its increase. Regarding the gentamicin group, significant renal damage occurs after 4 days of treatment. While reg IIIb appears in the urine at this time, urinary t-gelsolin appears on day 1 and its increase is permanent along with the treatment. As for CISP, renal dysfunction is also observed at day 4 but only t-gelsolin increases in the urine of these rats at day 2.

Table II.2 – Temporal variations of renal changes previously reported for the models employed.

	G (150 mg/Kg)	CISP (5 mg/Kg)
Day1	↑ urine t-gelsolin	
Day2		↑ urine t-gelsolin
Day3	Cytoplasmatic vacuolation of tubule epithelial cells	
Day4	↑ in plasma Cr; ↑ in urine: reg IIIb, proteinuria, NAG, KIM-1, NGAL and PAI-1	↑ in plasma Cr; ↑ in urine: KIM-1 and NAG
Day5		-
Day6	↑ urine fl-gelsolin	-

CISP: cisplatin; Cr: creatinine; fl-gelsolin: full-length gelsolin; G: gentamicin; KIM-1: kidney injury molecule 1; NAG: *N*-acetyl-β-D-glucosaminidase; NGAL: neutrophil gelatinase associated lipocalin; PAI-1: plasminogen activator inhibitor 1; reg IIIb: regenerating islet-derived protein III β; t-gelsolin: 43 kDa fragment of gelsolin.

CISP is an anti-cancer drug broadly used for treatment of different cancers. Its nephrotoxic effects are frequent and represents the major limitation in CISP-based chemotherapy. Several mechanisms contribute to kidney dysfunction elicited by CISP, including direct tubular toxicity in the form of apoptosis and necrosis that is mediated through inflammation, reactive oxygen species, calcium overload, phospholipase activation, GSH depletion, inhibition of mitochondrial respiratory chain function, opening of mitochondrial permeability of transition pore and ATP depletion (Arany and Safirstein, 2003; Pabla and Dong, 2008; Sánchez-González *et al.*, 2011; Sancho-Martínez *et al.*, 2012, 2018; Dasari and Tchounwou, 2014; Karasawa and Steyger, 2015; Vicente-Vicente *et al.*, 2015).

All these factors might suggest an interaction between the nephrotoxicity-induced by CISP and G and the detoxification of CysSSX in proximal tubular cells. Although both drugs are also hydrophilic (Hilmer *et al.*, 2011; England *et al.*, 2015), they have different mechanisms of elimination that might in a certain way explain the differences found regarding the detoxification of CysSSX. G is excreted unchanged by the kidneys mainly through glomerular filtration and eliminated in urine with no significant metabolism reported (Sande, 1985; Hilmer *et al.*, 2011). On the other hand, the renal clearance of CISP is performed by both glomerular filtration and tubular secretion (Miller *et al.*, 2010). Once inside the tubular cell, the metabolism of CISP is related with the mercapturate pathway. However, this interaction is an exception to the common assumption that this route is a mechanism of detoxification (Mathias and Bhymer, 2016). In fact, the conjugation of CISP with GSH seems to be the first step on the conversion of CISP into a potent nephrotoxin (Townsend *et al.*, 2003). Similarly to other GSH-*S*-conjugates, GSH-CISP is excreted into the lumen where undergoes hydrolysis by the brush border enzyme GGT (Griffith, 1981; Hanigan, 1998), forming the CysGly conjugate of CISP (CysGly-CISP) that is further metabolized by cysteinyl-glycine dipeptidase or aminopeptidase-M, also expressed at the brush border (Hughey *et al.*, 1978). The final Cys-CISP is transported into the proximal tubular cells where it is bioactivated through *β*-lyase activity, forming a reactive thiol that has nephrotoxic effects (Mistry, Lee and McBrien, 1989; Townsend *et al.*, 2003). In fact, the formation of toxic intermediates through this pathway has been strongly related to kidney injury (Dekant, Vamvakas and Anders, 1989; Mistry, Lee and McBrien, 1989; Möller-Hartmann and Siegers, 1991; Townsend *et al.*, 2003; Lash, 2007; Jung *et al.*, 2008; Soo *et al.*, 2018). This *β*-elimination route competes with the acetylation of Cys-*S*-conjugates by NAT8, producing

mercapturates (Veiga-da-Cunha *et al.*, 2010), that have polar, water-soluble and anionic features, rendering their elimination in urine (Hinchman and Ballatori, 1994; Veiga-da-Cunha *et al.*, 2010). Of note, mercapturates might also be metabolized by *β*-lyase, forming reactive intermediates that might evoke toxic effects similar to the ones described for the parent compound (Wolfgang *et al.*, 1989; Townsend *et al.*, 2003). However, this process is dependent on the prior deacetylation of the mercapturate (Dekant, Vamvakas and Anders, 1989; Wolfgang *et al.*, 1989).

A relevant role in CISP toxicity has been attributed to GGT, the first and limiting step of GSH-*S*-conjugates degradation, producing CysGly-*S*-conjugates and dictating the low half-life of GSH-*S*-conjugates. This step is essential for Cys recycling from the extracellular space and to provide the cell with Cys for intracellular *de novo* synthesis of GSH. A strong evidence that GGT is an important factor underlying CISP nephrotoxicity came from studies with GGT knock-out mice, where CISP (15 mg/Kg) was nephrotoxic in wild-type but not in GGT-deficient mice (Hanigan *et al.*, 2001). Furthermore, similar results were obtained when renal GGT activity was blocked with acivicin in rats (Hanigan *et al.*, 1994). However, despite this *in vivo* proof favouring the role of GGT in CISP toxicity, results from *in vitro* models are contradictory. On one hand, similar results to the one previously mentioned were obtained using the more selective GGT inhibitor OU749 while the addition of exogenous GGT lead to an increase in CISP cytotoxicity (Fliedl *et al.*, 2014). On the other hand, other studies describe GGT as the main detoxification mechanism, where GSH-CISP and CysGly-CISP renders a non-toxic profile (Daubeuf *et al.*, 2002, 2003; Paolicchi *et al.*, 2003). Further, a study performed by Wainford and co-authors (2008) showed that while inhibition of GGT in rats prevented CISP nephrotoxicity, cellular toxicity was still observed in both rat and human proximal tubular cell cultures (Wainford *et al.*, 2008). These results further support that GSH-CISP and other GSH-*S*-conjugates that are disulfides might be formed in other tissues and reach the proximal tubular cells.

Nevertheless, the intravenous administration of substantially higher concentrations of reduced GSH compared to the CISP dose (about 83-fold higher) seems to protect against CISP-induced nephrotoxicity (Cozzaglio *et al.*, 1990). As the major physiologic substrate of GGT (Hanigan and Pitot, 1985), the high concentration of GSH might inhibit the enzyme's activity, reducing the metabolism of GSH-CISP. In fact, a glutathione-disulfide

mimetic (NOV-002, oxidized glutathione with cisplatinum at an approximate 1000:1 ratio) acts as a competitive substrate for GGT and its administration to mice after treatment with CISP protected the kidneys from CISP-induced proximal tubule damage, including dilation of tubules and the presence of protein casts (Jenderny *et al.*, 2010).

The toxicity of this concentration needs to be elucidated in more complex organisms such as rats and humans, but it has been shown that high levels of reduced GSH inhibits growth and promote cell death in yeast strains (Kumar *et al.*, 2011). Nevertheless, the inhibition of GGT activity allows the inhibition of Cys-CISP reaching the tubular cell. This would avoid the accumulation of toxic metabolites through *β*-lyase activity in these cells. However, the activity of NAT8 would be redirected to the detoxification of Cys-CISP formed directly in tubular cells rather than acting on CysSSX that would continue to reach or be formed in the cells.

From these studies, one can assume that the dose of GSH disulfide required to inhibit the enzyme and avoid Cys-CISP induced toxicity is very high and that GGT might prefer GSH-CISP than other GSH-*S*-conjugates. This might also explain the reduction in urinary excretion of CysGly in the CISP model and increase in uCys, which was described to be increased in mixed disulfide forms in urine of both animals treated with GGT inhibitors and of a patient with severe GGT deficiency (Griffith and Meister, 1980). This could justify the absence of decrease found in the G group that do not form GSH conjugates. Moreover, Cys-CISP might also inhibit the entrance of CysSSX in cells, supporting its increase in urine. This increase in uCys was also observed in the G model, although in a lower magnitude. Nevertheless, the increase of uCys coincided with the increase in pCr in both models.

The premature decrease in the levels of uNAC in the CISP model was not observed in rats treated with G. In fact, changes in uNAC happened at the onset of the increase in pCr. As mentioned, G is actively eliminated in its unchanged form by glomerular filtration (Sande, 1985; Hilmer *et al.*, 2011) and seems to have no influence from the mercapturate pathway. However, after glomerular filtration, a small portion of the drug (3 to 5%) is reabsorbed by proximal tubular cells (Pattyn *et al.*, 1988; Verpooten *et al.*, 1989). This site-specific accumulation of G is related with the high expression at the proximal tubule of the megalin and cubilin complex, known to transport G and other aminoglycosides by endocytosis (Schmitz *et al.*, 2002; Sassen *et al.*, 2006). Afterwards, G accumulates mainly

in lysosomes, Golgi apparatus and ER (Silverblatt and Kuehn, 1979; Silverblatt, 1982). G binds to membrane phospholipids, changing their turnover and metabolism, causing lysosomal phospholipidosis, i.e., the accumulation of undigested phospholipids in lysosomes, that correlates tightly with the levels of G nephrotoxicity (Laurent, Kishore and Tulkens, 1990; Nonclercq *et al.*, 1992). Furthermore, extensive mitochondrial swelling and damage is also observed (Giuliano *et al.*, 1984; Mingeot-Leclercq and Tulkens, 1999).

However, it is at the ER level that G could impair the activity of NAT8, and hence, the detoxification of CysSSX. In fact, at the ER, G inhibits protein synthesis, disrupts translation accuracy and protein posttranslational modifications (Horibe *et al.*, 2004). Of note, NAT8 has been associated with the ability to acetylate correctly folded proteins, allowing the progression of these polypeptides through the secretory pathway and complete maturation, whereas non-acetylated proteins are disposed off (Ding *et al.*, 2014).

The effects of G above-mentioned leads to ER stress and activation of the unfolded protein response that, if continuously stimulated, induces apoptosis by caspase 12 and calpain (Peyrou, Hanna and Cribb, 2007). As so, NAT8 activity could be inhibited by G, which could explain the impairment on the detoxification of CysSSX, although in a less magnitude and belatedly in comparison with CISP treatment. This difference might be related with the fact that the interaction of CISP with NAT8 could happen not only at the mercapturate pathway but also due to the ER stress induced by this drug (Peyrou, Hanna and Cribb, 2007; Kong *et al.*, 2013; Xu, Wang and Li, 2014; Yan *et al.*, 2018).

Changes in uCysGly were not observed in the G group. Data regarding the levels of renal GSH in G-induced nephrotoxicity models are conflicting, with reports showing a decrease (Ateşşahin *et al.*, 2003; Parlakpinar *et al.*, 2005; Silan *et al.*, 2007; Derakhshanfar, Bidadkosh and Hashempour Sadeghian, 2009) or unchanged (Karahan *et al.*, 2005) levels. Nevertheless, the nephrotoxicity of G was attenuated when *N*-acetylcysteine and methionine were administered as precursors of GSH (Ali *et al.*, 2009; Derakhshanfar, Bidadkosh and Hashempour Sadeghian, 2009). The observed effect might also be related with its metal chelating properties (as iron chelators ameliorated oxidative stress induced by gentamicin) (Ali, 2003). The more strongly proposed mechanism underlying the nephroprotection conferred by *N*-acetylcysteine and methionine may be related to the

decrease in oxidative stress in renal cortex (Unnikrishnan and Rao, 1990; Priuska and Schacht, 1995).

These data seem to be a paradox, as both *N*-acetylcysteine and methionine would contribute to the increase in Cys, which in oxidative conditions could lead to the formation of CysSSX. Cys is a nonessential amino acid because it can be available from methionine via the transsulfuration pathway, which largely occurs at the liver of healthy organisms. *N*-acetylcysteine is a reasonable alternative to Cys because it is more stable, less toxic, and more readily soluble than Cys. In rat, *N*-acetylcysteine was superior to methionine as a source of Cys (Neuhäuser *et al.*, 1986; Pajares and Perez-Sala, 2017). *N*-acetylcysteine is converted in Cys through deacetylation by several acylases, an enzyme activity that is predominantly present in kidney and, to a lesser extent, in liver (Yamauchi *et al.*, 2002) and higher in rodents that in man. Although, this was not apparent in healthy volunteers who received *N*-acetylcysteine by intravenous infusion, since no increase in the plasma concentration of Cys was observed (Magnusson *et al.*, 1989). Cys in plasma, contrary to cells where it is GSH, is the predominant thiol and exists in oxidized form, particularly in a pool linked to proteins, CysSSP (disulfides with Cys residues in proteins) (Han *et al.*, 1997; Oliveira and Laurindo, 2018), that might protect Cys residues from irreversible oxidation at least until there is a mild threshold of oxidative stress (Dalle-Donne *et al.*, 2007; Hochgräfe *et al.*, 2007; Auclair, Johnson, *et al.*, 2013).

It has been shown that in plasma, *N*-acetylcysteine reacts with CysSSCys and produce mercapturates of cysteine (NAC-Cys), *N*-acetylcysteine symmetric disulfide (NAC-NAC) and Cys (Whillier *et al.*, 2009). As so, *N*-acetylcysteine is able to reduce CysSSX, forming mercapturates that are directly eliminated (NAC-Cys and NAC-NAC) and so reducing the toxic potential of CysSSX accumulation.

Nevertheless, Small and collaborators (2018) have recently show that progression to chronic kidney pathologies after AKI-induced by ischemia/reperfusion can be enhanced by *N*-acetylcysteine therapy, possibly by dampening endogenous antioxidant responses (by eliminating redox-sensitive endogenous cytoprotective Nrf2 signaling) and enhancing persistent kidney mitochondrial and metabolic dysfunction (Small *et al.*, 2018). Linking this evidence to our hypothesis, the supplementation with *N*-acetylcysteine therapy might promote the elimination in early formation of CysSSX that increase as an adaptive response – disulfide stress. This might lead to an increase in intracellular levels of Cys and GSH, which in it turn, could be further oxidized with

continuous injury, promoting the formation and accumulation of more CysSSX and of other endogenous Cys-*S*-conjugates increased in inflammatory/oxidative conditions (Alkhamees *et al.*, 2017). This will lead to an overload of NAT8 activity that might be more evident in drugs undergoing the mercapturate pathway or in patients with higher risk (e.g. lower NAT8 activity, chronic inflammatory conditions, among others).

The combination of the results obtained for the CISP model suggest that the impairment on the detoxification of CysSSX formed in proximal tubular cells is coincident with changes in GSH turnover and precede the increase in CysSSX levels in urine and pCr. This was, however, not observed for the G treatment. The impairment on CysSSX detoxification and increase in CysSSX urinary levels seem to be concomitantly with the increase in pCr. We were not able to obtain samples from day 1, which could determine if the variation on uNAC precedes the changes on GSH turnover. According to our hypothesis, when proximal tubular cells are exposed to oxidative injury, Cys is readily oxidized and changes on uNAC would happen before the ones related with GSH status. As a consequence, there is a reduction on the Cys available to form GSH and an accumulation of toxic Cys products. GSH would then oxidize in the form of disulfide, conjugating with CISP which are effluxed from cells, or with several endogenous molecules as catecholamines and inflammatory chemical mediators (Wang and Ballatori, 1998; Gonçalves-Dias *et al.*, 2019). Afterwards, they are catabolized to CysSSX and Cys-CISP or other Cys-*S*-conjugates that would compete for NAT8's activity, leading to an overload of the enzyme's capacity. The impairment of the detoxification of CysSSX might also be promoted by inhibition of NAT8's activity, of other enzymes of the mercapturate pathway and of the transporters involved on urinary elimination of the mercapturates. In all these scenarios, CysSSX either formed in tubular cell or the ones reaching them will accumulate and might promote the activation of pathways associated with toxicity in proximal tubular cells.

As for the G group, the impairment on CysSSX detoxification and increase in CysSSX urinary levels seem to be concomitantly with the increase in pCr. The interaction of G and the mercapturate pathway has not been reported, although it might affect NAT8's activity due to its ability to induce ER stress (Horibe *et al.*, 2004). The unavailability of samples from days prior to day 4 and 5 limits the possibility to investigate if changes in

uNAC could also be identified at earlier stages, although the results obtained at day 4 points the other direction.

The effects of Cys-*S*-conjugates have been underestimated, probably because the mercapturate pathway has been classically considered a detoxification route for xenobiotics. Cys-*S*-conjugates have primarily vascular and hemodynamic properties (Lewis and Austen, 1984), being potent vasoconstrictors (Rosenthal and Pace-Asciak, 1983; Badr, Brenner and Ichikawa, 1987; Shastri *et al.*, 2001) with ability to enhance the permeability of the postcapillary venules (Leng *et al.*, 1988). Moreover, they are involved in glucose-stimulated insulin secretion (Guo *et al.*, 2018), and have pro-inflammatory (Magnay *et al.*, 2001), cytotoxic (Townsend *et al.*, 2003; Stern, Bruno, Hennig, *et al.*, 2005; Stern, Bruno, Horton, *et al.*, 2005; Dvash *et al.*, 2015) and immunogenic (Salauze *et al.*, 2005) properties. As mentioned, Cys-CISP conjugate is more toxic to tubular cells than CISP (Townsend *et al.*, 2003). Another example, the Cys-*S*-conjugate of paracetamol is related to its nephrotoxicity, but not hepatotoxicity (Stern, Bruno, Hennig, *et al.*, 2005). Additionally, the accumulation of CysSSCys in lysosomes leads to proximal tubular dysfunction (renal Fanconi Syndrome) and ESRD (Besouw and Levtchenko, 2014). Therefore, the elimination of these conjugates could have important implications at the nephroprotection level.

As so, the level of interaction between the drug and the mercapturate pathway might have an influence on the temporal changes observed regarding the detoxification of CysSSX. While the different renal handling of CISP and G might induce changes on the time of uNAC decrease, the common tubular toxic effects induced by both drugs could be the reason why both models have decreased levels of uNAC and increased levels of uCys.

II.5. Conclusions

In summary, uNAC might represent an early biomarker of drug induced-AKI, particularly for drugs undergoing the mercapturate pathway, such as CISP. Nevertheless, both drugs might inhibit the activity of NAT8 through their nephrotoxic effects. As so, CysSSX acetylation might represent the primary and early mechanism of detoxification upon acute insult.

In the future, considering the unavailability of genetic models neither selective inhibitors of NAT8, more studies are required to further investigate: 1) early points, especially day or even hours after injury, that we believe that will increase uNAC in the maximum levels of CysSSX in the tubular cell; 2) evaluate the change of NAT8 expression and CysSSX levels in kidney in a time-dependent manner, the effect of GGT inhibitors, administrations of NAC and comparison with other markers of tubular dysfunction; 3) measurement of other endogenous CysSCX and their mercapturates and also the effect of administration of exogenous CysSCX; and 4) assess this pathway in other acute models of renal disease such as ischemia/reperfusion and other tubular nephrotoxicants that undergo the mercapturate pathway (e.g. paracetamol) or not (e,g. tenofovir, TDF) (Gorgulho *et al.*, 2018).

CHAPTER III

Factors for uNAC inter-individual variability and uNAC as an indicator of kidney disease progression in HIV-infection

CHAPTER III

Factors for uNAC inter-individual variability and uNAC as an indicator of kidney disease progression in HIV-infection

III.1. Rationale & Objectives

Based on the previous data, we decided to determine the factors that would influence the inter-individual variability of uNAC in HIV-infected patients. The choice of this population is related with the fact that kidney disease is one of the major causes of morbidity and mortality in this condition (Wyatt, 2017; Swanepoel *et al.*, 2018).

Kidney disease prevalence, which keeps increasing and is predicted to rise even further (Palau *et al.*, 2018), might be linked not only to residual viremia, immunosuppression and chronic inflammation, well known traits of HIV-infection, but also to the contribution of the sub-toxic chronic effects of antiretroviral (ARVs) drugs (Campos, Ortiz and Soto, 2016). These factors might lead to chronic low-grade kidney insults (oxidative stress, DNA damage and mitochondrial injury) on the tubular epithelium, increasing epithelial cell sensitivity to new insults, maladaptive repair and progression to CKD (Ferenbach and Bonventre, 2015).

Thus, we have investigated the inter-individual variability of the excretion of mercapturates of CysSSX, through uNAC measurement, in a cross-sectional analysis of a HIV-infected population. Also, the relation of CysSSX formation through CysSSP was also measured in serum. As LTE4 is the best well known endogenous Cys-*S*-conjugate that is substrate of NAT8, the urinary levels of LTE4 (uLTE4) were also quantified and their association with uNAC was performed. Additionally, a prospective evaluation of uNAC changes with the progression of kidney disease was performed in this population.

III.2. Patients & Methods

III.2.1. Study population

As part of a prospective study of a cohort of HIV-infected patients, a cross-sectional analysis was performed in patients included in a consecutive manner. Pregnancy and age under 18 years old were set as exclusion criteria. Anthropometric and clinical data were recorded at study admission. The study was approved by the Hospital Prof. Dr. Fernando da Fonseca, EPE ethics committee and conducted in accordance with the Declaration of Helsinki. All patients gave their written informed consent.

III.2.1.1. Interventions

Urine and blood samples were collected after outpatient consult and immediately processed (in the case of the blood to obtain serum) and frozen at -80 °C until further analysis. Anthropometric, combined antiretroviral therapy (cART)-related and clinical data were collected and registered on a database. Laboratory data gathered included sCr, sCys C, HIV viral load (VL) and T-cells.

III.2.1.2. Definitions

eGFR was calculated by the Chronic Kidney Disease-Epidemiology Collaboration (CKD-EPI) equation using sCr, sCys C or both (sCr – sCys C) and the equation of the Modification of Diet in Renal Disease (MDRD) with sCr (Levey *et al.*, 2007, 2009; Inker *et al.*, 2012), presented as mL/min/1.73m^2.

III.2.2. Inter-individual variability of uNAC

To assess its inter-individual variability, uNAC was quantified in first morning urine of patients included consecutively, as previously described (**Chapter I**). Inter-individual variability was assessed through the calculation of the CV of uNAC quantified in all included patients.

III.2.2.1. Influence of kidney function on the levels of uNAC

To assess the association between uNAC and kidney function, we performed correlations between the levels of uNAC and the above mentioned eGFR equations in section III.2.1.2.

III.2.2.2. Effect of anthropometric factors in the levels of uNAC

Whenever applicable, correlations or group comparisons were performed with anthropometric factors that could potentially influence the inter-individual variability of uNAC. The analysis was performed with several factors including age, sex, race, body weight and BMI.

III.2.2.3. Impact of cART in uNAC

To understand the effect of cART-related data in the levels of uNAC, correlations or group comparisons were performed. Factors included on this analysis were the pharmacological control of the infection (patients under cART *versus* patients without cART), the time of cART initiation, cART scheme and the use of each ARV.

III.2.3. Variability of serum CysSSP and its association with uNAC

To obtain the CysSSP fraction of Cys in serum, the levels of total and free total Cys were quantified, as previously described. Serum CysSSP levels were obtained by subtracting was quantified as previously described (Grilo *et al.*, 2017). Both fractions were quantified using an initial volume of 50 μL of serum for each fraction. In brief, to obtain the total fraction, after reduction of sulfhydryl groups with 100g/L TCEP (30 min, RT), proteins were removed by precipitation with 100 g/L TCA containing 1 mM EDTA followed by centrifugation (13000 g, 10 min, 4°C). Afterwards, the supernatant was collected to a new tube containing 1.55 M NaOH, 125 mM $Na_2B_4O_7$, (pH 9.5) with 4 mM EDTA and 1g/L SBD-F in $Na_2B_4O_7$ buffer. The final mixture was vortexed and incubated in the dark, at 60 ºC for 1 h, to complete the derivatization of the free sulfhydryl groups. The free total fraction of Cys was obtained by first submitting the sample to protein precipitation with TCA followed by centrifugation (13000 g, 10 min, at 4ºC). Then, samples were reduced with TCEP (30 min, RT) and the protocol described above for derivatization was

followed. The CysSSP fraction was then obtained by subtracting the free total to the total values of Cys.

III.2.4. Association of uNAC with uLTE4

uLTE4 was measured in urine samples by ELISA (E-El-H1037, Elabscience), according with manufacturer's instructions. Briefly, 50 μL of serum was added to each well of the 96-well microplate pre-coated with human LTE4, upon which 50 μL of biotinylated detection antibody was immediately added. Then, after an incubation period of 45 min at 37 °C, the wells were washed and 100 μL of HRP conjugate was added to each well and incubated for 30 min at 37 °C. The microplate was once again washed and 90 μL of substrate reagent was added. A new incubation period of 15 min at 37 °C was performed where upon 50 μL of stop solution was used to stop the reaction. The levels of uLTE4 were immediately measured spectrophotometrically at 450 nm and expressed as pg/mL.

III.2.5. Variability of uNAC with the progression of kidney disease after one year of follow-up

We performed a one-year prospective study on patients that were included on the cross-sectional analysis. Only patients with samples collected at T0 and T12 months were included on this study. Patients were stratified according to their baseline eGFR values using CKD-EPI equation with sCr: normal controls (NC), with eGFR equal or higher than 90 mL/min/1.73m2; early kidney disease (EKD), with eGFR values lower to 90 and equal or higher to 60 mL/min/1.73m2 and CKD, with eGFR below 60 mL/min/1.73m2. Additionally, eGFR evolution throughout study time was used for stratification: non-progression (NP), for those patients with stable kidney function (no GFR changes, increased or decreased lower than 10% of baseline over 1-year of follow-up); and progression (P), for patients with decreased kidney function equal or higher to 10% (KDIGO CKD Work Group, 2013) from baseline values. uNAC quantified in samples from the T12 visit is presented as the % of the values attained at baseline (T0 visit).

III.2.6. Statistical analysis

Statistical analysis was performed using GraphPad Prism® version 7.0 (GraphPad Software Inc., San Diego, CA, USA) and Statistical Package for Social Sciences (SPSS) software version 23 (IBM Corp., Armonk, NY, USA). Data was presented in percentage, mean ± SEM or mean ± SD or median ± IQR, whenever applicable. Variability among data was expressed in CV (%). Non-normal continuous variables were analyzed with *Kruskal-Wallis* test with *Dunn's* multiple comparisons test, or *Mann-Whitney* test, while for normal variables One-way ANOVA with *Bonferroni's* multiple comparisons test, Unpaired t-test or Paired t-test analysis were performed. A step-wise multivariable regression models were performed to identify factors influencing the levels of uNAC. Two-way ANOVA with *Bonferroni's* multiple comparisons test was used when both baseline eGFR values and progression to kidney disease were analyzed. Statistical significance for all tests was set at $p < 0.05$.

III.3. Results

III.3.1. Anthropometric and clinical data

Table III.1. presents the anthropometric and clinical data of the 242 included patients.

Table III.1 – Anthropometric and clinical data of the included patients.

Men (%)	64
Black (%)	26
Age (years old) [a]	51 [44-58]
Body weight (Kg) [a]	70 [60-80]
BMI (Kg/m^2) [a]	24 [22-28]
HIV type-1 (%)	96
Time of HIV diagnosis (years) [a]	8 [4-13]
Undetectable VL (%)	69
CD4$^+$ T-cells (cells/µL) [a]	486 [332-693]
CD3$^+$ T-cells (cells/µL) [a]	1421 [1016-1859]
CD8$^+$ T-cells (cells/µL) [a]	868 [588-1175]
Patients on cART (%)	78
Time on cART (years) [a]	7 [3-12]
Patients on TDF (%)	49
cART scheme (%)	2N(t)RTI+NNRTI: 52; 2N(t)RTI+PI/r: 21; Other: 27
eGFR CKD-EPI sCr [a, c]	89 [76-101]
eGFR MDRD [a, c]	81 [69-96]
eGFR CKD-EPI sCr – sCys C [a, c]	94 [73-105]
eGFR CKD-EPI sCys C [a, c]	96 [68-109]

[a] Median [IQR]; [b] mg/g of uCr; [c] mL/min/1.73m^2

BMI: body mass index; cART: combined antiretroviral therapy; CD: cluster of differentiation; CKD-EPI: Chronic Kidney Disease-Epidemiology Collaboration; eGFR: estimated glomerular filtration rate; HIV: human-immunodeficiency virus; MDRD: Modification of Diet in Renal Disease; NNRTI: non-nucleoside reverse transcriptase inhibitor; N(t)RTI: nucleoside/nucleotide reverse transcriptase inhibitor; PI/r: ritonavir-boosted protease inhibitor; sCr: serum creatinine; sCys C: serum cystatin C; TDF: tenofovir; VL: viral load.

III.3.2. Inter-individual variability of uNAC

Our first approach consisted in investigating the inter-individual variability of uNAC. This was assessed by the calculation of the CV of the 242 uNAC values measured (**Figure III.1**). The median [IQR] values of obtained were 51 [31-72] μM. The levels of uNAC were highly variable, with > 30x differences between the lowest and the highest values (**Figure III.1**).

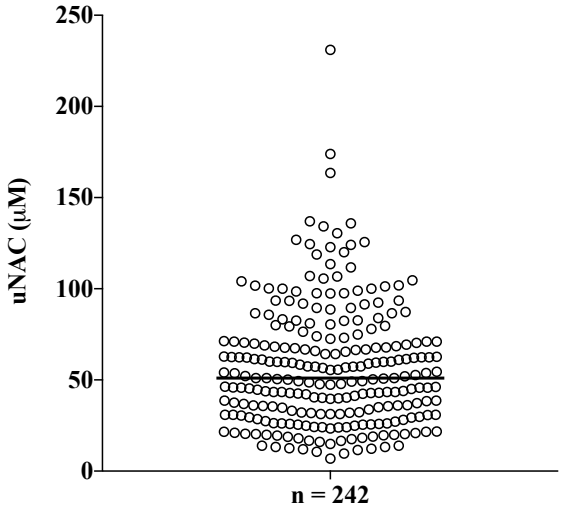

Figure III.1 – uNAC inter-individual variability among 242 included HIV-infected patients. Median [IQR] levels of uNAC were 51 [31-73] μM, varying between 7 μM and 231 μM, with a coefficient of variation of 59%.
uNAC: urinary surrogate of the mercapturates from cysteine-disulfides.

III.3.2.1. Influence of kidney function on the levels of uNAC

We further analyzed the contribution of renal function for uNAC's inter-individual variability. For this, kidney function, was evaluated through eGFR using the most applied equations in human diagnostic (Levey *et al.*, 2007, 2009; Inker *et al.*, 2012). Our results showed that patients with higher eGFR present higher uNAC levels, regardless of the used equation (*Spearman* r = 0.183, $p = 0.004$ for CKD-EPI with sCr – **Figure III.2A**; *Spearman* r = 0.175, $p = 0.006$ for MDRD – **Figure III.2B**; *Spearman* r = 0.165, $p = 0.016$ for CKD-EPI with both sCr and sCys C – **Figure III.2C**; and *Spearman* r = 0.146, $p = 0.034$ for CKD-EPI with sCys C – **Figure III.2D**).

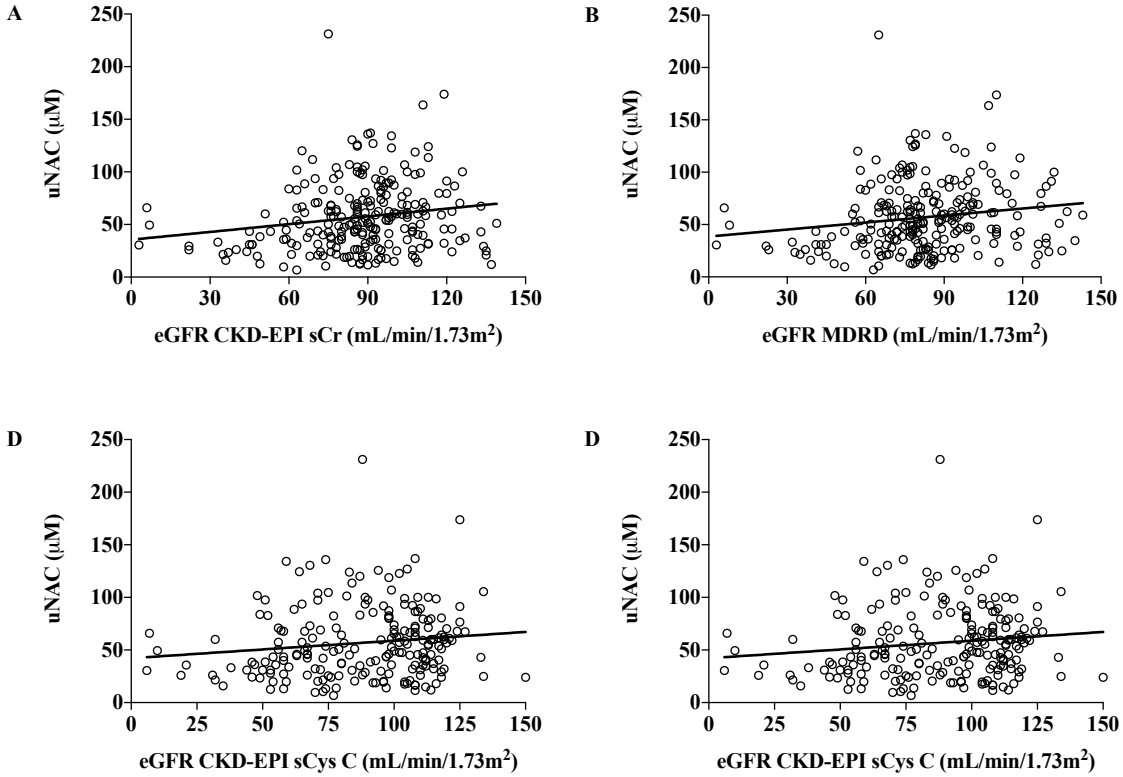

Figure III.2 – uNAC and eGFR. Higher levels of uNAC were observed in patients with increased GFR estimated using CKD-EPI with sCr (*Spearman* r = 0.183, *p* = 0.004 – **A**), MDRD (*Spearman* r = 0.175, *p* = 0.006 – **B**), CKD-EPI with sCr and sCys C (*Spearman* r = 0.165, *p* = 0.016 – **C**) and CKD-EPI with sCys C (*Spearman* r = 0.146, *p* = 0.034 – **D**) (n = 242 for CKD-EPI with sCr and MDRD and n = 212 for CKD-EPI with sCr and sCys C and CKD-EPI with sCys C).
CKD-EPI: chronic kidney disease-epidemiology collaboration; eGFR: estimated glomerular filtration rate; MDRD: modification of diet in renal disease; sCys C: serum cystatin C; sCr: serum creatinine; uNAC: urinary surrogate of the mercapturates from cysteine-disulfides.

III.3.2.2. Effect of anthropometric factors in the levels of uNAC

Next, we investigated other factors that could influence the levels of uNAC rather than eGFR. We observed that uNAC was influenced by sex, race and BMI (**Figure III.3**). Specifically, the levels of uNAC were lower in women (44 [26-66] µM) and Black patients (44 [26-60] µM), in comparison with men (59 [35-78] µM) and non-Black patients (57 [33-83] µM), respectively (*p* = 0.011 for sex – **Figure III.3A**; and *p* = 0.001 for race – **Figure III.3B**). Additionally, higher BMI was associated with decreased uNAC (*Spearman* r = -0.136, *p* = 0.042) (**Figure III.3C**), while no effect of age and body weight was observed.

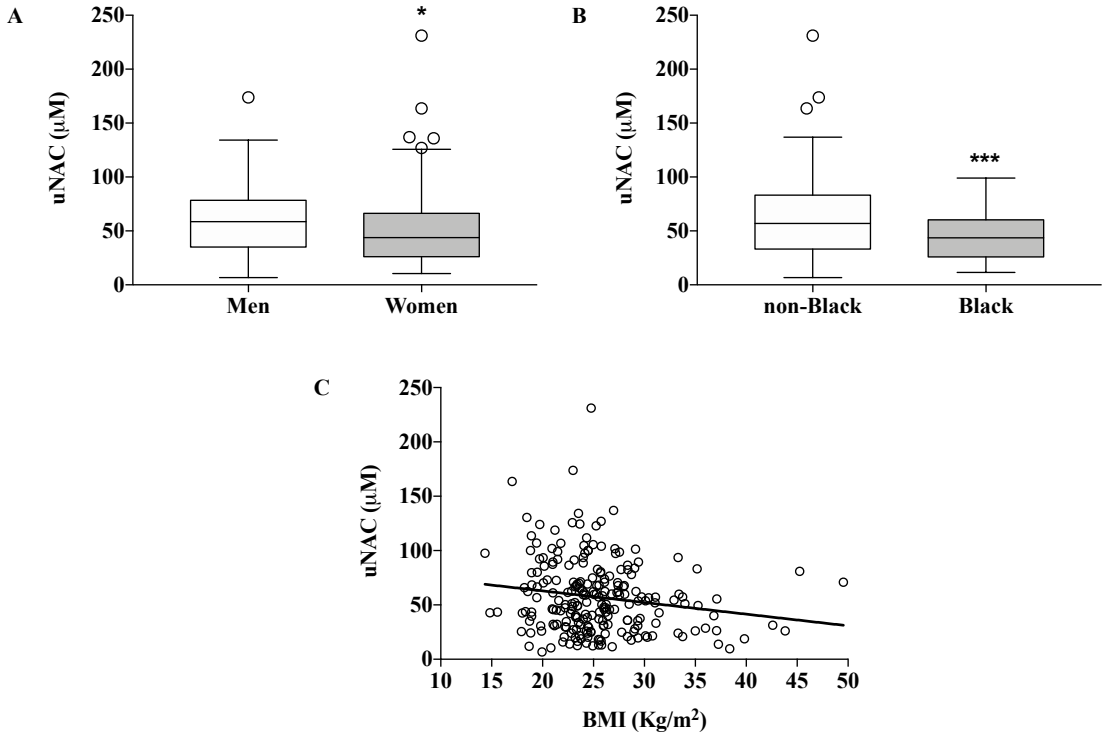

Figure III.3 – Influence of sex, race and BMI on the levels of uNAC. Female sex (**A**) and Black race (**B**) influenced negatively the levels of uNAC. On the other hand, higher BMI was associated with lower levels of uNAC (*Spearman* r = -0.136, $p = 0.042$ – **C**) (n = 154 men, 88 women, 180 non-Black, 62 Black and 226 for BMI).
* or *** *Mann-Whitney* test; BMI: body mass index; uNAC: urinary surrogate of the mercapturates from cysteine-disulfides; * $p < 0.05$; *** $p < 0.001$.

In a multivariable analysis including these anthropometric factors, the levels of uNAC were only influenced by Black race (B: -17.0, 95% CI [-26.7 – 7.2], $p = 0.001$). However, when eGFR was added to the model, uNAC levels were influenced both by Black race (B: -17.6, 95% CI [-27.2; -8.0], $p < 0.001$) and eGFR (B: 0.281, 95% CI [0.102 – 0.459], $p = 0.002$).

III.3.2.3. Impact of cART in uNAC

In order to assess if the pharmacological control of HIV-infection influenced uNAC, we compared uNAC levels in patients that were receiving cART with non-treated HIV-infected patients. The levels of uNAC were similar between patients receiving cART and patients without cART (**Figure III.4A**).

Then, we evaluated if the time on cART affected uNAC, but no association was found as well as no association was found between uNAC and time on cART.

Next, the influence on uNAC of the main cART schemes, i.e. combination of two nucleoside/nucleotide reverse transcriptase inhibitors (N(t)RTIs) with one non-nucleoside reverse transcriptase inhibitor (NNRTI) (2N(t)RTIs + NNRTI) or one protease inhibitors boosted with ritonavir (PI/r) (2(N(t)RTIs + PI/r) was assessed. No significant differences were found (**Figure III.4B**). Similarly, no differences were found when patients were stratified according to each of the NNRTI (**Figure III.4C**) or PI/r on the scheme (**Figure III.4D**).

Afterwards, the role of each N(t)RTI on the levels of uNAC was evaluated. Higher levels of uNAC were found in patients receiving cART with TDF (57 [37-77] μM and 46 [27-70] μM respectively for TDF and no-TDF) ($p = 0.043$) (**Figure III.4E**). In the opposite direction, uNAC levels were lower in patients on lamivudine (3TC)-containing cART (38 [26-58] μM and 56 [35-80] μM respectively for 3TC and no-3TC) ($p < 0.001$) (**Figure III.4F**) and abacavir (ABC)-containing cART (45 [26-61] μM and 55 [26-61] μM respectively for ABC and no-ABC) ($p = 0.027$) (**Figure III.4G**). Nevertheless, the differences found for emtricitabine (FTC) did not reach statistical significance ($p = 0.060$) (**Figure III.4H**). Similarly, no differences were found for raltegravir, nevirapine (NVP), etravirine (ETV), efavirenz (EFV), lopinavir (LPV), darunavir (DRV) and atazanavir (ATV).

Finally, we compared the eGFR in each N(t)RTI and observed that lower eGFR was found in patients under 3TC (90 [78-105] mL/min/1.73m^2 and 81 [59-93] mL/min/1.73m^2, respectively for no-3TC and 3TC) ($p < 0.001$) (**Figure III.5A**) and ABC (90 [79-105] mL/min/1.73m^2 and 85 [59-94] mL/min/1.73m^2, respectively for no-ABC and ABC) ($p < 0.001$) (**Figure III.5B**), while TDF and FTC use had no effect.

In a multivariable analysis where uNAC was the dependent variable, the levels of uNAC were influenced by Black race (B: -16.8, 95% CI [-26.1; -7.5], $p < 0.001$) and use of 3TC (B: -15.3, 95% CI [-25.3; -5.2], $p = 0.003$).

Secondly, the analysis was performed by including the four N(t)RTIs and eGFR. Both 3TC use and eGFR influenced uNAC in opposite ways (B: -13.1, 95% CI [-23.6; -2.7], $p = 0.015$ and B: 0.190, 95% CI [0.007; 0.373], $p = 0.042$, respectively for 3TC use and eGFR).

Lastly, the factors that influenced uNAC in the previous 2 models (3TC, race and eGFR) were included on a third multivariable analysis. All factors appeared to influence the

levels of uNAC. In fact, Black race was the most prominent influencer (B: -17.5, 95% CI [-26.8; -8.3], $p < 0.001$), followed by for 3TC use (B: -12.2, 95% CI [-22.5; 2.0], $p = 0.019$) and finally eGFR (B: 0.213, 95% CI [0.035; 0.392], $p = 0.020$).

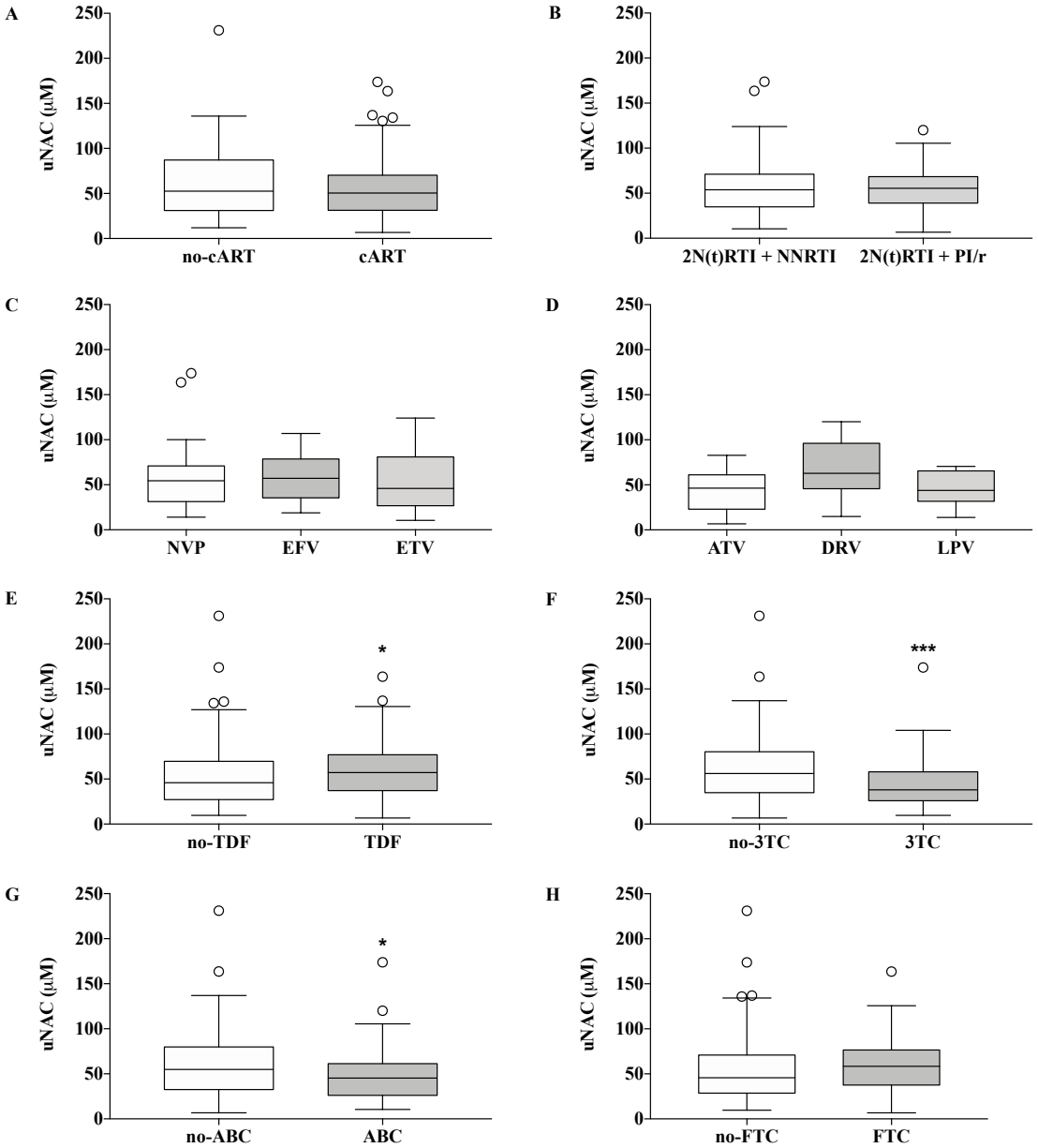

Figure III.4 – uNAC stratification by antiretroviral use. No differences were found on the levels of uNAC between patients under-cART or without cART (**A**) neither between the two different cART schemes (**B**) or different NNRTI (**C**) or PI/r used (**D**). While TDF use increased the levels of uNAC (**E**), the opposite was found for 3TC and ABC (**F** and **G**, respectively for 3TC and ABC). No differences were found for FTC use (**H**) (n = 54 no-cART, 188 cART, 97 2N(t)RTI + NNRTI, 36 2N(t)RTI + PI/r, 43 NVP, 45 EFV, 9 ETV, 9 ATV/r, 17 DRV/r, 8 LPV/r, 118 TDF, 124 no-TDF, 50 3TC, 192 no-3TC, 66 ABC and 176 no-ABC, 99 FTC and 143 no-FTC).
* or *** *Mann-Whitney* test; 3TC: lamivudine; ABC: abacavir; ATV: atazanavir; cART: combined antiretroviral therapy; DRV: darunavir; EFV: efavirenz; ETV: etravirine; FTC: emtricitabine; LPV: lopinavir; NNRTI: non-nucleoside reverse transcriptase inhibitor; N(t)RTI: nucleoside/nucleotide reverse transcriptase inhibitor; NVP: nevirapine; PI/r: protease inhibitor boosted with ritonavir; TDF: tenofovir; uNAC: urinary surrogate of the mercapturates from cysteine-disulfides; * $p < 0.05$; *** $p < 0.001$.

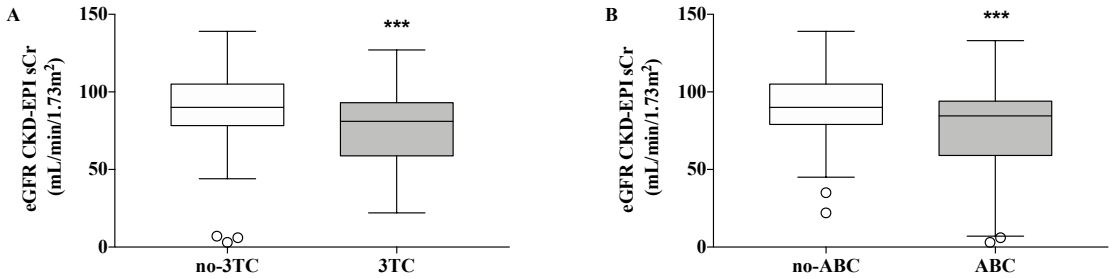

Figure III.5 – Influence of 3TC and ABC use on eGFR. Lower eGFR was found in patients under cART-containing 3TC (**A**) and ABC (**B**) (n = 50 3TC, 192 no-3TC, 66 ABC and 176 no-ABC).
*** *Mann-Whitney* test; 3TC: lamivudine; ABC: abacavir; eGFR CKD-EPI sCr: estimated glomerular filtration rate obtained by chronic kidney disease-epidemiology collaboration using serum creatinine; *** $p < 0.001$.

III.3.3. Variability of serum CysSSP and its association with uNAC

Serum levels of CysSSP were assessed due to its previously established relation with kidney disease (Regazzoni *et al.*, 2013; Nagumo *et al.*, 2014). Furthermore, cysteinylated proteins have been reported as one of the major sources of Cys and CysSSX for the proximal tubular cells (Thoene and Lemons, 1980; Sumayao, Newsholme and McMorrow, 2018). Median IQR levels of CysSSP were 174 [150-197] μM, with a CV of 22% (**Figure III.6**). An indirect association between CysSSP and kidney function was observed (*Spearman* r = -0.278, $p < 0.001$) (**Figure III.7A**) and we were unable to find an association between CysSSP and uNAC (**Figure III.7B**).

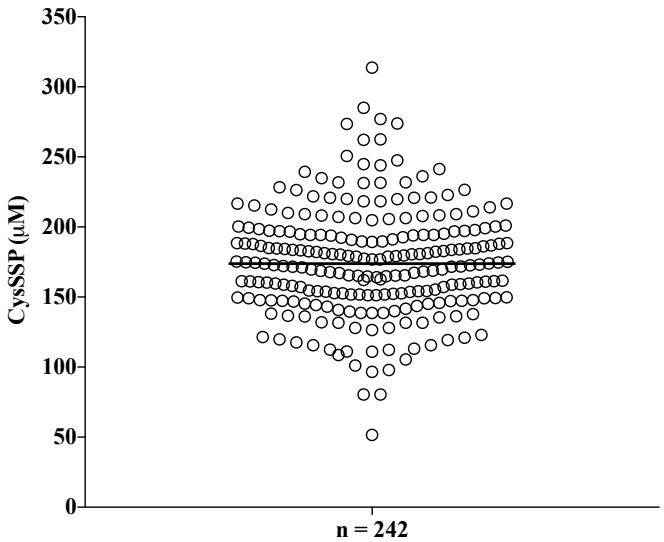

Figure III.6 – Serum CysSSP inter-individual variability among 242 included HIV-infected patients. Median [IQR] levels of serum CysSSP were 174 [150-197] μM, varying between 52 μM and 314 μM, with a coefficient of variation of 22%.
CysSSP: protein cysteinylation.

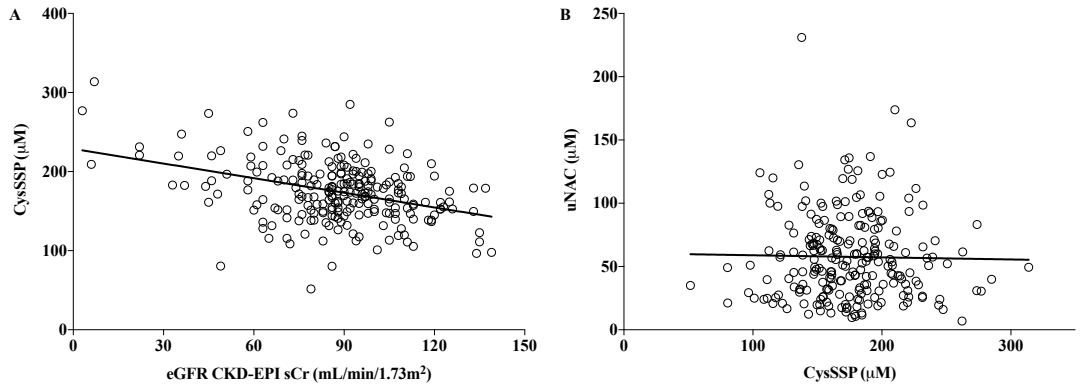

Figure III.7 – Serum CysSSP and its association with kidney function and uNAC. While patients with higher CysSSP had lower eGFR (*Spearman* r = -0.278, $p < 0.001$) (**A**), no association was found between CysSSP and uNAC (**B**).
CysSSP: protein cysteinylation; eGFR CKD-EPI sCr: estimated glomerular filtration rate obtained by chronic kidney disease-epidemiology collaboration using serum creatinine; uNAC: urinary surrogate of the mercapturates from cysteine-disulfides.

III.3.4. Association of uNAC with uLTE4

Since LTE4 is the most widely studied substrate of NAT8 (Veiga-da-Cunha *et al.*, 2010; Deol, 2015; Deol and Josephy, 2017), its urinary levels were quantified and related with uNAC in a subpopulation of the study (n = 40, median [IQR] age of 50 [44-60], 68% men, 25% Black). Whereas no association with eGFR was observed (**Figure III8.A**), uLTE4 levels were related with the levels of uNAC (*Spearman* r = 0.379, $p = 0.016$) (**Figure III8.B**).

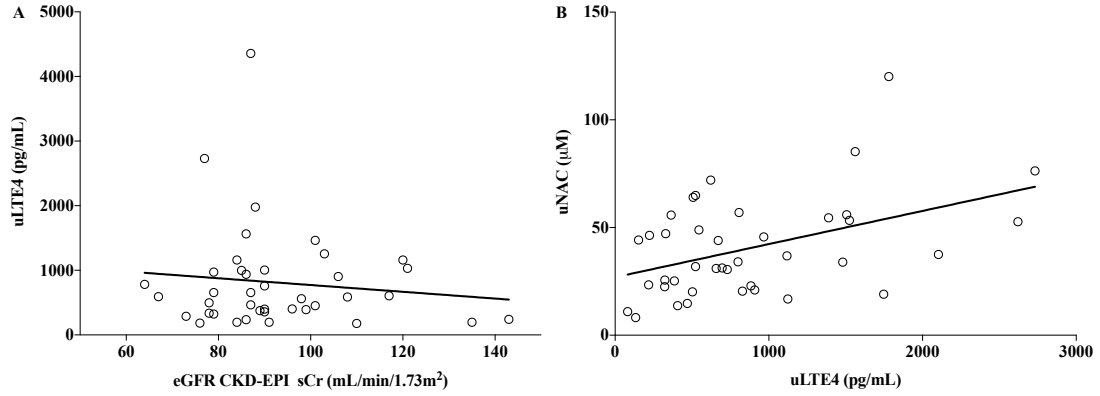

Figure III.8 – uLTE4 and its association with kidney function and uNAC. uLTE4 was not related with eGFR (**A**), whereas it was directly associated with the levels of uNAC (*Spearman* r = 0.379, $p = 0.016$) (**B**).
eGFR CKD-EPI sCr: estimated glomerular filtration rate obtained by chronic kidney disease-epidemiology collaboration using serum creatinine; uLTE4: urinary leukotriene 4; uNAC: urinary surrogate of the mercapturates from cysteine-disulfides.

III.3.5. Variability of uNAC with the progression of kidney disease after one year of follow-up

III.3.5.1. Patient's baseline (T0) status

A total of 118 HIV-infected patients fulfilled the criteria for inclusion on the one-year follow-up (samples collected at baseline, T0, and 12 months after, T12). Of them, 69% were men and 25% were Black. The median age of all patients included was 52 [42-60] years old and 96% were infected with HIV-type 1 virus.

At baseline, 90% of patients were on cART and cART schemes was distributed as follows: 52% with 2N(t)RTI+NNRTI, 19% with 2N(t)RTI+PI/r, 7% with PI/r+N(t)RTI and 22% with others cART schemes. A total of 63% of patients were on TDF-containing cART. Regarding baseline kidney function, 52 patients were NC, 51 were EKD and 15 were CKD. Of all, 52% showed progression of kidney disease, as shown by eGFR CKD-EPI obtained with serum creatinine. Anthropometric and clinical data at baseline for each group are presented in **Table III.2**.

Chi-square analysis showed significant differences among groups in what regards the number of patients under TDF-containing cART ($p = 0.001$) and on cART scheme ($p = 0.003$). No differences were found for anthropometric and hepatic function, with the exception of high density lipoprotein levels, which median levels were 52 [45-65] mg/dL for NC-NP, 58 [47-71 mg/dL for NC-P, 50 [38-55] mg/dL for EKD-NP, 48 [37-66] mg/dL for EKD-P, 68 [34-81] mg/dL for CKD-NP and 68 [58-74] for CKD-P ($p = 0.011$, data not shown). Concerning kidney function, baseline eGFR levels were similar between NP and P groups with the same baseline kidney function stratification. As patients were stratified according to baseline levels of eGFR, significant differences regarding this parameter were found, as expected ($p < 0.001$). Differences were also found for serum urea levels, urinary protein-to-creatinine ratio (uPCR), as well as the fractional excretions of sodium, potassium and phosphorus ($p < 0.001$ except for FePi, which was $p = 0.001$). Nevertheless, the fractional excretion of uric acid was similar among groups and there was not enough data regarding baseline urinary ACR (uACR). However, published guidelines for CKD screening in HIV-infected patients states that kidney function should be assessed by estimating eGFR and measuring proteinuria (Gupta *et al.*, 2005), as herein presented.

III.3.5.2. Patient's one-year of follow-up (T12) status

III.3.5.2.1 Clinical status at T12

We evaluated the patient's clinical status after one-year of follow-up regarding renal, hepatic and immunological function. Kidney function was assessed by eGFR CKD-EPI with sCr (**Figure III.9**). In comparison with NP groups, all P groups had decreased eGFR at T12 (median [IQR] of 84 [75-88], 83 [75-89] and 81 [72-86] % of T0, respectively for NC-P, EKD-P and CKD-P groups) ($p < 0.001$). On the other hand, EKD-NP patients had an increase in eGFR at T12 (107 [100-112] % of T0) than the remaining NP groups (98 [95-102] and 98 [93-117] % of T0, respectively for NC-NP and CKD-NP groups) ($p = 0.002$).

Liver function was assessed through transaminases levels. Alkaline phosphatase was increased in CKD-P group (110 [99-120] % of T0) in comparison with CKD-NP group (102 [71-245] % of T0) ($p = 0.016$, data not shown). On the other hand, lactate dehydrogenase was increased in EKD-NP group (107 [96-122] % of T0) compared to EKD-P group (99 [89-105] % of T0) ($p = 0.019$, data not shown). No further differences were found for the remaining parameters previously analyzed on baseline.

Table III.2 – Anthropometric and clinical data at baseline.

Parameter (Unit)	NC-NP (n = 25)	NC-P (n = 27)	EKD-NP (n = 27)	EKD-P (n = 24)	CKD-NP (n = 5)	CKD-P (n = 10)	*p* value
Men (%)	76	56	70	79	40	80	ns
Black (%)	24	26	33	17	20	30	ns
Age (years old) [a]	51 [43-56]	47 [44-58]	50 [42-56]	56 [49-63]	58 [44-66]	58 [50-83]	ns
Undetectable VL (%)	96	67	81	71	80	90	ns
$CD4^+$ T-cells (cells/μL) [a]	483 [339-771]	460 [207-636]	620 [380-783]	543 [388-648]	416 [356-1107]	448 [348-720]	ns
Patients on cART (%)	92	93	81	88	100	100	ns
Patients on TDF (%)	70	68	77	71	0	20	0.001 [b]
cART scheme (%)							
2N(t)RTI+NNRTI	83	68	37	33	20	30	
2N(t)RTI+PI/r	0	12	27	24	20	50	0.003 [b]
PI/r+N(t)RTI	0	4	18	14	0	0	
Other	17	16	18	29	60	20	
eGFR CKD-EPI sCr (mL/min/1.73m²) [a]	104 [94-109]	98 [93-110]	78 [75-86] ***, ###	80 [72-85] ***, ###	44 [22-58] ***, ###	47 [22-58] ***, ###	< 0.001 [c]
Serum Urea (mg/dL) [a]	30 [26-34]	31 [25-36]	36 [30-40]	38 [35-49] **, #	56 [42-190] **, #	62 [44-109] ***, ###, §	< 0.001 [c]
uPCR (mg/g of uCr) [a]	138 [99-193]	123 [105-205]	138 [108-194]	203 [125-344]	310 [97-2230]	677 [431-1315] ***, ###, §§§	< 0.001 [c]
FeNa (%) [a]	0.5 [0.3-0.8]	0.6 [0.4-0.9]	0.7 [0.4-1.1]	0.9 [0.7-1.5] *	1.2 [0.7-4.0]	1.7 [0.7-2.6] **, #	< 0.001 [c]
FeK (%) [a]	5.8 [4.0-8.2]	4.9 [3.7-7.3]	6.9 [4.3-12.7]	7.8 [5.1-12.1]	17 [13-18] *, ##	16 [11-18] **, ###	< 0.001 [c]
FePi (%) [a]	17 [11-22]	16 [10-21]	18 [13-22]	20 [15-25]	25 [21-54]	31 [19-39] *, ##	0.001 [c]

[a] Levels presented as median [IQR]; [b] *Chi*-square test; [c] *Kruskal-Wallis* test; *, **, ***, #, ##, ###, § or §§§ *Kruskal-Wallis* test with *Dunn's* multiple comparisons test (* *versus* NC-NP group; # *versus* NC-P group and § *versus* EKD-NP group); cART: combined antiretroviral therapy; CD: cluster of differentiation; CKD: chronic kidney disease; eGFR CKD-EPI sCr: estimated glomerular filtration rate with Chronic Kidney Disease-Epidemiology Collaboration equation using serum creatinine; EKD: early kidney disease; FeK: fractional excretion of potassium; FeNa: fractional excretion of sodium; FePi: fractional excretion of phosphate; NC: normal control; NNRTI: non-nucleoside reverse transcriptase inhibitor; NP: non-progression; N(t)RTI: nucleoside/nucleotide reverse transcriptase inhibitor; P: progression; PI/r: ritonavir-boosted protease inhibitor; TDF: tenofovir ; uPCR: urinary protein-to-creatinine ratio; VL: viral load; *, # or § $p < 0.05$; ** or ## $p < 0.01$; ***, ### or §§§ $p < 0.001$.

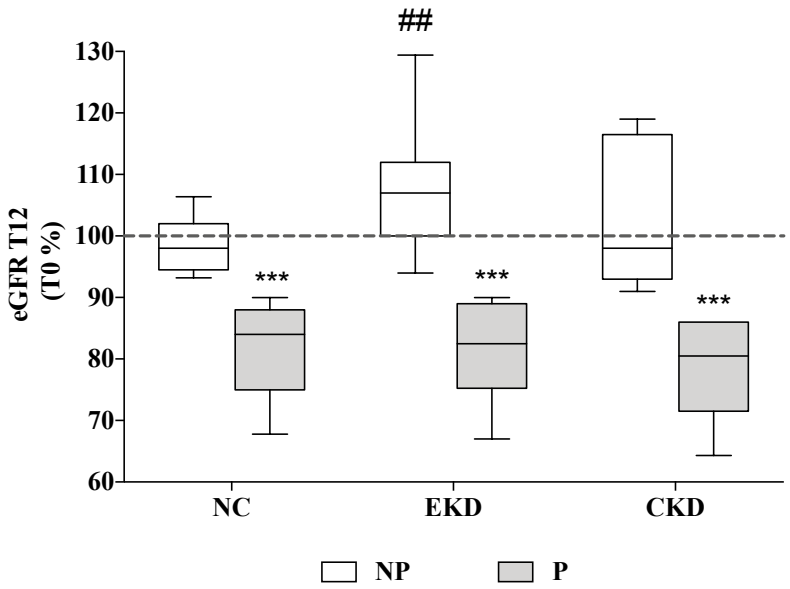

Figure III.9 – Variation of eGFR at T12. Patients from P groups showed a decrease in eGFR in comparison with NP groups. EKD-NP patients had an increase in eGFR in comparison with the other NP groups (n = 25 for NC-NP, 27 for NC-P, 27 for EKD-NP, 24 for EKD-P, 5 for CKD-NP and 10 for CKD-P).
eGFR presented as % of values attained at baseline; *** Two-way ANOVA with *Bonferroni's* multiple comparisons test (versus NP group); ## Kruskal-Wallis test, with *Dunn's* multiple comparisons test (versus NC-NP group); CKD: chronic kidney disease; eGFR: estimated glomerular filtration rate; EKD: early kidney disease; NC: normal control; NP: non-progression; P: progression; *** $p < 0.001$; ## $p < 0.01$.

III.3.5.2.2. uNAC at T12

Although the variation of uNAC at T12 was similar in NC groups (73 [56-131] and 73 [44-98] % of T0 respectively for NC-NP and NC-P groups), we found striking differences for the EKD and CKD groups (**Figure III.10**). Particularly, uNAC decreased significantly in the EKD-P group (56 [41-88] % of T0) comparatively to EKD-NP group (80 [65-119] % of T0) ($p = 0.009$). An even higher difference was found between CKD groups, with CKD-NP presenting a uNAC variation of 152 [123-188] % of T0 and while CKD-P group had 62 [56-80] % of T0 ($p < 0.001$). Furthermore, CKD-NP group had increased uNAC, relatively to the remaining NP groups ($p = 0.016$).

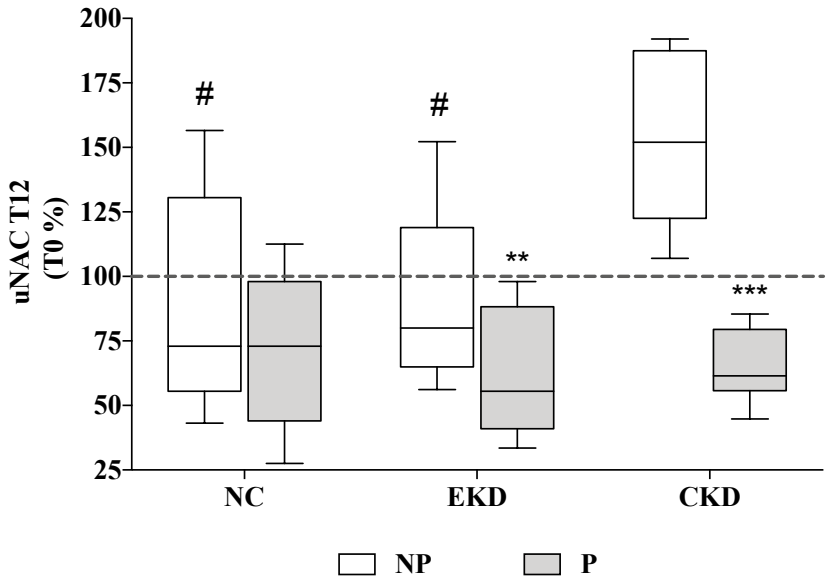

Figure III.10 – Variation of uNAC at T12. uNAC decreased in P groups in comparison with NP groups, particularly for EKD and CKD groups. Among NP groups, CKD patients had increased in uNAC (n = 25 for NC-NP, 27 for NC-P, 27 for EKD-NP, 24 for EKD-P, 5 for CKD-NP and 10 for CKD-P).
uNAC presented as % of values attained at baseline; ** or *** Two-way ANOVA with *Bonferroni's* multiple comparisons test (versus NP group); # Kruskal-Wallis test, with *Dunn's* multiple comparisons test (versus CKD-NP group); CKD: chronic kidney disease; EKD: early kidney disease; NC: normal control; NP: non-progression; P: progression; uNAC: urinary surrogate of the mercapturates from cysteine-disulfides; ** $p < 0.01$; *** $p < 0.001$; # $p < 0.05$.

In accordance with the results obtained in the cross-sectional study, *Spearman* correlation showed an association between the variation of uNAC and eGFR at T12 (*Spearman* r = 0.298, $p = 0.001$) (**Figure III.11**).

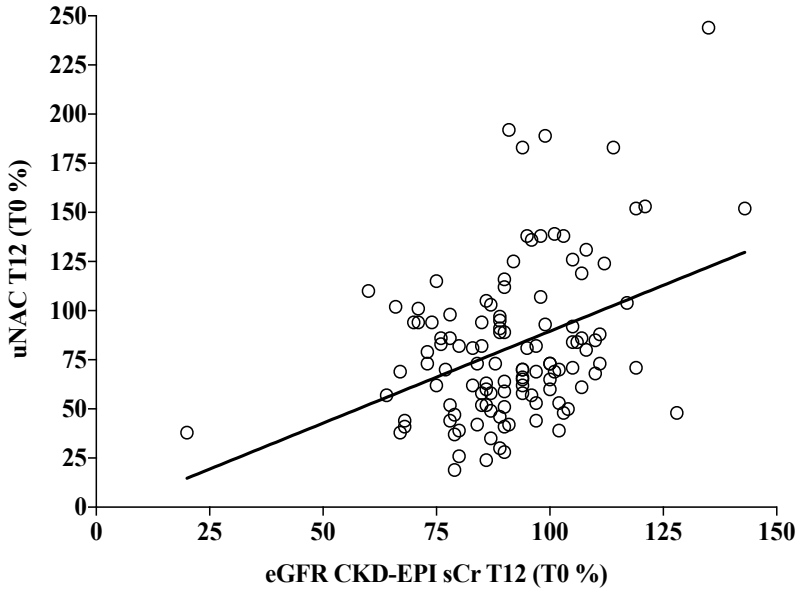

Figure III.11 – uNAC and eGFR at T12. The variation of uNAC was positively associated with eGFR (*Spearman* r = 0.298, $p = 0.001$) (n = 118).
Presented as % of values attained at baseline; eGFR CKD-EPI sCr: estimated glomerular filtration rate with Chronic Kidney Disease-Epidemiology Collaboration equation using serum creatinine; uNAC: urinary surrogate of the mercapturates from cysteine-disulfides.

III.4. Discussion

The present study showed that eGFR use of 3TC as well as Black race are factors that independently contribute for the high inter-individual variability found in uNAC levels. Notably, through a prospective analysis, we found that uNAC can discriminate patients with kidney disease progression from those that remain with stable kidney function, independently of their baseline eGFR values.

We found a high inter-individual variability on the capacity to detoxify CysSSX. While HIV-infected patients have a high prevalence of kidney disease, evidence for delineating the best therapeutic strategy in susceptible patients is limited by several factors. This include, for instance, the absence of accurate markers of kidney tubular function and the absence of long-term follow-up studies regarding the effects of chronic exposure to ARVs in a population affected by residual viremia and inflammation, immunosuppression and low antioxidant defenses (Swanepoel *et al.*, 2018).

While CysSSX might undergo glomerular filtration and tubular secretion (Crawhall *et al.*, 1967; Griffith, 1981; Commandeur, Stijntjes and Vermeulen, 1995), the detected uNAC, accordingly to our hypothesis and our results might be exclusively formed in tubular cells upon CysSSX acetylation by NAT8. This would explain the nephroprotective effect of NAT8 which has been reported mainly through genetic association studies (Juhanson *et al.*, 2008; Chambers *et al.*, 2010; Köttgen *et al.*, 2010; Tin *et al.*, 2013). Thus, changes in the levels of uNAC may reflect alterations solely happening in the proximal tubule. This might have important implications in the early detection of injury, since the proximal tubule has been identified as the primary sensor and effector in the progression of renal disease (Chevalier, 2016).

The widespread use of cART can be interpreted as a double-edged sword. Whereas cART has significantly reduced the incidence of the classic kidney disease associated with HIV-infection, HIV-associated nephropathy, it has also led to a concomitant increase in the prevalence of other kidney diseases (Swanepoel *et al.*, 2018). Additionally, as cART is chronically administrated throughout the patient's life (Cihlar and Fordyce, 2016), it is plausible to assume that cART could potentially induce or even exacerbate kidney injury at any time (Swanepoel *et al.*, 2018).

Oxidative stress has been increasingly implicated in HIV-associated kidney injury (Rai *et al.*, 2013) and several mechanisms have been reported for generating ARV-induced

oxidative stress. For instance, NRTIs are able to inhibit DNA polymerase gamma, further inhibiting mitochondrial DNA synthesis (Day and Lewis, 2004). On the other hand, decreased levels of oxidized glutathione (GSSG) were associated with the toxic effects of TDF (Morello *et al.*, 2018), which might indicate a decrease in GSH synthesis (Santangelo *et al.*, 2004; Shang *et al.*, 2016) or an increase in the conjugation of electrophiles with GSH (Wang and Ballatori, 1998). Additionally, protease inhibitors (PIs) trigger the increased production of reactive oxygen species, with downstream consequences that include impaired mitochondrial function and ubiquitin proteasome system dysregulation, and eventually cell death (Reyskens and Essop, 2014). ARVs were also reported to inhibit drug transporters and reduce tubular secretion of sCr (Yombi *et al.*, 2014). This might increase sCr and reduce eGFR although in the absence of change in the real GFR. For instance, TDF, 3TC, FTC, EFV and NVP are known inhibitors of multidrug-resistance-associated protein (MRPs) transporters, namely MRP1, MRP2 and MRP3 (Weiss *et al.*, 2007). ABC also inhibits MRP1 and MRP2 but has no effect on MRP3 (Weiss *et al.*, 2007). Therefore, both the inhibition of MRP2 and the GSH-conjugation of ARVs might influence the elimination of CysSSX. On the other hand, the cystinuria-related plasma membrane protein rBAT/SLC3A1, together with $b^{0,+}$AT/SLC7A9 (S1 segment) or AGT1/SLC7A13 (S3 segment) is responsible for CysSSCys reabsorption in the renal proximal tubules (Calonge *et al.*, 1995; Feliubadaló *et al.*, 1999; Nagamori *et al.*, 2016). The interaction between these transporters, as far as we know, remains to be investigated. The NNRTIs rilpivirine (Pereira *et al.*, 2012), EFV (Pereira *et al.*, 2012), NVP (Srivastava *et al.*, 2010) and ETV (Godinho *et al.*, 2018) are known to form reactive metabolites that are eliminated as mercapturates. The toxicity of these drugs is mostly associated with the liver, where they are mainly biotransformed (Pereira *et al.*, 2012). In fact, in the liver, GSH-conjugates are substrates of MRP2 (Keppler, 2005). Nevertheless, the susceptibility of this organ to this toxic mechanism is lower compared to the kidney, due to its increased capacity to produce GSH and to metabolize Cys, with consequent lower Cys/GSH ratio and hence lower susceptibility to oxidation (States, Foreman and Segal, 1987).

We observed that TDF use increased the levels of uNAC. This result was unexpected, as TDF has been associated with nephrotoxic events (Herlitz *et al.*, 2010; Scherzer *et al.*, 2012; Gupta *et al.*, 2014; Jotwani *et al.*, 2016), which includes Fanconi syndrome, characterized by an accumulation of CysSSCys (Cherqui and Courtoy, 2017). However, it is recommended this drug avoidance with eGFR bellow 60 mL/min/1.73m^2 or to stop

its prescription if eGFR drops 25% of baseline eGFR and to a level bellow 60 mL/min/1.73m^2 (Lucas *et al.*, 2014). This fact could explain the absence of differences in eGFR between patients receiving TDF and patients not receiving this drug. It can also explain the similar results obtained for FTC, since all patients from this group also had TDF on their cART scheme.

TDF is excreted by the kidneys through a combination of glomerular filtration and active tubular secretion (Barditch-Crovo *et al.*, 2001; Gutiérrez *et al.*, 2014) and is eliminated as an unchanged drug in urine since there is no hepatic biotransformation (Kearney *et al.*, 2006). Specifically, the basolateral uptake of TDF by proximal tubular cells is mediated by OAT1 and OAT3 while its efflux from tubular cells is mediated essentially by MRP4 (Kohler *et al.*, 2011). Evidence from both *in vitro* and *in vivo* models show that Cys-*S*-conjugates also enter the proximal tubular cells through OATs in both basolateral and brush border membranes (Lash and Anders, 1989; Commandeur, Stijntjes and Vermeulen, 1995; Groves *et al.*, 2003). As such, TDF and Cys-*S*-conjugates may compete for their basolateral uptake, which could explain the increased levels of uNAC in patients under TDF-containing cART. Another plausible explanation for this increase might be an adaptation to a nephrotoxic agent that leads to an over-production of CysSSX and/or acetylation of CysSSX to avoid injury. The transport of mercapturates for elimination still remains a debating issue, and there are only reports for the involvement of OATs, specifically OAT1, in the basolateral uptake when mercapturates are administered intravenously (Inoue, Okajima and Morino, 1981; Pombrio *et al.*, 2001), although the exact mechanism of transport across the brush border membrane is yet to be elucidated. Notably, TDF has higher affinity for OAT1 than OAT3 (approximately 20x more) although the expression of OAT3 in the proximal tubule is greater than OAT1 (Kohler *et al.*, 2011), which might also contribute for the results herein described.

On the other hand, ABC is extensively metabolized in liver, only with less than 2% being eliminated as an unchanged drug in urine. The major metabolites found in urine are inactive (a glucuronide and a carboxylate). The remaining percentage is divided between minor metabolites in urine and also faecal elimination (Yuen, Weller and Pakes, 2008). No differences were found on the pharmacokinetics of ABC in HIV-infected patients with kidney dysfunction from the profile observed in healthy adults (Izzedine *et al.*, 2001), which is consistent with the kidney's minor route of ABC elimination. Still, both ABC and 3TC have been implicated in case reports of Fanconi syndrome and nephrogenic diabetes insipidus (Ahmad, 2006; Nelson *et al.*, 2008). Moreover, 65% of ABC-patients

were treated with a combination containing 3TC, which was the only drug that independently influenced the levels of uNAC in this study. As so, the effect observed for ABC might be due to the simultaneous use of 3TC. Contrarily to ABC, renal clearance is the major route of elimination of 3TC. Indeed, about 70% of the unchanged drug is found in urine, being only 5 to 10% metabolized in liver to form a trans-sulfoxide metabolite which is then excreted by the kidney (Johnson *et al.*, 1998). Significant effects have been reported on the pharmacokinetics of 3TC with renal impairment (increase on peak concentration and half-life), and dose adjustment (dose reduction or lengthening of the dosing interval) is sometimes encouraged (Heald *et al.*, 1996). Moreover, the amount of the trans-sulfoxide metabolite excreted increases with decreasing renal function (Johnson *et al.*, 1998). The clinical relevance of these findings remains to be elucidated, since, as far as the author's knowledge, no toxicity studies have been reported for this metabolite.

Our results showed that Black race was the most important factor that independently determined the levels of uNAC, in a negative way. As a contributor to the calculation of eGFR (Levey *et al.*, 2009), racial differences are clearly evidenced regarding kidney disease. For instance, ESRD is disproportionately prevalent in Black people, its risk appears early in the course of kidney disease and is not explained by the survival advantage of Black people (Choi *et al.*, 2009). Specifically for HIV-infection, Black race is a traditional risk factor for the development of kidney disease (Winston *et al.*, 2008) and increases the risk of microalbuminuria and proteinuria by at least 2-fold (Szczech *et al.*, 2002, 2007).

A different, and yet very interesting explanation for the low uNAC in the Black race might be related with melanin. The formation of pheomelanin which is responsible for lighter colours (in opposition to eumelanin, responsible for darker colours) requires Cys. In fact, pheomelanogenesis has been proposed as a mechanism that contributes to the removal of excess Cys from the endogenous pool (Galván, Ghanem and Møller, 2012) potentially avoiding Cys oxidation in susceptible organs, as it is kidney.

The kidney is prone to receive a large quantity of CysSSX, owing to the high expression of its transporters (Calonge *et al.*, 1995; Feliubadaló *et al.*, 1999; Nagamori *et al.*, 2016). Moreover, the kidney is also susceptible to oxidation due to its dependence on oxidative phosphorylation to produce energy (Simmons, Bogusky and Humes, 1980; Basile, Anderson and Sutton, 2012; Chevalier, 2016). In fact, cysteinylated proteins are the major source of Cys and CysSSX for the proximal tubular cells (Thoene and Lemons, 1980;

Sumayao, Newsholme and McMorrow, 2018) and serum levels of CysSSP increase with the presence of kidney disease (Regazzoni *et al.*, 2013; Nagumo *et al.*, 2014). Our results are concordant with this, though no relation with uNAC was observed. This might suggest that CysSSX detoxification is somehow independent of CysSSP regulation and that uNAC do not allow to predict CysSSP. For instance, part of the lysosomal CysSSCys pool has been shown to be originated upon the uptake of extracellular CysSSCys mediated by the previous mentioned transporters (rBAT/SLC3A1, $b^{0,+}$AT/SLC7A9, AGT1/SLC7A13) (Calonge *et al.*, 1995; Feliubadaló *et al.*, 1999; Nagamori *et al.*, 2016). The efflux of CysSSCys into the cytosol is mediated by cystinosin. Under non-oxidative conditions, CysSSCys is reduced to Cys by the cytosolic reducing systems which leads to the formation of GSSG (Sumayao, Newsholme and McMorrow, 2018). An impairment in this system might lead to an accumulation of CysSSCys with consequent overload of NAT8 that is trying to detoxify these compounds. On the other hand, NAT8 function might also be overloaded due to the formation of other Cys-*S*-conjugates rather than CysSSX, such the case of LTE4. In fact, increased formation of mercapturates from CysSSX was associated with an increase in uLTE4 levels, probably suggesting that NAT8 is acetylating CysSSX rather than LTE4. Nevertheless, these results should be analyzed with caution. Besides the reduced sample size (n = 40 patients), the method herein used to measure LTE4 levels is limited by existing techniques. The manufacture state that cross reaction may still exist, as it is impossible to complete the cross-reactivity detection between human LTE4 and all the analogues (LTC4 and LTD4). Moreover, ideally, *N*-acetyl-LTE4 would be measured and the cross-reactivity with this compound is unknown.

Regarding the prospective analysis of the population, we observed that uNAC decreased with the progression of kidney disease, a result that was independent of the baseline eGFR, particularly for EKD and CKD patients. CKD-NP patients were the ones that had higher increases in uNAC for one year, suggesting that despite their lower kidney function, they are able to eliminate CysSSX and maintain stable their function even if it is low. This might also indicate that the decrease in uNAC levels observed is not due to lower activity of drug transporters, as CKD-NP patients have increased uNAC. As so, uNAC might represent a marker of tubular dysfunction, due to the predominance of the mercapturate pathway in the tubular cell (Chambers *et al.*, 2010; Veiga-da-Cunha *et al.*, 2010). Having into account the fact that the proximal tubule is the primary sensor and effector on the progression of kidney disease (Chevalier, 2016), this might have important implications for the early management and detection of kidney dysfunction. In this

scenario, patients with lower ability to detoxify CysSSX might be at a higher risk for the development and progression of kidney disease, a condition that could be further increased with the presence of factors like the exposure to nephrotoxic drugs.

III.5. Conclusions

In conclusion, our data shows that uNAC has a high person to person variability and that nucleosides backbone of cART, particularly 3TC, race and eGFR are factors for the high inter-individual variability observed. uNAC is able to identify patients that are progressing in their kidney disease related to a lower detoxification of CysSSX products. Moreover, it reveals that uNAC might be a candidate for a new biomarker for diagnosis of early events of tubulopathy and for theranostic purposes on this setting.

CHAPTER IV

Cysteine-disulfides dynamics in kidney tubule differs between models of pre-diabetes

CHAPTER IV

Cysteine-disulfides dynamics in kidney tubule differs between models of pre-diabetes

IV.1. Rationale & Objectives

Based on the data obtained in the previous chapter (**Chapter III**), we questioned how the dynamics of CysSSX will occur in the progression to CKD. For this purpose, as tubulointerstitial inflammation and oxidative stress have been described as events underlying it, we selected models of pre-diabetes. Growing evidence is now supporting the concept of diabetic tubulopathy as an underlying cause of DKD (Zeni *et al.*, 2017). The tubulocentric-concept of DKD links tubulointerstitial inflammation, oxidative stress, hypoxia and fibrosis with kidney dysfunction (Vallon, 2011), understanding the mechanisms underlying the progression of diabetic tubulopathy is in its infancy. As proximal tubule underlies the initiation and progression of the early pathogenesis of the diabetic kidney (Zeni *et al.*, 2017), we considered that Cys-*S*-conjugates dynamics and NAT8 are relevant players to be investigated (Dias et al, 2018).

As previously mentioned, the kidney is rich in Cys (States, Foreman and Segal, 1987; Guan *et al.*, 2003) and an organ highly susceptible to oxidation under inflammatory conditions (Simmons, Bogusky and Humes, 1980; Basile, Anderson and Sutton, 2012; Chevalier, 2016). Cys has a lower reductant capacity than GSH and is a first target for oxidative conditions (Jones *et al.*, 2000; Grunwell *et al.*, 2015). The total net content of Cys can dynamically exchange between distinct pools, which are influenced by the redox status of the tissue involved. The free Cys pool includes the free reduced (CysSH) and oxidized (when Cys forms a disulfide bond with other LMW thiol-containing molecule, CysSSX) fractions. The latter one contains symmetric disulfides (CysSSCys) and asymmetric disulfides such as CysSSG, CysSSCoA and CysSSHCys (Moreno *et al.*, 2014; Coelho *et al.*, 2018). Additionally, CysSSP is generated when a disulfide bond is formed between a free reduced Cys and a Cys protein residue (Rossi *et al.*, 2009).

Although the impact of these changes for kidney redox homeostasis and tubular disease progression is still to be fully understood, we hypothesized that the redox couple CysSH/CysSSX controls the rapid response to tubular injury and that the formation of disulfides is a protective mechanism, especially for the regulation of proteins.

Nevertheless, the formation of LWM disulfides might induce an opposite reaction and should be eliminated through acetylation. As so, the early events of injury should be an increase in CysSSX (and consequently uNAC) and CysSSP as an adaptive response.

Besides the toxic profile elicited by CysSSX (Vina *et al.*, 1983; Munday, 1989; Moreno *et al.*, 2014; Poole, 2015; Sumayao *et al.*, 2016; Coelho *et al.*, 2018), plasma Cys has been pointed out as one of the top uremic toxins (Duranton *et al.*, 2012). CysSSX might be detoxified through the action of NAT8, an enzyme that has been associated with the control of both blood pressure and kidney function (Juhanson *et al.*, 2008) and can be followed by uNAC elimination (**Chapter I**).

Herein, we studied the temporal variation of uNAC in two models of pre-diabetes, namely high-fructose (HFruct) and hypercaloric (HFat) diets and its association with renal NAT8 expression, Cys dynamics and kidney dysfunction. We hypothesize that changes in tubular CysSSX dynamics underlies the pathogenesis of diabetes-induced renal disease and that the monitoring of uNAC can be used as a marker of disease progression.

IV.2. Animals & Methods

IV.2.1 Animal models and study design

Experiments were performed using male C57BL/6 mice obtained from the NOVA Medical School rodent facility. Animals were housed in polycarbonate cages with wire lids and maintained under standard laboratory conditions as follows: artificial 12 h light/dark cycles at RT, with *ad libitum* access to food and water. Animals were specific-pathogen-free according to FELASA recommendations (Mähler *et al.*, 2014). All applicable institutional and governmental regulations concerning the ethical use of animals were followed, according to the NIH Principles of Laboratory Animal Care (NIH Publication 85 23, revised 1985), the European guidelines for the protection of animals used for scientific purposes (European Union Directive 2016/63/EU) and the Portuguese Law nº 113/2013. The experimental procedures received prior approval by the Portuguese Directorate-General for Food and Veterinary that regulates the animal care and use in research (protocol nº 0421/000/000/2017).

Animals were divided into three groups, each one exposed to a different type of diet. The mice were given *ab libitum* access to a normal diet containing 3.6 g/Kg of methionine

and 3.5 g/Kg of CysSSCys (Chow Group) (SDS diet RM3, *Special Diets Services*) or a high-fructose diet with 35% m/v of fructose (FRUC-00T-500, *Enzymatic*) in drinking water (HFruct group) or a hypercaloric diet with 58% fat by kcal, 175 g/Kg of sucrose and 2 g/Kg of DL-methionine (HFat group) (D12331, *Research Diet, Inc.*) for 15 weeks.

Animal's weight was weekly recorded, and food and water intake were recorded during the first six weeks of diet and caloric intake was obtained. Blood from tail tip and urine samples were collected throughout study-time. At the end of the experiments, animals were euthanized, and both kidneys were collected, weighed and stored until further analysis. The time at each sample was collected as well as the recording of data and performance of experiences is shown in **Figure IV.1**.

Week of study	0	1	2	3	4	5	6	7	8	9	10	11	12	13	14	15
Sample collection																 
Weight	x	x	x	x	x	x	x	x	x	x	x	x	x	x	x	x
Food intake	x	x	x	x	x	x	x									
Water intake	x	x	x	x	x	x	x									
Caloric intake	x	x	x	x	x	x	x									
IPGTT							x						x			
Baseline insulin													x			
Kidney histology																x
Kidney weight																x
Kidney qPCR																x
uCr	x	x	x		x				x							x
uACR	x								x							x
Kidney Cys																x
uNAC	x								x							x

Figure IV.1 – Study design. The "x" represents the time at each sample was collected and/or the experiment was performed.
Cys: cysteine; IPGTT: intra-peritoneal glucose tolerance test; ITT: insulin tolerance test; qPCR: quantitative real-time polymerase chain reaction; uACR: urinary albumin-to-creatinine ratio; uCr: urinary creatinine; uNAC: urinary surrogate of the mercapturates from cysteine-disulfides.

IV.2.2. Assessment of glucose tolerance and insulin resistance

Glucose tolerance was assessed by intra-peritoneal glucose tolerance test (IPGTT), performed at 6 and 12 weeks of diet in overnight-fasted conscious animals. Blood glucose was measured using a standard glucometer in samples collected from a small incision made at the tip of the tail immediately before glucose administration (2 g/Kg of body weight; G8270, *Sigma-Aldrich*) and 15, 30, 60, 90 and 120 afterwards. The area under the curve (AUC) describing blood glucose levels was then calculated. Insulin levels were measured at the baseline at 12 weeks of diet. The homeostasis model assessment of insulin resistance (HOMA-IR) was calculated using the formula: HOMA-IR = fasting insulin x fasting glucose / 22.5 to assess insulin resistance.

IV.2.3. Kidney parameters

IV.2.3.1. Weight and histology

After collection, both kidneys were weighted, and histological analysis was performed in 10% formaldehyde-fixed paraffin embedded left kidney. Sections from 3 mice *per* group were stained with H&E.

IV.2.3.2. Urinary creatinine (uCr)

The levels of uCr were quantified by a methodology adapted from George and collaborators (2006) (George *et al.*, 2006). Briefly, after centrifugation (800g, 5 min, 4 °C), urine samples were diluted (1:20 to 1:40) in reverse osmosis water. A total volume of 20 µL was analyzed by high-performance liquid chromatography with ultraviolet detection (HPLC-UV) on an Agilent 1100 Series equipment (*Agilent Technologies*), using a reversed-phase Luna C18 (250 mm x 4.6 mm; 5 µm; 100 Å; *Phenomenex*), at 25 °C. The mobile phase was a 10 mM potassium dihydrogen phosphate solution (pH 4.7) (104877, *Merck*). Cr (retention time 4.3 min) was separated in an isocratic elution mode, with a flow rate of 1 mL/min and UV detection at 220 nm. The concentration of Cr from urine samples was extrapolated from calibration curves constructed with standards with known concentrations of Cr (C4255-10G, *Sigma-Aldrich*) that were submitted to the same procedure described for urine samples.

IV.2.3.3. uACR

Albuminuria levels were measured using the Bromocresol Green Albumin (BCG) Assay Kit (MAK124, *Sigma-Aldrich*). The assay was performed in duplicate following the manufacturer's instructions in a 96-well flat bottom plate. First, 5 µL of urine sample or standards were transferred into each well followed by the addition of 200 µL of BCG reagent. After an incubation period of 5 min at RT, the absorbance was measured at 620 nm in a microplate reader (Biotrack II plate reader, *Amersham Biosciences*). Then, uACR was obtained by dividing albumin by uCr levels.

IV.2.3.4. Gene expression

Right kidney tissue was collected and homogenized in Trizol® (T9424, *Sigma-Aldrich*) using a tissue homogenizer (Heidolph DIAX 900). Total RNA extraction was performed according to the Trizol® manufacturer's instructions. The RNA concentration was determined prior to cDNA synthesis by measuring the absorbance at 260 nm on a Nanodrop 2000 (*Thermo Scientific*). cDNA was synthesized from 1 µg of RNA, according to manufacturer's instructions (MB12501, *nzytech*). Mouse specific primers were used for the housekeeping gene (*Hprt*) as wells as for the target genes. The selected genes and the primer sequences are shown in **Table IV.1**.

The experiments were performed using LightCycler® 480 SYBR Green I Master Mix (04887352001, Roche), according to manufacturer's protocol. Quantitative real-time PCR (qPCR) was performed on a LightCycler® 480 II real-time PCR system (*Roche*). Experiments were performed in biological triplicates. The relative quantification was performed using the comparative CT method (2 - ΔΔCt) with LightCycler® 480 Software release 1.5.0 SP4.

Table IV.1 - Primer sequences of housekeeping gene and target genes.

Gene	Forward 5'-3'	Reverse 5'-3'
Hprt	GGACTGATTATGGACAGACTGG	GTAATCCAGCAGGTCAGCAAAG
Nat8	CAGAACTGTCCTCCAGTTTGC	GTATGTCCACGAAGGATTCACC
Fn	TGACTGGCCTTACCAGAGGG	CATCTGTAGGCTGGTTCAGGC
Col1a2	GGTCCCCGAGGCAGAGAT	CCATTAAACCCATTGGTCCAGG
Tgfb1	GAAGAACTGCTGTGTGCGGC	CTCCACCTTGGGCTTGCGA
Vim	CCGAGGAATGGTACAAGTCCA	CTCTTCCATCTCACGCATCTG
Hspa5	GTCTTCTCAGCATCAAGCAAGG	CCAACACTTTCTGGACAGGCT
Ccl2	TAGGCTGGAGAGCTACAAGAGGAT	AGACCTCTCTCTTGAGCTTGGTGA
Tnfa	GGGTGATCGGTCCCCAAAG	TTGAGATCCATGCCGTTGGC
Fbpase	AGCCTTCTGAGAAGGATGCTC	GTCCAGCATGAAGCAGTTGAC
Chrebp	CTGGGGACCTAAACAGGAGC	GAAGCCACCCTATAGCTCCC
Srebp1a	GGCCGAGATGTGCGAACT	TTGTTGATGAGCTGGAGCA TGT
Elovl2	CCTGCTCTCGATATGGCTGG	AAGAAGTGTGATTGCGAGGTTAT
Glut2	TTTCTTTGCCCTGACTTCCT	GGCTAATTTCAGGACTGGTT
Sglt2	TAGAGGCACAGTTGGTGGCTA	CGAGGAGCAGCACCACGA

Ccl2: chemokine (C-C motif) ligand 2; Chrebp: carbohydrate-responsive element-binding protein; Col1a2: collagen, type I, alfa 2; Elovl2: elongation of very long chain fatty acids like 2; Fbpase: fructose 1,6 biphosphatase; Fn: fibronectin; Glut2: glucose transporter 2; Hprt: hypoxanthine guanine phosphoribosyl transferase; Hspa5: heat shock protein 5; Nat8: *N*-acetyltransferase 8; Sglt2: sodium/glucose co-transporter 2; Srebp1a: sterol regulatory element binding protein; Tgfb1: transforming growth factor, beta 1; Tnfa: tumor necrosis factor, alfa; Vim: vimentin;

IV.2.4. CysSSX and related metabolites

IV.2.4.1. Quantification of Cys fractions in kidney

Renal total and free total fractions of Cys were quantified using a fourth (between 30 to 60 mg) of the right kidney. The tissue was homogenized in 400 µL of iced PBS 1x (P4417-100TAB, *Sigma-Aldrich*) in a tissue homogenizer (Heidolph DIAX 900). The quantification was performed by an HPLC-FD method, as previously reported (Grilo *et al.*, 2017; Coelho *et al.*, 2018) (**Chapter III**).

IV.2.4.2. Quantification of uNAC, uCys and uCysGly

The levels of uNAC, uCys (as a measure of CysSSX filtration and reabsorption) and uCysGly (as a measure of GSH turnover) were quantified in urine by HPLC-FD (**Chapter I**) (Grilo *et al.*, 2017; Coelho *et al.*, 2018).

IV.2.5. Statistical analysis

Statistical analysis was performed using GraphPad Prism® version 7.0 (GraphPad Software Inc., San Diego, CA, USA). Data are presented in % of effect or as mean ± SD. Whenever applicable, data was analysed through, Unpaired t-test, One-way ANOVA with *Dunnett's* multiple comparisons test or Two-way ANOVA with *Bonferroni's* multiple comparisons test. Statistical significance for all tests was set at the level of $p < 0.05$.

IV.3. Results

IV.3.1. Animals

At the beginning of the experiments, animals (n = 6 animals *per group*) were age-matched (6 weeks of age) and no differences were found regarding total body weight (mean ± SD BW of 16 ± 3 g, 18 ± 2 g and 18 ± 4 g, respectively for Chow, HFruct and HFat groups). However, the HFat group gained significantly more weight throughout study time in comparison with the remaining groups (**Figure IV.2**). Specifically, the HFat group presented higher weight variation than the Chow group right after 4 weeks of diet ($p < 0.023$), further increasing until the end of the study. A similar result was obtained between HFat and HFruct groups ($p < 0.001$) (**Figure IV.2**).

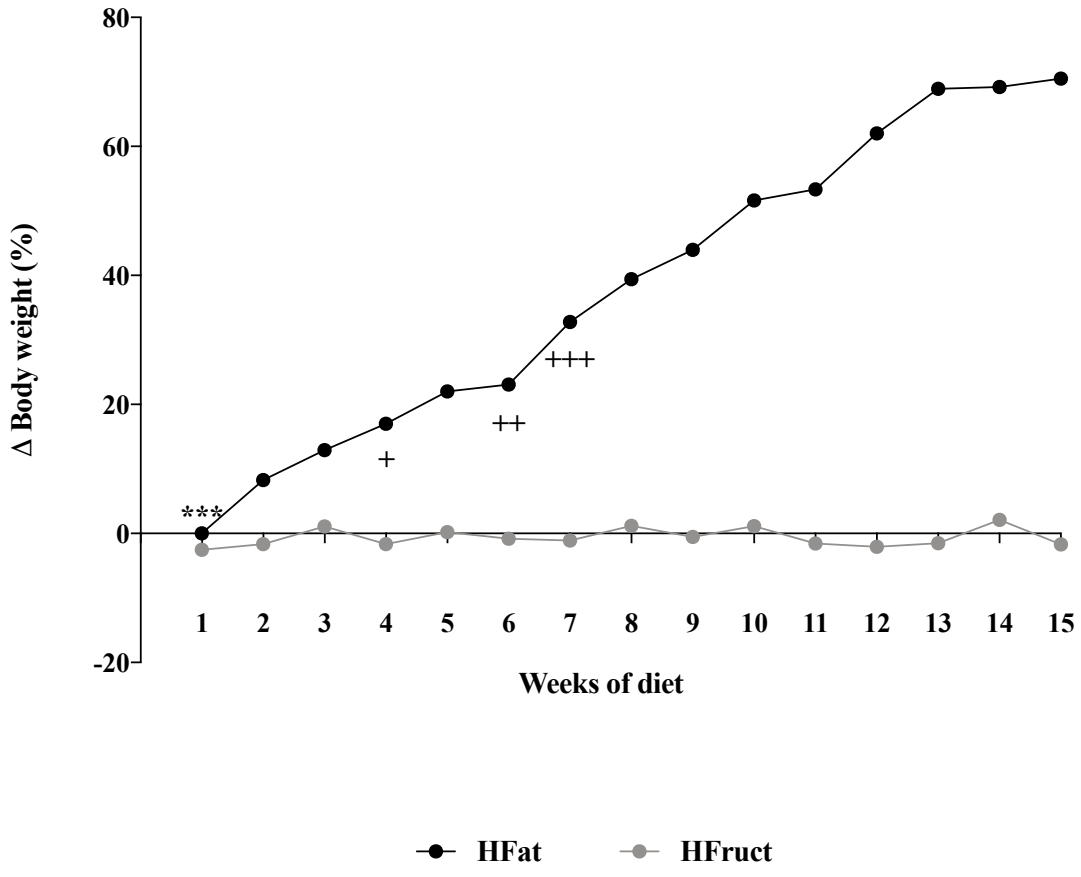

Figure IV.2 – Weight variation throughout study time. After 4 weeks of diet, the HFat group gained significantly more weight than the Chow group, a difference that further increased until the end of the experiment. This difference was also observed between the HFat and the HFruct group (n = 6 animals per group).
Body weight was normalized by the values attained at week 0 and is presented as percentage of effect from Chow group; *** Two-way ANOVA with *Bonferroni's* multiple comparisons test, versus HFruct group of the same week; +, ++ or +++ Unpaired t-test, versus Chow group of the same week; HFat: hypercaloric diet group; HFruct: high-fructose diet group.; + $p < 0.05$; ++ $p < 0.01$; +++ or *** $p < 0.001$.

Daily records during the first six weeks of diet showed that both models had a decrease in ingestion of food and water in comparison with the Chow group ($p < 0.001$ for food and $p = 0.003$ for water intake) **(Figure IV.3A and IV.3B**). Additionally, HFruct animals presented lower ingestion of food than the HFat model ($p < 0.001$).

However, this decrease was not translated in a decrease on caloric intake (**Figure IV.3C**). In fact, a tendency for an increase in caloric intake in the HFat group was observed after 5 weeks of diet.

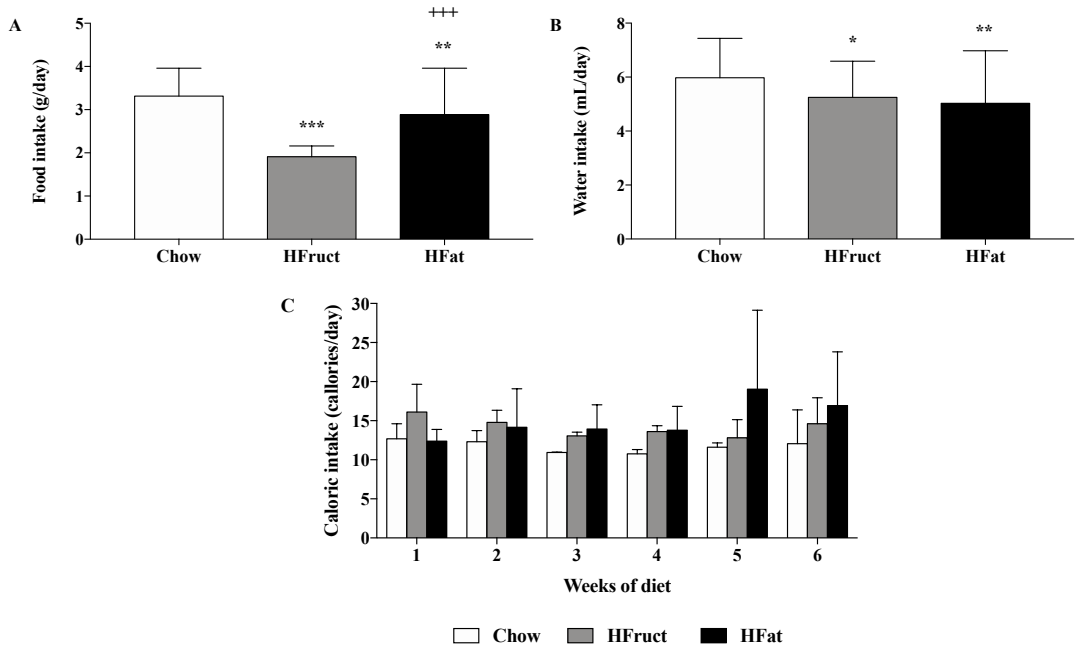

Figure IV.3 – Daily food and water intake and caloric intake during the first six weeks of diet. HFat and HFruct groups had lower ingestion of food (**A**) and water (**B**) than the Chow group during the first six weeks of diet. However, for caloric intake a tendency for an increase was observed after 5 weeks of diet (**C**) (n = 6 animals per group).
Values presented as mean ± SD; *, **, *** or +++ One-way ANOVA with *Bonferroni's* multiple comparisons test (*, ** or *** versus Chow group and +++ versus HFruct group); HFat: hypercaloric diet group; HFruct: high-fructose diet group; * $p < 0.05$; ** $p < 0.01$; *** or +++ $p < 0.001$.

IV.3.2. Assessment of glucose tolerance and insulin resistance

To assess glucose tolerance of these animals, we performed the IPGTT in two different time-points. At 6 weeks, blood glucose curve was significantly different after 60 min for HFat and after 90 min for HFruct groups ($p < 0.001$) (**Figure IV.4A**). However, the AUC parameter was not different among groups (**Figure IV.4B**). In contrast, 12 weeks of diet induced changes in the blood glucose curve of the HFat group after 30 min of injection ($p = 0.02$ for 30 min, $p = 0.002$ for 60 min, $p < 0.001$ for 90 min and $p = 0.001$ for 120 min) (**Figure IV.4C**) that was translated in an impaired glucose tolerance in comparison with both the Chow and HFruct diets, as evidenced by the increased AUC for glucose ($p < 0.001$) (**Figure IV.4D**). Furthermore, we also assessed insulin resistance at 12 weeks of diet through the calculation of HOMA-IR (**Figure IV.5**). Similarly, the HFat group presented higher HOMA-IR in comparison with the Chow group ($p = 0.035$) as well as with the HFruct group ($p = 0.049$), compatible with the presence of insulin resistance in these animals.

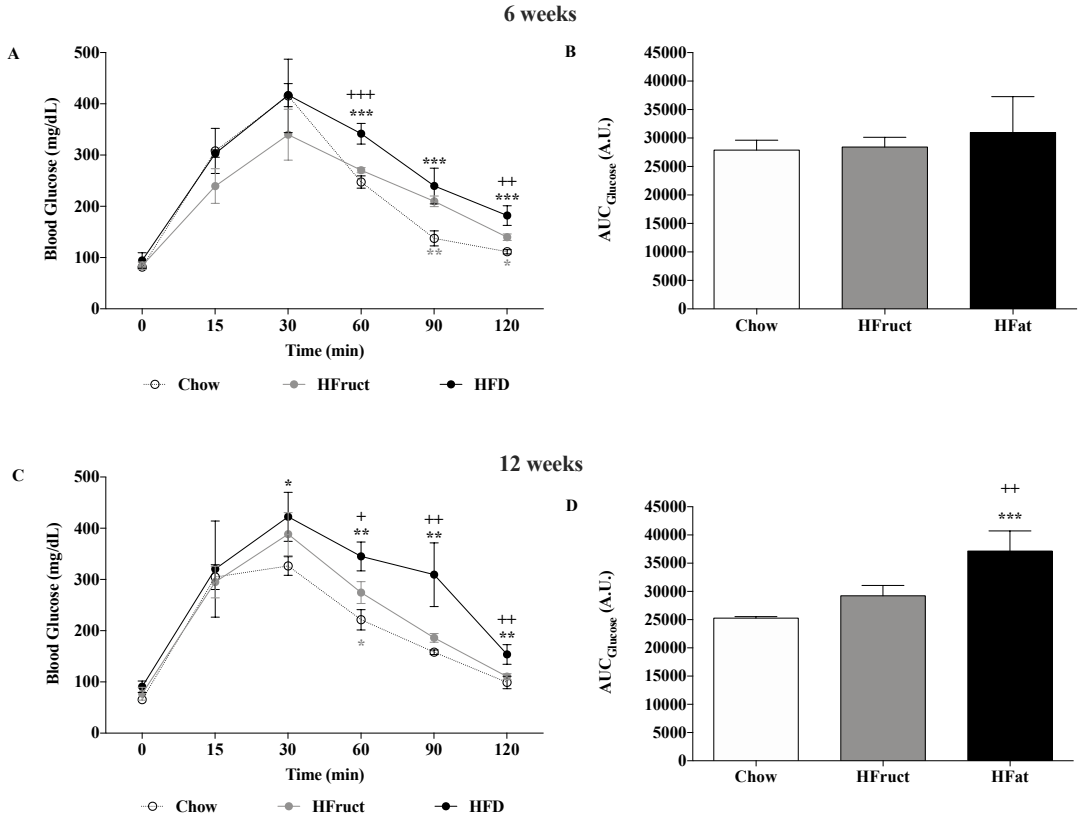

Figure IV.4 – Intra-peritoneal glucose tolerance test. Glucose tolerance was similar between groups at 6 weeks of diet (**A** and **B**). However, at 12 weeks, mice from HFat group were intolerant to glucose, as shown by the increase on the area under the curve (**C** and **D**) (n = 3 to 6 animals per group).
Values presented as mean ± SD; *, **, ***, +, ++ One-way ANOVA with *Bonferroni's* multiple comparisons test (*, **, *** versus Chow group, where black symbols are for HFat and grey symbols are for HFruct group; and + or ++ versus HFruct group); AUC: area under the curve; HFat: hypercaloric diet group; HFruct: high-fructose diet group; * or + $p < 0.05$; **, ++ $p < 0.01$; *** $p < 0.001$.

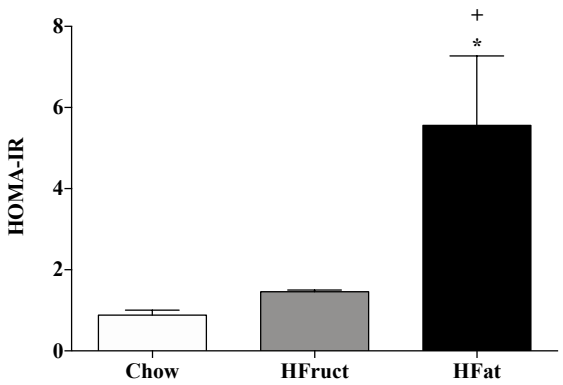

Figure IV.5 – Insulin resistance test. At 12 weeks of diet, the HFat group presented higher HOMA-IR in relation to both the Chow and the HFruct groups, characteristic of a phenotype of insulin resistance (n = 3 to 4 animals per group).
Values presented as mean ± SD; * or + Unpaired t-test (* versus Chow group and + versus HFruct group); HFat: hypercaloric diet group; HFruct: high-fructose diet group; HOMA-IR: homeostasis model assessment of insulin resistance; * or + $p < 0.05$.

IV.3.3. Kidney parameters

IV.3.3.1. Weight and histology

The weights of both kidneys were assessed as additional reflections of diet on kidney status. The HFat group showed higher kidney weights in comparison with the remaining groups ($p < 0.001$) (**Figure IV.6A and IV.6B**). On the other hand, H&E staining-histological analysis revealed a normal architecture with no clear pathology on the left kidney of all animals examined (**Figure IV.7**).

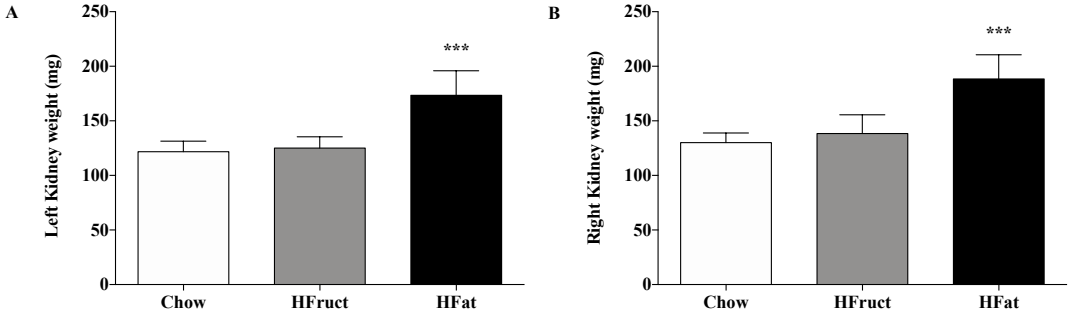

Figure IV.6 – Left and right kidney weights. The HFat group presented higher weight of both kidneys (**A** for left kidney and **B** for right kidney) (n = 6 animals per group).
*** One-way ANOVA with *Bonferroni's* multiple comparisons test, versus Chow and HFruct groups; HFat: hypercaloric diet group; HFruct: high-fructose diet group; *** $p < 0.001$.

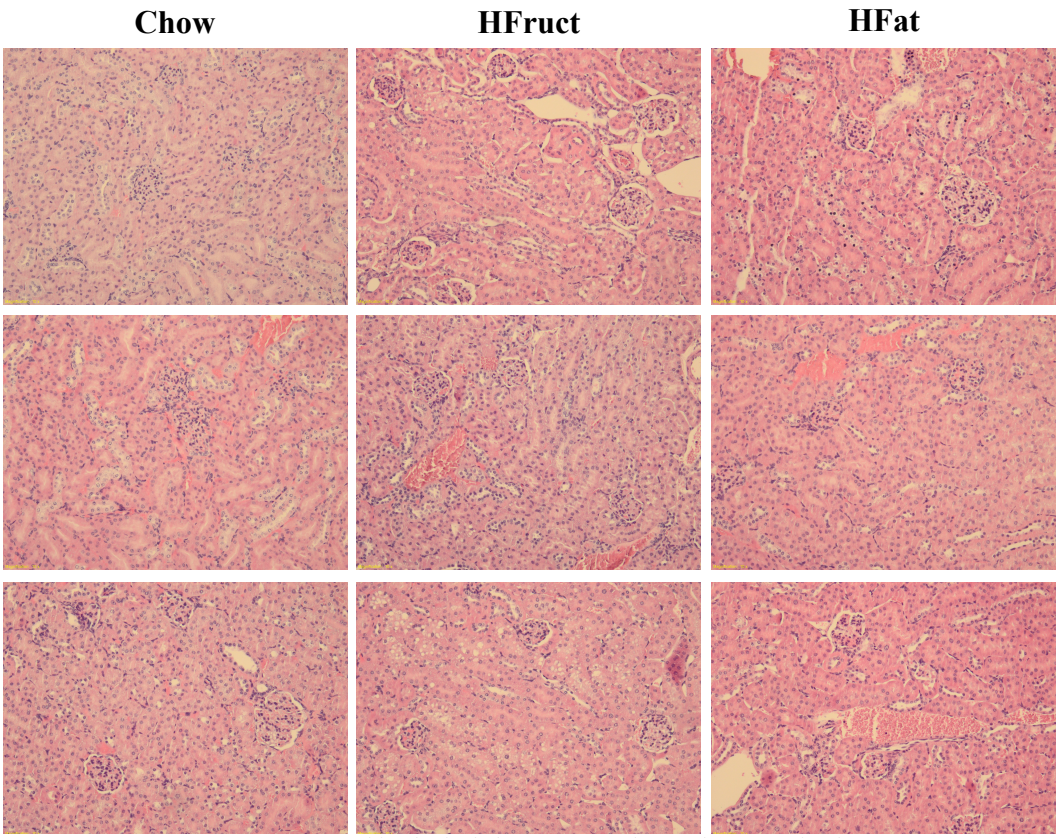

Figure IV.7 – Left kidney histology. No histological changes were observed (n = 3 animals per group).
Staining was performed in 10% formaldehyde-fixed paraffin embedded left kidney sections using H&E; Magnification: 10x; HFat: hypercaloric diet group; HFruct: high-fructose diet group.

IV.3.3.2. uCr

uCr was quantified in order to normalize albuminuria as well as the urinary concentration of metabolites herein described (uCys, uNAC, uCysGly) (**Figure IV.8**). An increase on creatinuria was observed in the HFat model right after 2 weeks of diet and until the end of the study in comparison with the Chow group ($p = 0.006$ for weeks 2 and 4 and $p < 0.001$ for weeks 8 and 15 of diet). As for the HFruct group, changes in uCr levels were only visible at 8 weeks of diet ($p = 0.009$).

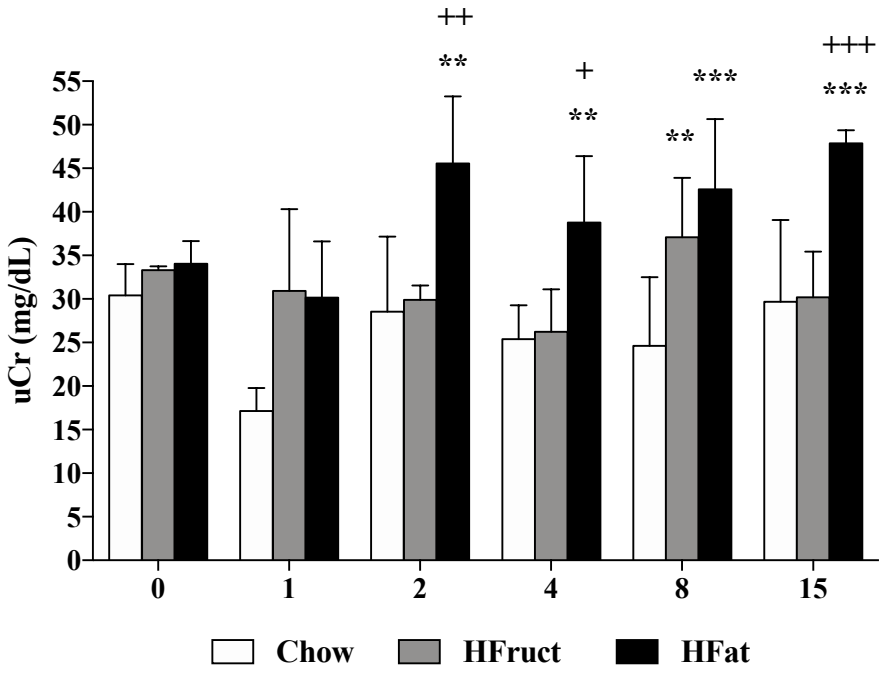

Figure IV.8 – uCr levels. While an increase in creatinuria was observed right after 2 weeks of HFat diet, mice from the HFruct group presented increased creatinuria only at 8 weeks of diet (n = 3 to 6 animals per group).
, *, +, ++, +++ Two-way ANOVA with *Bonferroni's* multiple comparisons test (** or *** versus Chow group and +, ++ or +++ versus HFruct group); HFat: hypercaloric diet group; HFruct: high-fructose diet group; uCr: urinary creatinine; + $p < 0.05$; ** or ++ $p < 0.01$; *** or +++ $p < 0.001$.

IV.3.3.3. uACR

The temporal variation of uACR (**Figure IV.9**) was evaluated as a measure of kidney function. uACR was stable throughout study time in the Chow group (872 ± 355 mg/g of uCr, 953 ± 276 mg/g of uCr and 914 ± 418 mg/g of uCr, respectively for weeks 0, 8 and 15 of diet). We were able to observe increases in uACR in both HFruct and HFat groups

after 8 and 15 weeks of diet. This increase was significantly higher for the HFat group in both time-points ($p < 0.001$ for week 8 and $p = 0.001$ for week 15) (**Figure IV.9**).

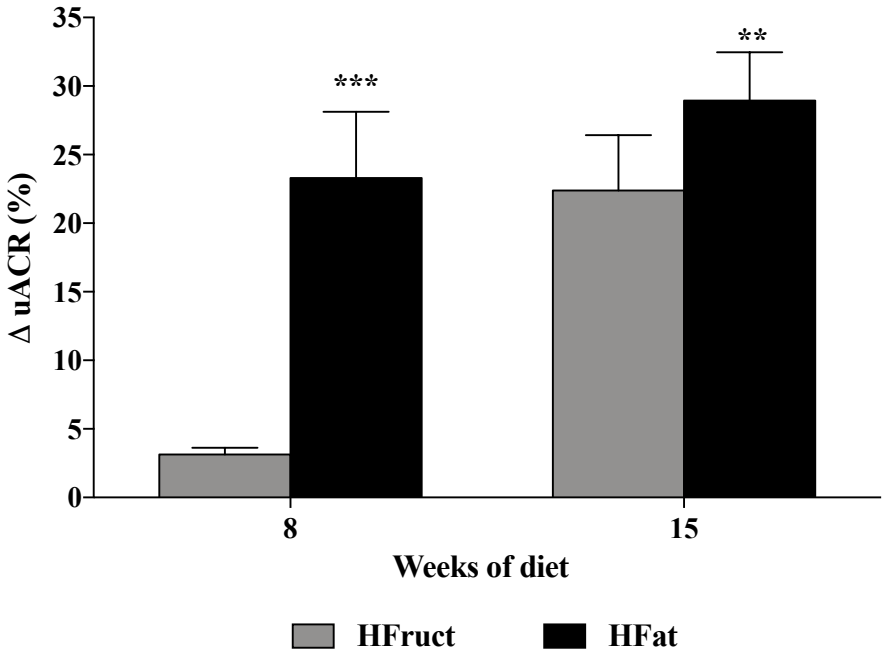

Figure IV.9 – uACR variation at 8 and 15 weeks of diet. Although not statistically significant, HFruct and HFat diets increased uACR throughout study time, an increase that was more pronounced for the HFat group (n = 3 to 6 per group, per week).
uACR was normalized by the values attained at week 0 and is presented as percentage of effect from Chow group; ** or *** Two-way ANOVA with *Bonferroni's* multiple comparisons test, versus HFruct group of the same week; HFat: hypercaloric diet group; HFruct: high-fructose diet group; uACR: urinary albumin-to-creatinine ratio; ** $p < 0.01$; *** $p < 0.001$.

IV.3.3.4. Gene expression

The renal expression of several genes involved in different processes that might influence kidney status was also quantified and the results are depicted in **Figure IV.10**. We first analyzed the expression of *Nat8*, as the enzyme responsible for the detoxification of CysSSX, and observed an increase in its expression for the HFat group ($p = 0.001$) (**Figure IV.10A**). As this enzyme is expressed in the ER, we have also evaluated a markers of ER stress as heat shock protein 5 (*Hspa5*, also known as *Grp78*) was quantified and was increased in both pre-diabetic models ($p < 0.001$) (**Figure IV.10A**).

Secondly, we wanted to assess the renal expression of genes related with inflammation, fibrosis and epithelial to mesenchymal transition (EMT) (**Figure IV.10B**). We analyzed the expression of chemokine (C-C motif) ligand 2 (*Ccl2*, also known as *Mcp1*) and tumor necrosis factor alfa (*Tnfa*), observing increases in both HFruct and HFat diets ($p < 0.001$

and $p = 0.002$, respectively for *Ccl2* and *Tnfa*). A marked increased in the expression of fibronectin (*Fn*), collagen type 1 alfa 2 (*Col1a2*) and *Tgfb1* was found in the HFat group, whilst the levels of vimentin (*Vim*) were increased in both HFruct and HFat ($p < 0.001$ for *Fn* and *Col1a2*; $p = 0.007$ for *Tgfb1* and *Vim*) (**Figure IV.10B**).

Finally, we evaluated markers of glucose and lipid metabolism and dynamics (**Figure IV.10C**) revealing an increase in the of expression of fructose 1,6 biphosphatase (*Fbpase*) in the kidney of HFat mice ($p < 0.001$). Additionally, the HFat group also presented higher expression of sterol regulatory element binding protein (*Srebp1a*) and elongation of very long chain fatty acids like 2 (*Elovl2*) ($p = 0.029$ and $p = 0.020$, respectively for *Srebp1a* and *Elovl2*). Both HFruct and HFat diets induced higher expression of carbohydrate-responsive element-binding protein (*Chrebp*) ($p < 0.001$). We also assessed the expression of glucose transporter 2 (*Glut2*) and sodium/glucose co-transporter 2 (*Sglt2*), the later was increased mice fed with HFruct diet ($p = 0.019$) (**Figure IV.10C**).

IV.3.4. CysSSX and related metabolites

IV.3.4.1. Quantification of Cys fractions in kidney

To investigate the status of CysSSX availability and dynamics in pre-diabetes, Cys fractions were quantified in kidney homogenates upon exposure to the different diets. Animals from the Chow group presented a Cys total net of 14 ± 1 μM/mg of tissue. The free Cys pool (containing both the reduced and oxidized fractions of Cys) represented the major fraction of Cys in this tissue (11 ± 1 μM/mg of tissue) whereas a small proportion (about 21%) of Cys levels were found bound to proteins (3 ± 1 μM/mg of tissue). Exposure to the pre-diabetic-inducing diets lead to different outcomes ($p < 0.001$ for all fractions in both diets) (**Figure IV.11**). While an increase in all fractions was found for the HFruct group in comparison with the Chow diet ($p = 0.046$, $p = 0.045$ and $p = 0.017$, respectively for total, free total and CysSSP fractions), the HFat diet decreased all fractions ($p = 0.028$, $p = 0.065$ and $p = 0.049$, respectively for total, free total and CysSSP fractions) (**Figure IV.11**)

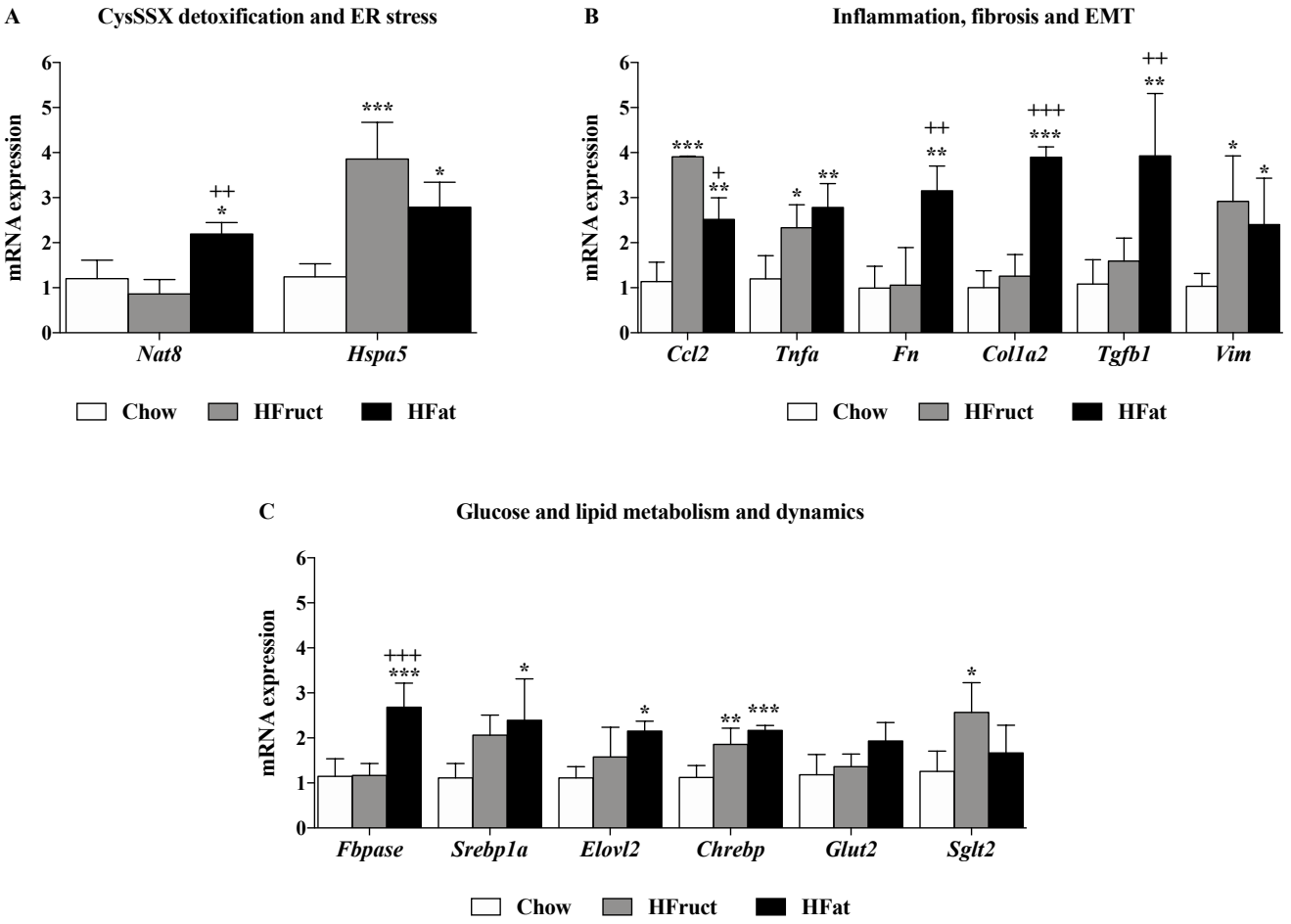

Figure IV.10 – Renal gene expression at 15 weeks of diet. The HFat group presented increased renal expression of Nat8, Ccl2, Tnfa, Fn, Col1a2, Tgfb1, Vim, Hspa5, Fbpase, Chrebp, Srebp1a and Elovl2. On the hand the HFruct group has increased expression of Vim, Hspa5, Ccl2, Tnfa, Chrebp and Sglt2 (n = 6 animals per group)

Gene expression was normalized by Hprt; *, **, ***, +, ++ or +++ One-way ANOVA with *Bonferroni's* multiple comparisons test (*, ** or *** versus Chow group and +, ++ or +++ versus HFruct group); Ccl2: chemokine (C-C motif) ligand 2; Chrebp: carbohydrate-responsive element-binding protein; Col1a2: collagen, type I, alfa 2; Elovl2: elongation of very long chain fatty acids like 2; Fbpase: fructose 1,6 biphosphatase; Fn: fibronectin; Glut2: glucose transporter 2; HFat: hypercaloric diet; HFruct: high-fructose diet; Hspa5: heat shock protein 5; Nat8: N-acetyltransferase 8; Sglt2: sodium/glucose co-transporter 2; Srebp1a: sterol regulatory element binding protein; Tgfb1: transforming growth factor, beta 1; Tnfa: tumor necrosis factor, alfa; Vim: vimentin; * or + $p < 0.05$; ** or ++ $p < 0.01$; *** or +++ $p < 0.001$.

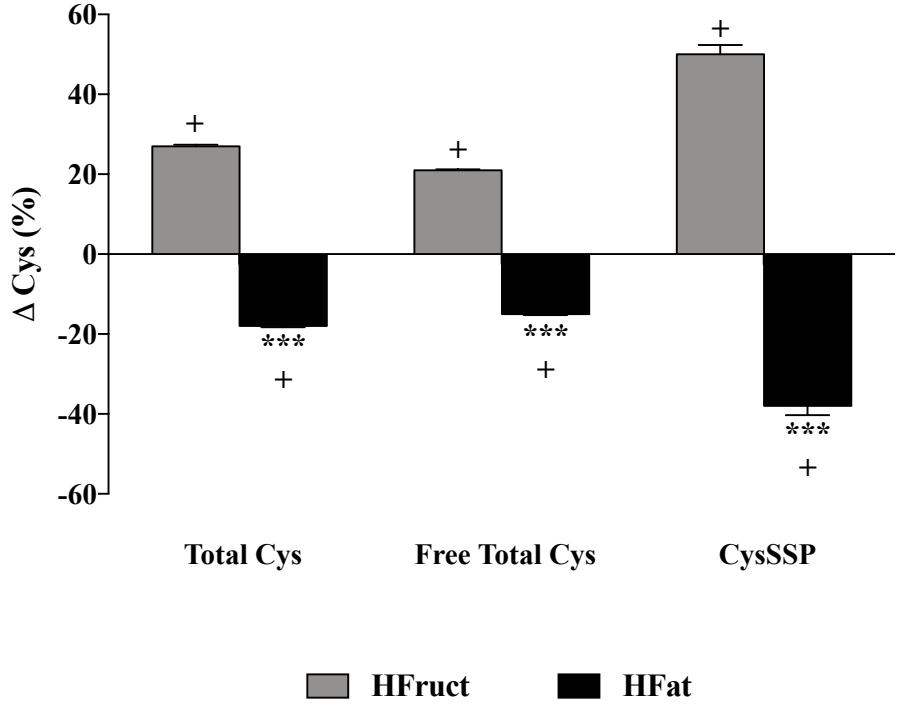

Figure IV.11 – Cys fractions in kidney homogenates after 15 weeks of diet. HFruct group presented increases in all fractions, while the HFat diet induced decreases (n = 4 animals per group).
Cys fractions were normalized by tissue weight and are presented as the percentage of effect from Chow group; *** Two-way ANOVA with *Bonferroni's* multiple comparisons test, versus HFruct group; + Unpaired t-test, versus Chow group; Cys: cysteine; CysSSP: cysteine protein-bound fraction; HFat: hypercaloric diet; HFruct: high-fructose diet; + $p < 0.05$; *** $p < 0.001$.

IV.3.4.2. Quantification of uNAC, uCys and uCysGly

The levels of uNAC were evaluated in order to explore the effect of diets on the detoxification of CysSSX. uNAC levels were similar among weeks 0, 1, 2, 4, 8 and 15 for the Chow group, with mean values varying between 7.5 to 9.4 μM/mg of uCr.

The temporal variation of uNAC in the pre-diabetic models is shown in **Figure IV.12**. uNAC varied significantly between the pre-diabetic models ($p < 0.001$). Regarding the HFruct group, a small increase in uNAC elimination was observed in the first week, which was abolished with the chronicity of exposure to this diet ($p < 0.001$). As for the HFat, this effect was not observed, which by the end of week 1 had already a reduction of more than 20% of uNAC elimination that further decreased along study time ($p < 0.001$). Overall, both pre-diabetic diets induced significant reductions in uNAC elimination, reaching a difference of -17 for HFruct and -47% for HFat after 15 weeks of diet. However, comparing to the Chow group, these differences were only significant for the HFat group at weeks 8 and 15 of diet ($p = 0.016$ and $p = 0.005$, respectively for week 8 and 15).

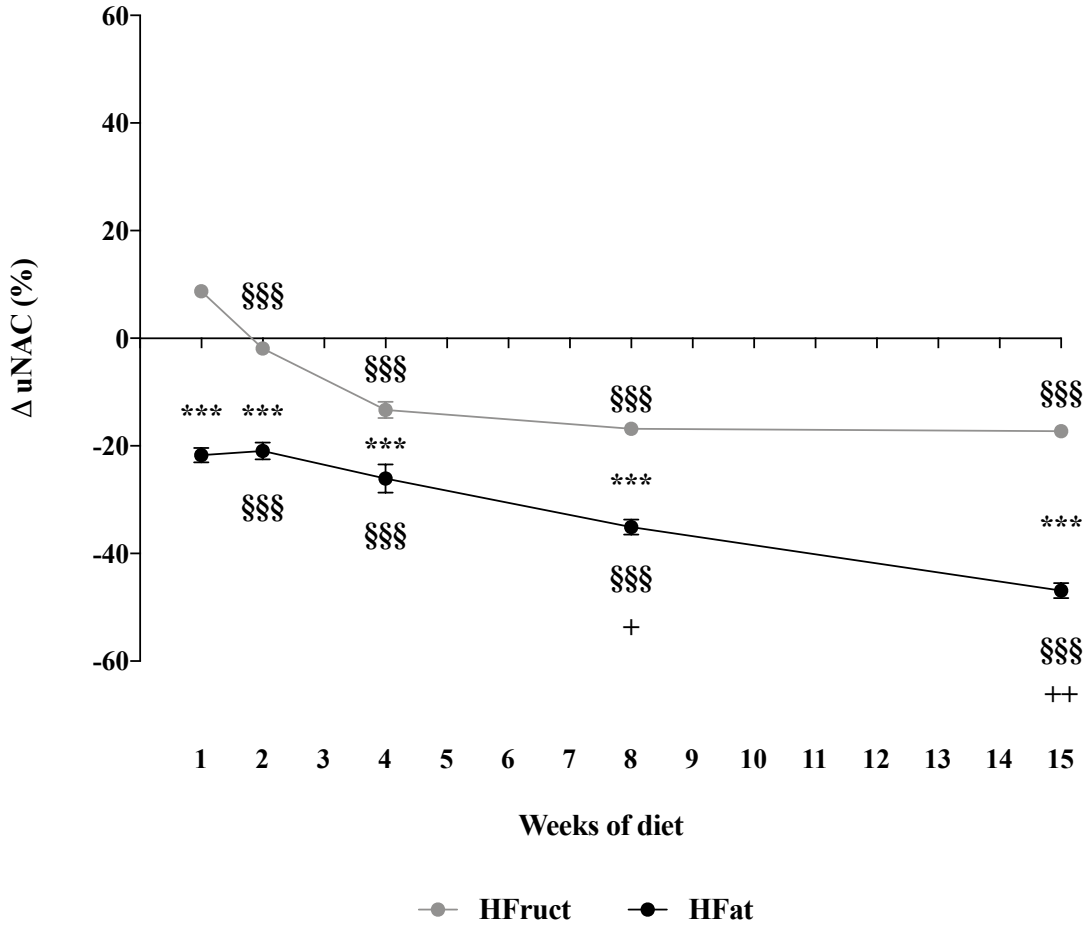

Figure IV.12 – Temporal variation of uNAC in HFruct and HFat groups. Both pre-diabetic models induced significant reductions in uNAC elimination (n = 3 to 6 animals per group, per week).
uNAC was normalized by uCr and the values attained at week 0 and is presented as percentage of effect from Chow group; *** Two-way ANOVA with Bonferroni's multiple comparisons test, versus HFruct group; §§§ One-way ANOVA with *Bonferroni's* multiple comparisons test, versus week 1; + or ++ Unpaired t-test, versus Chow group of the same week; HFat: hypercaloric diet; HFruct: high-fructose diet; uNAC: urinary surrogate of mercapturates of cysteine-disulfides; + $p < 0.05$; ++ $p < 0.01$; *** or §§§ $p < 0.001$.

IV.3.4.3. Quantification of uCys and uCysGly

The effect of pre-diabetic diets on the urinary levels of CysSSX was assessed through the quantification of uCys (**Figure IV.13**). The levels of uCys were stable in the Chow group throughout study time, with mean values of each week ranging from 6.2 to 11.5 μM/mg of uCr.

The levels of uCys were significantly different between HFat and HFruct groups in the time-course performed (p <0.001). After 1 week of diet, both HFruct and HFat groups presented lower uCys in comparison with the Chow group, (p = 0.020 and p = 0.003, respectively for HFruct and HFat groups). With the chronicity of diet uCys was similar to Chow in HFruct and lower than Chow in the HFat group with tendency to increase.

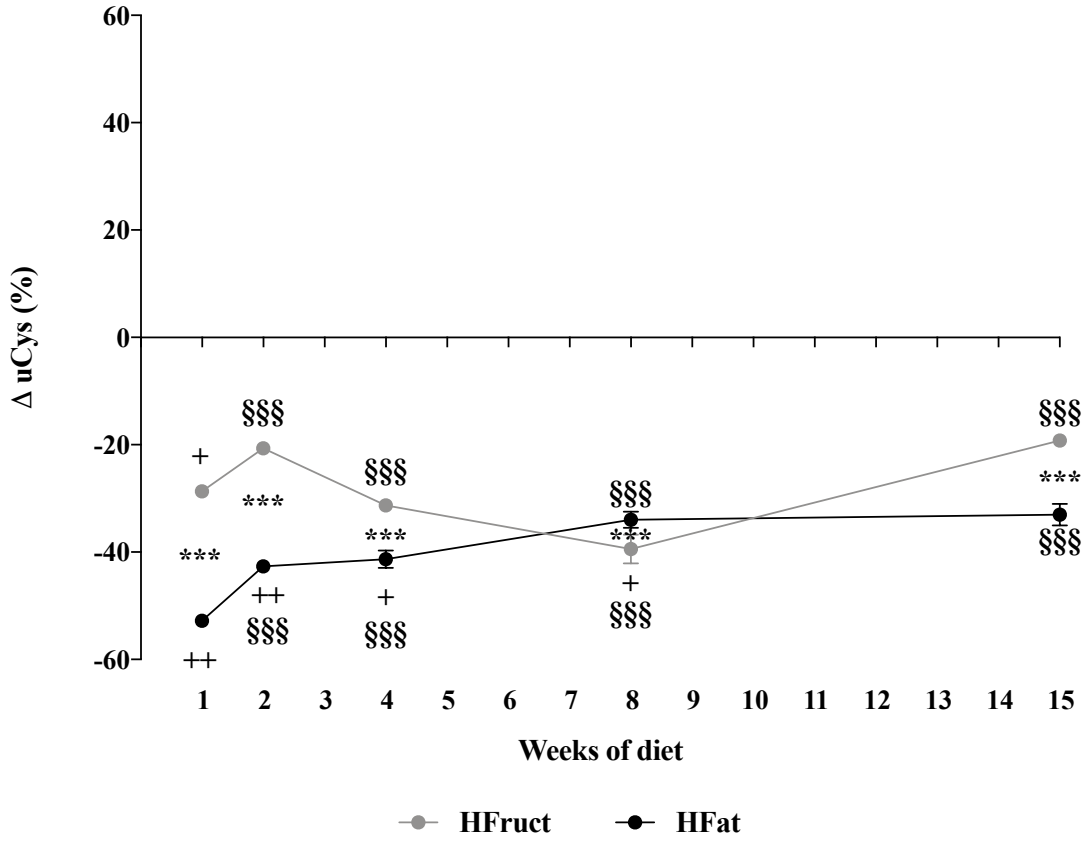

Figure IV.13 – Temporal variation of uCys in in HFruct and HFat groups. uCys initial decreases in week 1 in both groups. With the chronicity of diet uCys was similar to Chow in HFruct and lower than Chow in the HFat group with tendency to increase.
uCys was normalized by uCr and the values attained at week 0 and is presented as percentage of effect from Chow group; *** Two-way ANOVA with Bonferroni's multiple comparisons test, versus HFruct group; §§§ One-way ANOVA with *Bonferroni's* multiple comparisons test, versus week 1; + or ++ Unpaired t-test, versus Chow group of the same week; HFat: hypercaloric diet; HFruct: high-fructose diet; uCys: urinary cysteine; + $p < 0.05$; ++ $p < 0.01$; *** or §§§ $p < 0.001$.

We also assessed changes in GSH turnover by measuring the levels of uCysGly (**Figure IV.14**). As for the uCysGly, the mean levels in the Chow group varied between 3.9 and 7.7 μM/mg of uCr, with differences observed between week 0 (3.9 ± 1.4 μM/mg of uCr) and weeks 1 (7.7 ± 2.5) and 4 (7.0 ± 0.7 μM/mg of uCr) ($p = 0.007$). Similar to uCys, the variation on the levels of uCysGly was different between pre-diabetic models ($p < 0.001$). Nevertheless, no differences were found between pre-diabetic and chow diets. There was a progressive increment on the levels of uCysGly in urine for the HFat model in comparison with week 1 ($p < 0.001$) while the differences found in the HFruct group were linear, although significantly different from the values attained at week 1 ($p < 0.001$).

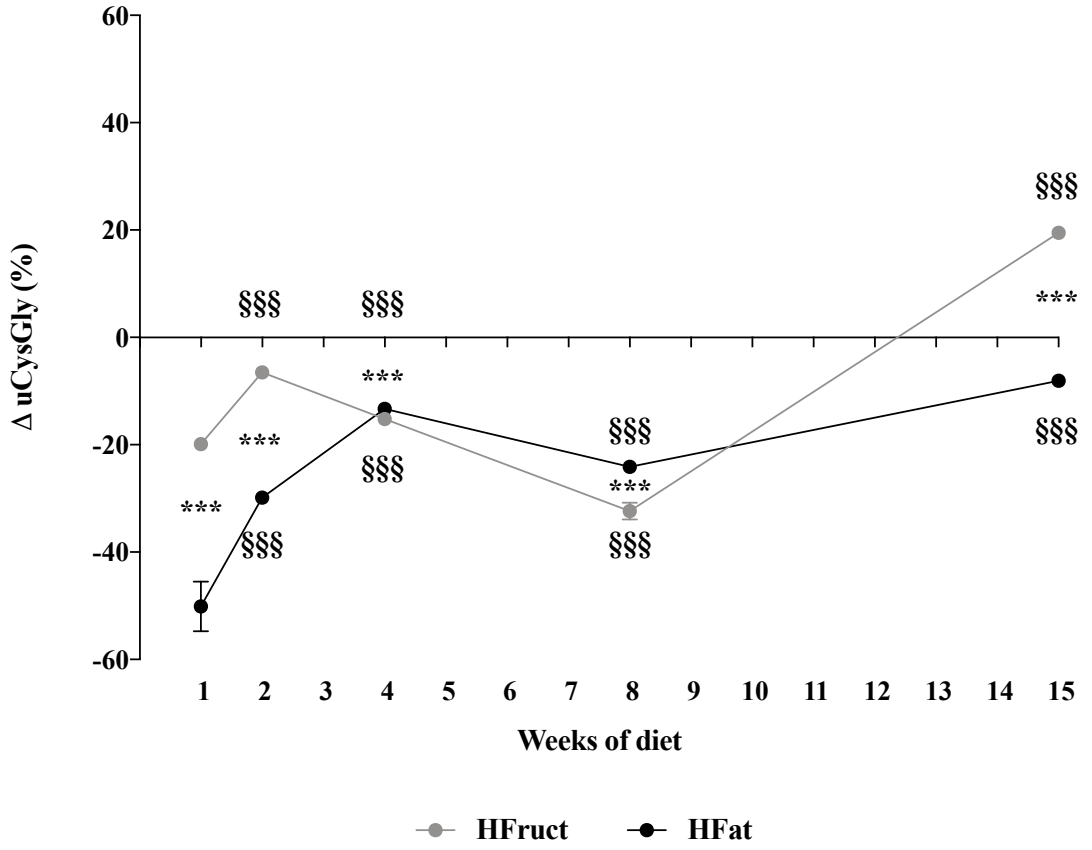

Figure IV.14 – Temporal variation of uCysGly in in HFruct and HFat groups. uCysGly varied widely between pre-diabetic diets, although no significant differences were found in comparison with the Chow group (n = 3 to 6 animals per group, per week).
uCysGly was normalized by uCr and the values attained at week 0 and is presented as percentage of effect from Chow group; *** Two-way ANOVA with Bonferroni's multiple comparisons test, versus HFruct group; §§§ One-way ANOVA with *Bonferroni's* multiple comparisons test, versus week 1; HFat: hypercaloric diet; HFruct: high-fructose diet; uCysGly: urinary cysteine-glycine; *** or §§§ $p < 0.001$.

Tables IV.2 and **IV.3** summarizes the overall results obtained.

Table IV.2 – Summary of findings of the study at week 15 for kidney function and CysSSX dynamics.

	Body Weight	Kidney weight	Renal histology	uACR	Total Cys	Free total Cys	CysSSP	uNAC	uCys	uCysGly
HFruct	=	=	=		↑	↑	↑			
HFat	↑	↑	=		↓	↓	↓	↓		

↑ or ↓ represents increase or decrease relatively to Chow group; grey color represents increase relatively to the other pre-diabetic diet; Cys: cysteine; CysSSP: protein-bound cysteine fraction; HFat: hypercaloric diet; HFruct: high fructose diet; uACR: urinary albumin to creatinine ratio; uCys: urinary cysteine; uCysGly: urinary cysteine-glycine; uNAC: urinary surrogate of the mercapturates of cysteine-disulfides.

Table IV.3 – Summary of findings of the study at week 15 for gene expression in kidney.

	Nat8	Hspa5	Ccl2	Tnfa	Fn	Col1a2	Tgfb1	Vim	Fbpase	Srebp1a	Elovl2	Chrebp	Sglt2
HFruct		↑	↑	↑				↑				↑	↑
HFat	↑	↑	↑	↑	↑	↑	↑	↑	↑	↑	↑	↑	

↑ represents increase relatively to Chow group; grey color represents increase relatively to the other pre-diabetic diet; Ccl2: chemokine (C-C motif) ligand 2; Chrebp: carbohydrate-responsive element-binding protein; Col1a2: collagen, type I, alfa 2; Elovl2: elongation of very long chain fatty acids like 2; Fbpase: fructose 1,6 biphosphatase; Fn: fibronectin; HFat: hypercaloric diet; HFruct: high-fructose diet; Hspa5: heat shock protein 5; Nat8: *N*-acetyltransferase 8; Sglt2: sodium/glucose co-transporter 2; Srebp1a: sterol regulatory element binding protein; Tgfb1: transforming growth factor, beta 1; Tnfa: tumor necrosis factor, alfa; Vim: vimentin

IV.4. Discussion

We herein investigated changes in CysSSX dynamics with chronicity of exposure to pre-diabetic diets and how these changes were related to kidney dysfunction and to our marker uNAC. Using uNAC as a surrogate of the mercapturates derived from CysSSX, we demonstrate that pre-diabetic states are characterized by lower mercapturates of CysSSX in urine that might indicate a decrease on the formation or on the detoxification of CysSSX, a condition that aggravates with the progressive exposure to the pre-diabetic diets. This fact was particularly evident for the HFat diet.

Differently from HFruct diet, after 15 weeks of diet, the HFat group has an increase in NAT8 expression and decreased uNAC. Additionally, while no histological changes were observed, there was an increase in the expression of fibrotic markers.

A recent work by Guo and co-authors (2017) showed that C57BL/6 mice fed with a HFat diet for 3 weeks have a slight, yet not significant, increase in NAT8 expression in liver (Guo *et al.*, 2017), that might indicate that NAT8 increases with a reduced exposure to the diet. The increase observed in our study suggest that these mice are on an initial stage of kidney injury, as suggested by the increased uACR. Nevertheless, the elimination of CysSSX is already impaired, further supporting that uNAC might be an indicator of kidney disease progression. This decrease could also mean that although NAT8 expression is increased, its function could be overloaded by other Cys-*S*-conjugates that can compete with CysSSX. In fact, the production of CysLTs is increased in adipocytes of HFat mice (Mothe-Satney *et al.*, 2012). Furthermore, the elimination of Cys-*S*-conjugates in diabetic conditions has been reported. For instance, the urinary excretion of LTE4 is increased in streptozotocin-induced diabetic rats (Hardy *et al.*, 2001) and also in patients with type 1 diabetes (Hardy *et al.*, 2005). Cys is also able to form a stable and irreversible conjugate with glucose (Glucose-Cys), a reaction reported to be much faster than the one between GSH and glucose. Interestingly, urinary Glucose-Cys levels were increased in patients with diabetes (Szwergold, 2006).

Also, NAT8 action can be counteracted by the action of sirtuin 1 (SIRT1), a deacetylase that suppresses gluconeogenesis in proximal tubular cells (Sasaki *et al.*, 2017). To date, no studies have been reported regarding the ability of NAT8 to acetylate Cys residues of proteins.

As NAT8 is a microsomal enzyme, we investigated the expression of a markers of ER stress, *Hspa5*, which was increased in both pre-diabetic groups. ER stress, oxidative stress and oxidative DNA are all factors that have been associated with kidney dysfunction (Ozbek, 2012; Cao and Kaufman, 2014). Moreover, ER stress activates CysLTs pathway, the best well known endogenous substrate that undergoes the mercapturate pathway, mediating ER stress-triggered kidney damage, apoptosis, oxidative DNA damage and morbidity *in vivo* (Dvash *et al.*, 2015).

On the other hand, a remarkable difference in Cys dynamics was observed for both pre-diabetic groups. The HFruct model, that does not present insulin resistance at week 12, has an increase in renal Cys availability, both in the free and CysSSP forms, and lower uACR while the HFat model, with marked increase in insulin resistance and glucose intolerance, displayed exactly an opposite profile, with worse kidney markers. These results might indicate that changes in Cys redox homeostasis in kidney that course with the increase in CysSSP might have a protective role.

In accordance, cysteinylation of SOD1 has reported to protect it from oxidation under conditions of oxidative stress (Auclair, Brodkin, *et al.*, 2013). On the other hand, it is known that albumin cysteinylation in ESRD patients is greatly increased in respect to healthy subjects, consequently hindering the protective functions of albumin, particularly its antioxidant activity (Regazzoni *et al.*, 2013). The cysteinylation of the only free Cys residue of albumin (Cys34) correlates with oxidative stress related pathological conditions, namely chronic liver disease, CKD and diabetes mellitus (Nagumo *et al.*, 2014). Furthermore, CysSSP increases with age (Rossi *et al.*, 2009), this increase might be related to protection of reactive Cys in albumin but also because it can represent an important source of Cys to the proximal tubular cell.

In fact, a major source of cytosolic Cys is the lysosomal CysSSCys pool, normally generated inside the lysosomes via endoproteolysis of disulphide-containing proteins (Thoene and Lemons, 1980). The proximal tubular cells are responsible for almost all of the protein reabsorption in kidney via receptor-mediated endocytosis from the brush border membrane. Afterwards, vesicles are fused with the lysosomes, allowing lysosomal internalization of CysSSCys-containing proteins. These proteins undergo cathepsin-catalyzed degradation, leading to the formation of CysSSCys, which is then effluxed into the cytosol, a process mediated by cystinosin. Under non-oxidative conditions, CysSSCys

is reduced to Cys by the cytosolic reducing systems which leads to the formation of GSSG (Sumayao, Newsholme and McMorrow, 2018).

On the other hand, part of the lysosomal CysSSCys pool has been shown to be originated upon the uptake of extracellular CysSSCys, which in proximal tubular cells is mediated by the plasma membrane protein rBAT/SLC3A1, together with $b^{0,+}$AT/SLC7A9 (S1 segment) or AGT1/SLC7A13 (S3 segment) (Calonge *et al.*, 1995; Feliubadaló *et al.*, 1999; Fernández *et al.*, 2002; Nagamori *et al.*, 2016). Importantly, mutations in these genes are associated with a cystinuria phenotype, characterized by excessive wasting of CySSCys into the urine (Feliubadaló *et al.*, 1999; Fernández *et al.*, 2002). In addition, cystinosin-LKG has been recently identified (Bellomo *et al.*, 2016).

Both thiol availability and redox status were shown to influence the expression of cystinosin (Bellomo *et al.*, 2010). In specific, reduced intracellular Cys and GSH was followed by a concomitant increase in reactive oxygen species production was observed in HK-2 cells under thiol-free conditions. Moreover, these authors observed a shift towards a more oxidized status of Cys and GSH with progressive increase in the mRNA levels of cystinosin gene (Bellomo *et al.*, 2010). Thus, it would be interesting to understand how these targets change Cys dynamics in order to maintain cellular redox homeostasis in kidney and its impact in kidney disease progression and uNAC.

The healthy human kidney cortex has only about 8% of Cys represented as CysSSCys (Crawhall and Segal, 1967). Uremia-triggered oxidative stress affects the reduction of CysSSCys and correlated with increased pCr. Furthermore, the accumulation of CysSSCys is a hallmark of cystinosis and leads to loss of renal function (Gahl, Thoene and Schneider, 2002). This dysfunction elicited by Cys accumulation is associated with increased intracellular H_2O_2, reduced GSSG/total GSH ratio, catalase activity and ATP production and impairment in GSH synthesis (Wilmer *et al.*, 2007; Bellomo *et al.*, 2010; Sansanwal *et al.*, 2010).

The HFat model seems to have a more pronounced kidney dysfunction comparatively to the HFruct model. In addition to the decreased uNAC elimination and renal cysteine availability, HFat animals also have increased kidney weight, higher renal fibrosis (showed by increase expression of Fn, Col1a2 and Tgfb1) and higher expression of enzymes involved in the glucose and lipid metabolism and dynamics than the HFruct group.

Nevertheless, increased CysSSP observed in the HFrcut animals might contribute for kidney dysfunction, as cysteinylated proteins are transported to the lysosomes of tubular epithelial cells where undergo proteolysis, generating CysSSCys (Sumayao, Newsholme and McMorrow, 2018). If there is a defect on the transport of CysSSCys, its consequent accumulation in the lysosome will elicit toxic effects, including elevated intracellular reactive oxygen species production, reduced antioxidant capacity, induction of redox-sensitive proteins, altered mitochondrial integrity and augmented cell death (Sumayao *et al.*, 2016). While the cellular pathways required for protein cysteinylation are not fully elucidated, evidence shows that cystathionine beta-synthase (CBS) might have a relevant role on this setting since no cysteinylated albumin was detected in CBS deficient mouse (Bar-Or *et al.*, 2004). In fact, renal expression of CBS in HFat mice is decreased (Liu *et al.*, 2018), hence probably explaining the decrease in CysSSP observed in this group.

Kidney glutamate/cystine antiporter (xCT, responsible for uptake of CysSSX) protein expression is decreased in diabetic mice induced by streptozotocin. In addition, mice models of type II diabetes have increased expression of renal GST, the enzyme responsible for the formation of GSH-*S*-conjugates (Fujita *et al.*, 2001).

It is important to highlight the relative resistance to kidney dysfunction presented by the C57BL/6 mice. Albuminuria and renal pathological changes are less commonly observed in diabetic C57BL/6 animals (Brosius *et al.*, 2009; Soler, Riera and Batlle, 2012; Kitada, Ogura and Koya, 2016). These facts might justify the results herein obtained.

The detection of mercapturates in urine can be used for biomonitoring of disease progression (Mathias and Bhymer, 2016; Dias *et al.*, 2017). In fact, an increase on the levels of mercapturates derived from acrolein were found in patients with diabetes (Daimon *et al.*, 2003) whereas the mercapturates from 4-hydroxynonenal were lower in patients with impaired glucose tolerance (Ntimbane *et al.*, 2008). Our results are in accordance with this last aforementioned report.

IV.5. Conclusions

The present study shows an impaired elimination of mercapturates derived from CysSSX with the progression of disease, as denoted by a decrease on the elimination of uNAC in urine throughout study time. This is, for the extent of our knowledge, the first study reporting an association between DKD progression and the detoxification of CysSSX.

This effect seems to more pronounced in the HFat group, a model associated with weight gain and a higher degree of kidney dysfunction. The results support the involvement of CysSSX and the mercapturate pathway on the early events of tubulopathy in DKD.

CHAPTER V

Cysteine-disulfides in an animal model of hypertension-induced by chronic intermittent hypoxia

CHAPTER V

Cysteine-disulfides in an animal model of hypertension-induced by chronic intermittent hypoxia

V.1. Rationale & Objectives

As the elimination of CysSSX seems to be through their acetylation by the activity of NAT8 (**Chapter I**), which has been associated not only with the mercapturate pathway (Veiga-da-Cunha *et al.*, 2010) but also with the regulation of blood pressure (Juhanson *et al.*, 2008), both processes mostly dependent on the kidney, we aimed to test our hypothesis in a model of hypertension associated with increased oxidative stress and inflammation. We have previously described that CysSSX formation increases at rat kidney upon exposition to chronic intermittent hypoxia (CIH) (Coelho *et al.*, 2018), a model of model of hypertension associated to sleep apnea (Diogo et al, 2015), characterized by increased oxidative stress and inflammation, contributing to damage of various tissue and organs (May and Mehra, 2014; Lavie, 2015).

The specific aims in this chapter were to measure the temporal variation of uNAC in this model and its association with the establishment of hypertension and changes in kidney function. Moreover, uNAC variation was also related with CysSSX formation at the kidney.

V.2. Animals & Methods

V.2.1. Animals

Experiments were performed using male Wistar rats Crl:WI (Han) obtained from the NOVA Medical School rodent facility. Animals (two per cage) were housed in polycarbonate cages with wire lids (Tecniplast) under 12h light/dark cycles (8am-8pm), at room temperature (22 ± 2 °C) and a relative humidity of 60 ± 10%. Rats were maintained on a standard laboratory diet (SDS diets RM1, Special Diets Services) and reverse osmosis water, which was provided *ab libitum*. Corncob bedding (Probiológica)

was used and changed every week. Animals were specific-pathogen-free according to FELASA recommendations (Mähler *et al.*, 2014).

All applicable institutional and governmental regulations concerning the ethical use of animals were followed, according to the NIH Principles of Laboratory Animal Care (NIH Publication 85 23, revised 1985), the European guidelines for the protection of animals used for scientific purposes (European Union Directive 2016/63/EU) and the Portuguese Law nº 113/2013. The experimental procedures received prior approval by the Institutional Ethics Committee of the NOVA Medical School for animal care and use in research (protocol nº 15/2017/CEFCM).

V.2.1.1. Experimental design

The experimental design is outlined in **Figure V.1**. Rats were randomly assigned and divided into different groups, which were exposed to CIH during 1, 7, 14, 21 and 60 days. Four different control groups of animals were kept in the same room under normoxic (Nx) conditions (21% O_2 and 79% N_2) for 7 (control of both 1 and 7 days of exposure to CIH), 14, 21, and 60 days. All animals were weighed at baseline and once a week during the entire study. Water and food intake were also recorded every week. Additionally, urine samples were collected at day 0, 1, 7, 14, 21, 28, 35, 42, 49, 56 and 60 at approximately 9:00-10:00 am.

At day 1, 7, 14, 21 and 60 of each group, rats were anaesthetised by intraperitoneal injection with medetomidine (0.5 mg/kg body weight; Domitor®, Pfizer Animal Health) and ketamine (75 mg/kg body weight; Imalgene 1000®, Mérial). Cardiac puncture was performed for blood sampling, obtaining plasma that was stored at -80 °C until use. Renal sections, namely renal cortex (RC) and renal medulla (RM) were rapidly collected and a part was stored in Trizol® (*Life Technologies*) until further use.

The 3Rs police was employed to minimize the number of animals used in the experiments, meaning that the same rat was used for almost all experiments.

Days of exposure	0	1	7	14	21	28	35	42	49	56	60
Sample collection											
Weight	x		x	x	x	x	x	x	x	x	x
Food intake	x		x	x	x	x	x	x	x	x	x
Water intake	x		x	x	x	x	x	x	x	x	x
Kidney histology											x
Kidney/liver qPCR		x	x	x	x						x
uCr	x	x	x	x	x	x	x	x	x	x	x
uACR	x	x	x	x	x			x			x
Plasma/kidney/liver Cys fractions		x	x	x	x						x
uNAC	x	x	x	x	x	x	x	x	x	x	x

Figure V.1 – Study design. The "x" represents the time at each sample was collected and/or the experiment was performed.
Cys: cysteine; qPCR: quantitative real-time polymerase chain reaction; uACR: urinary albumin-to-creatinine ratio; uCr: urinary creatinine; uNAC: urinary surrogate of the mercapturates from cysteine-disulfides; uPCR: urinary protein-to-creatinine ratio.

V.2.1.2. CIH exposure

CIH-exposure was performed as previously published (Diogo *et al.*, 2015; Coelho *et al.*, 2018). Rats were kept in a eucapnic atmosphere inside medium A-chambers (76 x 51 x 51 cm^3, A-60274-p, Biospherix Ltd). The chambers were equipped with gas injectors and O_2 and CO_2 sensors levels to ensure the accuracy of CIH cycles. Accumulation of CO_2 was prevented by the continuous flow and circulation of the gases inside the chambers using vents and self-indicating soda lime (AnalaR Normapur®, *VWR*), which absorbs expired CO_2. Carbon dioxide levels inside the chamber never exceed 1%. Excess water was absorbed by a silica gel container (Chameleon® C 2-6 mm, *VWR*) that was also placed inside the chambers. Oxygen concentration inside the chambers was regulated by electronically regulated solenoid switches that controlled 100% N_2 and 100% O_2 gas input in a three-channel gas mixer and gradually lowered the oxygen in the chamber from 21%

to 5% O_2 (OxyCycler AT series, *Biospherix Ltd*). The chambers were infused with 100% N_2 for 3.5 min to briefly reduce the O_2 concentration to 5%; afterwards, the chambers were infused with 100% O_2 for 7 min to restore O_2 to ambient levels of 21% until the start of the next CIH cycle. Each CIH cycle had a duration of 10.5 min (5.6 CIH cycles/h) and the exposure period was during the rat's sleep period (light phase of light/dark cycle), corresponding to 10.5 h/day. During the remaining hours of the day, the chambers were ventilated with a constant flow of room air to maintain oxygen levels at 21%. Oxygen was purchased as regular bottles (*Gasin*), while N_2 was generated from the air by pressure swing absorption technology using a high-output nitrogen generator (Nitrogen 15 Plus, *PSA Technology*, *Sysadvance*).

V.2.2. Kidney parameters

V.2.2.1. Renal histology

Histological analysis was performed in 10% formaldehyde-fixed paraffin embedded left kidney from rats exposed to 60 days of CIH or Nx. Sections from 3 rats *per group* were stained with H&E.

V.2.2.2. uCr

The levels of uCr were quantified as previously described (**Chapter IV**).

V.2.2.3. uACR

Albuminuria levels were measured as described in **Chapter IV**. uACR was obtained by dividing albumin by uCr levels.

V.2.2.4. Gene expression

Right kidney cortex and medulla tissue were collected and homogenized in Trizol® (T9424, *Sigma-Aldrich*) using a tissue homogenizer (Heidolph DIAX 900). Total RNA extraction was performed according to the Trizol® manufacturer's instructions. The RNA

concentration was determined prior to cDNA synthesis by measuring the absorbance at 260 nm on a Nanodrop 2000 (*Thermo Scientific*). cDNA was synthesized from 1 µg of RNA, according to manufacturer's instructions (MB12501, *nzytech*). Rat specific primers were used for the housekeeping gene (*β-actin*) as wells as for the target gene *Nat8* and are shown in **Table V.1**.

The experiments were performed using LightCycler® 480 SYBR Green I Master Mix (04887352001, Roche), according to manufacturer's protocol. qPCR was performed on a LightCycler® 480 II real-time PCR system (*Roche*). Experiments were performed in biological triplicates. The relative quantification was performed using the comparative CT method (2 - ΔΔCt) with LightCycler® 480 Software release 1.5.0 SP4.

Table V.1 - Primer sequences of housekeeping gene (β-actin) and target gene (Nat8).

Gene	Forward 5'-3'	Reverse 5'-3'
β-actin	AAGTCCCTCACCCTCCCAAAAG	AAGCAATGCTGTCACCTTCCC
Nat8	CATCTGCGAGTACCAAGACAG	GATGCATACAACAGCCAGCAG

Nat8: *N*-acetyltransferase 8

V.2.3. CysSSX and related metabolites

V.2.3.1. Quantification of Cys fractions

Fractions of Cys were quantified in right kidney cortex and medulla sections as previously described (**Chapter IV**) (Grilo *et al.*, 2017; Coelho *et al.*, 2018). For this quantification, approximately 50 mg of each tissue was homogenized in 400 µL of iced phosphate buffered saline 1x (PBS1x) (P4417-100TAB, *Sigma-Aldrich*) in a tissue homogenizer (Heidolph DIAX 900). As for the free reduced fraction of Cys, the protocol employed for the quantification of the free fraction was used although samples were incubated with reverse osmosis water instead of TCEP in order to obtain the naturally reduced fraction. The free oxidized fraction was obtained by subtracting the free reduced to the total free fraction.

V.2.3.2. Quantification of uNAC, uCys and uCysGly

The levels of uNAC, uCys (as a measure of CysSSX filtration and reabsorption) uCysGly (as a measure of GSH turnover) were quantified in urine by HPLC-FD (**Chapter I**) (Grilo *et al.*, 2017; Coelho *et al.*, 2018).

V.2.4. Statistical analysis

Statistical analysis was performed using GraphPad Prism® version 7.0 (GraphPad Software Inc., San Diego, CA, USA). Data are presented in % of effect or as mean ± SEM. Whenever applicable, data was analysed through Unpaired t-test, One-way ANOVA with *Dunnett's* multiple comparisons test or Two-way ANOVA with *Bonferroni's* multiple comparisons test. Statistical significance for all tests was set at the level of $p < 0.05$.

V.3. Results

V.3.1. Animals

We have followed the changes in animal weight in both groups (n = 5-6 rats *per* group) that were age-matched (median [IQR] age of 12 [10-13] weeks) and had no differences regarding their total body weight at the baseline (mean ± SD BW of 293 ± 44 g). However, the curve of body weight variation throughout exposure time showed significantly less weight gain in animals exposed to CIH in comparison with Nx animals (**Figure V.2**). This was evident right after 14 days of exposure ($p = 0.033$), increasing over time ($p = 0.001$ from day 21 to 35 and $p < 0.001$ from day 42 until the end of the experiment).

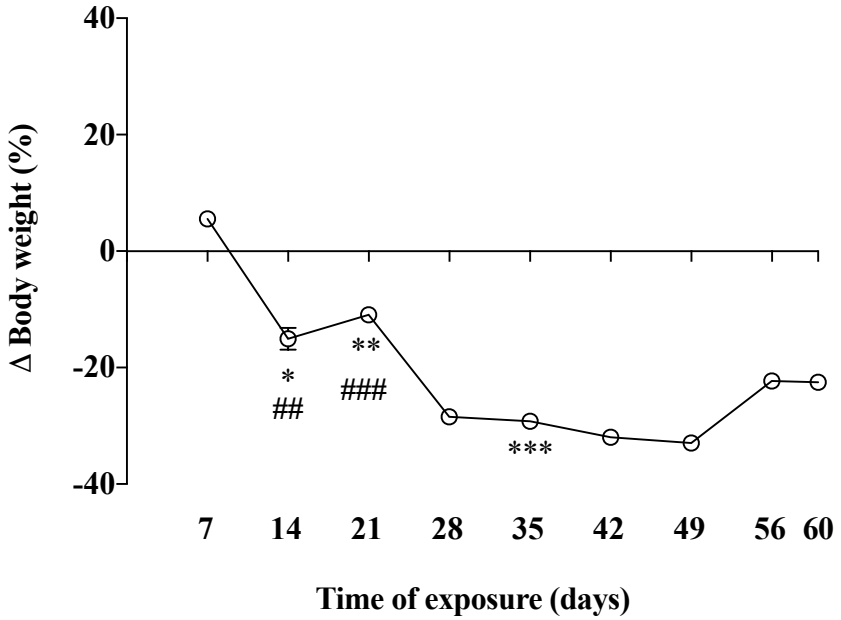

Figure V.2 – Body weight curves for rats exposed to Nx or CIH conditions. Animals exposed to CIH had significantly lower body weight gain in comparison with Nx animals. This difference was evident right after 14 days of exposure to CIH, increasing until the end of experiments (n= 5-6 animals per group).
Body weight was normalized as % of day 0 values and presented as mean ± SEM; *, ** or ***Unpaired t-test Nx versus CIH of the same day; ## or ### One-way ANOVA with *Dunnett's* multiple comparisons test, versus day 0; CIH: chronic intermittent hypoxia; Nx: normoxic; * $p < 0.050$; ** or ## $p < 0.010$; *** or ### $p < 0.001$.

The analysis of weekly records of food intake showed that CIH animals ingested lower amounts of food in comparison with the Nx group, a difference that was significant after 49 days of CIH exposure until the end of experiments ($p = 0.025$ and $p = 0.028$, respectively for days 49 and 56 of CIH exposure) (**Figure V.3A**). However, whereas CIH animals ingested a higher quantity of water on the first week of exposure comparatively to Nx animals, an opposite effect was found after 49 days of study ($p = 0.002$ for both days 7 and 49 and $p = 0.038$ for day 56) (**Figure V.3B**). Furthermore, Nx animals progressively ingested more water, while an inverse result was observed in the CIH group ($p < 0.001$ for Nx and $p = 0.010$ for CIH groups) (**Figure V.3B**).

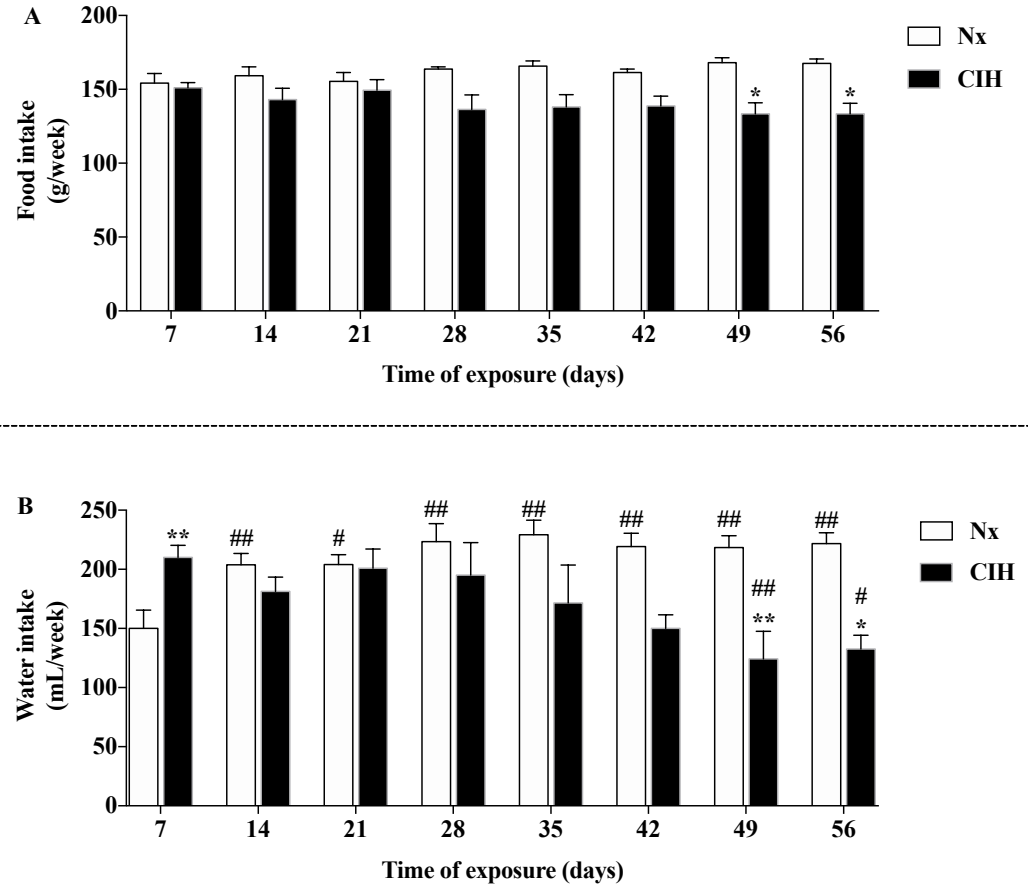

Figure V.3 - Food and water intake. By the end of the study period, CIH animals ingested lower amounts of both food (**A**) and water (**B**). Also, there was an increase in water intake throughout study time for the Nx group, while CIH animals decreased its consumption (**B**) (n = 5-6 animals per group).
Data presented as mean ± SEM; * or ** Two-way ANOVA with *Bonferroni's* multiple comparisons test, Nx versus CIH of the same day; # or ## One-way ANOVA with *Dunnett's* multiple comparisons test, versus day 7; CIH: chronic intermittent hypoxia; Nx: normoxic; * or # $p < 0.05$; ** or ## $p < 0.01$.

V.3.2. Renal parameters

V.3.2.1. Histology

Histological analysis through H&E staining revealed a normal architecture with no clear pathology on the left kidney of all animals examined after 60 days of study time (**Figure V.4**).

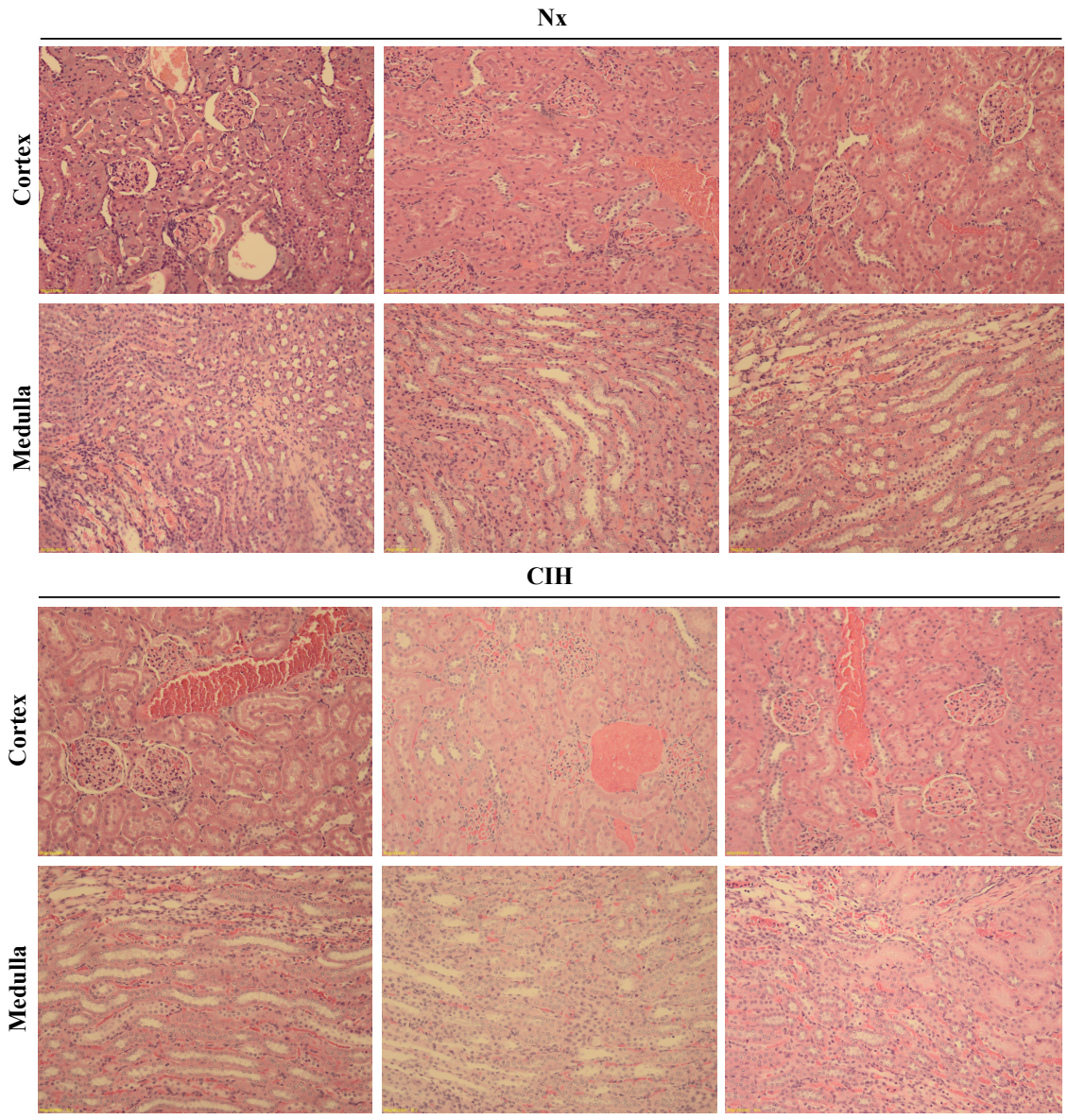

Figure V.4 – Left kidney histology. No histological changes were observed for the left kidney of all groups (n = 3 animals per group).
Staining was performed in 10% formaldehyde-fixed paraffin embedded left kidney sections using H&E; Magnification: 10x; CIH: chronic intermittent hypoxia; Nx: normoxic.

V.3.2.2. uCr

uCr was quantified in order to normalize albuminuria and proteinuria as well as the urinary concentration of metabolites herein described (uCys, uNAC, uCysGly). There were no differences for uCr levels throughout the study in both groups of animals (**Figure V.5**).

V.3.2.3. uACR

To evaluate kidney function, we quantified the temporal variation of uACR (**Figure V.6**). Although not reaching statistical meaning, CIH animals presented higher uACR in the majority of the analyzed time-points.

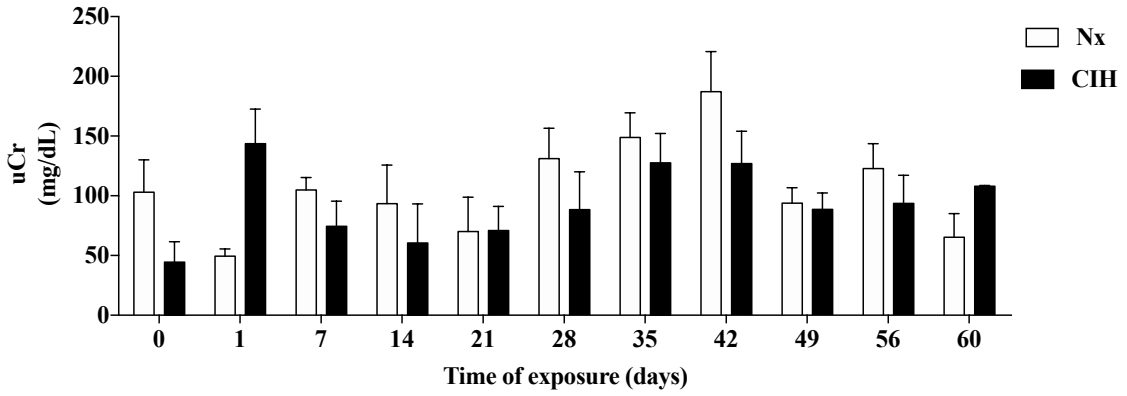

Figure V.5 – uCr levels. No differences were observed regarding the temporal variation of uCr in both groups (n = 5-6 animals per group, per week).
Data presented as mean ± SEM; CIH: chronic intermittent hypoxia; Nx: normoxic; uCr: urinary creatinine.

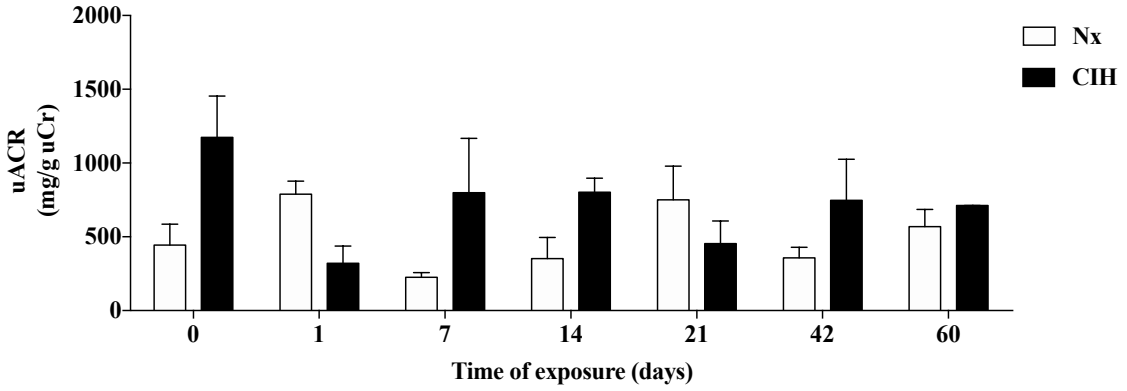

Figure V.6 – Temporal variation of uACR. Although without reaching statistical significance, the CIH group presented higher uACR in most time-points.
Data presented as mean ± SEM; CIH: chronic intermittent hypoxia; Nx: normoxic; uACR: urinary albumin-to-creatinine ratio.

V.3.2.4. Gene expression

In order to address the effect of chronicity of CIH in NAT8, its mRNA expression was evaluated in kidney sections, namely RC and RM. We observed differences between Nx and CIH groups in a time- and tissue-dependent manner (**Figure V.7**). Specifically, after 1 day of exposure, CIH animals presented lower *NAT8* in comparison with Nx group (*p*

= 0.006 for RC and $p = 0.041$ for RM), a difference that remained similar after 7 days of study time ($p = 0.021$ for RC and $p = 0.024$ for RM). However, while no differences were found between Nx and CIH animals after 14 days of exposure, a significant increase in this expression was observed only in RC of CIH animals at 21 days ($p = 0.007$). By the end of the study, CIH animals presented lower expression of NAT8 in comparison with Nx groups in both renal sections ($p = 0.037$ for RC and $p = 0.024$ for RM). On the other hand, when the temporal expression of *NAT8* was compared with the values attained after 1 day of study time, we observed an increase at days 14 and 21 for RC and RM ($p < 0.001$ for both days and both sections), while a slight decrease was observed in RM after 7 days of study time ($p < 0.001$).

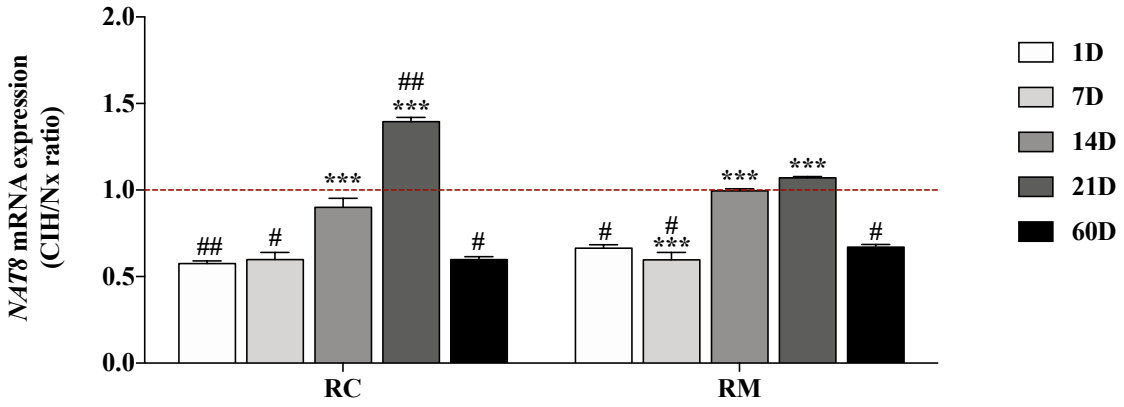

Figure V.7 – Temporal variation of NAT8 mRNA expression. The expression of NAT8 varied in a temporal- and tissue-dependent manner. Specifically, we observed that right after 1 day of exposure, CIH animals presented lower expression in both RC and RM. A similar result was obtained after 7 days of study time. However, by the 21st day of exposure, these animals presented higher expression in RC comparatively to Nx animals though only in RC. By the end of the study, NAT8 expression was once again reduced in the CIH group in both kidney sections. Notably, in comparison with day 1, the expression of NAT8 increased at days 14 and 21 in RC and RM sections while a slight, yet significant reduction was observed at 7 days of study time in RM (n = 5-6 animals per group).
Gene expression was normalized with *β-actin*. Data presented as the ratio of CIH by Nx groups; *** Two-way ANOVA with *Bonferroni's* multiple comparisons test, versus day 1 of each tissue; # or ## Unpaired t-test, Nx versus CIH of the same day; CIH: chronic intermittent hypoxia; D: day; NAT8: N-acetyltransferase 8; Nx: normoxic; RC: renal cortex; RM: renal medulla; # $p < 0.05$; ## $p < 0.01$; *** $p < 0.001$.

V.3.3. CysSSX and related metabolites

V.3.3.1. Quantification of Cys fractions

The influence of CIH in Cys availability and dynamics was investigated through the quantification of Cys fractions in RC and RM tissue (**Figure V.8**). At 1 day of study time, the total net content of Cys (i.e free plus protein-bound fraction) in CIH animals in both sections was similar to Nx (**Figure V.8A**). However, a significant increase was observed

after 7 days of exposure (p = 0.003 and p = 0.001, respectively for RC and RM). Afterwards, Cys availability decreased in both sections until the end of the experiment (p < 0.001).

In a similar manner, we observed increased CysSSP at day 7 in CIH animals in both RC and RM (p = 0.041 and p = 0.028, respectively for RC and RM) that progressively decreased throughout study time (p < 0.001) (**Figure V.8B**).

On the other hand, we also assessed the oxidative status of Cys through its redox couple, given by the ratio of CysSH divided by free oxidized Cys (i.e. cysteine disulfides, CysSSX) (**Figure V.8C**). A higher ratio was observed at day 7 in both sections (p = 0.008 and p = 0.017, respectively for RC and RM). However, Cys rapidly shift towards a more oxidized status, as shown by a lower ratio at days 14 and 21 (p < 0.001), returning to values closer to the ones attained in Nx conditions at 60 days of CIH exposure.

V.3.3.2. Quantification of uNAC

To explore the effect of CIH on the elimination of CysSSX, the levels of uNAC were quantified throughout study time (**Figure V.9**). After an increase of almost 100% on the elimination of uNAC after 1 day of exposure to CIH, a progressive decrease was observed in CIH animals until the end of the study (p < 0.001). However, differences between Nx and CIH groups were only significant at day 21 and then from day 42 until the end of the experiments (p = 0.010, p = 0.005, p = 0.034, p = 0.032 and p = 0.042, respectively for day 21, 42, 49, 56 and 60).

V.3.3.3. Quantification of uCys and uCysGly

We have evaluated the contribution of CysSSX trough the quantification of uCys (**Figure V.10**) and GSH turnover through uCysGly (**Figure V.11**). Both uCys and uCysGly were generally lower in CIH than in Nx.

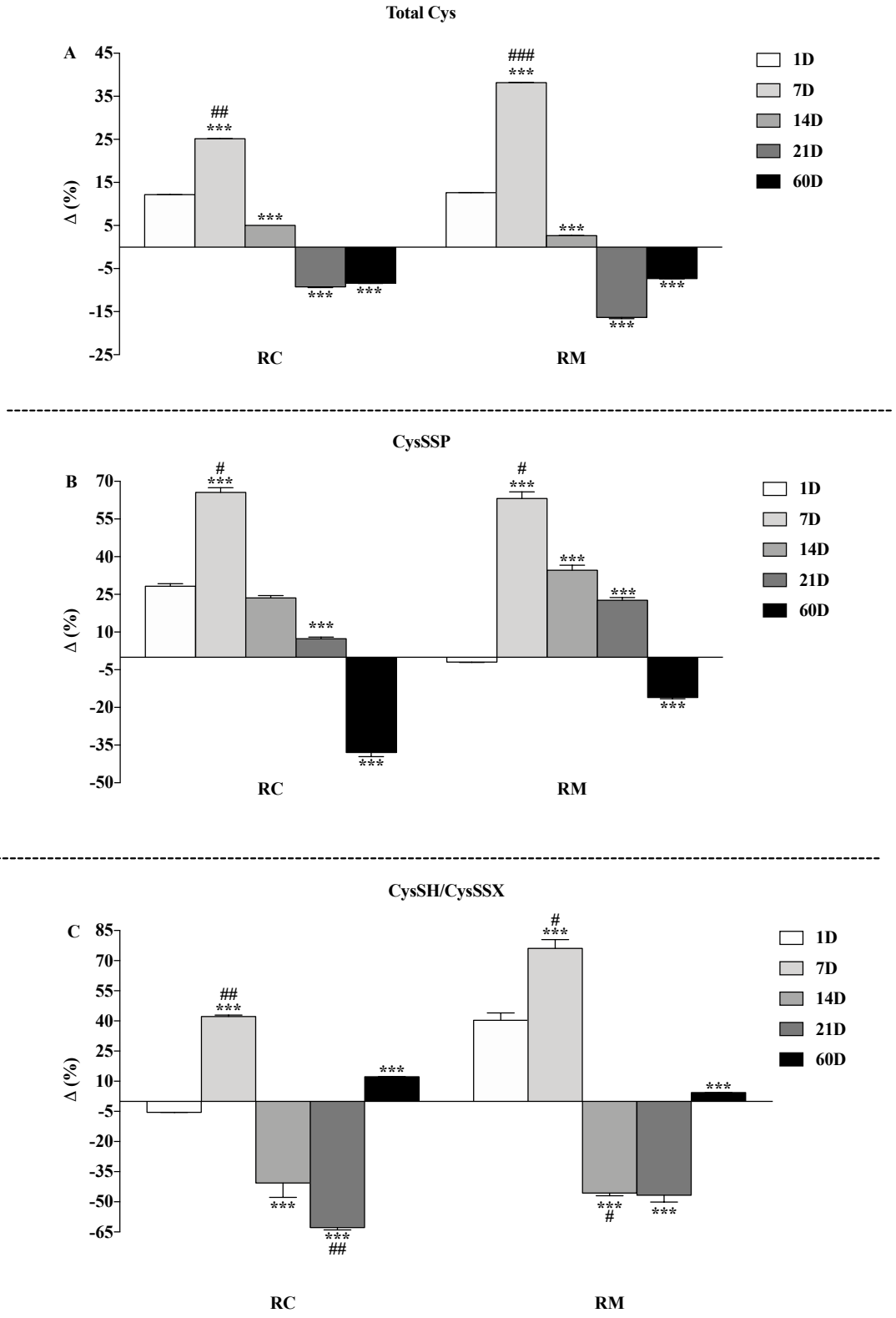

Figure V.8 – Cysteine availability and dynamics throughout study time. At 7 days of exposure to CIH, we observed an increase in both kidney fractions in total Cys (**A**) and CysSSP (**B**), decreasing with the increment on the temporal exposure to CIH. A significant increase was also observed in CysSH/CysSSX (**C**) at day 7, indicative of a more reduced state of Cys, decreasing from day 14 to 21 and returning to values closer to control conditions by the end of the experiment (n= 5-6 animals per group).

Cys fractions were normalized by tissue weight and are presented as the as percentage of effect from Nx group; *** Two-way ANOVA with *Bonferroni's* multiple comparisons test, versus day 1 of each tissue; # , ## or ### Unpaired t-test, versus Nx group of the same day; Cys: cysteine; CysSH: free reduced cysteine; CysSSP: cysteine protein-bound fraction; CysSSX: cysteine disulfides; D: day; RC: renal cortex; RM: renal medulla; # $p < 0.05$; ## $p < 0.01$; *** or ### $p < 0.001$.

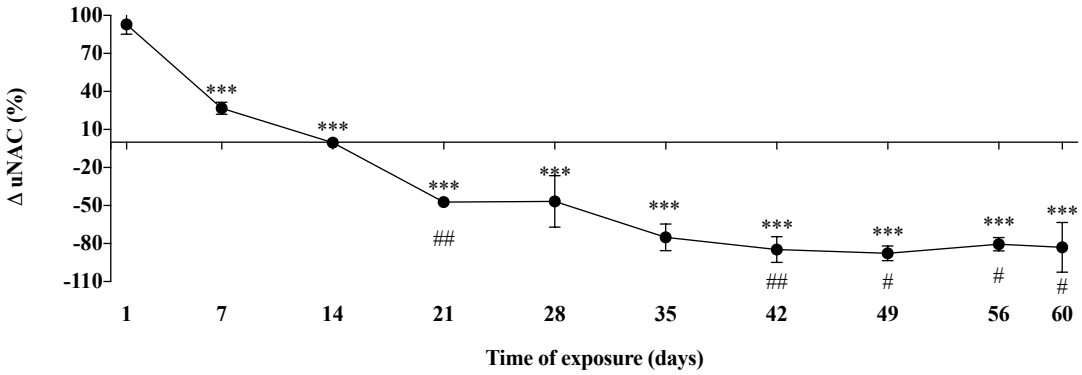

Figure V.9 – Temporal variation of uNAC. CIH rats presented increased elimination of uNAC after 1 day of exposure to CIH. Afterwards, this elimination progressively decreased throughout study time. Nevertheless, differences between Nx and CIH groups was only significant at day 21 and then from day 42 until the end of the study period (n = 5-6 animals per group per week).

uNAC was normalized by uCr and the values attained at day 0 and is presented as percentage of effect from Nx group; *** One-way ANOVA with *Bonferroni's* multiple comparisons test, versus day 1; # or ## Unpaired t-test, versus Nx group of the same day; uNAC: urinary surrogate of mercapturates of cysteine-disulfides; # $p < 0.05$; ## $p < 0.01$; *** $p < 0.001$

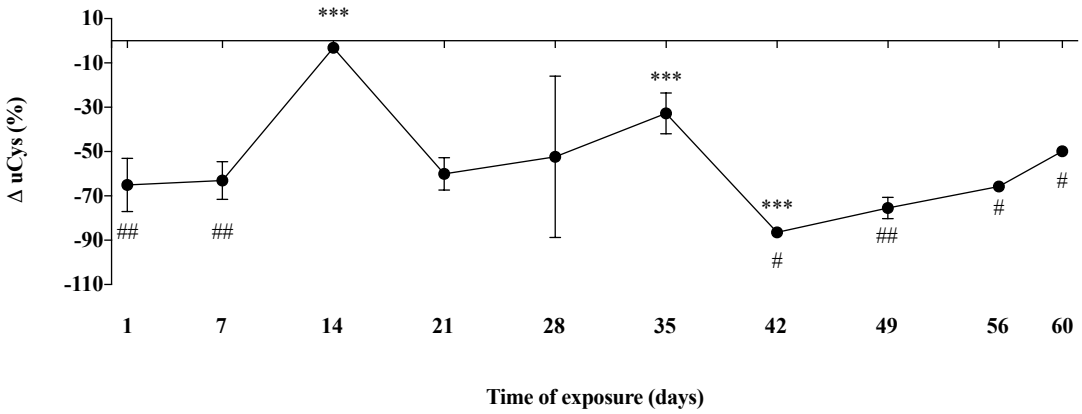

Figure V.10 – Temporal variation of uCys. uCys varied widely throughout study time in CIH animals, but was generally lower in this group in relation with Nx animals (n = 5-6 animals per group per week).

uCys was normalized by uCr and the values attained at day 0 and is presented as percentage of effect from Nx group; *** One-way ANOVA with *Bonferroni's* multiple comparisons test, versus day 1; # or ## Unpaired t-test, versus Nx group of the same day; uCys: urinary cysteine; # $p < 0.05$; ## $p < 0.01$; *** $p < 0.001$

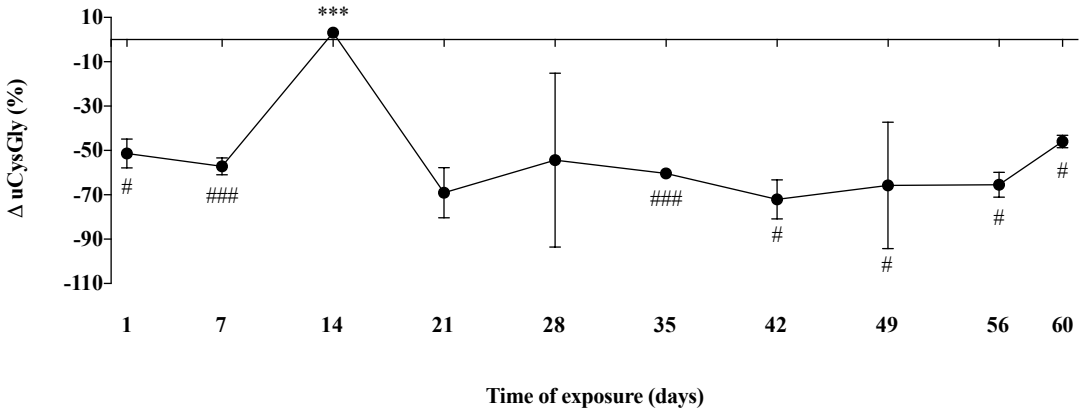

Figure V.11 – Temporal variation of uCysGly. The variation of uCysGly in the CIH group relatively to the Nx group exhibited a similar pattern to the one obtained for uCys (n = 5-6 animals per group per week).
uCysGly was normalized by uCr and the values attained at day 0 and is presented as percentage of effect from Nx group; *** One-way ANOVA with *Bonferroni's* multiple comparisons test, versus day 1; # or ### Unpaired t-test, versus Nx group of the same day; uCysGly: urinary cysteine-glycine; # $p < 0.05$; *** or ### $p < 0.001$.

V.4. Discussion

The present study shows that the progression of kidney dysfunction associated with hypertension-induced by CIH is accompanied by lower detoxification of CysSSX through the formation of their mercapturates. The decreased in the elimination of uNAC was accompanied by changes in renal Cys availability and dynamics as well as CysSSX filtration/reabsorption and GSH turnover. Herein, we observed an increase in the elimination of uNAC after acute exposure to CIH (1 day), indicative of an adaptive response to injury that is lost with the chronicity of exposure to CIH.

The model herein used mimics several co-morbidities of OSA, the most common sleep related breathing disorder (Foldvary-Schaefer and Waters, 2017). Features of the model employed include hypertension, insulin resistance and kidney dysfunction (Diogo *et al.*, 2015; Sacramento *et al.*, 2016; Coelho *et al.*, 2018). However, the paradigm of CIH employed does not induce obesity, allowing us to separate the mechanical and hypercapnic components of the obstruction, which is associated with obesity, from the effects of IH (O'donnell *et al.*, 1999; Schwartz *et al.*, 2008; Zammit *et al.*, 2010; Diogo *et al.*, 2015; Shetty and Parthasarathy, 2015). The absence of increase in weight observed in CIH animals is consistent with previous reports (Fenik *et al.*, 2012; Diogo *et al.*, 2015) and is not related with the decrease in food consumption, which only happened nearly at the end of the study. Instead, it seems to be associated with a significantly higher

metabolism and energy expenditure due to the increased work of breathing required in the CIH animals (Fenik *et al.*, 2012).

The association of sleep apnea and kidney dysfunction has been studied (Iseki *et al.*, 2008; Ahmed *et al.*, 2011; Chou *et al.*, 2011; Kanbay *et al.*, 2012; Nicholl *et al.*, 2012). For instance, CKD is highly prevalent in patients with sleep-related breathing disorders (Iseki *et al.*, 2008; Chou *et al.*, 2011). Moreover, a progressive decline in eGFR was detected as the severity of OSA increased (Kanbay *et al.*, 2012) and OSA patients with nocturnal hypoxia were at significant risk for accelerated loss of kidney function (Ahmed *et al.*, 2011). Still, this association is not a one-way street, as sleep apnea is also considered a relevant co-morbidity in CKD patients (Nicholl *et al.*, 2012; Aziz and Chaudhary, 2017).

Although the contribution of OSA *per se* or other confounding factors (e.g. obesity, hypertension, diabetes) for kidney injury remains unclear (Calvin *et al.*, 2009; X. I. A. Wang *et al.*, 2013; X. Wang *et al.*, 2013; Abuyassin *et al.*, 2015; Badran *et al.*, 2015; Rajan and Greenberg, 2015), OSA induces alterations known to stimulate functional and structural kidney damage such as increased activities of renin angiotensin-aldosterone system and sympathetic nervous system as well as the generation of systemic and local reactive oxygen species (Somers *et al.*, 1995; Carpagnano *et al.*, 2003; Adeseun and Rosas, 2010; Parati *et al.*, 2014).

A recent study revealed the presence of kidney injury in a mouse model of OSA-induced by IH that was characterized by glomerular hypertrophy, expansion of the glomerular mesangial matrix, increased expression of growth factors, renal cellular apoptosis and albuminuria (Abuyassin *et al.*, 2018). Our model seems to be a less severe form of kidney dysfunction, as no histological changes were observed neither significant increases uACR at the end of the study, probably due to the absence of glomerular hypertrophy (Cravedi and Remuzzi, 2013). However, rats exposed to our paradigm of CIH have increased renal expression of fibronectin (Coelho *et al.*, 2018) as well as inflammatory and EMT markers (unpublished data), further showing alterations at the kidney level. Moreover, these differences on the magnitudes of kidney dysfunction between both models might be due to the fact that the model employed by Abuyassin and co-authors is a more severe form of IH, with 60 cycels/h for 12 h/day (Abuyassin *et al.*, 2018), in comparison with the 5.6 cycles/h for 10.5/day obtained with our model (Diogo *et al.*, 2015; Coelho *et al.*, 2018). In fact, our paradigm of CIH approximates the impact of sleep apnea lasting for more than 2 years in humans and matches the clinical practice of OSA diagnosis (Diogo *et al.*,

2015). A AHI higher than 5 per hour is usually sufficient to consider someone as having OSA (Aziz and Chaudhary, 2017), although falling bellow the AHI cut-offs for moderate OSA in humans (> 15 events/h of sleep) (Berry *et al.*, 2012) even after correction for the higher metabolic activity in animlas (Germack *et al.*, 2002).

On the other hand, the effects of IH in the kidney seems to be time-dependent. Whereas short-term IH induces a protective response against renal oxidative damage, long-term IH induces damage to the kidneys (Sun *et al.*, 2013). This time-dependency of IH effects on the kidney are consistent with the initial increase in the elimination of uNAC observed in the present study as well as with the increase on free reduced Cys (increased CysSH/CysSSX) that precedes the increase in Cys oxidation (decreased CysSH/CysSSX). Interestingly, the increase in blood pressure denoted after 14 days of CIH exposure coincides with the time-point of changes on the elimination of uNAC. In fact, at this time-point, uNAC, uCys and uCysGly levels are similar among CIH and Nx animals. It is also at this time that a shift on the renal expression of NAT8 occurs, as shown by an increase in its expression mainly at the RC after 21 days of CIH exposure, coinciding also with an increase in renal fibronectin (Coelho *et al.*, 2018) and vimentin expression (unpublished data). This is probably due to the increase in Cys oxidation, that, under oxidative conditions is not able to be reduced to its free reduced formed, promoting toxicity. On the other hand, this can also be related with the increase on the oxidation of GSH in an attempt to reduce CysSSX. The increase in NAT8 mRNA expression is probably a mechanism to eliminate CysSSX and/or other Cys-*S*-conjugates. Alternative hypothesis might be related with NAT8's association with autophagy (Peng and Puglielli, 2016) and the possible acetylation of CysSSP, which has not been proven though there is evidence of its *in vitro* ability to acetylate protein lysine residues (Ko and Puglielli, 2009; Mak *et al.*, 2014). However, the activity might be reduced, as there is a progressive decline in the elimination of uNAC, reaching a difference of -80% in CIH than Nx animals by the end of the study, that also coincides with the decrease in NAT8 expression in kidney. This can also be explained by the action of the deacetylase SIRT1 (Sasaki *et al.*, 2017) or the fact that since Cys-*S*-conjugates are increased in inflammatory conditions (as reviewed in the **Introduction**) they might also compete with CysSSX for acetylation by NAT8, further contributing to the decrease elimination of uNAC. In a way, it seems that the increment on blood pressure underlies alterations in the mercapturate pathway and on CysSSX handling by the kidney. This fact is not surprising as NAT8 has been suggested as a positional candidate for blood pressure and renal regulation through a

resequencing, association and *in silico* study (Juhanson *et al.*, 2008). Specifically, the authors suggested a contribution of highly variable NAT8 promoter polymorphisms in determination of systolic blood pressure and eGFR, with minor alleles of these polymorphisms revealing a significant protective effect against elevated systolic blood pressure as well as kidney failure in hypertensive patients (Juhanson *et al.*, 2008).

V.5. Conclusions

The initial increase of uNAC upon short-term injury might be indicative of an adaptation response. However, with the chronicity of exposure to an inflammatory injury, the adaptation capacity is lost. This occurrence suggests the participation of CysSSX and the mercapturate pathway in the pathophysiological mechanism of kidney disease.

FINAL CONSIDERATIONS

FINAL CONSIDERATIONS

The starting point of this project was to discover a bioindicator of progression of kidney disease. The relevance of this work is related with huge global impact of kidney disease merged with the fact that there are no reliable markers to early predict and manage the progression of kidney disease. This was a hypothesis-oriented investigation, where it was aimed to implicate NAT8 activity into kidney disease progression by controlling the balance of Cys-*S*-conjugates and kidney redox homeostasis.

As so, the general aim was to discover a bioindicator of progression of tubular kidney disease and contribute to the knowledge of NAT8 function in the mechanisms underlying kidney tubular dysfunction with different etiologies.

Herein, the final considerations of this study are presented, divided into four different sections. First, the relevant findings and contributions of each chapter are summarized. The added value of this work is described in the second section, followed by its main limitations. Finally, future perspectives are presented. Due to this stratification, there is a possibility that some content herein presented overlaps with points stated in the discussion section of each chapter.

1. TOP 3 findings

The work herein presented contributes to the knowledge on the impact of renal cysteine disulfides renal dynamics and NAT8 activity in the development and progression of kidney dysfunction.

Development and validation of a non-invasive method to quantify uNAC that might be an indicator of Cys redox status in the kidney and evidence of a high person to person variability in the levels of uNAC

Using a mechanistic-based approach to kidney, we first developed a method to non-invasively measure tubular Cys redox status (cysteine disulfide stress) in kidney. This ability to measure uNAC was one of the major achievements of the present work. Thereby, we developed a method to quantify the mercapturates of CysSSX, using a surrogate that we named uNAC. In fact, this was the first report aiming at the quantification of uNAC as a surrogate of the urinary mercapturates derived from CysSSX and that provides first-hand evidence that its formation occurs in the kidney.

We also provide evidence on person-to-person variation in uNAC and factors associated to this variation, at least in the HIV-infected population. This high variability justifies that there are differences in patients in the way they eliminate CysSSX and it is relevant to understand these differences and its underlying consequence.

In fact, the study the temporal variation of uNAC along the progression of kidney dysfunction in animal models associated with metabolic inflammation, namely two pre-diabetic mice models and a rat model of hypertension and insulin resistance induced by CIH also contributed to this knowledge. In two of the three models, we observed an initial increase in uNAC, that might be indicative of an adaptive response, that was lost with the chronicity of exposure to injury. This decrease had different magnitudes and relations to CysSSP but was common to the three animal models. This provided evidence that it might exist particularities related to the etiology in the involvement of disulfide stress and cysteine disulfides dynamics in the pathophysiological mechanism of kidney disease and that uNAC might have a place in precision medicine of tubulopathy. Additionally, uNAC variation showed differences in CISP (that undergoes the mercapturate pathway) and G (that do not undergo mercapturate pathway) AKI-induced models, suggesting that there are mechanisms dependent on the mercapturate pathway and others that do not point in the same direction of the remaining models.

Evidence that uNAC might represent an early indicator of tubulopathy and is able to distinguish those at higher risk of disease progression regardless of the grade of kidney dysfunction progression

Using different models of kidney disease that course with tubulointerstitial oxidative stress and inflammation we evaluated temporal variations of uNAC. This was performed in acute and chronic models with different harmful stimulus (diet, CIH, infection, nephrotoxic drugs) in an attempt to approach as high as possible the relation of uNAC with tubular disease. The decrease in uNAC was consistent in all models used, and the more pronounced progression of kidney disease, the more uNAC decreases followed by a decrease in renal CysSSP.

As so, our translational approach shows a progressive decrease in the elimination of uNAC with the increment in kidney dysfunction. This is a concept that has never been addressed and that is common to all presented models, both in the clinical and in the *in vivo* setting. The limitations of pCr as a marker of kidney function have been discussed priorly (Waikar, Betensky and Bonventre, 2009; Ferguson and Waikar, 2012) and our results points towards the identification of uNAC as a valid early indicator of acute injury-induced by nephrotoxic drugs.

A remarkable evidence that was provided in the prospective study of the HIV-infected population was that uNAC allowed to discriminate patients with kidney disease progression from those that maintained a stable renal function throughout one-year of follow-up. This result suggests that uNAC is a strong candidate for a urinary biomarker for early diagnosis and theranostic purposes in kidney disease, particularly for tubular dysfunction.

Changes in cysteine disulfides dynamics and availability might underlie early events in kidney disease, promoting its progression, which might differ depending on the etiology

Our study shows that there are changes in Cys handling by the kidney in response to injury stimulus. Also, in animal models, it seems that renal CysSSP decreases in more pronounced stages of kidney disease progression. On the other hand, serum CysSSP increases with decreased renal function in our cross-sectional analysis of the HIV-infected population.

2. What is the added value and the impact of the present work to the field?

Notwithstanding the significant research in the field, there is still a lack of a valid reliable and accurate marker of kidney disease progression. Still, this scenario is far from reality, and several questions need to be addressed.

Tubular markers: a problem in the field

A major concern in the nephrology field is the lack of markers of proximal tubular cell function, since the proximal tubule has been recognized as the primary effector and sensor in kidney disease progression (Chevalier, 2016). Hence, our approach was to select a metabolic that was mainly expressed in proximal tubular cells, supported by association studies (Juhanson *et al.*, 2008; Chambers *et al.*, 2010; Köttgen *et al.*, 2010; Tin *et al.*, 2013), the mercapturate pathway. As far as the author knowledge, this is the first time that this concept has been employed to identify a tubular marker. This might be related with the fact that NAT8 has only been identified as the enzyme that acetylates Cys-*S*-conjugates in 2010 (Veiga-da-Cunha *et al.*, 2010), reflecting the low number of publications associated with the enzyme (only 18 publications in PubMed).

Herein, a hypothesis-driven method to quantify urinary mercapturates of CysSSX was developed and validated. The major advantage is the fact that this enables a non-invasive quantification, a relevant fact not only for its clinical application but also for the study of its temporal variation, minimizing the number of animals used.

Contribution for the knowledge of disulfide stress and CysSSP in renal tubule

While the study of renal disulfide stress and CysSSP are still in its early stages, the results herein presented pave the way for future studies in this field. Overall, disulfide stress and CysSSP are relevant players not only for metabolic inflammation mas but also on the interplay with environmental/food toxins and drugs, with potential to detect new mechanisms of action and adverse drug reactions.

Contribution for the understanding of the non-albuminuric phenotype in diabetic kidney disease

Classically, the progression of DKD is followed by a progressive increase in albuminuria and proteinuria with consequent decrease in GFR (Haneda *et al.*, 2014). Nevertheless, there is now growing evidence that this traditional pathway of DKD does not always happens, as reported in several clinical studies showing the regression or unchanged status of albuminuria upon decreases in GFR (Caramori, Fioretto and Mauer, 2003; Perkins *et al.*, 2010), the so called "non-albuminuric phenotype" (Viazzi *et al.*, 2017). As so, the concept of initial diabetic glomerular disease has now a direct competitor, diabetic tubulopathy, that has been stimulating research for better markers of prediction and management of DKD. Herein, we showed that the progression of kidney disease in pre-diabetic states is not directly related with increases in albuminuria. This shows the necessity of the identification of new biomarkers and also suggests that there are still mechanisms of kidney dysfunction that remain to be identified.

Contribution for the tubulocentric theory of inflammatory diseases

We have previously suggested that the formation of Cys-*S*-conjugates is associated with inflammatory conditions rather than kidney disease (Gonçalves-Dias *et al.*, 2019). The present study also contributes for this theory, as changes in uNAC were identified in HIV-infection, pre-diabetic and hypertensive conditions, all associated with inflammation (Deeks, Tracy and Douek, 2013; De Miguel *et al.*, 2015; Brahimaj *et al.*, 2017). Moreover, all Cys-*S*-conjugates have in common the detoxification by the proximal tubular cells as mercapturates, motivating a tubulocentric perspective for other inflammatory conditions.

A literature review was performed regarding the endogenous Cys-*S*-conjugates involved in inflammatory conditions. The mercapturate pathway is widely studied in the toxicology field to evaluate the exogenous exposure (Mathias and Bhymer, 2016). With this work, with cross the borders in an attempt to use this toxicology tools to evaluate the endogenous exposure and unravel the role of this tubular pathway in kidney disease and identify new markers of tubular dysfunction that are currently lacking in the clinical practice. Furthermore, a relation between renal metabolic inflammation and the

mercapturate pathway was established, where the Cys redox dynamics, the fibrotic mechanism and the identification of new therapeutic targets was included.

uNAC is an early marker of kidney tubular dysfunction

uNAC reflects mercapturates that are probably formed exclusively in proximal tubular cells through the acetylation of CysSSX provided by NAT8 activity, an enzyme that is almost exclusively expressed in kidney cortex (Chambers *et al.*, 2010). Furthermore, other enzymes that are involved in the mercapturate pathway are highly expressed at the brush border of proximal tubular cells (Hughey *et al.*, 1978; Griffith, 1981; Hanigan, 1998; De Carvalho *et al.*, 2011). Having into account that the proximal tubule is the primary effect and sensor of kidney disease progression (Chevalier, 2016) and that the mercapturate pathway is an almost exclusive feature of proximal tubular cells, the results herein obtain regarding uNAC variation might have tremendous impact in the clinical setting of both nephrotoxic and disease-associated kidney dysfunction.

Contribution for the development of strategies to minimize tubular dysfunction

Give the important role of proximal tubular cells in the progression of kidney disease, strategies aimed to minimize tubular dysfunction might contribute for prevention and/or management of kidney disease. We believe that targeting vital steps in the mercapturate pathway could be a relevant strategy to achieve this goal. For instance, studying patient's susceptibility to drugs undergoing the mercapturate pathway could be a valid option. This could be achieved through NAT8 genotyping. Although several SNPs in NAT8 coding sequence have been identified that could affect the activity of the enzyme, there is contradictory evidence. For instance, SNP rs13538 induces a non-synonymous amino acid change (F143S) that is likely to impact on the binding of acetyl-coA, the donor of the acetyl moiety of the mercapturates, and hence NAT8 function (Chambers *et al.*, 2010). However, in the same year of this report, Veiga-da-Cunha and co-authors performed a functional study and reported that the mutated F143S NAT8 had a similar enzymatic activity to the that of the wild-type protein (Veiga-da-Cunha *et al.*, 2010). A year later, Nicholson *et al*., showed that the mutation was associated with increased urinary concentrations of mercapturates, consistent with an increase in NAT8 efficiency (Nicholson *et al.*, 2011). However, whereas another rather frequent non-synonymous

amino acid change (E104K) does not influence the activity of the enzyme, a suppression on the activity was induced by the R149K mutation, that replaces an extremely conserved arginine (Veiga-da-Cunha *et al.*, 2010).

On the other hand, the stratification of patients through the levels of uNAC could also allow the identification of patients at higher risk for kidney disease progression. In this setting, the treatment choice will be focused solely on the individual's features, a concept associated with personalized medicine.

3. Which were the main limitations of this work?

As with all research projects, we are conscious regarding the limitations associated with this study.

Lack of sustained evidence that NAT8 acetylates CysSSX

The difficulty in developing NAT8 knockout rats (Fu *et al.*, 2014) and absence of tools to pharmacologically address NAT8 hinders to get hard evidence not only on the nephroprotective role of this enzyme, but also on the function of NAT8 to acetylate CysSSX. Nevertheless, our data points to the direction that, similarly to other Cys-*S*-conjugates, NAT8 is also able to acetylate CysSSX.

In an attempt to overcome this limitation, we tried to establish an *in vitro* model, an approach that is still ongoing. The main results obtained are displayed in attachment (**Attachment I**).

Lack of a gold standard measurement of kidney function

A major limitation of our clinical study is the lack of a gold standard measurement of true GFR rather than the use of eGFR equations with sCr, whose production is dependent on muscle mass and decreases in the presence of liver disease (Cocchetto, Tschanz and Bjornsson, 1983; Perrone, Madias and Levey, 1992), conditions associated with HIV-infection. Since establishing the true GFR is difficult due to the simultaneous occurrence

of the filtration process in all glomeruli, GFR can be measured by exogenous substances that are freely filtered at the glomeruli, with no associated secretion or reabsorption by the renal tubules, such the case of inulin (Mandel *et al.*, 1953; Rahn, Heidenreich and Brückner, 1999). However, the need for continuous infusion, multiple blood samples and urine collection, make it cumbersome and expensive to measure (Lopez-Giacoman and Madero, 2015). On the other hand, renal biopsy is also a useful tool for the clinical management of kidney disease (Dhaun *et al.*, 2014). Besides being an invasive procedure, its performance in this setting would not give enough information to stage the patients according the level of kidney function.

Having this into account, we believe that our choice for evaluation of kidney function was the best that we could perform in order to minimize the use of invasive and uncomfortable procedures in the patients.

Use of animal models and their associated differences

The use of animal models was unavoidable for our research purposes, mainly due to the fact that we needed to induce kidney injury and/or follow the progression of kidney disease from a starting point with no confounding factors (e.g. previous disease, medications, age, sex, race) that would be utopic to perform in human subjects. While not perfect, the respectful use of animal experimentation allows the study of pathophysiological mechanisms in an accelerated time frame. In this setting, the use of alternative *in vitro* models would not be suitable and. Nevertheless, the 3Rs policy (replacement, reduction and refinement) was always followed during the entire project. The number of animals used *per* experiment was reduced the minimum possible and the same biological sample was used for more than one assay, whenever applicable and all guidelines were followed. Furthermore, samples from the pre-diabetic and the drug-induced AKI models were obtained in collaborations with national and international laboratories, hence emphasizing the use of the 3Rs policy in this study.

It is noteworthy to state that the results obtained with animal models could be influenced by several factors. For instance, while some species complete their nephrogenesis after birth (rats, dogs, pigs and rabbits) in others it is ceased pre-natally (mice, monkey, man) (Frazier, 2017). Furthermore, we have to consider the fact that renal dysfunction in rats

is influenced by both gender and the genetic background of the strain (Baylis and Corman, 1998; Nogueira, Pires and Oliveira, 2017). Specifically, renal scarring begins earlier and becomes more severe in male rats that females and Sprague-Dawley rats are less resistant than other rat strains (Nogueira, Pires and Oliveira, 2017). In mice, the genetic background also influences the severity of the development of renal disease (Nishino *et al.*, 2010). For instance, C57Bl/6 animals harbor one single renin gene while other backgrounds have 2 renin genes (Wang *et al.*, 2002; Nishino *et al.*, 2010). This fact has important implications, since 2 renin genes induces a ten-fold higher plasma renin activity, angiotensin dependent hypertension, increased blood pressure and cardiac and renal hypertrophic responses to salt compared with 1 renin gene (Nishino *et al.*, 2010).

Moreover, the selection of the species could have an influence on the elimination of uNAC and hence impact the mercapturate pathway. In fact, rat livers dosed with l-chloro-2,4-dinitrobenzen excreted lower amounts of its mercapturate and higher quantity of the GSH-conjugate in bile whereas the opposite was found in guinea pig livers (Hinchman *et al.*, 1991). On the other hand, the metabolism of acrylamide in humans is apparently more prone for GSH conjugation rather than conversion to glycidamide when compared with rats and mice (Li *et al.*, 2016). Differences on the expression of the enzymes of the mercapturate pathway have also been reported. Rats and mice have very low hepatic but very high renal activities of GGT in comparison with guinea pig, pig, macaque monkey and man (Hinchman and Ballatori, 1990). Species differences were also found for dipeptidases activity, although in a lower magnitude than the one observed for GGT (Hinchman and Ballatori, 1990).

Lack of evaluation of changes in other endogenous Cys-S-conjugates and their mercapturates

We cannot exclude the hypothesis that the levels of other Cys-*S*-conjugates and their corresponding mercapturates might be changed in all models presented. In fact, evidence points to this fact (Gonçalves-Dias *et al.*, 2019). Unfortunately, we were not able to develop tools allowing their quantification, though we hope that in a near future this limitation will be overpassed.

Several parameters are still lacking in the animal models

Although we generated a substantially higher amount of data, some parameters were still no available for quantification in each one of the animal models used. Regarding the drug-induced AKI models, as we only had access to urine samples, it was not possible to quantify changes in renal NAT8 and CysSSX for the time being. We were also not able to quantify the protein levels of NAT8 in either one of the remaining models. This limitation was due to problems regarding the isolation of NAT8 for western blot analysis and the background noise observed in immunofluorescence/immunohistochemistry of histological cuts. Nevertheless, the techniques for its quantification are currently being developed and validated. Similarly, we had methodological problems on the quantification of pCr in the pre-diabetics and CIH models related with matrix interference. Lastly, the quantification of CysSH/CysSSX was also not possible for the pre-diabetic models since we only had access to frozen tissue. The quantification of CysSH requires the use of freshly collected samples, in order to avoid their spontaneous oxidation to CysSSX (McMenamin, Himmelfarb and Nolin, 2009).

Furthermore, other factors that might be lacking in this approach is the comparison of uNAC with other published markers and also the lack of mechanistic studies.

4. What is still unknown and should be addressed?

The knowledge on NAT8 actions has been hampered by its late association to both kidney disease and the mercapturate pathway (Juhanson *et al.*, 2008; Chambers *et al.*, 2010; Veiga-da-Cunha *et al.*, 2010). Furthermore, the unavailability of pharmacological tools and the plausible non-viable genetic animal models also contributes substantially for this gap in the knowledge (Ozaki *et al.*, 1998; Fu *et al.*, 2014).

Considering this, future studies should focus on assessing:

1. early changes in uNAC and renal CysSSX, specially right after injury;

2. changes of other endogenous Cys-*S*-conjugates rather than disulfides as well as their mercapturates in the progression of kidney disease

3. the mechanism of NAT8 regulation and the effect of exogenous Cys-*S*-conjugates in proximal tubular cells;

4. the mercapturate pathway in other acute models of renal disease such as ischemia/reperfusion, other tubular nephrotoxicants that undergo the mercapturate pathway (e.g. paracetamol) or not (e,g. tenofovir) (Gorgulho *et al.*, 2018) as well as in other diseases associated with kidney dysfunction;

5. the prospective evaluation in type II diabetic and OSA patients of uNAC and CysSSP, the identification of a pattern of mercapturates and NAT8 polymorphisms to evaluate the risk of kidney disease progression;

6. the evaluation of uNAC performance in drug-induced AKI or contrast-induced AKI in the clinical setting;

7. the identification of which specific proteins are cysteinylated;

8. if NAT8 regulated the effect of insulin and glucose in the proximal tubular cell.

Additionally, another fact that requires further elucidation is the possible role of NAT8 for the acetylation of protein Cys residues. Recently, NAT8 has been reported as a player in the acetylation of lysine residues of cargo proteins at the ER, controlling the homeostatic balance between quality control and autophagy (Peng and Puglielli, 2016). This acetylation is only performed in correctly folded polypeptides whereas non-acetylated polypeptides are prevented from leaving the ER and are disposed of. Moreover, autophagy is also controlled through acetylation. Specifically, acetylated ATG9A prevents the induction of autophagy while non-acetylated ATG9A stimulates it (Peng and Puglielli, 2016). Moreover, CD133 and BACE1 proteins have been suggested to be acetylated by NAT8 at lysine residues (Ko and Puglielli, 2009; Mak *et al.*, 2014). However, Veiga-da-Cunha and co-authors (2010) found that the catalytic efficiency of NAT8 to acetylate L-lysine residues and protein-bound lysine was 20-fold lower than for cys-*S*-conjugates (Veiga-da-Cunha *et al.*, 2010). Additionally, the mentioned reports of lysine acetylation by NAT8 were either *in vitro* (Ko and Puglielli, 2009) or in a line of human epithelial colorectal adenocarcinoma (Mak *et al.*, 2014), both context very apart from the proximal tubular cells where NAT8 is physiologically expressed to the greatest

extent. Therefore, this protein acetylation function of NAT8 remains unclear and should be further addressed.

Lastly, future work should also target the upstream steps of the mercapturate pathway to avoid the accumulation of toxic CysSSX. In fact, increasing GSH synthesis through other ways rather that the use of sulfur-containing supplements that may add to the Cys toxicity might be a valid long-term solution. There are antagonistic reports regarding the effect of *N*-acetylcysteine supplementation in kidney dysfunction, which further suggests the study of alternative approaches to avoid the dampening of endogenous antioxidant defenses in situations involving oxidation and inflammation.

ATTACHMENTS

ATTACHMENT I

AI.1. Comparison of the cytotoxicity of CISP *versus* Cys-CISP

To address cytotoxicity of cisplatin *versus* Cys-CISP, total cell death and its dose-dependency was evaluated in Mock cells. Cells were also exposed to Cys as a control. It was observed that increasing concentrations lead to a decrease in total cell death (p = 0.010), while the opposite variation was found for CISP (p = 0.004). No differences were observed for the three concentrations of Cys-CISP conjugate used that were associated with cell death similar to CISP 50 μM. Nevertheless, at 10 μM and 25 μM, the conjugate Cys-CISP was able to induce higher total cell death in comparison with the same concentrations of CISP, while the effect was similar between the two compounds at 50 μM (p = 0.034 and p = 0.022, respectively for 10 μM and 25 μM) (**Figure AI.1**).

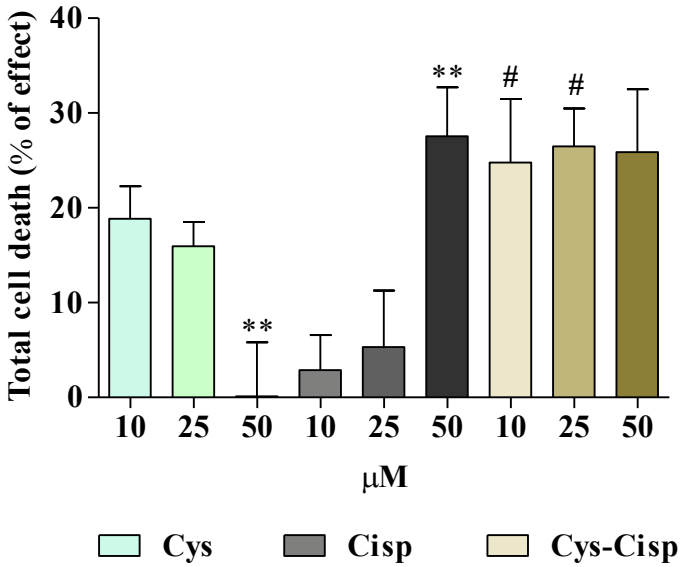

Figure AI.1 – Total cell death in mock cells. A decrease in total cell death was observed with increased concentration of Cys, while Cisp elicited an opposite effect. Although no differences were found on the total cell death elicited by the three concentrations of CysCisp conjugate, 10 μM and 25 μM of CysCisp were able to induce higher cell death then the same concentrations for Cisp. This effect was not served when the CISP 50 μM was used.
HK-2 cells were transiently transfected with pcDNA 3.1-mock and exposed to CTL (DMEM F-12 media), Cys, CISP or Cys-CISP for 24h. Data were normalized by the values observed in CTL condition and presented as mean ± SEM of 3 independent experiments. * One-way ANOVA with *Dunnett's* multiple comparisons test, versus 10 μM of each compound; # Two-way ANOVA with *Bonferroni's* multiple comparisons test, versus Cisp; CTL: control; Cisp: cisplatin; Cys: cysteine; Cys-Cisp: cysteine-cisplatin conjugate.

AI.2. Effect of NAT8 overexpression in CISP cytotoxicity

NAT8 overexpression lead to a decrease in total cell death elicited by CISP and Cys-CISP in comparison with the results obtained for mock cells, except for wt-NAT8. This is demonstrated by normalized values below 100% for most experimental conditions (one-sample t-test), considering that 100% corresponds to equal % of total cell death obtained for NAT8 overexpression in the same mock condition (**Figure AI.2**). This decrease was not so significant for the higher dose of Cys-CISP.

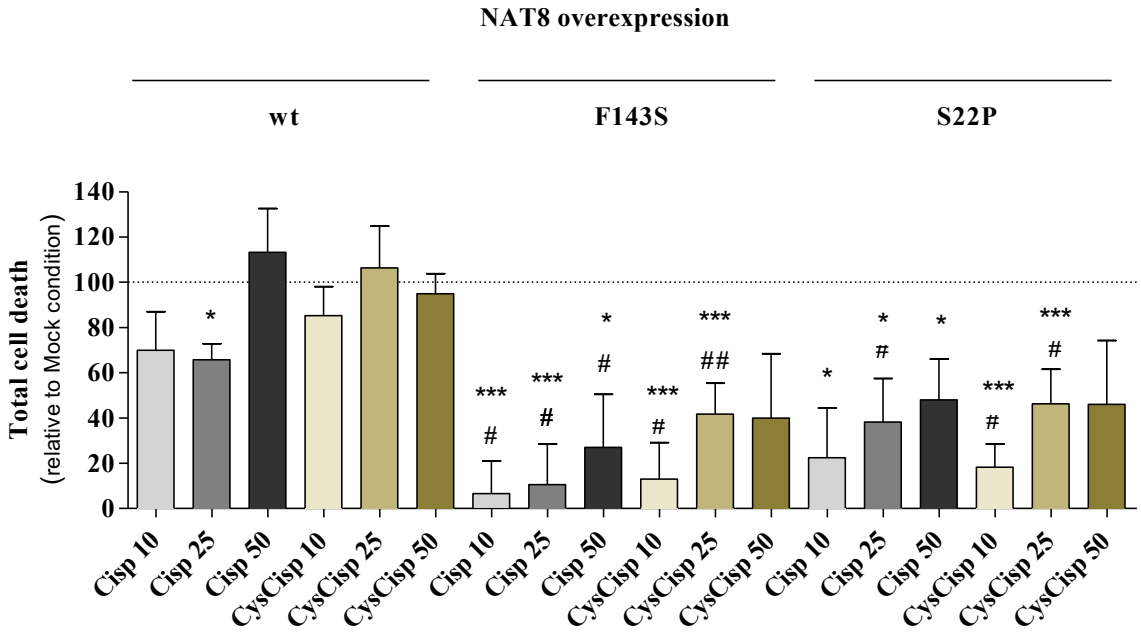

Figure AI.2 – Total cell death in NAT8 overexpressed cells exposed to CISP or Cys-CISP. The mutated forms of NAT8 showed significantly lower total cell death relatively to the wt form. In specific, the F143S mutation had lower cell death in cells exposed to CISP at 10 μM and 50 μM and Cys-CISP at 10 μM and 25 μM concentrations (Two-way ANOVA with *Bonferroni's* multiple comparisons test, p = 0.030, p = 0.004, p = 0.010 and p = 0.024, respectively for CISP 10 μM, CISP50 μM, Cys-CISP 10 μM and Cys-CISP 25 μM concentrations). Differences in S22P mutation were significant for CISP 50 μM, and Cys-CISP conjugate at 10 μM and 25 μM concentrations (Two-way ANOVA with *Bonferroni's* multiple comparisons test, p = 0.027, p = 0.019 and p = 0.039, respectively for CISP 50 μM, Cys-CISP 10 μM and Cys-CISP 25 μM concentrations).
HK-2 cells were transiently transfected with pcDNA 3.1-mock or pcDNA 3.1-NAT8-wt or pcDNA 3.1-NAT8-F143S or pcDNA 3.1-NAT8-S22P. Cells were exposed to CTL (DMEM F-12 media), Cys, CISP or Cys-CISP for 24h. Data were normalized by the values observed in CTL condition and expressed as the percentage of the values attained at each Mock condition. Values are presented as mean ± SEM of 3 independent experiments. # Two-way ANOVA with *Bonferroni's* multiple comparisons test versus wt; * One sample t-test for differences from 100.
CTL: control; Cisp: cisplatin; Cys: cysteine; CysCisp: cysteine-cisplatin conjugate; wt: wild-type.

REFERENCES

REFERENCES

Abdelsalam, M. *et al.* (2018) 'Urinary biomarkers for early detection of platinum based drugs induced nephrotoxicity', *BMC Nephrology*, 19:219.

Abuyassin, B. *et al.* (2015) 'Obstructive sleep apnea and kidney disease: a potential bidirectional relationship?', *Journal of Clinical Sleep Medicine*, 11:915–924.

Abuyassin, B. *et al.* (2018) 'Intermittent hypoxia causes histological kidney damage and increases growth factor expression in a mouse model of obstructive sleep apnea', *PLoS One*, 13: e0192084.

Adeseun, G. A. and Rosas, S. E. (2010) 'The impact of obstructive sleep apnea on chronic kidney disease', *Current Hypertension Reports*, 12:378–383.

Ahmad, M. (2006) 'Abacavir-induced reversible Fanconi syndrome with nephrogenic diabetes insipidus in a patient with acquired immunodeficiency syndrome', *Journal of Postgraduate Medicine*, 52:296–297.

Ahmed, S. B. *et al.* (2011) 'Nocturnal hypoxia and loss of kidney function', *PLoS One*, 6:e19029.

Aigner, A. *et al.* (1996) 'Purification and characterization of cysteine-S-conjugate N-acetyltransferase from pig kidney', *Biochemical Journal*, 317:213–218.

Al-Majed, A. A. *et al.* (2002) 'Protective effect of oral arabic gum administration on gentamicin-induced nephrotoxicity in rats', *Pharmacological Research*, 46:445–451.

Alary, J. *et al.* (1998) '1,4-Dihydroxynonene mercapturic acid, the major end metabolite of exogenous 4-hydroxy-2-nonenal, is a physiological component of rat and human urine', *Chemical Research in Toxicology*, 11:130–135.

Alge, J. L. and Arthur, J. M. (2015) 'Biomarkers of AKI: a review of mechanistic relevance and potential therapeutic implications', *Clinical Journal of the American Society of Nephrology*, 10:147–155.

Ali, B. H. (2003) 'Agents ameliorating or augmenting experimental gentamicin nephrotoxicity: some recent research', *Food and Chemical Toxicology*, 41:1447–1452.

Ali, B. H. *et al.* (2009) 'Comparative protective effect of N-acetyl cysteine and tetramethylpyrazine in rats with gentamicin nephrotoxicity', *Journal of Applied Toxicology*, 29:302–307.

Alkhamees, O. A. *et al.* (2017) 'Possible involvement of the lipoxygenase and leukotriene signaling pathways in cisplatin-mediated renal toxicity', *Cancer Chemotherapy and Pharmacology*, 80:55–64.

Allen, S. P. *et al.* (1993) 'Enhanced excretion of urinary leukotriene E4 in coronary artery disease and after coronary artery bypass surgery.', *Coronary Artery Disease*, 4:899–904.

Alvarez, J. A. *et al.* (2018) 'Vitamin D deficiency is associated with an oxidized plasma cysteine redox potential in critically ill children', *The Journal of Steroid Biochemistry and Molecular Biology*, 175:164–169.

Arany, I. and Safirstein, R. L. (2003) 'Cisplatin nephrotoxicity', *Seminars in Nephrology*, 23:460–464.

Ashfaq, S. *et al.* (2006) 'The relationship between plasma levels of oxidized and reduced thiols and early atherosclerosis in healthy adults', *Journal of the American College of Cardiology*, 47:1005–1011.

Ashfaq, S. *et al.* (2008) 'Endothelial function and aminothiol biomarkers of oxidative stress in healthy adults', *Hypertension*, 52:80–85.

Assem, E. S. and Abdullah, N. A. (1987) 'Release of thromboxane B2 and leukotriene C4 and reduction in renal perfusion in experimental anaphylactic reaction of isolated guinea pig kidney', *International Archives of Allergy and Applied Immunology*, 82:212–214.

Ateşşahin, A. *et al.* (2003) 'The effect of manganese chloride on gentamicin-induced nephrotoxicity in rats', *Pharmacological Research*, 48:637–642.

Auclair, J. R., Johnson, J. L., *et al.* (2013) 'Post-translational modification by cysteine protects Cu/Zn-superoxide dismutase from oxidative damage', *Biochemistry*, 52:6137–6144.

Auclair, J. R., Brodkin, H. R., *et al.* (2013) 'Structural consequences of cysteinylation of Cu/Zn-superoxide dismutase', *Biochemistry*, 52:6145–6150.

Aydinoz, S. *et al.* (2007) 'Effects of different doses of hyperbaric oxygen on cisplatin-induced nephrotoxicity', *Renal Failure*, 29:257–263.

Aziz, F. and Chaudhary, K. (2017) 'The triad of sleep apnea, hypertension, and chronic kidney disease: a spectrum of common pathology', *Cardiorenal Medicine*, 7:74–82.

Bäck, M. *et al.* (2007) 'Increased leukotriene concentrations in gingival crevicular fluid from subjects with periodontal disease and atherosclerosis', *Atherosclerosis*, 193:389–394.

Badr, K. F. *et al.* (1984) 'Renal and systemic hemodynamic responses to intravenous infusion of leukotriene C4 in the rat', *Circulation Research*, 54:492–499.

Badr, K. F., Brenner, B. M. and Ichikawa, I. (1987) 'Effects of leukotriene D4 on glomerular dynamics in the rat', *American Journal of Physiology*, 253:F239–F243.

Badran, M. *et al.* (2015) 'Epidemiology of sleep disturbances and cardiovascular consequences', *Canadian Journal of Cardiology*, 31:873–879.

Bagley, P. J. and Stipanuk, M. H. (1995) 'Rats fed a low protein diet supplemented with sulfur amino acids have increased cysteine dioxygenase activity and increased taurine production in hepatocytes', *The Journal of Nutrition*, 125:933–940.

Bailly, V. *et al.* (2002) 'Shedding of kidney injury molecule-1, a putative adhesion protein involved in renal regeneration', *Journal of Biological Chemistry*, 277:39739–39748.

Ballatori, N. *et al.* (2009) 'Glutathione dysregulation and the etiology and progression of human diseases', *Biological Chemistry*, 390:191–214.

Banfalvi, T. *et al.* (2000) 'Serum concentration of 5-S-cysteinyldopa in patients with melanoma', *European Journal of Clinical Investigation*, 30:900–904.

Bannai, S. and Tateishi, N. (1986) 'Role of membrane transport in metabolism and function of glutathione in mammals', *The Journal of Membrane Biology*., 89:1–8.

Bar-Or, D. *et al.* (2004) 'Plasma albumin cysteinylation is regulated by cystathionine β-synthase', *Biochemical and Biophysical Research Communications*, 325:1449–1453.

Barditch-Crovo, P. *et al.* (2001) 'Phase I/II trial of the pharmacokinetics, safety, and antiretroviral activity of tenofovir disoproxil fumarate in human immunodeficiency virus-infected adults', *Antimicrobial Agents and Chemotherapy*, 45:2733–2739.

Bargman, J. and Skorecki, K. (2015) 'Chronic kidney disease', in Kasper, D. et al. (eds) *Harrison's Principles of Internal Medicine*. 19th edn. McGraw-Hill Education, pp. 1811–1821.

Basile, D. P., Anderson, M. D. and Sutton, T. A. (2012) 'Pathophysiology of acute kidney injury', *Comprehensive Physiology*, 2:1303-1353.

Baylis, C. and Corman, B. (1998) 'The aging kidney: insights from experimental studies.', *Journal of the American Society of Nephrology*, 9:699–709.

Bella, D. L. *et al.* (1999) 'Mechanisms involved in the regulation of key enzymes of cysteine metabolism in rat liver in vivo', *American Journal of Physiology*, 276:E326–E335.

Bella, D. L., Hahn, C. and Stipanuk, M. H. (1999) 'Effects of nonsulfur and sulfur amino acids on the regulation of hepatic enzymes of cysteine metabolism', *American Journal of Physiology*, 277:E144–E153.

Bellomo, F. *et al.* (2010) 'Modulation of CTNS gene expression by intracellular thiols', *Free Radical Biology and Medicine*, 48:865–872.

Bellomo, F. *et al.* (2016) 'Carboxyl-terminal SSLKG motif of the human cystinosin-LKG plays an important role in plasma membrane sorting', *PloS One*, 11:e0154805.

Bernstrom, K. and Hammarstrom, S. (1986) 'Metabolism of leukotriene E4 by rat tissues: formation of N-acetyl leukotriene E4', *Archives of Biochemistry Biophysics*, 244:486–491.

Berry, R. B. *et al.* (2012) 'Rules for scoring respiratory events in sleep: update of the 2007 AASM manual for the scoring of sleep and associated events', *Journal of Clinical Sleep Medicine,* 8:597–619.

Bertram, J. F. *et al.* (2011) 'Human nephron number: implications for health and disease', *Pediatric Nephrology*, 26:1529-1533.

Bertram, J., Schettgen, T. and Kraus, T. (2016) 'Isotope-dilution method for the determination of 1-vinyl-2-pyrrolidone-mercapturic acid as a potential human biomarker for 1-vinyl-2-pyrrolidone via online SPE ESI-LC/MS/MS in negative ionization mode', *Journal of Chromatography B*, 1033–1034:321–327.

Besouw, M. T. and Levtchenko, E. N. (2014) 'Improving the prognosis of nephropathic cystinosis', *International Journal of Nephrology and Renovascular Disease*, 7:297–302.

Boizel, R. *et al.* (2010) 'Regulation of oxidative stress and inflammation by glycaemic control: evidence for reversible activation of the 5-lipoxygenase pathway in type 1, but not in type 2 diabetes', *Diabetologia*, 9:2068–2070.

Bonventre, J. V. (2015) 'Adaptation of the kidney to injury', in Kasper, D. et al. (eds) *Harrison's Principles of Internal Medicine*. 19th edn. New York: McGraw-Hill Education, p. 333e1-333e4.

Bonventre, J. V and Yang, L. (2011) 'Cellular pathophysiology of ischemic acute kidney injury', *The Journal of Clinical Investigation*, 121:4210–4221.

Boyland, E. and Chasseaud, L. F. (1969) 'The role of glutathione and glutathione S-transferases in mercapturic acid biosynthesis', *Advances in Enzymology and Related Areas of Molecular Biology*, 32:173–219.

Bradley, H. *et al.* (1994) 'Sulfate metabolism is abnormal in patients with rheumatoid arthritis. Confirmation by in vivo biochemical findings.', *The Journal of Rheumatology*, 21:1192–1196.

Brahimaj, A. *et al.* (2017) 'Novel inflammatory markers for incident pre-diabetes and type 2 diabetes: the Rotterdam Study', *European Journal of Epidemiology*, 32:217–226.

Brosius, F. C. *et al.* (2009) 'Mouse models of diabetic nephropathy', *Journal of the American Society of Nephrology*, 20:2503–2512.

Burckhardt, B. C. and Burckhardt, G. (2003) 'Transport of organic anions across the basolateral membrane of proximal tubule cells', *Reviews of Physiology, Biochemistry and Pharmacology*, 146:95–158.

Burckhardt, G. (2012) 'Drug transport by organic anion transporters (OATs)', *Pharmacology & Therapeutics*, 136:106–130.

Burns, J. A. *et al.* (1991) 'Selective reduction of disulfides by tris(2-carboxyethyl)phosphine', *Journal of Organic Chemistry*, 56:2648–2650.

Butterly, D. W. *et al.* (2000) 'A role for leukotrienes in cyclosporine nephrotoxicity', *Kidney International*, 57:2586–2593.

Calonge, M. J. *et al.* (1995) 'Assignment of the gene responsible for cystinuria (rBAT) and of markers D2S119 and D2S177 to 2p16 by fluorescence in situ hybridization', *Human Genetics*, 95:633–636.

Calvin, A. D. *et al.* (2009) 'Obstructive sleep apnea, inflammation, and the metabolic syndrome', *Metabolic Syndrome and Related Disorders*, 7:271–277.

Campos, P. *et al.* (2016) 'Is there a role for soluble α-Klotho in kidney and immune dysfunction of HIV-infected patients?', *Nephrology Dialysis Transplantation*, 31:i437–i437.

Campos, P., Ortiz, A. and Soto, K. (2016) 'HIV and kidney diseases: 35 years of history and consequences', *Clinical Kidney Journal*, 9:772–781.

Cao, S. S. and Kaufman, R. J. (2014) 'Endoplasmic reticulum stress and oxidative stress in cell fate decision and human disease', *Antioxidants & Redox Signaling*, 21:396–413.

Caramori, M. L., Fioretto, P. and Mauer, M. (2003) 'Low glomerular filtration rate in normoalbuminuric type 1 diabetic patients: an indicator of more advanced glomerular lesions', *Diabetes*, 52:1036-1040.

Carlsson, A. and Fornstedt, B. (1991) 'Catechol metabolites in the cerebrospinal fluid as possible markers in the early diagnosis of Parkinson's disease', *Neurology*, 41:50–51.

Carpagnano, G. E. *et al.* (2003) '8-Isoprostane, a marker of oxidative stress, is increased in exhaled breath condensate of patients with obstructive sleep apnea after night and is reduced by continuous positive airway pressure therapy', *Chest*, 124:1386–1392.

Carry, M. *et al.* (1992) 'Increased urinary leukotriene excretion in patients with cardiac ischemia: in vivo evidence for 5-lipoxygenase activation', *Circulation*, 85:230–236.

De Carvalho, J. A. M. *et al.* (2011) 'Assessment of urinary γ-glutamyltransferase and alkaline phosphatase for diagnosis of diabetic nephropathy', *Clinica Chimica Acta*, 412(:1407–1411.

Celik, D. *et al.* (2013) 'Cysteinyl leukotrienes in exhaled breath condensate of smoking asthmatics', *Clinical Chemistry and Laboratory Medicine*, 51:1069–1073.

Chambers, J. C. *et al.* (2010) 'Genetic loci influencing kidney function and chronic kidney disease', *Nature Genetics*, 42:373–375.

Chasseaud, L. F. (1979) 'The role of glutathione and glutathione S-transferases in the metabolism of chemical carcinogens and other electrophilic agents', *Advances in Cancer Research*, 29:175–274.

Cheng, F.-C. *et al.* (1996) 'Elevated 5-S-cysteinyldopamine/homovanillic acid ratio and reduced homovanillic acid in cerebrospinal fluid: possible markers for and potential insights into the pathoetiology of Parkinson's disease', *Journal of Neural Transmission*, 103:433–446.

Cherqui, S. and Courtoy, P. J. (2017) 'The renal Fanconi syndrome in cystinosis: pathogenic insights and therapeutic perspectives', *Nature Reviews Nephrology*, 13:115–131.

Chevalier, R. L. (2016) 'The proximal tubule is the primary target of injury and progression of kidney disease:

role of the glomerulotubular junction', *American Journal of Physiology Renal Physiology*, 311:F145–F161.

De Chiara, B. *et al.* (2012) 'Plasma total cysteine and cardiovascular risk burden: action and interaction', *The Scientific World Journal*, 2012:303654.

Choi, A. I. *et al.* (2009) 'White/black racial differences in risk of end-stage renal disease and death', *The American Journal of Medicine*, 122:672–678.

Chou, Y.-T. *et al.* (2011) 'Obstructive sleep apnea: a stand-alone risk factor for chronic kidney disease', *Nephrology Dialysis Transplantation*, 26:2244–2250.

Cihlar, T. and Fordyce, M. (2016) 'Current status and prospects of HIV treatment', *Current Opinion in Virology*, 18:50–56.

Cocchetto, D. M., Tschanz, C. and Bjornsson, T. D. (1983) 'Decreased rate of creatinine production in patients with hepatic disease: implications for estimation of creatinine clearance', *Therapeutic Drug Monitoring*, 5:161-168.

Coelho, N. R. *et al.* (2018) 'Cysteine oxidative dynamics underlies hypertension and kidney dysfunction induced by chronic intermittent hypoxia', in Gauda, E. et al. (eds) *Arterial Chemoreceptors - New Directions and Translational Perspectives*. Springer, Cham, p. 83–88, vol 1071.

Commandeur, J. N., Stijntjes, G. J. and Vermeulen, N. P. (1995) 'Enzymes and transport systems involved in the formation and disposition of glutathione S-conjugates. Role in bioactivation and detoxication mechanisms of xenobiotics.', *Pharmacological Reviews*, 47:271–330.

Cooper, A. J. L., Younis, I. R., *et al.* (2008) 'Metabolism of the cysteine S-conjugate of busulfan involves a β-lyase reaction', *Drug Metabolism and Disposition*, 36:1546–1552.

Cooper, A. J. L., Pinto, J. T., *et al.* (2008) 'Substrate specificity of human glutamine transaminase K as an aminotransferase and as a cysteine S-conjugate beta-lyase', *Archives of Biochemistry and Biophysics*, 474:72–81.

Cooper, A. J. L. *et al.* (2011) 'Cysteine S-conjugate β-lyases: important roles in the metabolism of naturally occurring sulfur and selenium-containing compounds, xenobiotics and anticancer agents', *Amino Acids*, 41:7–27.

Cooper, A. J. L. and Pinto, J. T. (2006) 'Cysteine S-conjugate β-lyases', *Amino Acids*, 30:1–15.

Cosnier, F. *et al.* (2012) 'Mercapturic acids derived from toluene in rat urine samples: identification and measurement by gas chromatography-tandem mass spectrometry', *Analytical and Bioanalytical Chemistry*, 404:1907–1917.

Cowland, J. B. *et al.* (2003) 'Neutrophil gelatinase-associated lipocalin is up-regulated in human epithelial cells by IL-1β, but not by TNF-α', *The Journal of Immunology*, 171:6630–6639.

Cozzaglio, L. *et al.* (1990) 'A feasibility study of high-dose cisplatin and 5-fluorouracil with glutathione protection in the treatment of advanced colorectal cancer', *Tumori Journal*, 76:590–594.

Cravedi, P. and Remuzzi, G. (2013) 'Pathophysiology of proteinuria and its value as an outcome measure in chronic kidney disease', *British Journal of Clinical Pharmacology*, 76:516–523.

Crawhall, J. C. *et al.* (1967) 'The renal clearance of amino acids in cystinuria', *The Journal of Clinical Investigation*, 46:1162–1171.

Crawhall, J. C. and Segal, S. (1967) 'The intracellular ratio of cysteine and cystine in various tissues', *Biochemical Journal*, 105:891–896.

Cristofori, P., Sauer, A. V. and Trevisan, A. (2015) 'Three common pathways of nephrotoxicity induced by halogenated alkenes', *Cell Biology and Toxicology*, 31:1–13.

Daimon, M. *et al.* (2003) 'Increased urinary levels of pentosidine, pyrraline and acrolein adduct in type 2 diabetes', *Endocrine Journal*, 50:61–67.

Dalle-Donne, I. *et al.* (2007) 'S-glutathionylation in protein redox regulation', *Free Radical Biology and Medicine*., 43:883–898.

Dasari, S. and Tchounwou, P. B. (2014) 'Cisplatin in cancer therapy: molecular mechanisms of action', *European Journal of Pharmacology*, 740:364–378.

Datta, S. K. *et al.* (2010) 'Association of glutathione S-transferase M1 and T1 gene polymorphism with oxidative stress in diabetic and nondiabetic chronic kidney disease', *Renal Failure*, 32:1189–1195.

Daubeuf, S. *et al.* (2002) 'Enhanced resistance of HeLa cells to cisplatin by overexpression of γ-glutamyltransferase', *Biochemical Pharmacology*, 64:207–216.

Daubeuf, S. *et al.* (2003) 'Different mechanisms for γ-glutamyltransferase-dependent resistance to carboplatin and cisplatin', *Biochemical Pharmacology*, 66:595–604.

Davis, S. R. *et al.* (2006) 'Plasma glutathione and cystathionine concentrations are elevated but cysteine flux is unchanged by dietary vitamin B-6 restriction in young men and women', *The Journal of Nutrition*, 136:373–378.

Dawn, J. F. R. W. W. and Ballatori, C. N. (1998) 'Glutathione S-conjugate formation and metabolism in HepG2 cells: a cell model of mercapturic acid biosynthesis', *Journal of Toxicology and Environmental Health Part A*, 53:651–663.

Day, B. J. and Lewis, W. (2004) 'Oxidative stress in NRTI-induced toxicity', *Cardiovascular Toxicology*, 4:207–216.

Deeks, S. G., Tracy, R. and Douek, D. C. (2013) 'Systemic effects of inflammation on health during chronic HIV infection', *Immunit*, 39:633–645.

Dekant, W., Vamvakas, S. and Anders, M. W. (1989) 'Bioactivation of nephrotoxic haloalkenes by glutathione conjugation: formation of toxic and mutagenic intermediates by cysteine conjugate β-lyase', *Drug Metabolism Reviews*, 20:43–83.

Deol, R. (2015) 'Substrate specificity of human N-acetyltransferase 8 for aromatic cysteine conjugates - Master Thesis'

Deol, R. and Josephy, P. D. (2017) 'Acetylation of aromatic cysteine conjugates by recombinant human N-acetyltransferase 8', *Xenobiotica*, 47:202–207.

Derakhshanfar, A., Bidadkosh, A. and Hashempour Sadeghian, M. (2009) 'L-methionine attenuates gentamicin nephrotoxicity in male Wistar rat: pathological and biochemical findings', *Iranian Journal of Veterinary Research*, 10:323–328.

Dhaun, N. *et al.* (2014) 'Utility of renal biopsy in the clinical management of renal disease', *Kidney International*, 85:1039–1048.

Dhawan, S. S. *et al.* (2011) 'The role of plasma aminothiols in the prediction of coronary microvascular dysfunction and plaque vulnerability', *Atherosclerosis*, 219:266–272.

Dias, C., Casimiro, N. F., *et al.* (2015) 'Lactonase activity and kidney function in HIV-infected patients under combined antiretroviral therapy', *Toxicology Letters*, 238:S163.

Dias, C., Maia, S., *et al.* (2015) 'Soluble α-Klotho in HIV-infected patients and kidney dysfunction', *Journal of the American Society of Nephrology*, 26:931A.

Dias, C. *et al.* (2017) 'Kidney disease progression in HIV-infected patients related with the detoxification of endogenous electrophilic species', *Nephrology Dialysis Transplantation*, 32:iii540-iii541.

Ding, Y. *et al.* (2014) 'The endoplasmic reticulum-based acetyltransferases, ATase1 and ATase2, associate with the oligosaccharyl-transferase to acetylate correctly folded polypeptides', *Journal of Biological Chemistry*, 289: 32044-32055.

Diogo, L. N. *et al.* (2015) 'Efficacy of carvedilol in reversing hypertension induced by chronic intermittent hypoxia in rats', *European Journal of Pharmacology*, 765:58–67.

Dröge, W. *et al.* (1991) 'Modulation of lymphocyte functions and immune responses by cysteine and cysteine derivatives', *The American Journal of Medicine,* 91:140S-144S.

Duranton, F. *et al.* (2012) 'Normal and pathologic concentrations of uremic toxins', *Journal of the American Society of Nephrology*, 23:1258–1270.

Dvash, E. *et al.* (2015) 'Leukotriene C4 is the major trigger of stress-induced oxidative DNA damage', *Nature Communications*, 6:10112.

England, C. G. *et al.* (2015) 'Release kinetics of paclitaxel and cisplatin from two and three layered gold nanoparticles', *Eur J Pharm Biopharm*, 92:120–129.

European Medicines Agency (2012) 'Guideline on bioanalytical method validation', *EMA Guideline*, 44:1–23.

Ezaki, T. *et al.* (2017) 'Metabolomics for the early detection of cisplatin-induced nephrotoxicity', *Toxicology Research*, 6:843–853.

Faubel, S. *et al.* (2007) 'Cisplatin-induced acute renal failure is associated with an increase in the cytokines interleukin (IL)-1β, IL-18, IL-6, and neutrophil infiltration in the kidney', *Journal of Pharmacology and Experimental Therapeutics*, 322:8–15.

Feehally, J. (2016) 'The ISN 0by25 global snapshot study', *Annals of Nutrition and Metabolism*, 68:29–31.

Feliubadaló, L. *et al.* (1999) 'Non-type I cystinuria caused by mutations in SLC7A9, encoding a subunit (b o,+ AT) of rBAT', *Nature Genetic*, 23:52–57.

Fenik, V. B. *et al.* (2012) 'Glucoregulatory consequences and cardiorespiratory parameters in rats exposed to chronic–intermittent hypoxia: effects of the duration of exposure and losartan', *Frontiers in Neurology*, 3:51.

Ferenbach, D. A. and Bonventre, J. V. (2015) 'Mechanisms of maladaptive repair after AKI leading to accelerated kidney ageing and CKD', *Nature Reviews Nephrology*, 11:264–276.

Ferguson, M. A. and Waikar, S. S. (2012) 'Established and emerging markers of kidney function', *Clinical Chemistry*, 58:680–689.

Fernández, E. *et al.* (2002) 'rBAT-b0,+ AT heterodimer is the main apical reabsorption system for cystine in the kidney', *American Journal of Physiology Renal Physiology*, 283:F540–F548.

Feroe, A. G., Attanasio, R. and Scinicariello, F. (2016) 'Acrolein metabolites, diabetes and insulin resistance', *Environmental Research*, 148:1–6.

Ferreira, L. *et al.* (2011) 'Urinary levels of regenerating islet-derived protein III b and gelsolin differentiate gentamicin from cisplatin-induced acute kidney injury in rats', *Kidney International*, 79:518–528.

Finkelstein, J. D., Martin, J. J. and Harris, B. J. (1986) 'Effect of dietary cystine on methionine metabolism in rat liver', *The Journal of Nutrition*, 116:985–990.

Fliedl, L. *et al.* (2014) 'Controversial role of gamma-glutamyl transferase activity in cisplatin nephrotoxicity', *Alternatives to Animal Experimentation*, 31:269–278.

Flo, T. H. *et al.* (2004) 'Lipocalin 2 mediates an innate immune response to bacterial infection by sequestrating iron', *Nature*, 432:917-921.

Foldvary-Schaefer, N. R. and Waters, T. E. (2017) 'Sleep-disordered breathing', *CONTINUUM: Lifelong Learning in Neurology*, 23:1093–1116.

Forman, H. J., Maiorino, M. and Ursini, F. (2010) 'Signaling functions of reactive oxygen species', *Biochemistry*, 49:835–842.

Fornstedt, B. *et al.* (1989) 'The apparent autoxidation rate of catechols in dopamine-rich regions of human brains increases with the degree of depigmentation of substantia nigra', *Journal of Neural Transmission Parkinson's Disease and Dementia Section*, 1:279–295.

Frazier, K. S. (2017) 'Species differences in renal development and associated developmental nephrotoxicity', *Birth Defects Research*, 109:1243–1256.

Fu, J. *et al.* (2014) 'The role of N-acetyltransferase 8 in mesenchymal stem cell-based therapy for liver ischemia/reperfusion injury in rats', *PLoS One*, 9:e103355.

Fujita, H. *et al.* (2001) 'Increased expression of glutathione S-transferase in renal proximal tubules in the early stages of diabetes: a study of type-2 diabetes in the Akita mouse model', *Nephron Experimental Nephrology*, 9:380–386.

Funk, C. D. (2001) 'Prostaglandins and leukotrienes: advances in eicosanoid biology', *Science*, 294:1871–1875.

Gahl, W. A., Thoene, J. G. and Schneider, J. A. (2002) 'Cystinosis', *New England Journal of Medicine*, 347:111–121.

Gaikwad, N. W. *et al.* (2008) 'The molecular etiology of breast cancer: evidence from biomarkers of risk', *International Journal of Cancer*, 122:1949–1957.

Gaikwad, N. W., Yang, L., Weisenburger, D. D., *et al.* (2009) 'Urinary biomarkers suggest that estrogen-DNA adducts may play a role in the aetiology of non-Hodgkin lymphoma', *Biomarkers*, 14:502–512.

Gaikwad, N. W., Yang, L., Pruthi, S., *et al.* (2009) 'Urine biomarkers of risk in the molecular etiology of breast cancer', *Breast Cancer*, 3:1–8.

Gaikwad, N. W. *et al.* (2011) 'Imbalanced estrogen metabolism in the brain: possible relevance to the etiology of Parkinson's disease', *Biomarkers*, 16:434–444.

Galván, I., Ghanem, G. and Møller, A. P. (2012) 'Has removal of excess cysteine led to the evolution of pheomelanin?', *BioEssays*, 34:565–568.

Garnier, N. *et al.* (2014) 'The novel arsenical darinaparsin is transported by cystine importing systems', *Molecular Pharmacology*, 85:576–585.

Gautier-Veyret, E. *et al.* (2018) 'Cysteinyl-leukotriene pathway as a new therapeutic target for the treatment of atherosclerosis related to obstructive sleep apnea syndrome', *Pharmacological Research*, 134:311–319.

Di Gennaro, A. and Haeggström, J. Z. (2012) 'The leukotrienes: immune-modulating lipid mediators of disease', *Advances in Immunology*, 116:51–92.

George, A. and Neilson, E. (2015) 'Cellular and molecular biology of the kidney', in Kasper, D. et al. (eds) *Harrison's Principles of Internal Medicine*. 19th edn. New York: McGraw-Hill Education, p. 332e1-332e11.

George, B., Joy, M. S. and Aleksunes, L. M. (2018) 'Urinary protein biomarkers of kidney injury in patients receiving cisplatin chemotherapy', *Experimental Biology and Medicine*, 243:272–282.

George, S. K. *et al.* (2006) 'Improved HPLC method for the simultaneous determination of allantoin, uric acid and creatinine in cattle urine', *Journal of Chromatography B: Analytical Technologies in the Biomedical and Life Sciences*, 832:134-137.

Germack, R. *et al.* (2002) 'Effect of intermittent hypoxia on cardiovascular function, adrenoceptors and muscarinic receptors in Wistar rats', *Experimental Physiology*, 87:453–460.

Giuliano, R. A. *et al.* (1984) 'Recovery of cortical phospholipidosis and necrosis after acute gentamicin loading in rats', *Kidney International*, 26:838–847.

Giustarini, D. *et al.* (2006) 'Age-related influence on thiol, disulfide, and protein-mixed disulfide levels in human plasma', *The Journals of Gerontology Series A: Biological Sciences and Medical Sciences*, 61:1030–1038.

Godinho, A. L. A. *et al.* (2018) 'High resolution mass spectrometry-based methodologies for identification of etravirine bioactivation to reactive metabolites: in vitro and in vivo approaches', *European Journal of Pharmaceutical Sciences*, 119:70–82.

Goldstein, D. S. *et al.* (2013) 'Determinants of buildup of the toxic dopamine metabolite DOPAL in Parkinson's disease', *Journal of Neurochemistry*, 126:591–603.

Goldstein, D. S. *et al.* (2015) 'Decreased vesicular storage and aldehyde dehydrogenase activity in multiple system atrophy', *Parkinsonism & Related Disorders*, 21:567–572.

Goldstein, D. S. *et al.* (2016) 'Elevated cerebrospinal fluid ratios of cysteinyl-dopamine/3, 4-dihydroxyphenylacetic acid in parkinsonian synucleinopathies', *Parkinsonism & Related Disorder*, 31:79–86.

Goldstein, R. S. and Mayor, G. H. (1983) 'The nephrotoxicity of cisplatin', *Life Sciences*, 32:685–690.

Gonçalves-Dias, C. *et al.* (2019) 'Mercapturate pathway in the tubulocentric perspective of diabetic kidney disease', *Nephron*, 9:1-7.

Gordon, C. *et al.* (1992) 'Abnormal sulphur oxidation in systemic lupus erythematosus', *The Lancet*, 339:25–26.

Gorgulho, R. *et al.* (2018) 'Usefulness of zebrafish larvae to evaluate drug-induced functional and morphological renal tubular alterations', *Archives of Toxicology*, 92:411–423.

Grácio, P. (2017) 'Changes in N-acetyltransferase 8 in kidney tubular cell. Injury, recovery and mesenchymal stem/stromal cell treatment - Master thesis'.

Grácio, P. *et al.* (2018) 'Changes in N-acetyltransferase 8 in kidney tubular cell. Injury, recovery and mesenchymal stromal cell-based therapy', *IEEE Xplore (submitted)*.

Green, S. A. *et al.* (2004) 'Increase in urinary leukotriene LTE4 levels in acute asthma: correlation with airflow limitation', *Thorax*, 59:100–104.

Griffith, O. W. (1981) 'The role of glutathione turnover in the apparent renal secretion of cystine', *Journal of Biological Chemistry*, 256:2263–2268.

Griffith, O. W. and Meister, A. (1980) 'Excretion of cysteine and gamma-glutamylcysteine moieties in human and experimental animal gamma-glutamyl transpeptidase deficiency', *Proceedings of the National Academy of Sciences*, 77:3384–3387.

Grilo, N. M. *et al.* (2017) 'Unmasking efavirenz neurotoxicity: time matters to the underlying mechanisms', *European Journal of Pharmaceutical Sciences*, 105:47–54.

Groves, C. E. *et al.* (2003) 'Interaction of cysteine conjugates with human and rabbit organic anion transporter 1', *Journal of Pharmacology and Experimental Therapeutics*, 304:560–566.

Grunwell, J. R. *et al.* (2015) 'Comparison of glutathione, cysteine, and their redox potentials in the plasma of critically ill and healthy children', *Frontiers in Pediatrics*, 3:46.

Guan, X. *et al.* (2003) 'A simultaneous liquid chromatography/mass spectrometric assay of glutathione, cysteine, homocysteine and their disulfides in biological samples', *Journal of Pharmaceutical and Biomedical Analysis*, 31:251–261.

Guéraud, F. *et al.* (2006) 'Enzyme immunoassay for a urinary metabolite of 4-hydroxynonenal as a marker of lipid peroxidation', *Free Radical Biology and Medicine*, 40:54–62.

Guhlmann, A., Hagmann, W. and Keppler, D. (1987) 'Enterohepatic circulation of N-acetyl-leukotriene E4', *Prostaglandins*, 34:63–70.

Guo, R. *et al.* (2018) 'Cysteinyl leukotriene receptor 1 regulates glucose-stimulated insulin secretion (GSIS)', *Cellular Signalling*, 46:129–134.

Guo, Y. *et al.* (2017) 'Effect of nine diets on mRNAs of phase-II conjugation enzymes in livers of mice', *Xenobiotica*, 47:645–654.

Gupta, S. K. *et al.* (2005) 'Guidelines for the management of chronic kidney disease in HIV-infected patients: recommendations of the HIV medicine association of the infectious diseases society of america', *Clinical Infectious Diseases*, 40:1559-1585.

Gupta, S. K. *et al.* (2014) 'Fanconi syndrome accompanied by renal function decline with tenofovir disoproxil fumarate: a prospective, case-control study of predictors and resolution in HIV-infected patients', *PLoS One*, 9:e92717.

Gutiérrez, F. *et al.* (2014) 'Renal tubular transporter-mediated interactions of HIV drugs: implications for patient management', *AIDS Reviews*, 16:199–212.

Habig, W. H., Pabst, M. J. and Jakoby, W. B. (1974) 'Glutathione S transferases. The first enzymatic step in mercapturic acid formation', *Journal of Biological Chemistry*, 249:7130–7139.

Haeggström, J. Z. and Funk, C. D. (2011) 'Lipoxygenase and leukotriene pathways: biochemistry, biology, and roles in disease', *Chemical Reviews*, 111:5866–5896.

Han, D. *et al.* (1997) 'Lipoic acid increases de novo synthesis of cellular glutathione by improving cystine utilization', *Biofactors*, 6:321–338.

Han, W. K. *et al.* (2002) 'Kidney injury molecule-1 (KIM-1): a novel biomarker for human renal proximal tubule injury', *Kidney International*, 62:237–244.

Haneda, M. *et al.* (2014) 'Classification of diabetic nephropathy 2014', *Japanese Journal of Nephrology*, 56:547-552.

Hanigan, M. H. *et al.* (1994) 'Inhibition of γ-glutamyl transpeptidase activity by acivicin in vivo protects the kidney from cisplatin-induced toxicity', *Cancer Research*, 54:5925–5929.

Hanigan, M. H. (1998) 'γ-Glutamyl transpeptidase, a glutathionase: its expression and function in carcinogenesis', *Chemico-Biological Interactions*, 111:333–342.

Hanigan, M. H. *et al.* (2001) 'γ-Glutamyl transpeptidase-deficient mice are resistant to the nephrotoxic effects of cisplatin', *The American Journal of Pathology*, 159:1889–1894.

Hanigan, M. H. and Pitot, H. C. (1985) 'Gamma-glutamyl transpeptidase–its role in hepatocarcinogenesis', *Carcinogenesi*, 6:165–172.

Hannested, U. and Sörbo, B. (1979) 'Determination of 3-mercaptolactate, mercaptoacetate and N-acetylcysteine in urine by gas chromatography', *Clinica Chimica Acta*, 95:189–200.

Hardy, G. *et al.* (2001) 'Cysteinyl leukotrienes modulate angiotensin II constrictor effects on aortas from streptozotocin-induced diabetic rats', *Arteriosclerosis, Thrombosis, and Vascular Biology*, 21:1751–1758.

Hardy, G. *et al.* (2005) 'Urinary leukotriene E4 excretion is increased in type 1 diabetic patients: a quantification by liquid chromatography-tandem mass spectrometry', *Prostaglandins and Other Lipid Mediators*, 78:291–299.

Heafield, M. T. *et al.* (1990) 'Plasma cysteine and sulphate levels in patients with motor neurone, Parkinson's and Alzheimer's disease', *Neuroscience Letters,* 110:216–220.

Heald, A. E. *et al.* (1996) 'Pharmacokinetics of lamivudine in human immunodeficiency virus-infected patients with renal dysfunction', *Antimicrobial Agents and Chemotherapy*, 40:1514–1519.

Herlitz, L. C. *et al.* (2010) 'Tenofovir nephrotoxicity: acute tubular necrosis with distinctive clinical, pathological, and mitochondrial abnormalities', *Kidney International*, 78:1171–1177.

Hilmer, S. N. *et al.* (2011) 'Gentamicin pharmacokinetics in old age and frailty', *British Journal of Clinical Pharmacology*, 71:224–231.

Hinchman, C. A. *et al.* (1991) 'Intrahepatic conversion of a glutathione conjugate to its mercapturic acid. Metabolism of 1-chloro-2, 4-dinitrobenzene in isolated perfused rat and guinea pig livers.', *Journal of Biological Chemistry*, 266:22179–22185.

Hinchman, C. A. and Ballatori, N. (1990) 'Glutathione-degrading capacities of liver and kidney in different species', *Biochemical Pharmacology*, 40:1131–1135.

Hinchman, C. A. and Ballatori, N. (1994) 'Glutathione conjugation and conversion to mercapturic acids can occur as an intrahepatic process', *Journal of Toxicology and Environmental Health*, 41:387–409.

Hinchman, C. A., Rebbeor, J. F. and Ballatori, N. (1998) 'Efficient hepatic uptake and concentrative biliary excretion of a mercapturic acid', *American Journal of Physiology*, 275:G612–G619.

Hirakawa, D. A. and Baker, D. H. (1985) 'Sulfur amino acid nutrition of the growing puppy: determination of dietary requirements for methionine and cystine', *Nutrition Research*, 5:631–642.

Hochgräfe, F. *et al.* (2007) 'S-cysteinylation is a general mechanism for thiol protection of Bacillus subtilis proteins after oxidative stress', *Journal of Biological Chemistry*, 282:25981–25985.

Homsi, E., Janino, P. and De Faria, J. B. L. (2006) 'Role of caspases on cell death, inflammation, and cell cycle in glycerol-induced acute renal failure', *Kidney International*, 69:1385–1392.

Hopkins, M. H. *et al.* (2010) 'Antioxidant micronutrients and biomarkers of oxidative stress and inflammation in colorectal adenoma patients: results from a randomized, controlled clinical trial', *Cancer Epidemiology and Prevention Biomarkers*, 19:1055–9965.

Horibe, T. *et al.* (2004) 'Gentamicin binds to the lectin site of calreticulin and inhibits its chaperone activity', *Biochemical and Biophysical Research Communications*, 323:281–287.

Horsley, L. *et al.* (2013) 'A phase 1 trial of intravenous 4-(N-(S-glutathionylacetyl) amino) phenylarsenoxide (GSAO) in patients with advanced solid tumours', *Cancer Chemotherapy and Pharmacology*, 72:1343–1352.

Hosohata, K. (2016) 'Role of oxidative stress in drug-induced kidney injury', *International Journal of Molecular Sciences*, 17:E1826.

Hoste, E. A. J. *et al.* (2015) 'Epidemiology of acute kidney injury in critically ill patients: the multinational AKI-EPI study', *Intensive Care Medicine*, 41:1411–1423.

Hsu, C. *et al.* (2004) 'The incidence of end-stage renal disease is increasing faster than the prevalence of chronic renal insufficiency', *Annals of Internal Medicine*, 141:95–101.

Hsu, C. Y. *et al.* (2008) 'The risk of acute renal failure in patients with chronic kidney disease', *Kidney International*, 74:101–107.

Huber, M. *et al.* (1990) 'Metabolism of cysteinyl leukotrienes in monkey and man', *European Journal of Biochemistry*, 194:309–315.

Hughey, R. P. *et al.* (1978) 'Specificity of a particulate rat renal peptidase and its localization along with other enzymes of mercapturic acid synthesis', *Archives of Biochemistry and Biophysics*, 186:211–217.

Ichimura, T. *et al.* (1998) 'Kidney injury molecule-1 (KIM-1), a putative epithelial cell adhesion molecule containing a novel immunoglobulin domain, is up-regulated in renal cells after injury', *Journal of Biological Chemistry*, 273:4135–4142.

Ichimura, T. *et al.* (2004) 'Kidney injury molecule-1: a tissue and urinary biomarker for nephrotoxicant-induced renal injury', *American Journal of Physiology Renal Physiology*, 286:F552–F563.

Ichimura, T. *et al.* (2008) 'Kidney injury molecule–1 is a phosphatidylserine receptor that confers a phagocytic phenotype on epithelial cells', *The Journal of Clinical Investigation*, 118:1657–1668.

Imai, K., Toyo'oka, T. and Watanabe, Y. (1983) 'A novel fluorogenic reagent for thiols: ammonium 7-fluorobenzo-2-oxa-1,3-diazole-4-sulfonate', *Analytical Biochemistry*, 128:471–473.

Inker, L. A. *et al.* (2012) 'Estimating glomerular filtration rate from serum creatinine and cystatin C', *The New England Journal of Medicine*, 367:20–29.

Inoue, M., Okajima, K. and Morino, Y. (1981) 'Renal transtubular transport of mercapturic acid in vivo', *Biochimica et Biophysica Acta*, 641:122–128.

Iseki, K. *et al.* (2008) 'High prevalence of chronic kidney disease among patients with sleep related breathing disorder (SRBD)', *Hypertension Research*, 31:249–255.

Izzedine, H. *et al.* (2001) 'Pharmacokinetics of abacavir in HIV-1-infected patients with impaired renal function', *Nephron*, 89:62–67.

Jaikumkao, K. *et al.* (2016) 'Amelioration of renal inflammation, endoplasmic reticulum stress and apoptosis underlies the protective effect of low dosage of atorvastatin in gentamicin-Induced nephrotoxicity', *PloS One*, 11:e0164528.

Jakubowski, H. and Głowacki, R. (2011) 'Chemical biology of homocysteine thiolactone and related metabolites', in Makowski, G. (ed.) *Advances in Clinical Chemistry*. Elsevier, pp. 81–103.

James, M. T., Hemmelgarn, B. R. and Tonelli, M. (2010) 'Early recognition and prevention of chronic kidney disease', *The Lancet*, 375:1296–1309.

Janicka, M. *et al.* (2010) 'Isoprostanes-biomarkers of lipid peroxidation: their utility in evaluating oxidative stress and analysis', *International Journal of Molecular Sciences*, 11:4631–4659.

Jenderny, S. *et al.* (2010) 'Protective effects of a glutathione disulfide mimetic (NOV-002) against cisplatin induced kidney toxicity', *Biomedicine & Pharmacotherapy*, 64:73–76.

Jha, V. *et al.* (2013) 'Chronic kidney disease: global dimension and perspectives', *The Lancet*, 382:260–272.

Jian, W. *et al.* (2009) 'Rapid detection and characterization of in vitro and urinary N-acetyl-L-cysteine conjugates using quadrupole-linear ion trap mass spectrometry and polarity switching', *Chemical Research in Toxicology*, 22:1246–1255.

Johnson, M. A. *et al.* (1998) 'Single dose pharmacokinetics of lamivudine in subjects with impaired renal function and the effect of haemodialysis', *British Journal of Clinical Pharmacology*, 46:21–27.

Jonas, C. R. *et al.* (2000) 'Plasma antioxidant status after high-dose chemotherapy: a randomized trial of parenteral nutrition in bone marrow transplantation patients', *The American Journal of Clinical Nutrition*, 72:181–189.

Jones, D. P. *et al.* (2000) 'Redox state of glutathione in human plasma', *Free Radical Biology and Medicine*, 28:625–635.

Jones, D. P. (2006) 'Redefining oxidative stress', *Antioxidants & Redox Signaling*, 8:1865–1879.

Jones, T. W. *et al.* (1988) 'Immunohistochemical localization of glutamine transaminase K, a rat kidney cysteine conjugate beta-lyase, and the relationship to the segment specificity of cysteine conjugate nephrotoxicity.', *Molecular Pharmacology*, 34:621–627.

Jotwani, V. *et al.* (2016) 'Cumulative tenofovir disoproxil fumarate exposure is associated with biomarkers of tubular injury and fibrosis in HIV-infected men.', *Journal of acquired immune deficiency syndromes*, 73, pp. 177–181.

Juhanson, P. *et al.* (2008) 'N-acetyltransferase 8, a positional candidate for blood pressure and renal regulation: resequencing, association and in silico study', *BMC Medical Genetics*, 9:25.

Jung, H. S. *et al.* (2008) 'Loss of autophagy diminishes pancreatic β cell mass and function with resultant hyperglycemia', *Cell Metabolism*, 8:318–324.

Kacew, S. and Bergeron, M. G. (1990) 'Pathogenic factors in aminoglycoside-induced nephrotoxicity', *Toxicology Letters*, 51:241–259.

Kanaoka, Y. and Boyce, J. A. (2014) 'Cysteinyl leukotrienes and their receptors; emerging concepts', *Allergy Asthma and Immunology Research*, 6:288–295.

Kanaoka, Y., Maekawa, A. and Austen, K. F. (2013) 'Identification of GPR99 protein as a potential third cysteinyl leukotriene receptor with a preference for leukotriene E4 ligand', *Journal of Biological Chemistry*, 288:10967–10972.

Kanbay, A. *et al.* (2012) 'Obstructive sleep apnea syndrome is related to the progression of chronic kidney disease', *International Urology and Nephrology*, 44:535–539.

Karahan, I. *et al.* (2005) 'Protective effect of lycopene on gentamicin-induced oxidative stress and nephrotoxicity in rats', *Toxicology*, 215:198–204.

Karasawa, T. and Steyger, P. S. (2015) 'An integrated view of cisplatin-induced nephrotoxicity and ototoxicity', *Toxicology Letters*, 237:219–227.

Kashani, K. *et al.* (2017) 'No increase in the incidence of acute kidney injury in a population-based annual temporal trends epidemiology study', *Kidney International*, 92:721–728.

Kassebaum, N. J. *et al.* (2016) 'Global, regional, and national disability-adjusted life-years (DALYs) for 315 diseases and injuries and healthy life expectancy (HALE), 1990–2015: a systematic analysis for the Global Burden of Disease Study 2015', *The Lancet*, 388:1603–1658.

KDIGO AKI Work Group (2012) 'KDIGO clinical practice guideline for acute kidney injury', *Kidney International Supplement*, 2:1–138.

KDIGO CKD Work Group (2013) 'KDIGO 2012 clinical practice guideline for the evaluation and management of chronic kidney disease', *Kidney International Supplements*, 3:1–150.

Kearney, B. P. *et al.* (2006) 'Pharmacokinetics and dosing recommendations of tenofovir disoproxil fumarate in hepatic or renal impairment', *Clinical Pharmacokinetics*, 45:1115–1124.

Keppler, D. (2005) 'Uptake and efflux transporters for conjugates in human hepatocytes', *Methods in Enzymology*, 400:531–542.

Kitada, M., Ogura, Y. and Koya, D. (2016) 'Rodent models of diabetic nephropathy: their utility and limitations', *International Journal of Nephrology and Renovascular Disease*, 9:279-290.

Klein, J. *et al.* (2016) 'The role of urinary peptidomics in kidney disease research', *Kidney International*, 89:539–545.

Knight, E. L. *et al.* (2004) 'Factors influencing serum cystatin C levels other than renal function and the impact on renal function measurement', *Kidney International,* 65:1416-1421.

Ko, M. H. and Puglielli, L. (2009) 'Two endoplasmic reticulum (ER)/ER golgi intermediate compartment-based lysine acetyltransferases post-translationally regulate BACE1 levels', *Journal of Biological Chemistry*, 284:2482–2492.

Kohler, J. J. *et al.* (2011) 'Tenofovir renal proximal tubular toxicity is regulated by OAT1 and MRP4 transporters', *Laboratory Investigation,* 91:852–858.

Kong, D. *et al.* (2013) 'Erythropoietin protects against cisplatin-induced nephrotoxicity by attenuating endoplasmic reticulum stress-induced apoptosis.', *Journal of Nephrology*, 26:219–227.

Kotani, K., Kimura, S. and Gugliucci, A. (2011) 'Paraoxonase-1 and ischemia-modified albumin in patients with end-stage renal disease', *Journal of Physiology and Biochemistry*, 67:437–441.

Köttgen, A. *et al.* (2010) 'Multiple new loci associated with kidney function and chronic kidney disease: the CKDGen consortium', *Nature Genetics*, 42:376–384.

Kuiper, H. C. *et al.* (2008) 'Mercapturic acid conjugates of 4-hydroxy-2-nonenal and 4-oxo-2-nonenal metabolites are in vivo markers of oxidative stress', *Journal of Biological Chemistry*, 283:17131–17138.

Kuiper, H. C. *et al.* (2010) 'Quantitation of mercapturic acid conjugates of 4-hydroxy-2-nonenal and 4-oxo-2-nonenal metabolites in a smoking cessation study', *Free Radical Biology and Medicine*, 48:65–72.

Kumar, C. *et al.* (2011) 'Glutathione revisited: a vital function in iron metabolism and ancillary role in thiol-redox control', *The EMBO Journal*, 30:2044–2056.

Kuśmierek, K. *et al.* (2009) 'Determination of endogenous thiols and thiol drugs in urine by HPLC with ultraviolet detection', *Journal of Chromatography B: Analytical Technologies in the Biomedical and Life Sciences*, 877:3300–3308.

Kuśmierek, K. and Bald, E. (2008) 'Determination of N-acetylcysteine and thioglycolic acid in human urine', *Chromatographia*, 67:23–29.

Lash, H. and Anders, W. (1989) 'Uptake of nephrotoxic S-conjugates by isolated rat renal proximal tubular cells', The *Journal of Pharmacology and Experimental Therapeutics*, 248:531–537.

Lash, L. H. (2007) 'Glutathione-dependent bioactivation', *Current Protocols in Toxicology*, 6:1–16.

Laurent, G., Kishore, B. K. and Tulkens, P. M. (1990) 'Aminoglycoside-induced renal phospholipidosis and nephrotoxicity', *Biochemical Pharmacology*, 40:2383–2392.

Lavie, L. (2015) 'Oxidative stress in obstructive sleep apnea and intermittent hypoxia–revisited–the bad ugly and good: implications to the heart and brain', *Sleep Medicine Reviews*, 20:27–45.

Leng, W. *et al.* (1988) 'Role of leukotrienes in vascular changes in the rat mesentery and skin in anaphylaxis.', *The Journal of Immunology*, 140:2361–2368.

Leung, K. C. W., Tonelli, M. and James, M. T. (2013) 'Chronic kidney disease following acute kidney injury — risk and outcomes', *Nature Reviews Nephrology*, 9:77-85.

Levey, A. S. *et al.* (2007) 'Expressing the modification of diet in renal disease study equation for estimating glomerular filtration rate with standardized serum creatinine values', *Clinical Chemistry*, 53:766–772.

Levey, A. S. *et al.* (2009) 'A new equation to estimate glomerular filtration rate', *Annals of Internal Medicine*, 150:604–612.

Levin, A. *et al.* (2017) 'Global kidney health 2017 and beyond: a roadmap for closing gaps in care, research, and policy', *The Lancet,* 390:1888-1917.

Levonen, A.-L. *et al.* (2014) 'Redox regulation of antioxidants, autophagy, and the response to stress:

implications for electrophile therapeutics', *Free Radical Biology and Medicine*, 71:196–207.

Lewis, R. A. and Austen, K. F. (1984) 'The biologically active leukotrienes. Biosynthesis, metabolism, receptors, functions, and pharmacology', *Journal of Clinical Investigation*, 73:889–897.

Lewy, P. R. *et al.* (1973) 'Renal energy metabolism and sodium reabsorption', *Annual Review of Medicin,* 24:365–384.

Li, D. *et al.* (2016) 'Metabolism of acrylamide: interindividual and interspecies differences as well as the application as biomarkers', *Current Drug Metabolism*, 17:317–326.

Li, Y. and Wingert, R. A. (2013) 'Regenerative medicine for the kidney: stem cell prospects & challenges', *Clinical and Translational Medicine*, 2:11.

Lindell, Å., Denneberg, T. and Jeppsson, J.-O. (1995) 'Urinary excretion of free cystine and the tiopronin-cysteine-mixed disulfide during long-term tiopronin treatment of cystinuria', *Nephron*, 71:328–342.

Liu, M. *et al.* (2018) 'Specific downregulation of cystathionine β-synthase expression in the kidney during obesity', *Physiological Reports*, 6:e13630.

Liu, R.-M. and Pravia, K. A. G. (2010) 'Oxidative stress and glutathione in TGF-β-mediated fibrogenesis', *Free Radical Biology and Medicine*, 48:1–15.

Lock, E. A. *et al.* (2006) 'Changes in gene expression in human renal proximal tubule cells exposed to low concentrations of S-(1, 2-dichlorovinyl)-l-cysteine, a metabolite of trichloroethylene', *Toxicology and Applied Pharmacology*, 216:319–330.

Loghman-Adham, D. M. *et al.* (2012) 'Detection and management of nephrotoxicity during drug development', *Expert Opinion on Drug Safety*, 11:581–596.

Lopez-Giacoman, S. and Madero, M. (2015) 'Biomarkers in chronic kidney disease, from kidney function to kidney damage', *World Journal of Nephrology*, 4:57–73.

López-Novoa, J. M. *et al.* (2011) 'New insights into the mechanism of aminoglycoside nephrotoxicity: an integrative point of view', *Kidney International*, 79:33–45.

Lu, S. C. (1999) 'Regulation of hepatic glutathione synthesis: current concepts and controversies', *The FASEB Journal*, 13:1169–1183.

Lu, S. C. (2009) 'Regulation of glutathione synthesis', *Molecular Aspects of Medicine*, 30:42–59.

Lucas, G. M. *et al.* (2014) 'Clinical practice guideline for the management of chronic kidney disease in patients infected with HIV: 2014 update by the HIV medicine association of the infectious diseases society of America', *Clinical Infectious Diseases*, 59:e96–e138.

Luyckx, V. A., Tonelli, M. and Stanifer, J. W. (2018) 'The global burden of kidney disease and the sustainable development goals', *Bulletin of the World Health Organization*, 96:414-422D.

Van Maanen, M. J. and Beijnen, J. H. (1999) 'Liquid chromatographic-mass spectrometric determination of the novel, recently identified thioTEPA metabolite, thioTEPA-mercapturate, in urine', *Journal of Chromatography B: Biomedical Sciences and Applications*, 732:73–79.

Macdonald, J. *et al.* (2006) 'GFR estimation using cystatin C is not independent of body composition', *American Journal of Kidney Diseases*, 48:712-719.

MacFarlane, M. *et al.* (1989) 'Cysteine conjugate β-lyase of rat kidney cytosol: characterization, immunocytochemical localization, and correlation with hexachlorobutadiene nephrotoxicity', *Toxicology and Applied Pharmacology*, 98:185–197.

Madias, N. E. and Harrington, J. T. (1978) 'Platinum nephrotoxicity', *The American Journal of Medicine*, 65:307–314.

Magnay, J. L. *et al.* (2001) 'Production of cysteinyl-dopamine during intravenous dopamine therapy', *Kidney International*, 59:1891–1898.

Magnusson, I. *et al.* (1989) 'N-acetyl-L-tyrosine and N-acetyl-L-cysteine as tyrosine and cysteine precursors during intravenous infusion in humans', *Metabolism*, 38:957–961.

Mähler, M. *et al.* (2014) 'FELASA recommendations for the health monitoring of mouse, rat, hamster, guinea pig and rabbit colonies in breeding and experimental units', *Laboratory Animals*, 48:178–192.

Mak, A. B. *et al.* (2014) 'Post-translational regulation of CD133 by ATase1/ATase2 mediated lysine acetylation', *Journal of Molecular Biology*, 426:2175–2182.

Makris, K. and Spanou, L. (2016) 'Acute kidney injury: diagnostic approaches and controversies', *The Clinical Biochemist Reviews*, 37:153–175.

Mally, A. *et al.* (2007) 'Are 4-hydroxy-2 (E)-nonenal derived mercapturic acids and 1H NMR metabonomics potential biomarkers of chemically induced oxidative stress in the kidney?', *Toxicology*, 230:244–255.

Mandel, E. E. *et al.* (1953) 'Renal excretion of creatinine and inulin in man', *The Journal of Laboratory and Clinical Medicine*, 42:621–637.

Markowitz, G. S. and Perazella, M. A. (2005) 'Drug-induced renal failure: a focus on tubulointerstitial disease', *Clinica Chimica Acta*, 351:31–47.

Mårtensson, J. and Hermansson, G. (1984) 'Sulfur amino acid metabolism in juvenile-onset nonketotic and ketotic diabetic patients', *Metabolism*, 33:425–428.

Mather, A. and Pollock, C. (2011) 'Glucose handling by the kidney', *Kidney International*, 79:S1–S6.

Mathias, P. I. and Bhymer, C. (2016) 'Mercapturic acids: recent advances in their determination by liquid chromatography/mass spectrometry and their use in toxicant metabolism studies and in occupational and environmental exposure studies', *Biomarkers*, 21:293–315.

May, A. M. and Mehra, R. (2014) 'Obstructive sleep apnea: role of intermittent hypoxia and inflammation', *Seminars in Respiratory and Critical Care Medicine*, 35:531–544.

McDuffie, J. E. (2018) 'Brief overview: assessment of compound-induced acute kidney injury using animal models, biomarkers, and in vitro platforms', *Toxicology Pathology*, 46:978–990.

McMenamin, M. E., Himmelfarb, J. and Nolin, T. D. (2009) 'Simultaneous analysis of multiple aminothiols in human plasma by high performance liquid chromatography with fluorescence detection', *Journal of Chromatography B*, 877:3274–3281.

McWilliam, S. J. *et al.* (2018) 'Urinary biomarkers of aminoglycoside-induced nephrotoxicity in cystic fibrosis: kidney injury molecule-1 and neutrophil gelatinase-associated lipocalin', *Scientific Reports*, 8:5094.

Melnikov, V. Y. *et al.* (2001) 'Impaired IL-18 processing protects caspase-1–deficient mice from ischemic acute renal failure', *The Journal of Clinical Investigation*, 107:1145–1152.

De Miguel, C. *et al.* (2015) 'Inflammation and hypertension: new understandings and potential therapeutic targets', *Current Hypertension Reports*, 17:507.

Miller, R. P. *et al.* (2010) 'Mechanisms of cisplatin nephrotoxicity', *Toxins*, 2:2490–2518.

Mingeot-Leclercq, M.-P. and Tulkens, P. M. (1999) 'Aminoglycosides: nephrotoxicity', *Antimicrobial Agents and Chemotherapy*, 43:1003–1012.

Mishra, J. *et al.* (2003) 'Identification of neutrophil gelatinase-associated lipocalin as a novel early urinary biomarker for ischemic renal injury', *Journal of the American Society of Nephrology*, 14:2534–2543.

Mishra, J., Mori, K., Ma, Q., Kelly, C., Yang, J., *et al.* (2004) 'Amelioration of ischemic acute renal injury by neutrophil gelatinase-associated lipocalin', *Journal of the American Society of Nephrology*, 15:3073–3082.

Mishra, J., Mori, K., Ma, Q., Kelly, C., Barasch, J., *et al.* (2004) 'Neutrophil gelatinase-associated lipocalin: a novel early urinary biomarker for cisplatin nephrotoxicity', *American Journal of Nephrology*, 24:307–315.

Mishra, J. *et al.* (2005) 'Neutrophil gelatinase-associated lipocalin (NGAL) as a biomarker for acute renal injury after cardiac surgery', *The Lancet*, 365:1231–1238.

Mistry, P., Lee, C. and McBrien, D. C. H. (1989) 'Intracellular metabolites of cisplatin in the rat kidney', *Cancer Chemotherapy and Pharmacology*, 24:73–79.

Mohorko, N. *et al.* (2015) 'Elevated serum levels of cysteine and tyrosine: early biomarkers in asymptomatic adults at increased risk of developing metabolic syndrome', *BioMed Research International*, 2015:418681.

Möller-Hartmann, W. and Siegers, C. P. (1991) 'Nephrotoxicity of paracetamol in the rat - mechanistic and therapeutic aspects', *Journal of Applied Toxicology*, 11:141–146.

Morello, J. *et al.* (2018) 'Zebrafish larvae are a suitable model to investigate the metabolic phenotype of drug-induced renal tubular injury', *Frontiers in Pharmacology*, 9:1193.

Moreno, M.-L. *et al.* (2014) 'Disulfide stress: a novel type of oxidative stress in acute pancreatitis', *Free Radical Biology and Medicine*, 70:265–277.

Mori, K. *et al.* (2005) 'Endocytic delivery of lipocalin-siderophore-iron complex rescues the kidney from ischemia-reperfusion injury', *The Journal of Clinical Investigation*, 115:610–621.

Mothe-Satney, I. *et al.* (2012) 'Adipocytes secrete leukotrienes: contribution to obesity-associated inflammation and insulin resistance in mice', *Diabetes*, 61:2311–2319.

Munday, R. (1989) 'Toxicity of thiols and disulphides: involvement of free-radical species', *Free Radical*

Biology and Medicine, 7:659–673.

Nagamori, S. *et al.* (2016) 'Novel cystine transporter in renal proximal tubule identified as a missing partner of cystinuria-related plasma membrane protein rBAT/SLC3A1', *Proceedings of the National Academy of Sciences of the United States of America*, 113:775–780.

Nagumo, K. *et al.* (2014) 'Cys34-cysteinylated human serum albumin is a sensitive plasma marker in oxidative stress-related chronic diseases', *PLoS One*, 9:e85216.

El Nahas, A. M. and Bello, A. K. (2005) 'Chronic kidney disease: the global challenge', *The Lancet*, 365:331–340.

Nelson, M. *et al.* (2008) 'Fanconi syndrome and lactic acidosis associated with stavudine and lamivudine therapy', *AIDS*, 22:1374–1376.

Neuhäuser, M. *et al.* (1986) 'Utilization of methionine and N-acetyl-L-cysteine during long-term parenteral nutrition in the growing rat', *Metabolism*, 35:869–873.

Nicholl, D. D. M. *et al.* (2012) 'Declining kidney function increases the prevalence of sleep apnea and nocturnal hypoxia', *Chest*, 141:1422–1430.

Nicholson, G. *et al.* (2011) 'A genome-wide metabolic QTL analysis in Europeans implicates two loci shaped by recent positive selection', *PLoS Genetics*, 7:e1002270.

Nielsen, B. S. *et al.* (1996) 'Induction of NGAL synthesis in epithelial cells of human colorectal neoplasia and inflammatory bowel diseases', *Gut*, 38:414–420.

Nishino, T. *et al.* (2010) 'Genetic background strongly influences the severity of glomerulosclerosis in mice', *Journal of Veterinary Medical Science*, 72:1313–1318.

Nogueira, A., Pires, M. J. and Oliveira, P. A. (2017) 'Pathophysiological mechanisms of renal fibrosis: a review of animal models and therapeutic strategies', *In vivo*, 31:1–22.

Nolin, T. D., McMenamin, M. E. and Himmelfarb, J. (2007) 'Simultaneous determination of total homocysteine, cysteine, cysteinylglycine, and glutathione in human plasma by high-performance liquid chromatography: application to studies of oxidative stress', *Journal of Chromatography B: Analytical Technologies in the Biomedical and Life Sciences*, 852:554–561.

Nonclercq, D. *et al.* (1992) 'Tubular injury and regeneration in the rat kidney following acute exposure to gentamicin: a time-course study', *Renal Failure*, 14:507–521.

Ntimbane, T. *et al.* (2008) 'Oxidative stress and cystic fibrosis-related diabetes: a pilot study in children', *Journal of Cystic Fibrosis*, 7:373–384.

Nunes, S. and Serpa, J. (2018) 'Glutathione in ovarian cancer: a double-edged sword', *International Journal of Molecular Sciences*, 19:E1882.

O'donnell, C. P. *et al.* (1999) 'Leptin prevents respiratory depression in obesity', *American Journal of Respiratory and Critical Care Medicine*, 159:1477–1484.

Oliveira, J. F. P. *et al.* (2009) 'Prevalence and risk factors for aminoglycoside nephrotoxicity in intensive care units', *Antimicrobial Agents and Chemotherapy*, 53:2887–2891.

Oliveira, P. V. S. and Laurindo, F. R. M. (2018) 'Implications of plasma thiol redox in disease', *Clinical Science*, 132:1257–1280.

Omata, M. *et al.* (2016) 'Hepatocyte nuclear factor-1β induces redifferentiation of dedifferentiated tubular epithelial cells', *PLoS One*, 11,:e0154912.

Ono, E. *et al.* (2011) 'Increase in salivary cysteinyl-leukotriene concentration in patients with aspirin-intolerant asthma', *Allergology International*, 60:37–43.

Ortiz, A. *et al.* (2014) 'Epidemiology, contributors to, and clinical trials of mortality risk in chronic kidney failure', *The Lancet*, 383:1831–1843.

Ozaki, K. *et al.* (1998) 'Isolation and mapping of a novel human kidney- and liver-specific gene homologous to the bacterial acetyltransferases', *Journal of Human Genetics*, 43:255–258.

Ozbek, E. (2012) 'Induction of oxidative stress in kidney', *International Journal of Nephrology*, 2012:465897.

Özkan, Y., Özkan, E. and Şimşek, B. (2002) 'Plasma total homocysteine and cysteine levels as cardiovascular risk factors in coronary heart disease', *International Journal of Cardiology*, 82: 269–277.

Ozkok, A. and Edelstein, C. L. (2014) 'Pathophysiology of cisplatin-induced acute kidney injury', *BioMed Research International*, 2014:967826.

Ozkok, S. and Ozkok, A. (2017) 'Contrast-induced acute kidney injury: a review of practical points', *World Journal of Nephrology*, 6:86–99.

Pabla, N. and Dong, Z. (2008) 'Cisplatin nephrotoxicity: mechanisms and renoprotective strategies', *Kidney International,* 73:994–1007.

Pajares, M. A. and Perez-Sala, D. (2017) 'Mammalian sulfur amino acid metabolism: a nexus between redox regulation, nutrition, epigenetics, and detoxification', *Antioxidants & Redox Signaling*, 29:408-452.

Palau, L. *et al.* (2018) 'HIV-associated nephropathy: links, risks and management', *HIV AIDS,* 10:73–81.

Paolicchi, A. *et al.* (2003) 'γ-Glutamyl transpeptidase catalyses the extracellular detoxification of cisplatin in a human cell line derived from the proximal convoluted tubule of the kidney', *European Journal of Cancer*, 39:996–1003.

Parakh, S. and Atkin, J. D. (2015) 'Novel roles for protein disulphide isomerase in disease states: a double edged sword?', *Frontiers in Cell and Developmental Biology*, 3:30.

Parati, G. *et al.* (2014) 'Obstructive sleep apnea syndrome as a cause of resistant hypertension', *Hypertension Research*, 37:601–613.

Parlakpinar, H. *et al.* (2005) 'Protective role of caffeic acid phenethyl ester (cape) on gentamicin-induced acute renal toxicity in rats', *Toxicology*, 207:169–177.

Pastore, A. *et al.* (2015) 'Homocysteine, cysteine, folate and vitamin B12 status in type 2 diabetic patients with chronic kidney disease', *Journal of Nephrology*, 28:571–576.

Patel, R. S. *et al.* (2016) 'Novel biomarker of oxidative stress is associated with risk of death in patients with coronary artery disease', *Circulation*, 133:361–369.

Pattyn, V. M. *et al.* (1988) 'Effect of hyperfiltration, proteinuria and diabetes mellitus on the uptake kinetics of gentamicin in the kidney cortex of rats.', *Journal of Pharmacology and Experimental Therapeutics*, 244:694–698.

Pedraza-Chaverrí, J. *et al.* (2000) 'Garlic ameliorates gentamicin nephrotoxicity: relation to antioxidant enzymes', *Free Radical Biology and Medicine*, 29:602–611.

Peiro, G. *et al.* (2005) 'Dihydroxynonene mercapturic acid, a urinary metabolite of 4-hydroxynonenal, as a biomarker of lipid peroxidation', *Biofactors*, 24:89–96.

Pelclova, D. *et al.* (2012) 'Leukotrienes B4, C4, D4 and E4 in the exhaled breath condensate (EBC), blood and urine in patients with pneumoconiosis', *Industrial Health*, 50:299–306.

Peng, H. *et al.* (2012) 'Thiol reactive probes and chemosensors', *Sensors,* 12:15907–15946.

Peng, Y. and Puglielli, L. (2016) 'Nϵ-lysine acetylation in the lumen of the endoplasmic reticulum: a way to regulate autophagy and maintain protein homeostasis in the secretory pathway', *Autophagy*, 12:1051–1052.

Perazella, M. A. (2005) 'Drug-induced nephropathy: an update', *Expert Opinion on Drug Safety*, 4:689–706.

Perazella, M. A. (2009) 'Renal vulnerability to drug toxicity', *Clinical Journal of the American Society of Nephrology*, 4:1275–1283.

Perazella, M. A. and Luciano, R. L. (2015) 'Review of select causes of drug-induced AKI', *Expert Review of Clinical Pharmacology*, 8:367–371.

Pereira, S. A. *et al.* (2012) 'Insights into the role of bioactivation mechanisms in the toxic events elicited by non-nucleoside reverse transcriptase inhibitors', in Fishbein, J. (ed.) *Advances in Molecular Toxicology*. Elsevier, pp. 1–39.

Perkins, B. A. *et al.* (2010) 'In patients with type 1 diabetes and new-onset microalbuminuria the development of advanced chronic kidney disease may not require progression to proteinuria', *Kidney International*, 77:57-64.

Perrone, R. D., Madias, N. E. and Levey, A. S. (1992) 'Serum creatinine as an index of renal function: new insights into old concepts', *Clinical Chemistry*, 38:1933-1953.

Petric, R. and Ford-Hutchinson, A. W. (1994) 'Elevated cysteinyl leukotriene excretion in experimental glomerulonephritis', *Kidney International*, 46,1322–1329.

Petric, R., Nicholson, D. W. and Ford-Hutchinson, A. W. (1995) 'Renal leukotriene C4 synthase: characterization, partial purification and alterations in experimental glomerulonephritis', *Biochimica et Biophysica Acta*, 1254:207–215.

Peyrou, M., Hanna, P. E. and Cribb, A. E. (2007) 'Cisplatin, gentamicin, and p-aminophenol induce markers of endoplasmic reticulum stress in the rat kidneys', *Toxicological Sciences*, 99:346–353.

Pitts, O. M. (1995) 'Con A cytotoxicity: a model for the study of key signaling steps leading to lymphocyte apoptosis in AIDS?', *Medical Hypotheses*, 45:311-315.

Pluym, N. *et al.* (2015) 'Analysis of 18 urinary mercapturic acids by two high-throughput multiplex-LC-MS/MS methods', *Analytical and Bioanalytical Chemistry*, 407:5463–5476.

Pombrio, J. M. *et al.* (2001) 'Mercapturic acids (N-acetylcysteine S-conjugates) as endogenous substrates for the renal organic anion transporter-1', *Molecular Pharmacology*, 60:1091–1099.

Poole, L. B. (2015) 'The basics of thiols and cysteines in redox biology and chemistry', *Free Radical Biology and Medicine*, 80:148–157.

Priuska, E. M. and Schacht, J. (1995) 'Formation of free radicals by gentamicin and iron and evidence for an iron/gentamicin complex', *Biochemical Pharmacology*, 50:1749–1752.

de Prost, N. *et al.* (2011) 'Changes in cysteinyl leukotrienes during and after cardiac surgery with cardiopulmonary bypass in patients with and without chronic obstructive pulmonary disease', *The Journal of Thoracic and Cardiovascular Surgery*, 141:1496–1502.

Qasem, H., Al-Ayadhi, L. and El-Ansary, A. (2016) 'Cysteinyl leukotriene correlated with 8-isoprostane levels as predictive biomarkers for sensory dysfunction in autism', *Lipids in Health and Disease*, 15:130.

Quiros, Y. *et al.* (2010) 'An integrative overview on the mechanisms underlying the renal tubular cytotoxicity of gentamicin', *Toxicological Sciences*, 119:245–256.

Rafnsson, A. and Bäck, M. (2013) 'Urinary leukotriene E4 is associated with renal function but not with endothelial function in type 2 diabetes', *Disease Markers*, 35:475–480.

Rahn, K. H., Heidenreich, S. and Brückner, D. (1999) 'How to assess glomerular function and damage in humans', *Journal of Hypertension*, 17:309–317.

Rai, P. *et al.* (2013) 'mTOR plays a critical role in p53-induced oxidative kidney cell injury in HIVAN', *American Journal of Physiology Renal Physiology*, 305:F343–F354.

Rajan, P. and Greenberg, H. (2015) 'Obstructive sleep apnea as a risk factor for type 2 diabetes mellitus', *Nature and Science of Sleep*, 7:113–125.

Ramsay, E. E. and Dilda, P. J. (2014) 'Glutathione S-conjugates as prodrugs to target drug-resistant tumors', *Frontiers in Pharmacology*, 5:181.

Randjelovic, P. *et al.* (2012) 'Protective effect of selenium on gentamicin-induced oxidative stress and nephrotoxicity in rats', *Drug and Chemical Toxicology*, 35:141–148.

Randjelovic, P. *et al.* (2017) 'Gentamicin nephrotoxicity in animals: current knowledge and future perspectives', *EXCLI Journal*, 16:388–399.

Rathbun, W. B. and Murray, D. L. (1991) 'Age-related cysteine uptake as rate-limiting in glutathione synthesis and glutathione half-life in the cultured human lens', *Experimental Eye Research*, 53:205–212.

Regazzoni, L. *et al.* (2013) 'Human serum albumin cysteinylation is increased in end stage renal disease patients and reduced by hemodialysis: mass spectrometry studies', *Free Radical Research*, 47:172–180.

Reilly, R., Bulger, R. and Kriz, W. (2007) 'Structural-functional relationships in the kidney', in Schrier, R. (ed.) *Diseases of the Kidney and Urinary Tract*. 8th edn. Philadelphia: Lippincott Williams & Wilkins, pp. 2–53.

Reyskens, K. M. S. E. and Essop, M. F. (2014) 'HIV protease inhibitors and onset of cardiovascular diseases: a central role for oxidative stress and dysregulation of the ubiquitin-proteasome system', *Biochimica et Biophysica Acta - Molecular Basis of Disease*, 1842:256–268.

Rodrigues, S. D. *et al.* (2012) 'Plasma cysteine/cystine reduction potential correlates with plasma creatinine levels in chronic kidney disease', *Blood Purification*, 34:231–237.

Rosenthal, A. and Pace-Asciak, C. R. (1983) 'Potent vasoconstriction of the isolated perfused rat kidney by leukotrienes C4 and D4', *Canadian Journal of Physiology and Pharmacology*, 61:325–328.

Rossi, R. *et al.* (2009) 'Cysteinylation and homocysteinylation of plasma protein thiols during ageing of healthy human beings', *Journal of Cellular and Molecular Medicine*, 13:3131-3140.

Rubinstein, M. and Dvash, E. (2018) 'Leukotrienes and kidney diseases', *Current Opinion in Nephrology and Hypertension*, 27:42–48.

Rysz, J. *et al.* (2017) 'Novel biomarkers in the diagnosis of chronic kidney disease and the prediction of its outcome', *International Journal of Molecular Sciences*, 18:1702.

Sacramento, J. F. *et al.* (2016) 'Insulin resistance is associated with tissue-specific regulation of HIF-1α and

HIF-2α during mild chronic intermittent hypoxia', *Respiratory Physiology & Neurobiology*, 228:30–38.

Salauze, L. *et al.* (2005) 'Circulating antibodies to cysteinyl catecholamines in amyotrophic lateral sclerosis and Parkinson's disease patients', *Amyotrophic Lateral Sclerosis and Other Motor Neuron Disorders*, 6:226–233.

Samani, N. J. (2003) 'Genome scans for hypertension and blood pressure regulation', *American Journal of Hypertension*, 16:167-171.

Samuelsson, B. *et al.* (1987) 'Leukotrienes and lipoxins: structures, biosynthesis, and biological effects', *Science*, 237:1171–1176.

Sánchez-González, P. D. *et al.* (2011) 'An integrative view of the pathophysiological events leading to cisplatin nephrotoxicity', *Critical Reviews in Toxicology*, 41:803–821.

Sancho-Martínez, S. M. *et al.* (2012) 'Subcellular targets of cisplatin cytotoxicity: an integrated view', *Pharmacology & Therapeutics*, 136:35–55.

Sancho-Martínez, S. M. *et al.* (2018) 'N-acetylcysteine transforms necrosis into apoptosis and affords tailored protection from cisplatin cytotoxicity', *Toxicology and Applied Pharmacology*, 349:83–93.

Sande, M. A. (1985) 'Antimicrobial agents. The aminoglycosides', in Goodman AG, Gilman A, R. and F, T. and M. (eds) *The pharmacological basis of therapeutics*. New York: Macmillian, pp. 1150–1169.

Sansanwal, P. *et al.* (2010) 'Mitochondrial autophagy promotes cellular injury in nephropathic cystinosis', *Journal of the American Society of Nephrology*, 21,:272–283.

Santangelo, F. *et al.* (2004) 'Restoring glutathione as therapeutic strategy in chronic kidney disease', *Nephrology Dialysis Transplantation*, 19:1951–1955.

Sasaki, M. *et al.* (2017) 'Dual regulation of gluconeogenesis by insulin and glucose in the proximal tubules of the kidney', *Diabetes*, 66,:2339–2350.

Sassen, M. C. *et al.* (2006) 'Dysregulation of renal sodium transporters in gentamicin-treated rats', *Kidney International*, 70:1026–1037.

Sato, S. *et al.* (2003) 'Rectal malignant melanoma diagnosed by N-isopropyl-p-123I-iodoamphetamine single photon emission computed tomography and 5-S-cysteinyl dopa: report of a case', *Surgery Today*, 33:454–458.

Schedl, A. (2007) 'Renal abnormalities and their developmental origin', *Nature Reviews Genetics*, 8:791.

Scherzer, R. *et al.* (2012) 'Association of tenofovir exposure with kidney disease risk in HIV infection', *AIDS*, 26:867–875.

Schettgen, T., Musiol, A. and Kraus, T. (2008) 'Simultaneous determination of mercapturic acids derived from ethylene oxide (HEMA), propylene oxide (2-HPMA), acrolein (3-HPMA), acrylamide (AAMA) and N, N-dimethylformamide (AMCC) in human urine using liquid chromatography/tandem mass spectrometry', *Rapid Communications in Mass Spectrometry*, 22:2629–2638.

Schetz, M. *et al.* (2005) 'Drug-induced acute kidney injury', *Current Opinion in Critical Care*, 11:555–565.

Scheuch, E. *et al.* (2015) 'Quantitative LC–MS/MS determination of flupirtine, its N-acetylated and two mercapturic acid derivatives in man', *Journal of Pharmaceutical and Biomedical Analysis*, 102:377–385.

Schmitz, C. *et al.* (2002) 'Megalin deficiency offers protection from renal aminoglycoside accumulation', *Journal of Biological Chemistry*, 277:618–622.

Schwartz, A. R. *et al.* (2008) 'Obesity and obstructive sleep apnea: pathogenic mechanisms and therapeutic approaches', *Proceedings of the American Thoracic Society*, 5:185–192.

Sequist, L. V *et al.* (2009) 'Phase 1-2a multicenter dose-ranging study of canfosfamide in combination with carboplatin and paclitaxel as first-line therapy for patients with advanced non-small cell lung cancer', *Journal of Thoracic Oncology*, 4:1389–1396.

Shang, Y. *et al.* (2016) 'Downregulation of glutathione biosynthesis contributes to oxidative stress and liver dysfunction in acute kidney injury', *Oxidative Medicine and Cellular Longevity*, 2016:9707292.

Shastri, S. *et al.* (2001) 'Cysteinyl leukotrienes mediate enhanced vasoconstriction to angiotensin II but not endothelin-1 in SHR', *American Journal of Physiology Heart and Circulatory Physiology*, 281:H342–H349.

Shetty, S. and Parthasarathy, S. (2015) 'Obesity hypoventilation syndrome', *Current Pulmonology Reports*, 4:42–55.

Shih, V. E. and Schulman, J. D. (1969) 'N-acetylcysteine-cysteine disulfide excretion in the urine following N-acetylcysteine administration', *The Journal of Pediatrics*, 74:129–131.

Silan, C. *et al.* (2007) 'Gentamicin-induced nephrotoxicity in rats ameliorated and healing effects of resveratrol', *Biological and Pharmaceutical Bulletin*, 30:79–83.

Silverblatt, F. (1982) 'Pathogenesis of nephrotoxicity of cephalosporins and aminoglycosides: a review of current concepts', *Reviews of Infectious Diseases*, 4:S360–S365.

Silverblatt, F. J. and Kuehn, C. (1979) 'Autoradiography of gentamicin uptake by the rat proximal tubule cell', *Kidney International*, 15:335–345.

Simmons, C. F., Bogusky, R. T. and Humes, H. D. (1980) 'Inhibitory effects of gentamicin on renal mitochondrial oxidative phosphorylation', *Journal of Pharmacology and Experimental Therapeutics*, 214:709–715.

Small, D. M. *et al.* (2018) 'N-acetyl-cysteine increases cellular dysfunction in progressive chronic kidney damage after acute kidney injury by dampening endogenous antioxidant responses', *American Journal of Physiology Renal Physiology*, 314:F956–F968.

Soler, M. J., Riera, M. and Batlle, D. (2012) 'New experimental models of diabetic nephropathy in mice models of type 2 diabetes: efforts to replicate human nephropathy', *Experimental Diabetes Research*, 2012:616313.

Somers, V. K. *et al.* (1995) 'Sympathetic neural mechanisms in obstructive sleep apnea.', *The Journal of Clinical Investigation*, 96:1897–1904.

Soni, H. *et al.* (2018) 'Cisplatin-induced oxidative stress stimulates renal Fas ligand shedding', *Renal Failure*, 40:314–322.

Soo, J. Y.-C. *et al.* (2018) 'Advances in predictive in vitro models of drug-induced nephrotoxicity', *Nature Reviews Nephrology*, 14:378–393.

Soto, K. *et al.* (2016) 'The risk of chronic kidney disease and mortality are increased after community-acquired acute kidney injury', *Kidney International*, 90:1090–1099.

Soto, K. and Devarajan, P. (2016) 'Acute kidney injury biomarkers – from bench to clinical use', *Portuguese Journal of Nephrology and Hypertension*, 30:166–169.

Spencer, J. P. E. *et al.* (1998) 'Conjugates of catecholamines with cysteine and GSH in Parkinson's disease: possible mechanisms of formation involving reactive oxygen species', *Journal of Neurochemistry*, 71:2112–2122.

Srivastava, A. *et al.* (2010) 'Quantifying the metabolic activation of nevirapine in patients by integrated applications of NMR and mass spectrometries', *Drug Metabolism and Disposition*, 38:122–132.

Stanke-Labesque, F. *et al.* (2009) 'Increased urinary leukotriene E4 excretion in obstructive sleep apnea: effects of obesity and hypoxia', *Journal of Allergy and Clinical Immunology*, 124:364–370.

States, B., Foreman, J. W. and Segal, S. (1987) 'Cysteine and glutathione levels in developing rat kidney and liver', *Pediatric Research*, 22:605–608.

Stephenson, S. T. *et al.* (2015) 'Cysteine oxidation impairs systemic glucocorticoid responsiveness in children with difficult-to-treat asthma', *Journal of Allergy and Clinical Immunology*, 136:454–461.

Stern, S. T., Bruno, M. K., Horton, R. A., *et al.* (2005) 'Contribution of acetaminophen-cysteine to acetaminophen nephrotoxicity II. Possible involvement of the γ-glutamyl cycle', *Toxicology and Applied Pharmacology*, 202:160–171.

Stern, S. T., Bruno, M. K., Hennig, G. E., *et al.* (2005) 'Contribution of acetaminophen-cysteine to acetaminophen nephrotoxicity in CD-1 mice: I. Enhancement of acetaminophen nephrotoxicity by acetaminophen-cysteine', *Toxicology and Applied Pharmacology*, 202:151–159.

Stevens, J. and Jones, D. (1989) 'The mercapturic acid pathway: biosynthesis, intermediary metabolism, and physiological disposition', in Dolphin, D., Avramovic, O., and Poulson, R. (eds) *Glutathione: Chemical, Biochemical, and Medical Aspects. Part B*. New York: John Wiley and Sons, pp. 45–84.

Stipanuk, M. H. *et al.* (2002) 'Enzymes and metabolites of cysteine metabolism in nonhepatic tissues of rats show little response to changes in dietary protein or sulfur amino acid levels', *The Journal of Nutrition*, 132:3369–3378.

Stipanuk, M. H. *et al.* (2006) 'Mammalian cysteine metabolism: new insights into regulation of cysteine metabolism', *The Journal of Nutrition*, 136:1652S–1659S.

Sumayao, R. *et al.* (2016) 'Lysosomal cystine accumulation promotes mitochondrial depolarization and induction of redox-sensitive genes in human kidney proximal tubular cells', *The Journal of Physiology*, 594:3353–3370.

Sumayao, R., Newsholme, P. and McMorrow, T. (2018) 'The role of cystinosin in the intermediary thiol metabolism and redox homeostasis in kidney proximal tubular cells', *Antioxidants*, 7:E179.

Sun, W. *et al.* (2013) 'Intermittent hypoxia-induced renal antioxidants and oxidative damage in male mice: hormetic dose response', *Dose Response*, 11:385–400.

Sutton, T. R. *et al.* (2018) 'A robust and versatile mass spectrometry platform for comprehensive assessment of the thiol redox metabolome', *Redox Biology*, 16:359–380.

Suzuki, S. *et al.* (2018) 'Plasma cystine levels and cardiovascular and all-cause mortality in hemodialysis patients', *Therapeutic Apheresis and Dialysis*, 22:476–484.

Suzuki, Y. *et al.* (2014) 'Close relationship between redox state of human serum albumin and serum cysteine levels in non-diabetic CKD patients with various degrees of renal function.', *Clinical Nephrology*, 82:320–325.

Swanepoel, C. R. *et al.* (2018) 'Kidney disease in the setting of HIV-infection: conclusions from a Kidney Disease: Improving Global Outcomes (KDIGO) Controversies Conference', *Kidney International*, 93:545–559.

Sweet, D. H., Miller, D. S. and Pritchard, J. B. (1999) 'Localization of an organic anion transporter-GFP fusion construct (rROAT1-GFP) in intact proximal tubules', *American Journal of Physiology Renal Physiology*, 276:F864–F873.

Szczech, L. A. *et al.* (2002) 'Predictors of proteinuria and renal failure among women with HIV infection', *Kidney International*, 61:195–202.

Szczech, L. A. *et al.* (2007) 'Microalbuminuria in HIV-infection', *AIDS*, 21:1003–1009.

Szwergold, B. S. (2006) 'α-Thiolamines such as cysteine and cysteamine act as effective transglycating agents due to formation of irreversible thiazolidine derivatives', *Medical Hypotheses*, 66:698–707.

Taber, S. S. and Mueller, B. A. (2006) 'Drug-associated renal dysfunction', *Critical Care Clinics*, 22:357–374.

Taguchi, K., Motohashi, H. and Yamamoto, M. (2011) 'Molecular mechanisms of the Keap1–Nrf2 pathway in stress response and cancer evolution', *Genes to Cells*, 16:123–140.

Tan, H. L., Yap, J. Q. and Qian, Q. (2016) 'Acute kidney injury: tubular markers and risk for chronic kidney disease and end-stage kidney failure', *Blood Purification*, 41:144–150.

Tenstad, O. *et al.* (1996) 'Renal handling of radiolabelled human cystatin C in the rat', *Scandinavian Journal of Clinical and Laboratory Investigation*, 56:409-414.

Thoene, J. G. and Lemons, R. (1980) 'Modulation of the intracellular cystine content of cystinotic fibroblasts by extracellular albumin', *Pediatric Research*, 14:785–787.

Thompson-Souza, G. A., Gropillo, I. and Neves, J. S. (2017) 'Cysteinyl leukotrienes in eosinophil biology: functional roles and therapeutic perspectives in eosinophilic disorders', *Frontiers in Medicine*, 4:106.

Tin, A. *et al.* (2013) 'Using multiple measures for quantitative trait association analyses: application to estimated glomerular filtration rate', *Journal of Human Genetics*, 58:461–466.

Tojo, A. *et al.* (1999) 'Immunohistochemical localization of multispecific renal organic anion transporter 1 in rat kidney', *Journal of the American Society of Nephrolog*, 10:464–471.

Tonolo, G. and Cherchi, S. (2014) 'Tubulointerstitial disease in diabetic nephropathy', *International Journal of Nephrology and Renovascular Disease*, 7:107-115.

Townsend, D. M. *et al.* (2003) 'Metabolism of cisplatin to a nephrotoxin in proximal tubule cells', *Journal of the American Society of Nephrology*, 14:1–10.

Tramonti, G. and Kanwar, Y. S. (2013) 'Review and discussion of tubular biomarkers in the diagnosis and management of diabetic nephropathy', *Endocrine*, 43:494–503.

Tsikas, D. *et al.* (1998) 'Analysis of cysteine and N-acetylcysteine in human plasma by high- performance liquid chromatography at the basal state and after oral administration of N-acetylcysteine', *Journal of Chromatography B: Biomedical Science Applications*, 708:55–60.

Tsou, H.-H. *et al.* (2018) 'Alterations in acrolein metabolism contribute to Alzheimer's disease', *Journal of Alzheimer's Disease*, 61:571–580,.

Tsuboyama-Kasaoka, N. *et al.* (1999) 'Human cysteine dioxygenase gene: structural organization, tissue-specific expression and downregulation by phorbol 12-myristate 13-acetate', *Bioscience, Biotechnology, and Biochemistry*, 63:1017–1024.

Tsuboyama, N. *et al.* (1996) 'Structural organization and tissue-specific expression of the gene encoding rat cysteine dioxygenase', *Gene*, 181:161–165.

Umemura, H. *et al.* (2017) 'Usefulness of serum 5-S-cysteinyl-dopa as a biomarker for predicting prognosis and detecting relapse in patients with advanced stage malignant melanoma', *The Journal of Dermatology*, 44:449–454.

Unnikrishnan, M. K. and Rao, M. N. A. (1990) 'Anti-inflammatory activity of methionine, methionine sulfoxide and methionine sulfone', *Agents and Actions*, 31:110–112.

Vaidya, V. S. *et al.* (2008) 'Urinary biomarkers for sensitive and specific detection of acute kidney injury in humans', *Clinical and Translational Science*, 1:200–208.

Vallon, V. (2011) 'The proximal tubule in the pathophysiology of the diabetic kidney', *American Journal of Physiology Regulatory, Integrative and Comparative Physiology,* 300:R1009–R1022.

Veiga-da-Cunha, M. *et al.* (2010) 'Molecular identification of NAT8 as the enzyme that acetylates cysteine S-conjugates to mercapturic acids', *Journal of Biological Chemistry*, 285:18888–18898.

Venkatachalam, M. A. *et al.* (2010) 'Acute kidney injury: a springboard for progression in chronic kidney disease', *American Journal of Physiology Renal Physiolog*, 298:F1078–F1094.

Ventura, P. *et al.* (1999) 'N-acetyl-cysteine reduces homocysteine plasma levels after single intravenous administration by increasing thiols urinary excretion', *Pharmacological Research*, 40:345–350.

Vergote, I. *et al.* (2010) 'Randomized phase III study of canfosfamide in combination with pegylated liposomal doxorubicin compared with pegylated liposomal doxorubicin alone in platinum-resistant ovarian cancer', *International Journal of Gynecological Cancer*, 20:772–780.

Verpooten, G. A. *et al.* (1989) 'Once-daily dosing decreases renal accumulation of gentamicin and netilmicin', *Clinical Pharmacology & Therapeutics*, 45:22–27.

Viazzi, F. *et al.* (2017) 'Association of kidney disease measures with risk of renal function worsening in patients with hypertension and type 2 diabetes', *Journal of Diabetes and its Complications*, 31:419–426.

Vicente-Vicente, L. *et al.* (2015) 'Sub-nephrotoxic cisplatin sensitizes rats to acute renal failure and increases urinary excretion of fumarylacetoacetase', *Toxicology Letters*, 234:99–109.

Vicente-Vicente, L. *et al.* (2017) 'A systematic meta-analysis on the efficacy of pre-clinically tested nephroprotectants at preventing aminoglycoside nephrotoxicity', *Toxicology*, 377:14–24.

Vina, J. *et al.* (1983) 'The effect of cysteine oxidation on isolated hepatocytes', *Biochemical Journal*, 212:39–44.

Waikar, S. S., Betensky, R. A. and Bonventre, J. V (2009) 'Creatinine as the gold standard for kidney injury biomarker studies?', *Nephrology Dialysis Transplantation*, 24:3263–3265.

Waikar, S. S. and Bonventre, J. V. (2015) 'Acute kidney injury', in Kasper, D. et al. (eds) *Harrison's Principles of Internal Medicine*. 19th edn. New York: McGraw-Hill Education, pp. 1799–1811.

Wainford, R. D. *et al.* (2008) 'Cisplatin nephrotoxicity is mediated by gamma glutamyltranspeptidase, not via a CS lyase governed biotransformation pathway', *Toxicology*, 249:184–193.

Wakamatsu, K. *et al.* (2002) 'Evaluation of 5-S-cysteinyldopa as a marker of melanoma progression: 10 years' experience', *Melanoma Research*, 12:245–253.

Walker, P. D., Barri, Y. and Shah., S. V. (1999) 'Oxidant mechanisms in gentamicin nephrotoxicity', *Renal Failure*, 21:433–442.

Wang, H. *et al.* (2016) 'Global, regional, and national life expectancy, all-cause mortality, and cause-specific mortality for 249 causes of death, 1980–2015: a systematic analysis for the Global Burden of Disease Study 2015', *The Lancet*, 388:1459–1544.

Wang, Q. *et al.* (2002) 'Blood pressure, cardiac, and renal responses to salt and deoxycorticosterone acetate in mice: role of Renin genes', *Journal of the American Society of Nephrology*, 13:1509–1516.

Wang, W. and Ballatori, N. (1998) 'Endogenous glutathione conjugates: occurrence and biological functions', *Pharmacological Reviews*, 50:335–356.

Wang, X. *et al.* (2013) 'Obstructive sleep apnea and risk of cardiovascular disease and all-cause mortality: a meta-analysis of prospective cohort studies', *International Journal of Cardiology*, 169:207–214.

Wang, X. I. A. *et al.* (2013) 'Obstructive sleep apnoea and the risk of type 2 diabetes: a meta-analysis of prospective cohort studies', *Respirology*, 18:140–146.

Weiner, D. E. (2009) 'Public health consequences of chronic kidney disease', *Clinical Pharmacology &*

Therapeutics, 86:566–569.

Weiss, J. *et al.* (2007) 'Inhibition of MRP1/ABCC1, MRP2/ABCC2, and MRP3/ABCC3 by nucleoside, nucleotide, and non-nucleoside reverser transcriptase inhibitors', *Drug Metabolism and Disposition*, 35:340–344.

Whillier, S. *et al.* (2009) 'Role of N-acetylcysteine and cystine in glutathione synthesis in human erythrocytes', *Redox Report*, 14:115–124.

Wilmer, M. J. *et al.* (2007) 'Cystine dimethylester model of cystinosis: still reliable?', *Pediatric Research*, 62:151-155.

Wimmer, I. *et al.* (1997) 'Prognostic value of serum 5-S-cysteinyldopa for monitoring human metastatic melanoma during immunochemotherapy', *Cancer Research*, 57:5073–5076.

Winking, M. *et al.* (1998) 'Cysteinyl-leukotriene levels in intracerebral hemorrhage: an edema-promoting factor?', *Cerebrovascular Diseases*, 8:318–326.

Winston, J. *et al.* (2008) 'Kidney disease in patients with HIV-infection and AIDS', *Clinical Infectious Diseases*, 47:1449–1457.

Wlodek, P. J. *et al.* (2001) 'Various forms of plasma cysteine and its metabolites in patients undergoing hemodialysis', *Clinica Chimica Acta*, 304:9–18.

Wolfgang, G. H. I. *et al.* (1989) 'N-acetyl S-(1, 2-dichlorovinyl)-L-cysteine produces a similar toxicity to S-(1, 2-dichlorovinyl)-L-cysteine in rabbit renal slices: differential transport and metabolism', *Toxicology and Applied Pharmacology*, 101:205–219.

Wonnacott, A. *et al.* (2014) 'Epidemiology and outcomes in community-acquired versus hospital-acquired AKI', *Clinical Journal of the American Society of Nephrology*, 9:1007–1014.

Wyatt, C. M. (2017) 'Kidney disease and HIV-Infection', *Topics in Antiviral Medicine*, 25:13–16.

Xu, Y., Wang, C. and Li, Z. (2014) 'A new strategy of promoting cisplatin chemotherapeutic efficiency by targeting endoplasmic reticulum stress', *Molecular and Clinical Oncology*, 2:3–7.

Yamauchi, A. *et al.* (2002) 'Tissue distribution of and species differences in deacetylation of N-acetyl-L-cysteine and immunohistochemical localization of acylase I in the primate kidney', *Journal of Pharmacy and Pharmacology*, 54:205–212.

Yan, M. *et al.* (2018) 'Endoplasmic reticulum stress in ischemic and nephrotoxic acute kidney injury', *Annals of Medicine*, 50:381–390.

Yang, H. *et al.* (2011) 'Cysteinyl leukotrienes synthesis is involved in aristolochic acid I-induced apoptosis in renal proximal tubular epithelial cells', *Toxicology*, 287:38–45.

Yang, J. *et al.* (2002) 'An iron delivery pathway mediated by a lipocalin', *Molecular Cell*, 10:1045–1056.

Yerramilli, M. *et al.* (2016) 'Kidney disease and the nexus of chronic kidney disease and acute kidney injury: the role of novel biomarkers as early and accurate diagnostics', *Veterinary Clinics: Small Animal Practice*, 46:961–993.

Yombi, J. C. *et al.* (2014) 'Antiretrovirals and the kidney in current clinical practice: renal pharmacokinetics, alterations of renal function and renal toxicity', *AIDS*, 28:621–632.

Yuen, G. J., Weller, S. and Pakes, G. E. (2008) 'A review of the pharmacokinetics of abacavir', *Clinical Pharmacokinetics*, 47:351–371.

Zahid, M. *et al.* (2013) 'Unbalanced estrogen metabolism in thyroid cancer', *International Journal of Cancer*, 133:2642–2649.

Zahid, M. *et al.* (2014) 'Unbalanced estrogen metabolism in ovarian cancer', *International Journal of Cancer*, 134:2414–2423.

Zammit, C. *et al.* (2010) 'Obesity and respiratory diseases', *International Journal of General Medicine*, 3:335-343.

Zandi-Nejad, K., Luyckx, V. A. and Brenner, B. M. (2006) 'Adult hypertension and kidney disease: the role of fetal programming', *Hypertension*, 47:502–508.

Zeni, L. *et al.* (2017) 'A more tubulocentric view of diabetic kidney disease', *Journal of Nephrology*, 30:701–717.